THE NUMERICAL REPRESENTATION OF PUMP-TURBINE PERFORMANCE CHARACTERISTICS

by

N. WALMSLEY

Thesis submitted in partial fulfilment for the degree of Doctor of Philosophy.

University of Warwick, Engineering Department.

August 1986

THE NUMERICAL REPRESENTATION OF PUMP-TUBINE PERFORMANCE CHARACTERISTICS

N. Walmsley

Summary

This thesis investigates the hydraulic transient analysis of hydro-power plants.with particular emphasis being placed on the turbine and pump-turbine boundary conditions. A lack of suitable data, in the form of the machine performance characteristics, during the early stages of a hydro-power station's development led to the investigation of alternative sources of performance characteristics, not based on the testing of a hydraulically similar model turbine. Two methods of obtaining turbine performance characteristics were developed, one based on the published performance characteristics of typical reaction turbines and the second based on performance characteristics from a turbine of similar specific speed.

The problems particular to the unit parameter representation of four quadrant reversible pump-turbine performance characteristics for use in hydraulic transient analyses were investigated. A review of alternative forms of representation led to the solution of the pump-turbine boundary based on a modified unit parameter representation. The method reduces the multi-variable problem of the pump-turbine boundary condition to that of a single variable. The solution algorithm is equally successful for use with standard turbines.

A computer program for the analysis of hydraulic transients in hydro-power plants was developed and comparisons with site recordings,taken during a full load rejection at a typical pumped storage scheme, made. in order to verify the operation of the computer program. Further simulations demonstrate the combined boundary condition of turbine and relief valve.

To family and friends.

LIST OF CONTENTS

ACKNOWLEDGEMENTS

The work presented in this thesis was carried out under a Science and Engineering Research Council (SERC) Collaborative Award in Science and Engineering (CASE) scheme. The collaborating body were Ewbank Preece Consultants, Brighton. I wish to express my thanks to all at the Hydro Department in Brighton and in particular to Mr. J.C. Bennett for his expertise and guidance during my study periods in Brighton.

My greatest thanks goes to my supervisor, Dr. A.P. Boldy, for his stimulation and guidance throughout the period of the research. I am also grateful for his encouragement and unending patience in the writing of this thesis.

DECLARATION

I declare that the research reported in this thesis is my own work. It has never been submitted previously in support for an application for any degree or qualification in any other academic institution.

LIST OF FIGURES

NOTATION

a	=	wavespeed (m/s^2)
A	=	cross-sectional area of pipe (m^2)
D	=	turbine throat diameter (m)
f	=	friction coefficient
g	=	gravitational constant (m/s^2)
gvo	=	guide vane opening
GD^2	=	flywheel effect of rotating masses ($kg.m^2$)
h	=	normalised net head across turbine
H	=	net head across turbine (m)
H_s	=	head at spiral inlet (m)
H_d	=	head at draft tube outlet (m)
I	=	moment of inertia of turbine runner ($kg.m/s^2$)
M	=	out of balance torque (N.m)
M_{11}	=	unit torque
n	=	rotational speed of turbine (r.p.m.)
n_s	=	specific speed of turbine (m-kW)
n_{11}	=	unit speed
P	=	power output of turbine (kW)
Q	=	discharge through turbine (m^3/s)
Q_{11}	=	unit discharge
t	=	time (s)
Δt	=	specified time interval (s)
v	=	average fluid velocity (m/s)
v_s	=	average fluid velocity at spiral inlet (m/s)
v_d	=	average fluid velocity at draft tube outlet (m/s)
x	=	distance (m)
Δx	=	mesh length (m)
z	=	guide vane opening
z_f	=	maximum guide vane opening

NOTATION (continued)

α = normalised speed

β = normalised torque

η = normalised head

ν = normalised discharge

ρ = fluid density (kg/m^3)

ξ = hydraulic efficiency

ξ_{maj} = efficiency majoration

θ = runner blade angle (rad)

ϕ = inclination of pipe to horizontal (rad)

Subscripts

m = model parameter

p = prototype parameter

r = parameter value at rated conditions

Superscripts

$t-\Delta t$ = parameter value at time $t-\Delta t$

t = parameter value at time t

$t+\Delta t$ = parameter value at time $t+\Delta t$

CHAPTER 1

INTRODUCTION

Hydraulic transients are used to describe the disturbances in a fluid caused during a change from one steady state to another. The principal components of the disturbances are pressure changes which result from the propagation of pressure waves throughout the hydraulic system. The study of these disturbances and the factors that effect them is a subject of international interest.

Any system containing a fluid in motion is susceptible to hydraulic transients. These include many types of industrial installations such as water distribution systems, liquid cooling systems, pumping pipelines and hydro-power plants. Extreme caution is required in the design stage and subsequent operation of these installations to ensure that they are adequately protected against the adverse effects of hydraulic transients.

Hydro-power plants are particularly susceptible to the effects of hydraulic transients. Common causes of hydraulic transients in hydro-power plants are; changes in valve settings, starting or stopping of turbines or pump-turbines and changes in load requirements of the generators. These changes may be planned or accidental.. All conceivable changes of operation must be analysed to predict the severity of the resulting pressure changes. Measures can then be taken to protect the plant and its equipment from their adverse effects.

In the 1960s computer based solutions for the solution of hydraulic transient problems in hydro-power plants were developed. The most commonly used numerical solution, to date, is the method of characteristics. The characteristic method converts the two partial differential equations of

motion and continuity into four total differential equations. These equations are then expressed in a finite difference form, using the method of specified time intervals, and their solution carried out on digital computers. In addition to the equations of motion and continuity the characteristic method requires the governing equations or performance characteristics of each mechanical component in the system in order to solve the boundary conditions.

The majority of data required for a hydraulic transient analysis are available during the early design stages.However, a notable exception are the turbine or pump-turbine data. The turbine or pump-turbine is the most complex boundary condition to be found in a hydro-power plant and it plays a leading role in the overall transient response of the installation. An accurate modelling of the boundary is therefore necessary in the hydraulic transient analysis.

The data governing the operation of a turbine or pump-turbine are its performance characteristics. Performance characteristics are obtained from studies of a hydraulically similar turbine and give the net head, discharge, rotational speed and torque relationships for a discrete range of guide vane openings. The performance characteristics are generally presented in a graphical form in terms of the unit parameters; unit speed, unit discharge and unit torque. The model test studies, however, are not performed until the final stages of a hydro-power plant's design. Alternative sources of performance characteristics must be used prior to the model test studies.

This research investigates the possibility of obtaining turbine performance characteristics from alternative sources. Published performance characteristics for typical turbines and performance characteristics from turbines of a similar specific speed are used as the source material of these investigations.

Hydraulic transient analyses of hydro-power plants requires an accurate mathematical modelling of each mechanical component within the hydraulic system. These components, or boundary conditions, include; main inlet valves, surge tanks, pipe branches, reservoirs, pipe junctions, relief valves and turbines or pump-turbines. The majority of boundary conditions are well documented in the literature. However, a notable exception is the pump-turbine boundary condition. Although solutions for a turbine boundary have been published these are not applicable to a pump-turbine.

A generalised solution algorithm is developed in this thesis which is able to handle turbine and pump-turbine boundary conditions. The specialised problems associated with a pump-turbine, particularly relating to the representation of their performance characteristics and interpolation within the performance characteristics, are investigated and incorporated into the solution algorithm.

A computer program for the analysis of hydraulic transients in hydro-power plants is developed, based on the method of characteristics, which incorporates the turbine and pump-turbine solution algorithm. A novel method of representing the many varied layouts of hydro-power plants is also included in the program's development. The method is based on a numerical coding system which can be easily interpreted within the program.

The operation of the computer program is verified by comparison with recordings taken during a full load rejection of a typical pumped storage installation. Further simulations are undertaken to demonstrate the alternative modes of operation the computer program is capable of handling.

CHAPTER 2

HISTORICAL REVIEW

2.1 EARLY HYDRAULIC TRANSIENT STUDIES

The theory behind hydraulic transient analysis was being investigated during the late nineteenth century but it was not until the turn of the century that it gained widespread acknowledgement. In 1904 Joukowski's [1] classical paper on hydraulic transients was published. He conducted a series of large scale experiments and correlated the results to his analytical treatment of the phenomenon. Working independently of Joukowski, the Italian engineer Allievi developed a comprehensive treatise on hydraulic transients. His work was published in a number of papers between 1902-1913. An English translation was made in 1925 [2]. Allievi's method of analysis, the solution of a series of interlocking algebraic equations,continued to be used throughout the early 1900's for hydraulic transient studies. However, the method could only be applied to simple frictionless hydraulic systems and it was soon superseded by the more versatile graphical methods of solution.

A graphical method for the solution of hydraulic transients was first proposed by Allievi [2] but it was found to be cumbersome and impractical. In 1928 a superior method was developed by Lowy [3] which he used to study resonance and the effects of valve openings in simple pipelines. During the 1930's the method was extended by Schnyder [4] and Bergeron [5] and their method is now internationally recognised, hence the Schnyder-Bergeron graphical solution of hydraulic transients. Although these two authors received much credit for the development of the graphical technique significant contributions were made by others,

the most notable of which was Angus [6,7]. He was the first to outline the lumped friction approximation in hydraulic transient studies and this treatment of the frictional losses later became widely accepted. During the 1930's and 1940's the application of the Schnyder-Bergeron method was demonstrated in many publications. Complex hydraulic systems, together with a variety of differing boundary conditions, were being analysed [8,9]. However, the introduction of digital computers in the early 1960's led to the graphical method of solution being replaced by numerical methods.

2.2 RECENT DEVELOPMENTS

2.2.1 Numerical Techniques

The introduction of digital computers enabled numerical techniques to be developed for the solution of hydraulic transient problems. These proved to be superior to the graphical methods, being able to handle complex hydraulic systems and components, giving greater accuracy whilst making considerable savings in terms of man-hours.

In 1953 Gray [10] advocated a computer based solution for the analysis of hydraulic transients known as the method of characteristics. This approach was subsequently adopted by Streeter [11,12,13] and through his numerous papers the method of characteristics became widely publicised. Much of Streeter's earlier work has since been summarised in a joint publication with Wylie [14]. Their work on the method of characteristics was inspired by Courant and Friedrich [15], who applied a similar technique to supersonic flow in 1948, and by Lister [16], who suggested that the method was suitable for the solution of partial differential equations of the hyperbolic type. In the 1960's and 1970's the application of the method of characteristics was demonstrated by many authors [17,18,19,20]. In the latter years much of the research concentrated on the generalisation of the boundary conditions and its application to more complex hydraulic systems. Despite the recent advancement of other numerical techniques, the implicit finite difference and finite element schemes, the method of characteristics has remained the the most popular method of solution of hydraulic transients.

The implicit finite difference scheme has been used extensively in the solution of free surface transients [21] and gas transients [14] but

it has remained unpopular for the analysis of internal transient flows . However, in 1964 Perkins et al [22] selected this method of solution to compute hydraulic transients in hydro-power stations. Their justification in choosing this method lay in its non-dependence on the Courant condition, which is a time step restriction limiting the method of characteristics. A larger time step, therefore, could be selected between successive calculations and this leads to considerable savings in computer processor times. Streeter and Wylie [14], however, concluded that this was a false economy as it resulted in a smoothing out of the pressure peaks unless the implicit finite difference scheme did in fact adhere to the Courant condition.

The implicit finite difference scheme requires the simultaneous solution of the governing equations and the performance characteristics of each element within the hydraulic system. The method of characteristics, on the other hand, allows each element to be analysed separately. This has led to the latter method gaining popularity as complex boundaries can be solved independently, without the need to solve for the entire hydraulic system. After the work of Perkins et al [22] the implicit finite difference scheme, therefore, has received little attention in conjunction with hydro-power station transients. However, its use in conjunction with the method of characteristics was proposed by Streeter [13] which allowed the Courant condition to be relaxed over selected short pipe reaches whilst retaining a larger time step for the remaining hydraulic system. This reduces the number of calculation steps needed over a given time period and leads to a reduction in the computer processor time for the simulation run.

An alternative numerical method of solution was developed by Watt [23] in 1982. A finite element approach was used to solve hydraulic

transient problems in simple pipelines and a good correlation was achieved with his experimental results and solutions using the method of characteristics and an implicit finite difference scheme. Despite the success of the method it was concluded that it would be unsuitable for the more complex hydraulic systems and boundary conditions which are found in a typical hydro-power station.

The study of hydraulic resonance in hydro-power plants has become a major field of research during the last twenty years. Hydraulic resonance has been the cause of a number of incidents [24] which have resulted in the damage or complete failure of conduits and mechanical components. Analytical methods of analysis to predict the frequency response of a hydraulic system have in the main been based on the concept of impedance. A major contributor to development of the impedance method is Wylie [25] who used it to analyse the experimental data from an incident at the Bersimis II power plant.[26]. An alternative method of predicting the frequency response of hydraulic systems was developed by Chaudhry [27] in 1970. Chaudhry used the same basic equations for unsteady flow as Wylie but manipulated them by a transfer matrix method. The early work by Wylie and Chaudhry has continued to be developed and the analysis of hydraulic resonance has become a research area in its own right.

2.2.2 Hydraulic Machinery

In the early hydraulic transient studies of hydro-power stations the inertial effects of the turbine were neglected, the turbine was generally represented as an inline valve. Strowger and Kerr [28], in the mid 1920's, were the first to rectify this situation. They considered speed changes and variations in turbine efficiency due to sudden changes in the load. In order to include these variables it was necessary to utilise the turbine performance characteristics. These give the relationships of turbine head, speed, discharge and torque for a range of guide vane openings. Unfortunately, there is a dearth of literature on turbine performance characteristics; manufacturers are reluctant to publish such information, so much of the earlier work on hydraulic machinery was concentrated on pumping installations as pump performance characteristics are more readily available.

In 1931 Kitteridge [29] reported a number of studies he made related to pumps operating under normal and abnormal hydraulic conditions. He summarised his findings by plotting the results in graphical form on a pair of diagrams. One depicted the head, power and discharge relationships for a constant speed whilst the other depicted the head, power and speed relationships for a constant discharge. This early work on pump performance characteristics was extended in 1937 by Knapp [30] who condensed the information onto a single diagram commonly known as the Karman-Knapp circle diagram. Donsky [31] and Parmakian [32] used Knapp's pump performance characteristics, but expressed in a more convenient non-dimensional form, and demonstrated their use with the graphical method of solution. In this form of representation they proved ideal for use with the graphical method but were cumbersome for the computer orientated solutions developed in the 1960's. In 1964

Streeter [12] adopted a homologous non-dimensional representation for use with the method of characteristics. This reduced the number of performance curves to two and was, therefore, particularly suitable for computer storage. He choose to store the data as a set of discrete points whereas Harding [33] advocated the representation of the pump performance characteristics in a polynomial form. The major drawback of Streeter's representation was that it relied upon a dual co-ordinate system in order to keep the parameter values within finite bounds, infinite values being undesirable in digital computation. In 1966 Suter [34] overcame this problem by introducing a trigonometrical function into his representation. This brought the parameter values to within finite limits and produced a smooth and continuous performance characteristic curve which lent itself easily to computer storage. Suter's method of representation has remained popular throughout the years since its introduction and is still used extensively for the hydraulic transient analysis of pumping installations.

The vast experience gained in the pumping field has enabled rapid progress to be made in the hydraulic transient analysis of hydro-power stations. The basic handling routine of a pump boundary is effectively the same as that for a turbine boundary except that its performance characteristics take a slightly different form. In general, pumps operate under a fixed guide vane opening whereas turbines have moveable guide vanes. The performance characteristics of a turbine, therefore, need to specify the relationships between the turbine head, discharge, speed and torque for each guide vane position. In theory, an infinite number of guide vane positions are possible but in practice only a limited number of the guide vane openings are depicted on the performance characteristics.

Turbine manufacturers generally present their performance characteristics on the unit parameter plane, see Section 4.3. The unit speed versus unit discharge and unit speed versus unit torque relationships are given for a range of discrete guide vane openings. The analysis of hydraulic transients in hydro-power stations requires these relationships to be known at all guide vane openings, not just the discrete guide vane openings shown on the performance characteristics. A method of interpolating the intermediate guide vane curves was demonstrated by Chaudhry [35] for use with turbine performance characteristics, their guide vane curves being predominately parallel to the the unit speed axes. Boldy [36] showed that Chaudhry's method was unsuitable for use with pump-turbine performance characteristics, where the guide vane curves can become perpendicular to the unit speed axes under certain operating conditions, and developed an alternative method. An orthogonal curvilinear mesh was superimposed on the performance characteristics and linear interpolation along the mesh lengths gives the intermediate guide vane curves. This method was found to be suitable for turbine and pump-turbine performance charcateristics. In 1983 Enever [37] proposed an alternative solution to the problem based on piece-wise Lagrangian polynomials and demonstrated its use with turbines operating under governor control.

Although turbine performance characteristics have remained unpublished a number of researchers have published comparisons of hydraulic transient simulations with on-site recordings [35,38]. The results showed a good correlation with the on-site recordings and demonstrated the viability of the method of characteristics for use with hydro-power plant transients. The comparisons also demonstrated that the the method could be applied to a variety of hydraulic systems and hydraulic components, or boundary conditions.

The rapid development of pumped storage schemes in the early 1960's led to considerable research being focussed on their specific problems. Transient conditions resulting from rapid change over from pumping to turbining needed investigation in addition to those resulting from load rejection, variations in load and pump failure. In 1965 a symposium devoted to hydraulic transients in pumped storage schemes produced a number of papers relating to these problems. Hornberger and Rodriguez [39] described their studies for the Taum Sauk pumped storage plant drawing attention to the lack of model performance characteristics available during the studies. The published performance characteristics of a machine of similar specific speed were used but they felt these were only suitable for preliminary studies. A recommendation that performance characteristics derived from a hydraulically similar model pump-turbine be used for the final design stages was emphasised strongly. Bovet and Schaum [40] reported the development of a generalised computer program which was able to handle the specialised operating conditions of a pump-turbine. An analytical treatment of the problem was given by Borel and Mamin [41] which could be readily adapted for use with digital computers. In addition,a procedure to obtain the optimum guide vane closure following a turbining load rejection was included. Other contributers dealt with undesirable vibrations [42] and the problems associated with converting a machine to run in spinning reserve whilst on standby [43].

The advancement of pumped storage technology increased rapidly in throughout the 1970's. Design heads in excess of 600 metres are in use at present and power outputs are approaching 400 megawatts for a single pump-turbine. The requirement of close correlation between hydraulic transient analyses and prototype performance under differing hydraulic conditions is essential for the safe operation of pumped storage schemes.

Due to the nature of the operation of pumped storage installations the pump-turbine is required, under a constantly changing net head, to achieve a high efficiency over a wide range of hydraulic conditions. This led to greater interest being directed towards the performance characteristics of pump-turbines.

In 1971 Yamabe [44] performed a series of model test studies on pump-turbines operating in the turbining mode. A region of operation in which hysteresis was evident was identified. He further showed that the hysteresis phenomenon could be predicted as a function of the cavitation number, the guide vane opening and the specific speed. In a second paper Yamabe [45] suggested ways of improving the hysteresis characteristics of pump-turbines. Whippen et al [46] also identified this phenomenon and proposed that it could be utilised advantageously as an aid to hydraulic braking during runaway conditions. Attention was also being focussed on an unstable region of pump-turbine performance characteristics known as the 'S' or re-entrant characteristic. Taulan [47] described the mechanism which caused the re-entrant characteristic and Pejovic et al [48] demostrated how it could cause large pressure fluctuations in asymmetrical hydraulic layouts. Boldy and Walmsley [49] showed that incorrect simulation results could arise from improper handling of the pump-turbine boundary condition when passing through the re-entrant characteristic. An algorithm to eliminate these problems was demonstrated but the re-entrant characteristic and its associated problems have remained the subject of considerable research.

The re-entrant characteristic of pump-turbines renders the guide vane curves multi-valued. For a given unit speed there can be up to three corresponding values of unit discharge or unit torque. The location of the operating point in such cases must be selected with care if the correct

operating condition is to be identified. However, the multi-valued nature of the unit parameter performance characteristics can be eradicated if they are mapped onto alternative planes. One alternative plane of representation was proposed by Martin [50] in 1981. Although the plane of representation led to single valued guide vane curves it was not without other set backs when considering its use in hydraulic transient simulations. The fully closed guide vane curve cannot be represented on the plane and during the final closure of the guide vanes Martin suggested modelling the pump-turbine as though it was an in-line valve. In view of this added complication Boldy and Walmsley [51] reviewed a number of different planes of representation . This research has been continued and is reported in this thesis.

CHAPTER 3

HYDRAULIC TRANSIENT ANALYSIS OF HYDRO-POWER PLANTS

3.1 INTRODUCTION

Computer simulations of hydraulic transients in hydro-power stations form an integral part of their design stages. Simulations of differing plant designs and their associated equipment can be performed both quickly and efficiently. They provide a suitable alternative to physical model testing which is extremely expensive and restrictive. Computer simulations allow a whole range of layouts to be investigated by simply altering the input data. Changes in the input data also allow the sizing of the mechanical components within the system to be investigated in order to arrive at at an optimum arrangement for the whole plant. An individual physical model would be required for each of these arrangements. Computer simulations, therefore, are more versatile and relatively cheap compared with physical models.

Hydraulic transient analyses of hydro-power stations predict the magnitudes of the pressure waves resulting from a change in operation. These changes can be planned or accidental and all conceivable situations must be analysed so the plant and its equipment can be protected from the adverse pressures. Various methods of surge protection are available and their individual merits and drawbacks must be assessed. One of the prime advantages of computer modelling is that these can performed well in advance of the final design being selected.

3.2 DESCRIPTION AND CAUSES OF HYDRAULIC TRANSIENTS

Hydraulic transients occur in closed conduit flow systems when there is either an acceleration or deceleration of the fluid. Within hydro-power plants these flow variations result from changes in the system components which alter the steady state conditions. In going from one steady state to another the system passes through a transient state in which large pressure waves are produced. The pressure waves propagate throughout the entire system. The system only returns to a steady state, once more, when the pressure waves become damped out and all other factors remain constant. During the design and subsequent operation of a hydro-power station measures must be taken to ensure that the system and its components are adequately protected against these adverse pressures.

The common causes of hydraulic transients in hydro-power plants are :-

(a) changes in valve settings, particularly rapid changes,

(b) the starting or stopping of turbines or pump-turbines,

(c) changes in load requirements,

(d) the vibration of valves, valve seals and guide vane apparatus,

(e) draft tube instabilities due to vortexing, and

(f) unstable machine performance characteristics.

The severity of the hydraulic transients is dependent on many factors which must be thoroughly investigated in the design stages of a hydro-power plant's development. Despite the many precautions taken to protect against adverse pressure waves a number of accidents attributable to hydraulic transients have occurred.

Manufacturers and clients are reluctant to widely publicise damage or complete failures due to hydraulic transients. However, a number of incidents have been reported in the literature. The first case to be generally publicised for hydro-engineers was an accident at the Lac Blanc -Lac Noir pumping station in 1933 [24]. A number of deaths resulted from a pipe rupture, the cause of which was investigated by Bergeron [24]. He concluded that the pipe failure was attributable to the vibration of the guide vanes at the pump. Resonance developed in the water column and the resulting pressures were sufficient to rupture the pipe. Bergeron suspected a resonance of the fundamental although the possibility of an odd harmonic causing the damage has since been considered [24]. Resonance was also attributed to the cause of an incident at Kandergrund hydro-power station [24]. Large fissures appeared in the upstream tunnel and despite measures to rectify the situation, including the relining of the tunnel, these fissures appeared repeatedly. Eventually the fissures opened up to such a degree that water seeped into the surrounding pervious rock causing a landslide. Initially investigators attributed the fissures to exceptionally large transient pressure waves, despite there being a large surge tank at the downstream end of the tunnel. Jaeger [24], however, revealed that in all probability they were due resonance of an odd harmonic. It was not until the Bersimis II incident [24] that the importance and dangers of vibrations due to the higher harmonics was revealed. In 1961 large vibrations in valve number one were recorded during a routine load rejection of machine number one. The vibrations continued for several minutes and were only halted after the opening of a bypass valve. Later that year large vibrations were recorded at valve number three despite it being in the fully closed position. Investigations showed that the leakage past the valve was sufficient to initiate large resonant pressures throughout the hydraulic system. It was also found that the frequencies of the vibrations were those of the higher odd harmonics.

The incidents described thus far were due to a cyclic or resonant phenomena but failures due to non-resonant transient pressures have occurred. In 1960 sections of the Oigawa Power Station ruptured as a direct result of adverse pressure waves. The cause of the pressure waves was a combination of malfunctioning equipment and operating errors. Problems were also recorded at the Jordan River Redevelopment hydro-power station. The pipeline was dimensioned for a ten percent pressure rise but under certain operating conditions the pressure rise was found to be in excess of the design pressure. Appropriate measures had then to be introduced to prevent any damage due to the over-pressure. Reverse waterhammer is the cause of many incidents in hydro-power plants. In 1980 Pejovic et al [52] reported the substantial damage inflicted on a Kaplan turbine due to reverse waterhammer. During a rapid shutdown of the machine one of the blades was broken away from the runner and this inflicted further damage to other parts of the runner.

3.3 OPERATIONAL REQUIREMENTS OF A HYDRO-POWER PLANT

Modern hydro-power plants are required to undertake a variety of standard operational mode changes. These must be performed quickly and efficiently in order not to lose valuable generating capacity. In addition, these mode changes must not result in the production of excessive transient pressures. Modern technology and greater experience have led to hydro-power plants operating under increased heads and flow velocities and this has led to greater dangers from hydraulic transients. The prediction of hydraulic transients, using computer simulations, plays an increasingly important role in the design of a safe but efficient hydro-power plant.

The standard operational mode changes of a hydro-power plant are as follows :-

(a) standstill to generation,

(b) generation to standstill, and

(c) adjustments to meet load requirements.

In addition to these basic mode changes a reversible pump-turbine must also meet the following additional requirements :-

(d) standstill to pumping,

(e) generation to pumping,

(f) pumping to generation, and

(g) pumping to standstill.

The basic sequencies involved in each of these mode changes are :-

(a) Standstill to generation. The main inlet valve or main gate is opened to pressurise the spiral casing. The governor then takes control to achieve a gradual opening of the guide vanes. As the machine speed increases the excitation is switched in. When the machine speed and voltage are within prescribed limits the generator is synchronised, either manually or more usually automatically, and the load applied.

(b) Generation to standstill. The load is removed from the generating set and the unit isolated from the electrical system. The unit is then tripped causing de-excitation of the generator and the guide vanes brought to the fully closed position. Depending on the type of trip the main inlet valve may or may not be closed. When natural retardation has brought the unit speed down to a preset level, usually 25%-30% of the synchronous speed, mechanical braking is applied to bring the set to a standstill.

(c) Adjustments in load requirements. The guide vanes are automatically adjusted by the governor in order to match the operating conditions to the load requirements, to preset active or reactive loading limits.

(d) Standstill to pumping. With the pump-turbine runner dewatered the unit is motored up to synchronous speed before water is re-admitted in to the runner. The discharge valve or discharge gate is opened and pumping commences with the opening of the guide vanes.

(e) Generation to pumping. The pump-turbine is taken off load and brought to rest as for (b). Pumping then commences as described in (d).

(f) Pumping to generation. In general, the guide vanes are closed, followed by the main inlet valve, once the driving load has been removed. The set is then brought to a standstill by natural retardation and mechanical breaking. The set is then re-started from standstill as given in (a). Alternatively, hydraulic reversal can be achieved through a partial closure of the guide vanes before tripping the set. The flow reversal rapidly deccelerates the runner causing a reversal of the runner rotation. As the speed increases in the generation direction the set is synchronised and the load applied.

(g) Pumping to standstill. With the driving load removed the guide vanes and discharge valve, or discharge gate, are closed. When natural retardation has lowered the speed to within a preset limit mechanical braking is applied bringing the the set to rest.

In order to reduce the sequence times of the mode changes the machine sets are often held in spinning reserve rather than at standstill. This eliminates the need to accelerate the machine set from rest to synchronous speed and therefore reduces the time taken for the mode change. This is applicable for both the generating and pumping modes. When held in spinning reserve the runner is dewatered, or blown-down, but water is re-admitted before proceeding with the mode change. However, one of the major factors in determining the sequence times of the mode changes, which result in the acceleration or deceleration of the water column, is the need to limit the transient pressure waves to within prescribed safety limits.

The operation requirements described previously are all for planned procedures. Some of the most severe transient conditions result from unplanned changes in operation. For example, if a machine is tripped by one of its many protective devices it is automatically disconnected from the electrical system. Alternatively the unit, or multiple units, may reject load as a result of electrical disconnection occurring at some remote point. In these events the guide vanes must be closed, or in some instances partially closed, such as to :-

(a) minimise the hydraulic pressure rise resulting from the guide vane closure, and

(b) control the overspeed of the unit to within acceptable design limits.

These are contradictory constraints and require a detailed optimisation of the guide vane closing time including cushioned final closure, generator inertia and, where applicable, pressure relief valve operating times.

3.4 HYDRAULIC TRANSIENT ANALYSIS DATA REQUIREMENTS

Computer simulations of hydraulic transients in hydro-power plants are dependent on accurate mathematical modelling of the physical system together with accurate data input. The data input covers both the fluid within the hydraulic system and its mechanical components. Inaccuracies in the input data will lead to inaccuracies in the simulation results. The input data must therefore be selected with care in order to avoid this problem.

The majority of the data required for a hydraulic transient analysis is available even during the early design stages. These include minimum and maximum reservoir levels, tunnel and pipe dimensions, valve, and where applicable surge tank, dimensions and locations, and the specifications of the turbine or pump-turbine. Although there may be more than one proposed layout for the scheme the majority of the required data will again be available. However,the most important piece of plant equipment is the turbine or pump-turbine and it is this which often suffers from a lack of the necessary input data in early studies.

A hydro-power plant operates over a range of hydraulic conditions under which it must produce a specific output. A turbine or pump-turbine of the appropriate specific speed and type is selected to meet these needs. This basic data is insufficient for use in hydraulic transient studies, where much more comprehensive information is needed in the form of the turbine or pump-turbine performance characteristics.

Prototype performance charcateristics are obtained from model test studies of a hydraulically similar machine. These tests are not generally carried out until the final stages of a hydro-power plant's development. Therefore in order to perform preliminary hydraulic transient studies a

representative machine performance characteristic must be obtained from alternative sources. Turbine and pump-turbine performance characteristics, and their use in hydraulic transient simulations, are discussed in Chapter 4 and Chapter 5.

CHAPTER 4

TURBINE PERFORMANCE CHARACTERISTICS

4.1 INTRODUCTION

Computer simulations of hydraulic transients in hydro-power stations rely upon the simultaneous consideration of two factors :-

(a) the equations of motion and continuity of the fluid within the hydraulic system and

(b) the performance characteristics, or governing equations, of each component within the system.

Accurate computer simulations are, therefore, heavily dependent upon the input data of the individual components, or boundary conditions. In practice this data is readily available for the majority of the components to be found in a hydro-power station such as pipe reaches, reservoirs, surge tanks,inlet valves and relief valves. However, accurate data for the turbine, or pump-turbine, may not be readily obtainable, particularly during the initial stages of a hydro-power plant's inception.

The data required for computer simulations of stations which include turbines, or pump-turbines, are their performance characteristics. These are obtained from tests performed on a hydraulically similar model turbine and whenever available these should be used in hydraulic transient simulations. However, simulations are often required prior to the testing of a model turbine and in such cases alternative sources of their performance characteristics must be found.

4.2 CLASSIFICATION AND SELECTION OF TURBINES

4.2.1 Introduction

The classification of turbines for hydro-power stations falls into four main categories. These are :-

(a) Pelton wheels,

(b) Kaplan turbines,

(c) Francis turbines and

(d) reversible, Francis-type, pump-turbines.

The selection of a turbine for a particular hydro-power plant is dependent upon a variety of factors. These include physical factors such as head variations , power capability, water release capability, efficiency and cost of maintainance, together with the economic viability of the plant and its overall role within the generation grid.

4.2.2 Pelton Turbines

The Pelton wheel is the only turbine in general use of the impulse type. It is best suited to high heads, above 90 metres, and has a moderate peak efficiency. The Pelton wheel is a simple and robust machine consisting of a circular wheel with a number of buckets, usually twenty or more, placed around its outer edge. Water jets are directed onto the buckets, tangentially to the wheel's radials, via nozzles to give the driving force of the turbine. The conversion of static to dynamic head takes place within the anchored nozzles. The rate of discharge through the nozzles is controlled by the use of spear valves which in turn regulate the power output of the turbine. At the peak efficiency point the buckets travel at about half the speed of the water jet. The absolute water velocity as it leaves the buckets is therefore very small and results in a relatively low kinetic energy wastage.

Pelton wheels are generally mounted with their shafts horizontal and have no more than two jets per wheel. The jets are positioned such that they do not interfere with each other under any circumstances. Pelton wheels mounted on vertical shafts are in use but these are uncommon. One of the advantages of this arrangement is that it allows a greater number of jets to be used. Up to six jets can be positioned around each wheel without fear of interference with one another as the water jet leaves the buckets in a downward direction, away from the other water jets.

4.2.3 Kaplan Turbines

Kaplan turbines are a development of the fixed blade propellor turbines. The latter display a very peaked efficiency curve but it was found that if the pitch of the blades was altered a much flatter efficiency curve was possible. Turbines such as these, variable pitch propellor turbines, are known as Kaplan turbines.

Kaplan turbines are suited to low heads, generally below 50 metres. The flow enters the runner via the spiral casing and the guide vane apparatus, passing over the turbine blades, before being discharged downwards and out through the draft tube. As the flow moves across the turbine blades it is accelerated, relative to the turbine blades, which results in a pressure differential across the blade which produces the rotation. The pressure at the blade surface can, under certain conditions, fall below atmospheric pressure which produces cavitation. In order to avoid this the submergence of the turbine is chosen such that excessive cavitation is eradicated.

A dual control system is required for a Kaplan turbine, one for the guide vane apparatus and one for the pitch of the blades. Combinations of these two factors result in differing efficiency curves for a given

hydraulic situation. The best efficiency curve, therefore, is achieved by an optimum combination of the two factors which will also vary as the hydraulic conditions vary. The control of the relationship between the guide vane apparatus and blade angle is maintained automatically by a device known as the combinator.

4.2.4 Francis Turbines

Francis turbines are inward flowing reaction turbines for use in the medium head range, 18 to 600 metres. The water enters the turbine runner at all points on its periphery having first passed through the spiral casing and guide vane apparatus. The guide vanes are adjustable to allow the angle of entry of the water to be varied with respect to the runner blades. The guide vane adjustment allows the turbine to operate with a high efficiency over a wide range of operating conditions.

The Francis turbine is a reaction turbine. As the water passes through the runner it is accelerated and directed downwards. A pressure differential is created between the runner inlet and runner outlet which causes the runner to rotate. At the design conditions, point of maximum efficiency, the flow leaves the runner with a low axial velocity and very little swirl. Under these conditions the kinetic energy of the fluid is almost entirely converted into rotational energy of the runner.

Francis turbines are generally mounted with their axles vertical, although horizontally mounted machines are also in use. A common problem with all Francis turbines is cavitation. The pressure within the runner can fall below atmospheric pressure causing the formation of air bubbles; on collapsing these cause erosion of the mechanical parts. The submergence of the turbine must therefore be such that excessive cavitation is avoided.

4.2.5 Reversible Pump-Turbines

Reversible, Francis-type, pump-turbines are similar in basic design and operation to a standard Francis turbine. However, the reversible machines are designed to operate in a pumping mode as well as in a turbining mode. These single runner machines have come to replace the individual pump and turbine systems previously used. The replacement of two hydraulic machines with a single pump-turbine is not achieved without technical problems. The operational requirements are: high efficiency in two flow directions, a high ratio of turbine output power to pump input power, and reasonably free cavitational operations. These requirements have been satisfied but not without much ingenuity and expenditure.

Pump-turbines are nowadays in great demand throughout the world. The number of sites available for standard hydro-power installations is decreasing yearly as the suitable, natural, locations are developed. Pumped storage installations provide a viable alternative to an otherwise unsuitable site for the generation of power. Pumped storage installations can provide the peak power requirements in a generation grid and provide a means of utilising excess power, during the off peak periods.

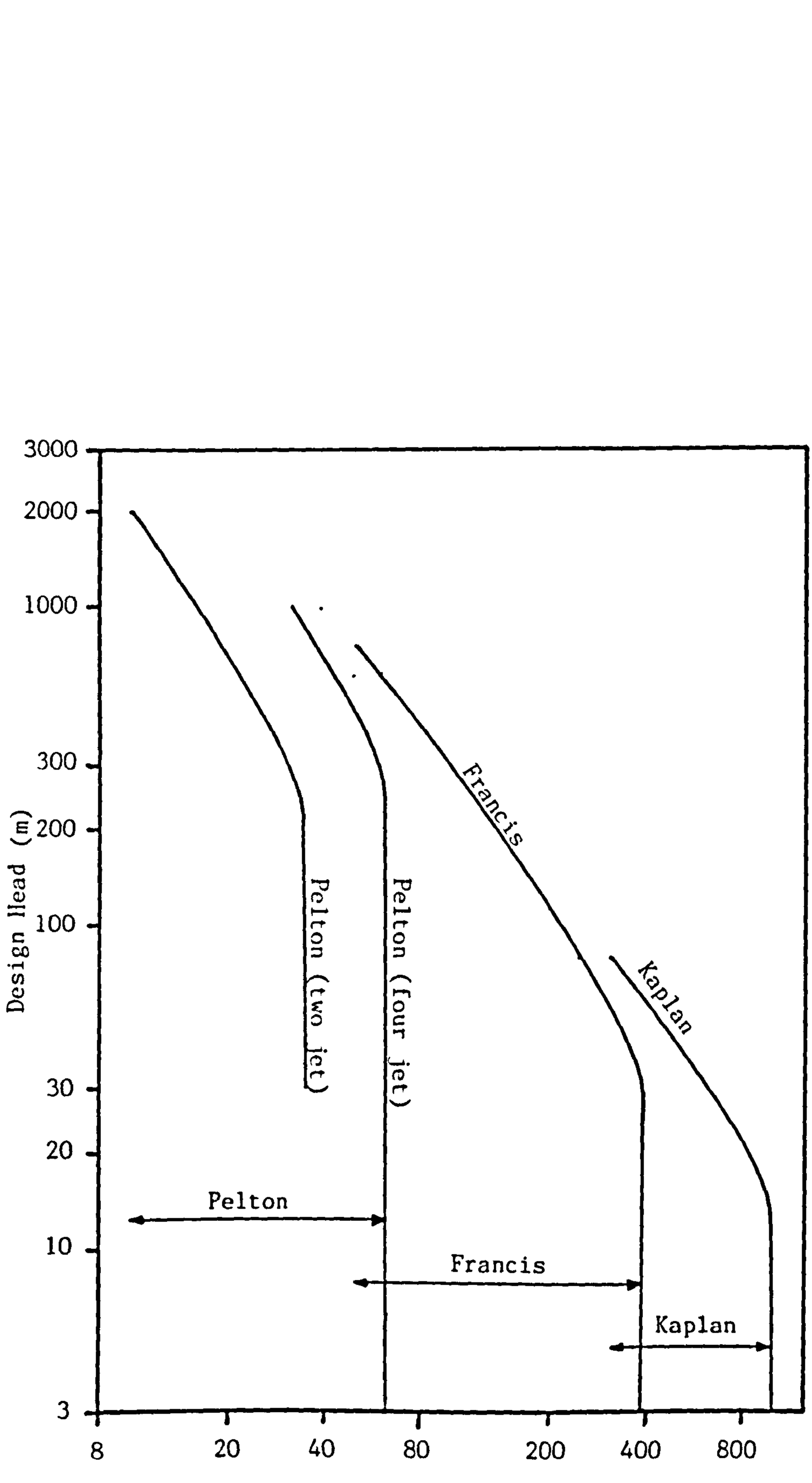

Figure 4.1 : Guide lines for turbine selection based on specific speed and design head.

4.2.6 Selection of Turbines

Hydraulic turbines are subjected to a wide variety of hydraulic conditions. Heads range from 10 metres to over 600 metres with power outputs ranging from a fraction of a megawatt to over 600 megawatts are in use at present. The number of combinations of head, power output and rotational speed is enormous. In order to summarise the hydraulic characteristics of a turbine reference is made to an index known as the specific speed, n_s, of the turbine.

The specific speed of a turbine is defined as the speed, in revolutions per minute, at which the turbine would rotate if reduced homologically in size to produce unit power under unit head, at full guide vane opening. The specific speed is defined as :-

$$n_s = \frac{n P^{0.5}}{H^{1.25}} \quad \ldots\ldots\ldots\ldots \quad (4.2.1)$$

in which

n_s = specific speed (r.p.m.)

n = rotational speed (r.p.m.)

P = power output (kW)

H = net head (m)

Equation 4.2.1 is not satisfied dimensionally and the value of the specific speed, n_s, is dependent on the units used for the variables of speed, power output and head. The specific speed given above is referred to as the metric specific speed, n_s(m-kW).

Experience has led to guide lines being established which relate the selection of a turbine to the specific speed of the turbine and the net head under which it will operate. Figure 4.1 gives these guide lines for the three main categories of turbines, Pelton, Kaplan and

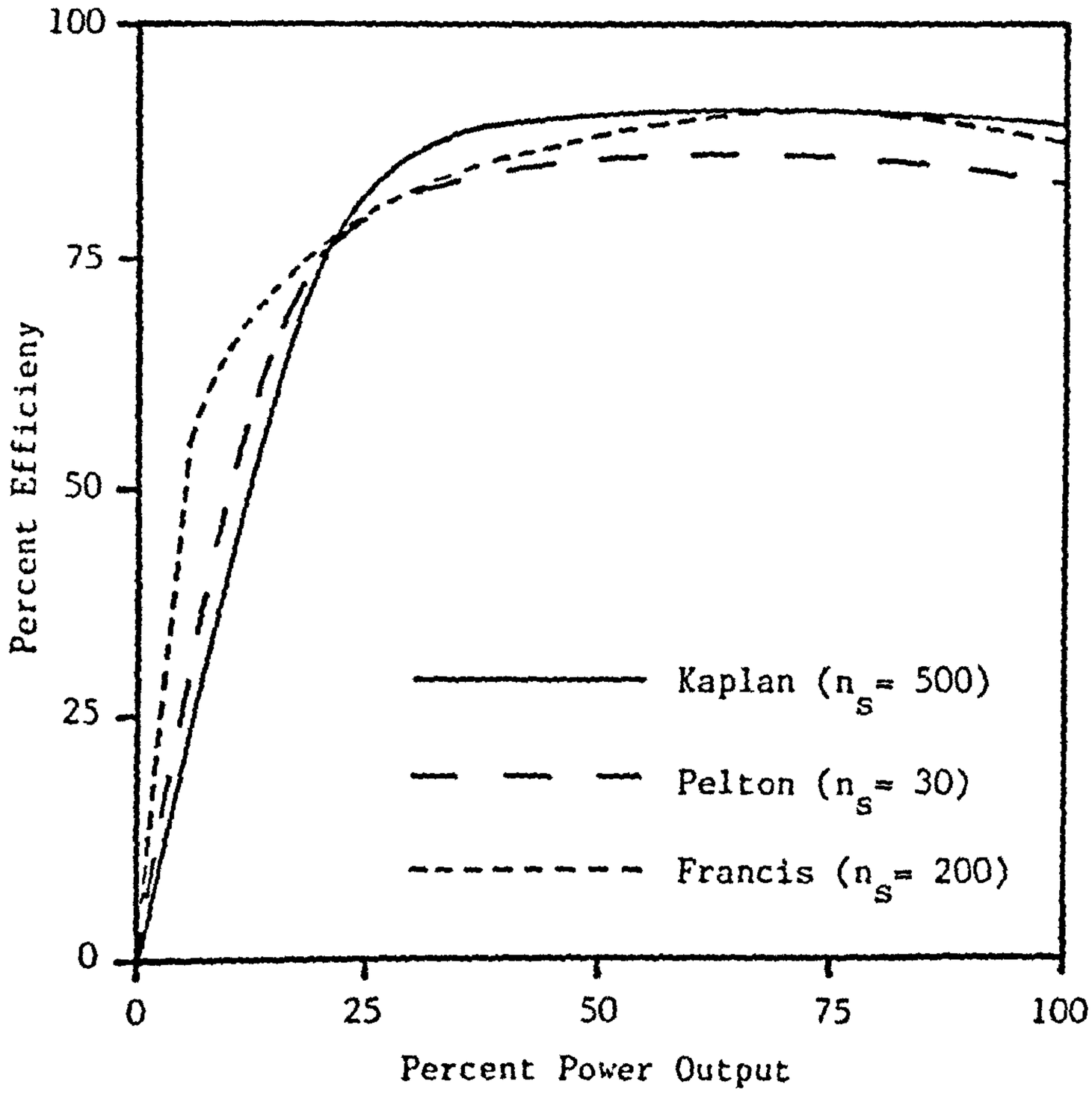

Figure 4.2 : Efficiencies at various power outputs for three turbines of different classifications.

Francis turbines. The diagram gives the recommended upper limits of specific speed for a given operating head. These are only guidelines and the selection of a turbine with a lower specific speed is common practice and equally valid.

Each turbine category is best suited to a fixed range of operating heads with upper limits set on the specific speed. In general, Kaplan turbines are used for low heads, Francis turbines for medium heads and Pelton turbines for high heads. Under certain head ranges there occurs an overlap in the curves which leads to choice of two types of turbines. Within these head ranges the advantages and disadvantages of each turbine must be assessed and an optimum solution chosen. Of particular importance in such cases is the period of time under which the turbine is expected to operate at part loads. The hydraulic efficiency of the turbine over the full range of operating conditions plays an important role in the selection of the turbine type in these situations.

The percentage efficiency versus percentage load curves differ for each type of turbine. Some typical examples are shown in Figure 4.2 . Adjustable blade Kaplan turbines display the flattest efficiency curves. A high hydraulic efficiency is achieved over a wide range of operating loads. Pelton turbines also show a relatively flat efficiency curve for loads above the half-load mark. The most marked peak efficiency curve is that for a Francis turbine. Relatively high efficiencies are possible for loads above the three-quarters mark but the efficiency decreases rapidly as the load is reduced. If a case arose where there were a choice between a Francis turbine and a Kaplan turbine and the station is required to operate for long periods under part loads the Kaplan turbine has a distinct advantage in terms of efficiency. This would then be considered against the plant and power house costs for the two installations before

making the final selection. Similarly, in the medium to high head range, there is an overlap between the selection of a Francis turbine and a Pelton turbine. Although the Pelton turbine gives a flatter efficiency curve all other considerations must be taken into account before a final selection can be made.

4.3 MODEL TURBINE TEST STUDIES

4.3.1 Introduction

Prototype turbine performance characteristics are obtained from tests performed on hydraulically similar model turbines. There are two basic criteria which the model turbines must adhere to :-

(a) geometrical similarity and

(b) geometrical similarity of their velocity vector diagrams at the runner entrance and exit.

In order to achieve complete similarity the same Reynolds number for the flow through both the model and prototype turbines should also be used. In practice, however, the latter condition cannot be met if the former two constraints are to be adhered to. This discrepancy in the Reynolds numbers means that viscous effects in the model-prototype correlation must be neglected. However, these are included by employing a majoration factor between the model and prototype performance characteristic conversion, see Section 4.3.3 .

The model test studies enable the relationships between the following parameters :-

(a) net head, defined as the difference in total pressure head between the spiral inlet and the draft tube outlet, (H),

(b) discharge through the runner (Q),

(c) rotational speed of the runner (n) and

(d) out of balance torque (M)

to be established for a fixed guide vane opening (gvo) and runner blade angle (θ).

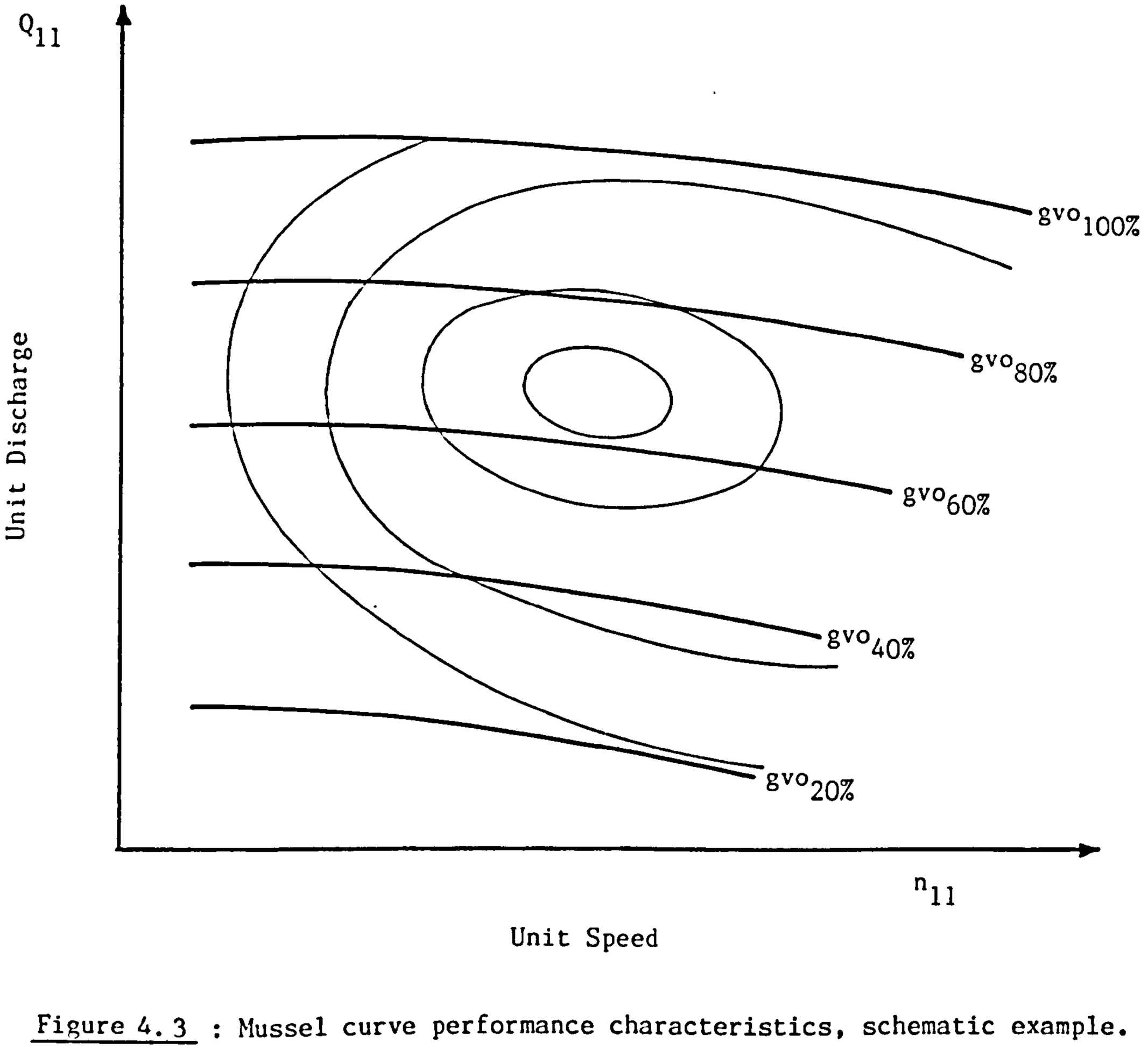

Figure 4.3 : Mussel curve performance characteristics, schematic example.

Model test studies are performed under strict codes of practice laid down by the International Electromechanical Commission (I.E.C), [53]. This aims to eliminate any discrepancies which may otherwise occur between the various test laboratories. The code outlines the object and scope of the model test studies and defines the appropriate terms, units and symbols. The nature and extent of technical guarantees such as maximum output efficiencies, overspeeding and cavitation are discussed and recommendations laid down. The report presents a standard test procedure, together with the test conditions to be fulfilled, and includes methods of measurement, the computation of results and their respective errors. Guidelines to the preparation and contents of a final model test report are also included in the code.

4.3.2 Model Turbine Performance Characteristics

Model turbine test studies are performed for a wide range of operating conditions for differing turbine heads, discharges, speeds, power outputs and guide vane openings. Once the numerical data has been collated from these numerous tests it becomes necessary to present this data in a convenient form. Turbine manufacturers generally adopt a graphical method of presentation based on the unit parameter relationships. The use of unit parameters is universally accepted where these are defined as :-

unit speed $$n_{11} = \frac{n\,D}{\sqrt{H}} \quad \ldots\ldots\ldots\ldots\ldots \quad (4.3.1)$$

unit discharge $$Q_{11} = \frac{Q}{D^2\sqrt{H}} \quad \ldots\ldots\ldots\ldots\ldots \quad (4.3.2)$$

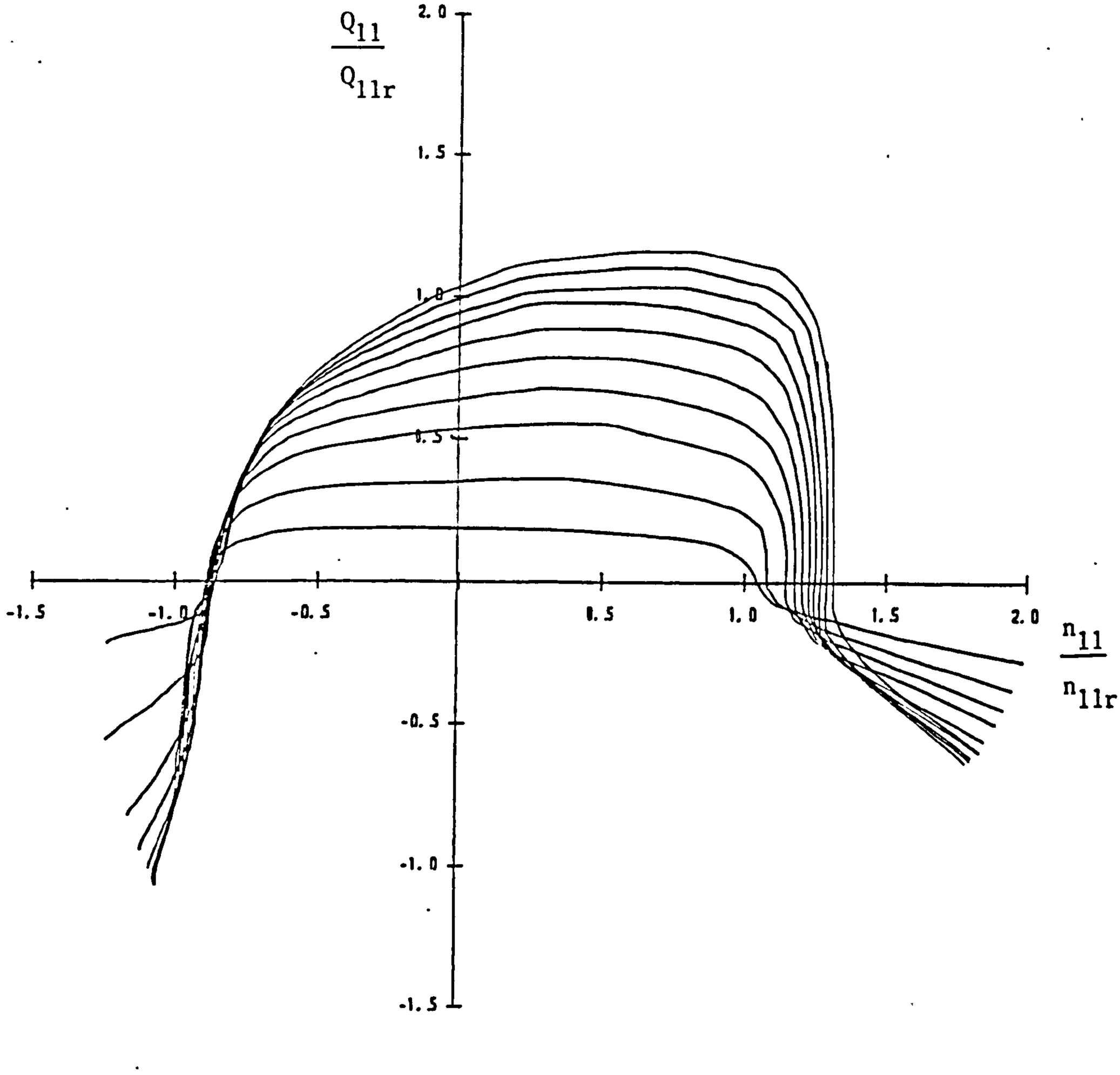

Figure 4.4 : Unit discharge versus unit speed performance characteristics, normalised.

$$\text{unit torque} \qquad M_{11} = \frac{M}{D^3 H} \qquad \text{.....} \qquad (4.3.3)$$

where n = rotational speed (r.p.m.)

H = net head (m)

Q = discharge (m^3/s)

M = torque (N.m)

D = runner diameter (m)

Two graphical forms of turbine performance characteristics are commonly found which use the unit parameters. Firstly, there is the mussel curve or hill chart. Axes of unit speed versus unit dicharge depict the guide vane relationships for a number of discrete guide vane openings. Superimposed upon these curves are a set of efficiency contours, shown in Figure 4.3 . In general, the mussel curve only gives the turbine performance characteristics for a single quadrant, the turbining quadrant. The second form of representation is as a pair of complementary curves. One set of curves (opposite) gives the unit speed versus un: discharge relationship and the other gives the unit speed versus unit torque relationship, each for a discrete range of guide vane openings. A typical set of performance characteristics in this form is shown in Figures 4.4 and 4.5 . These are for a reversible, Francis-type, pump -turbine and cover the full four quadrants of operation, pumping, braking, turbining and reverse pumping. To depict the full four quadrants on a mussel curve diagram proves to be cumbersome so the mussel curve is only used for turbines which are designed to operate exclusively in the turbining mode.

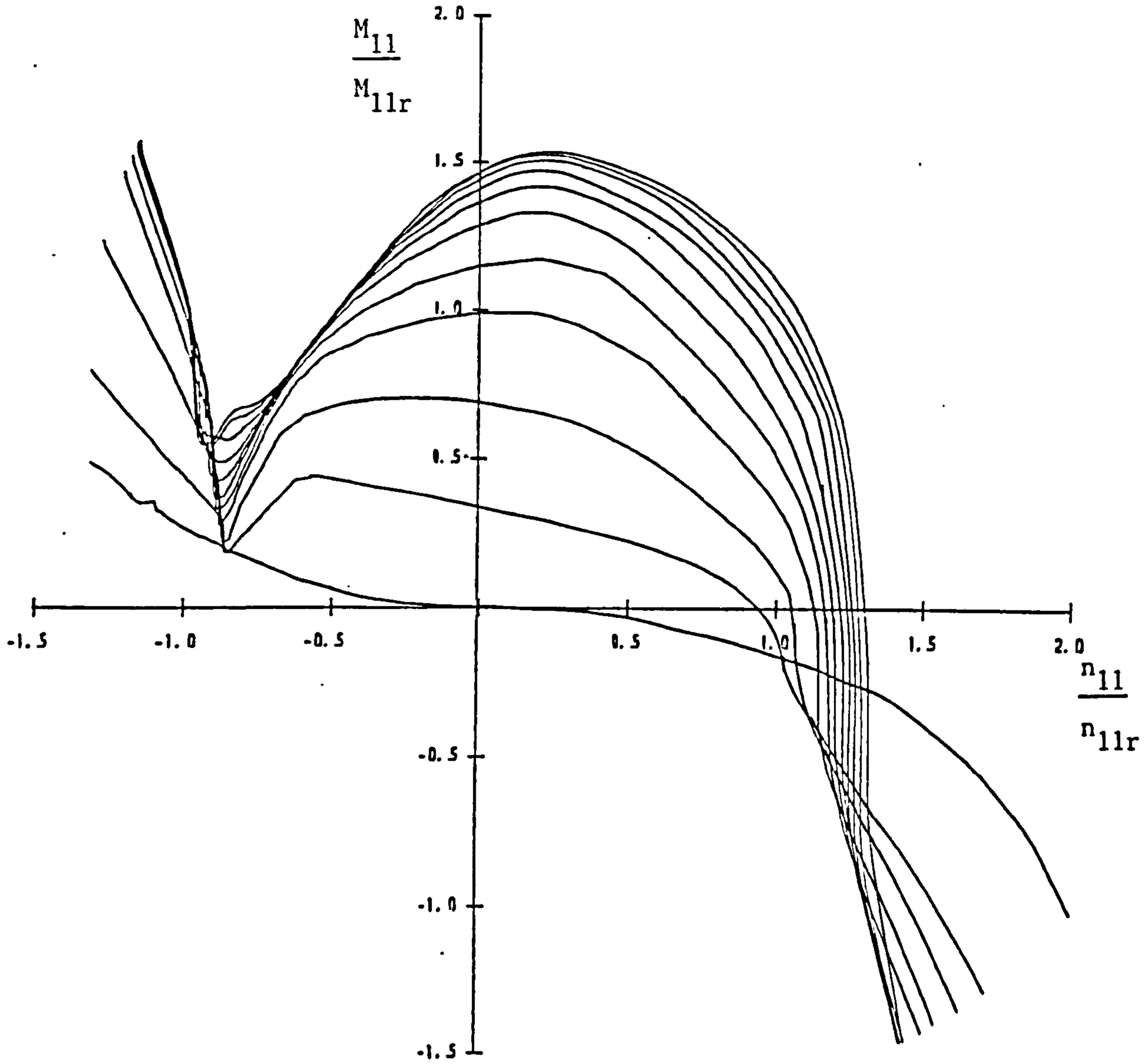

Figure 4.5 : Unit torque versus unit speed performance characteristics, normalised.

The information given by the two forms of representation of the turbine characteristics are identical and conversion from one to the other is easily achieved. The hydraulic power of a turbine is defined as :-

$$P = \xi \rho g Q H \qquad \ldots\ldots\ldots\ldots\ldots \quad (4.3.4)$$

where P = power (W)

H = net head (m)

Q = discharge (m^3/s)

g = gravitational constant (m/s^2)

ρ = fluid density (kg/m^3)

ξ = hydraulic efficiency

therefore

$$\xi = \frac{M \omega}{\rho g Q H} \qquad \ldots\ldots\ldots\ldots\ldots \quad (4.3.5)$$

where M = torque (N.m)

ω = rotational speed (rad/s)

From the definition of unit parameters, Equations 4.3.1, 4.3.2 and 4.3.3, the turbine speed (n), discharge (Q) and torque (M) are re-writen in terms of the unit parameters as :-

$$n = \frac{n_{11} \sqrt{H}}{D} \qquad \ldots\ldots\ldots\ldots\ldots \quad (4.3.6)$$

$$Q = Q_{11} D^2 \sqrt{H} \qquad \ldots\ldots\ldots\ldots\ldots \quad (4.3.7)$$

$$M = M_{11} D^3 H \qquad \ldots\ldots\ldots\ldots\ldots \quad (4.3.8)$$

Substituting Equations 4.3.6, 4.3.7 and 4.3.8 into Equation 4.3.2 gives :-

$$\xi = \frac{M_{11} n_{11} 2\pi}{\rho g Q_{11} 60} \qquad \ldots\ldots\ldots\ldots\ldots \quad (4.3.9)$$

or

$$M_{11} = \xi \rho g \frac{Q_{11} 60}{n_{11} 2\pi} \qquad \ldots\ldots\ldots\ldots\ldots \quad (4.3.10)$$

Equations 4.3.9 and 4.3.10 provide the necessary conversions between the two forms of representation of the turbine performance characteristics.

Model test studies provide the most comprehensive information of prototype turbine performance characteristics. However, these quasi-steady state performance characteristics may not correspond exactly with those followed during rapidly changing transient conditions. Although some research has been undertaken on transient performance characteristics there is, at present, very little literature on the subject. Engineers, therefore, continue to use the quasi-steady state turbine performance characteristics in hydraulic transient simulations.

4.3.3 Efficiency Majoration

The viscous effects in the model-prototype correlation are neglected during the model testing of a turbine, Section 4.3.1. The associated frictional losses of the turbines, due to differing surface finishes and dimensional tolerances, are not included in the model turbine performance characteristics. These losses directly effect the relative efficiencies of the model and prototype turbines and must be corrected for when deriving the prototype performance characteristics.

In order to compensate for the differing frictional losses it is necessary to introduce an efficiency majoration factor when converting from the model to prototype performance characteristics. The efficiency majoration factor is simply a constant efficiency factor which is added to the model efficiency to give that of the prototype. A number of efficiency majoration formulae are available but no all-purpose formulae has yet been adopted internationally. Two of the more prominent formulae to be used were developed by Moody, the latter in 1942, where the

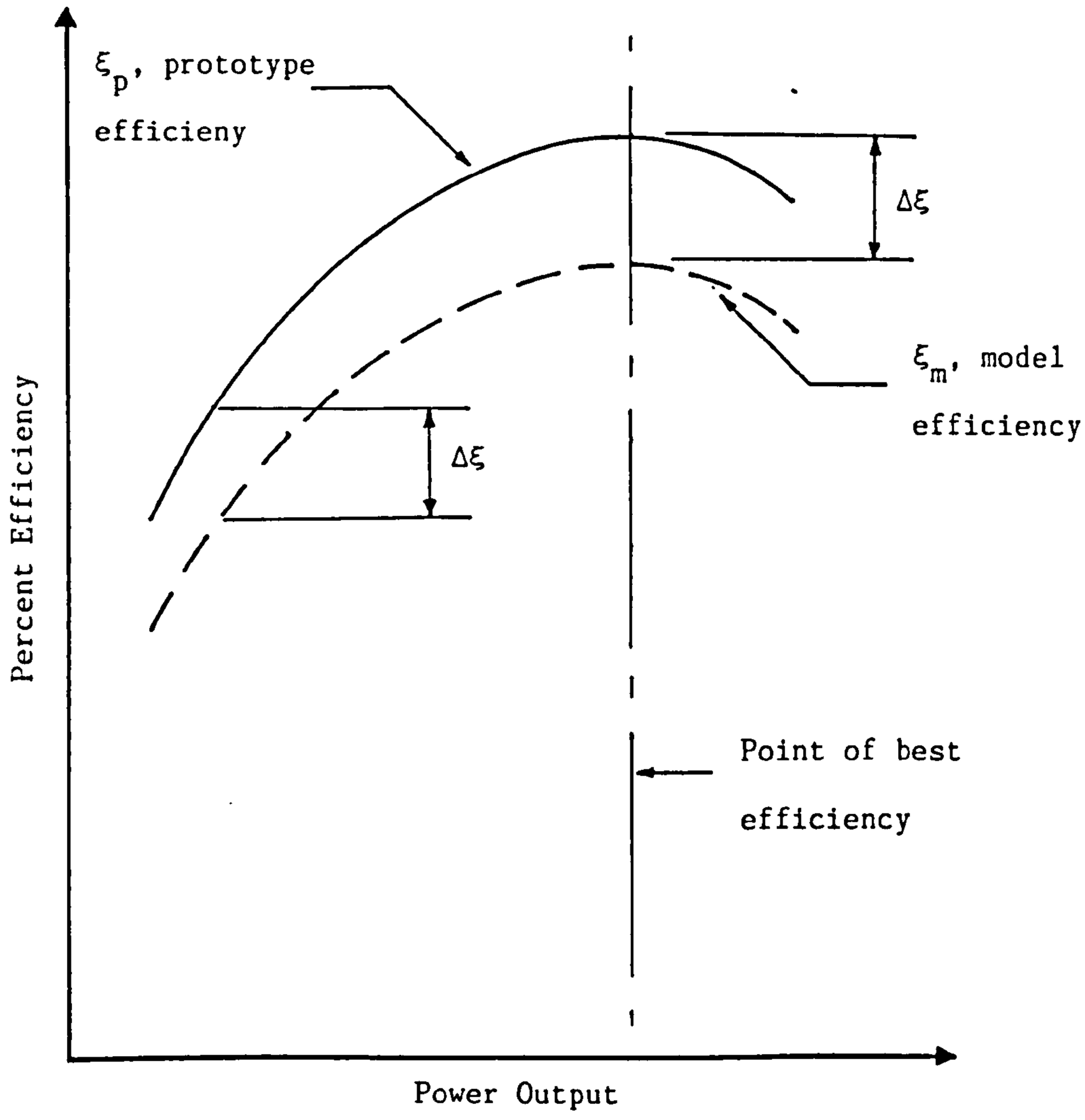

Figure 4.6 : Efficiency majoration, calculated at point of maximum efficiency, used as a step-up factor between model and prototype.

efficiency majorations are given by :-

$$\Delta\xi = [\,1-\xi_m\,]\,[\,1-(\frac{D_m}{D_p})^{0.2}\,] \qquad \ldots\ldots\ldots\ldots\ldots \quad (4.3.11)$$

and

$$\Delta\xi = [\,1-\xi_m\,]\,[\,1-(\frac{D_m}{D_p})^{0.25}(\frac{H_m}{H_p})^{0.01}\,] \qquad \ldots\ldots\ldots \quad (4.3.12)$$

in which

D_m = model runner diameter

D_p = prototype runner diameter

H_m = model net head

H_p = prototype net head

ξ_m = model efficiency

$\Delta\xi$ = efficiency majoration

The relationship between the model and prototype efficiencies, ξ_m and ξ_p, becomes :-

$$\xi_p = \xi_m + \Delta\xi \qquad \ldots\ldots\ldots\ldots\ldots \quad (4.3.13)$$

The efficiency majorations given above are strictly applicable to the point of best efficiency. For practical purposes the step-up formula, calculated at the point of best efficiency, is applied to all operating conditions. The majoration efficiency, therefore, is applied throughout as shown in Figure 4.6 .

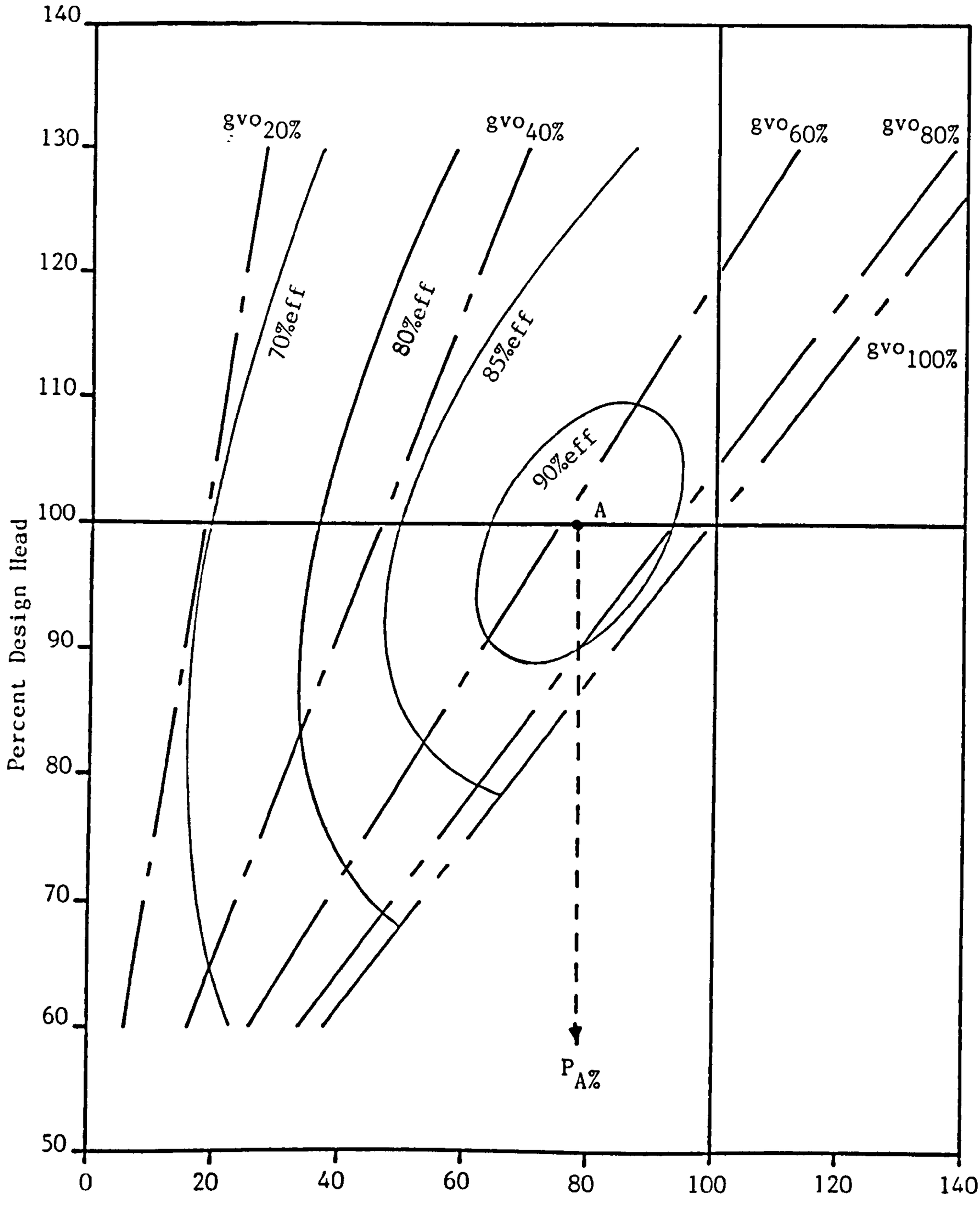

Figure 4.7 : Percent design power versus percent design head (schematic example from BUREC publication).

4.4 ALTERNATIVE SOURCES OF TURBINE PERFORMANCE CHARACTERISTICS

4.4.1 Introduction

The use of turbine performance characteristics, obtained from model test studies, is universally adopted for analysing hydraulic transients in hydro-power stations. However, situations often arise where the studies are required prior to the model testing of the turbine. In such cases, the turbine performance characteristics have to be obtained from alternative sources. There are two methods of obtaining the information required. Firstly, if the turbine performance characteristics are available for a turbine of similar specific speed these can be adapted for use with the turbine in question. Secondly, the publication 'Selecting Hydraulic Reaction Turbines' issued by the United States Department of the Interior, Bureau of Reclamation (BUREC), [54], gives example turbine performance characteristics which again can be adapted for use in hydraulic transient simulations.

4.4.2 BUREC Curves

The BUREC publication [54] presents a series of typical turbine performance characteristics each for a given range of spcific speeds. The curves are in the form of mussel curves but with their axes being given as percentages of the design conditions. Each range of specific speeds comprises two sets of complementary curves, shown schematically in Figures 4.7 and 4.8 . Figure 4.7 depicts the relationship of percent design power versus percent design head with the efficiency contours superimposed. Figure 4.8 depicts the relationship of percent discharge versus percent design head with the efficiency contours, once again, superimposed. Each set of curves gives the information for a range of

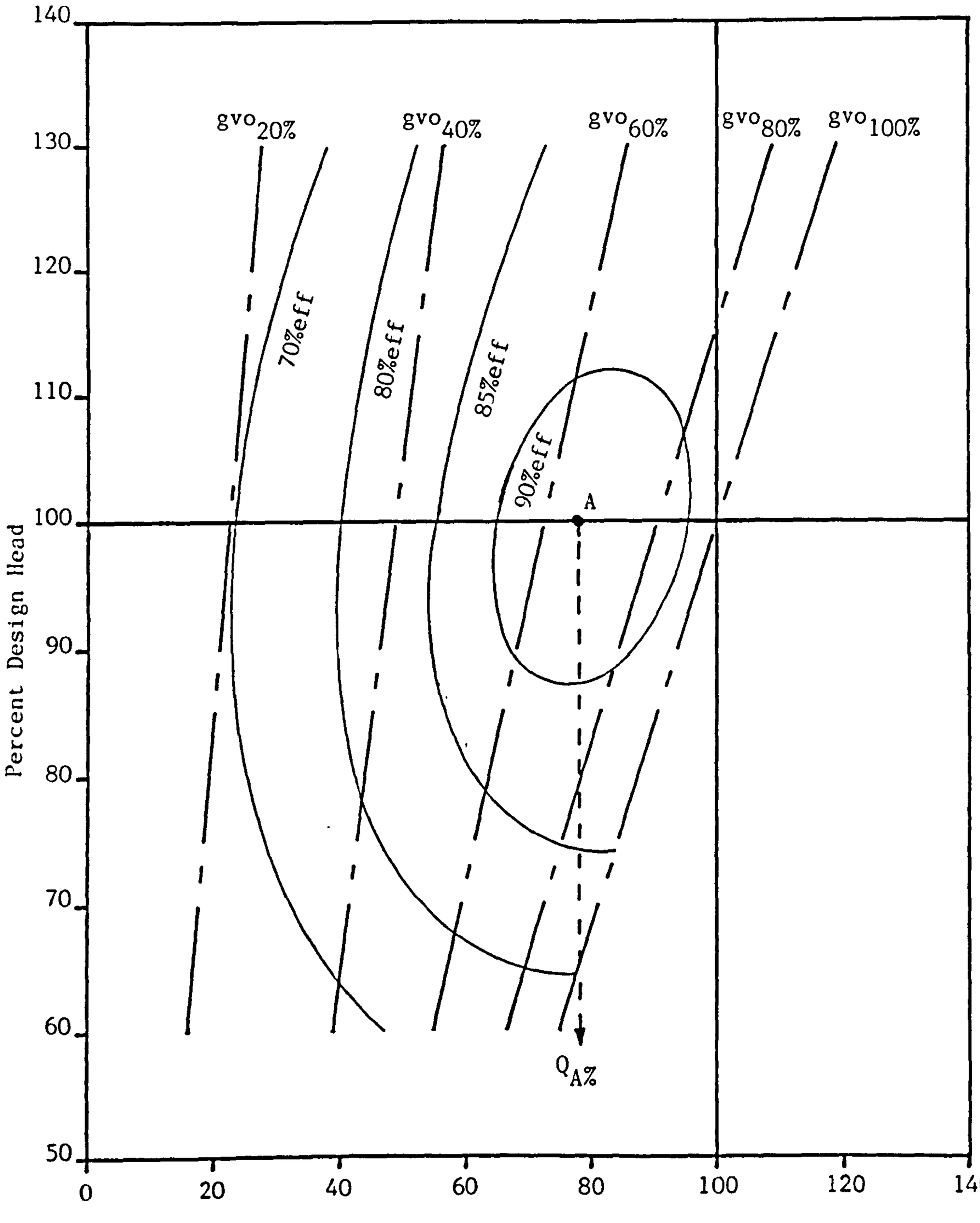

Figure 4.8 : Percent discharge versus percent design head (schematic example from BUREC publication).

guide vane openings where the design guide vane opening is taken as 65% of the maximum guide vane opening. The point of maximum efficiency, therefore, corresponds to the operating conditions which are defined as those at 100% design head with a 65% guide vane opening.

In this generalised form the BUREC curves are unsuitable for use in hydraulic transient simulations. However, they can be transformed to represent the turbine performance characteristics of a specific, individual, turbine.

4.4.3 Conversion of BUREC Curves onto the Unit Parameter Plane

During the initial design stages of a hydro-power station the hydraulic conditions under which the turbine is to operate will be known. The known design parameters are :-

(a) the design net head (H)

(b) the design power output (P) and

(c) the rotational speed (n).

Given these parameters the specific speed, n_s, of the turbine is defined as :-

$$n_s = \frac{n P^{0.5}}{H^{1.25}} \qquad \ldots\ldots\ldots\ldots\ldots \quad (4.4.1)$$

from which the appropriate set of BUREC curves is selected for use in the conversion. The hydraulic power of a turbine is defined as :-

$$P = \xi \rho g Q H \qquad \ldots\ldots\ldots\ldots\ldots \quad (4.4.2)$$

and at the point of maximum efficiency is given by :-

$$P = \xi_{max} \rho g Q H \qquad \ldots\ldots\ldots\ldots\ldots \quad (4.4.3)$$

The point of maximum efficiency is shown as point A in Figure 4.7 and Figure 4.8 . From Figure 4.8 the percent disharge at point A is $Q_{A\%}$ and

from Figure 4.7 the percent power output at point A is $P_{A\%}$. The actual discharge at the point of maximum efficiency, Q_A , is calculated from equation 4.4.3 giving :-

$$Q_A = \frac{P}{\xi_{max}\,\rho\,g\,H} \qquad \ldots\ldots\ldots\ldots \qquad (4.4.4)$$

The 100% discharge follows from :-

$$Q_{100\%} = \frac{Q_A}{Q_{A\%}} \qquad \ldots\ldots\ldots\ldots \qquad (4.4.5)$$

From the definition of the unit discharge, equation 4.3.2, the unit discharge can be written in terms of the 100% head, the known design head, and the 100% discharge, calculated from equation 4.4.5, to give :-

$$Q_{11} = \frac{(Q_\%\, Q_{100\%})}{D^2 \surd (H_\%\, H_{100\%})} \qquad \ldots\ldots\ldots\ldots \qquad (4.4.6)$$

in which

$H_\%$ = percent of the $100_\%$ head

$Q_\%$ = percent of the $100_\%$ discharge

Similarly, the unit speed, equation 4.3.1, is given by :-

$$n_{11} = \frac{n\,D}{\surd (H_\%\, H_{100\%})} \qquad \ldots\ldots\ldots\ldots \qquad (4.4.7)$$

in terms of percent of the 100% head.

The unit discharge versus unit speed curves are constucted by firstly selecting a percent head, $H_\%$, and percent guide vane opening, $gvo_\%$. The corresponding percent discharge, $Q_\%$, is found from Figure 4.8 . Substituting these values into equations 4.4.6 and 4.4.7 will give the corresponding unit discharge and unit speed values, Q_{11} and n_{11}, for the selected percent head and guide vane opening, $H_\%$ and $gvo_\%$. Repeating this procedure to cover a full range of heads and guide vane openings gives a full set of unit discharge versus unit speed performance characteristics.

A similar approach is adopted to transform Figure 4.7 onto the unit torque versus unit speed plane. At the point of maximum efficiency the power output is the design power output, P . This corresponds to point A in Figure 4.7 . The percent power output at this point is given by $P_{A\%}$. The 100% power output follows from :-

$$P_{100\%} = \frac{P}{P_{A\%}} \qquad \ldots\ldots\ldots\ldots\ldots \quad (4.4.8)$$

The power output of the turbine is equivalent to :-

$$P = M\omega \qquad \ldots\ldots\ldots\ldots\ldots \quad (4.4.9)$$

where

M = out of balance torque

ω = angular velocity of the turbine

In terms of the rotational speed, in r.p.m. , equation 4.4.9 becomes :-

$$P = M \frac{2\pi n}{60} \qquad \ldots\ldots\ldots\ldots\ldots \quad (4.4.10)$$

From the definition of unit torque, equation 4.3.3, the unit torque can be written in terms of the 100% power output and the 100% head, or design head, with the out of balance torque term, M ,being replaced from equation 4.4.10 to give :-

$$M_{11} = \frac{(P_{\%}\, P_{100\%})}{D^3\, (H_{\%}\, H_{100\%})} \frac{60}{2\pi n} \qquad \ldots\ldots\ldots\ldots\ldots \quad (4.4.11)$$

in which

$H_{\%}$ = percent of the 100% head

$P_{\%}$ = percent of the $100_{\%}$ power output

The corresponding unit speed value is given by equation 4.4.7.

The unit torque versus unit speed curves are constructed by selecting a percent head, $H_{\%}$, and a percent guide vane opening, $gvo_{\%}$. From Figure 4.7 the associated percent power output, $P_{\%}$, is identified. Substituting these

parameters into equations 4.4.11 and 4.4.7 gives the unit torque and unit speed values, M_{11} and n_{11}, respectively. Repeating the procedure over the full range of heads and guide vane openings gives the full set of unit torque versus unit speed performance characteristics.

One of the problems in using the BUREC curves in hydraulic transient studies is that they only provide a limited amount of information. The BUREC curves only provide peformance characteristics in the turbining quadrant. During a full load rejection of a turbine the locus of the operating point is likely to enter the reverse pumping quadrant if the guide vanes close rapidly. The only means of generating the required range of the performance characteristics from the BUREC curves is to use extrapolation. Having made the conversion onto the unit parameter planes the guide vane curves can be extrapolated by hand into the reverse pumping quadrant. This extrapolation, however, is open to interpretation and may clearly result in errors. For this reason, it is recommended that the BUREC curves are only used during early design studies.

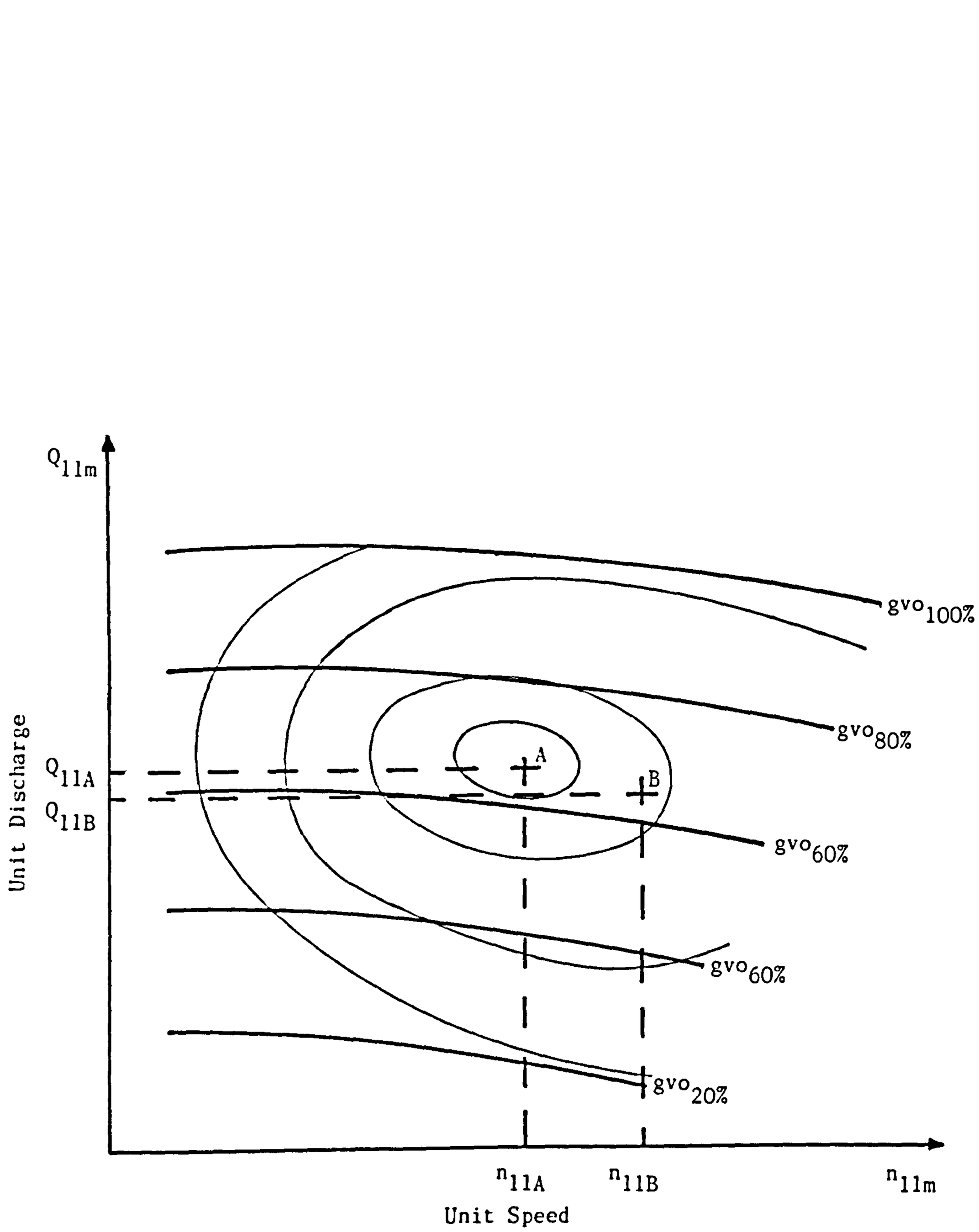

Figure 4.9 : Model turbine performance characteristic given as a mussel curve.

4.4.4 Turbine Performance Characteristics of Similar Specific Speed

Hydraulic transient studies are frequently required prior to the testing of a model turbine. Section 4.4.2 describes how this problem can be overcome by utilising the typical performance characteristics given in the BUREC publication. An alternative solution to the problem is to adapt the performance characteristics of a turbine with a similar specific speed to approximate those of the proposed turbine.

Consider a model turbine performance characteristic, of similar specific speed, presented as a mussel curve as shown in Figure 4.9 . At the point of maximum efficiency , point A in Figure 4.9 , the unit speed and unit discharge values are n_{11A} and Q_{11A} respectively. For the prototype turbine let the unit speed and unit discharge values at the point of maximum efficiency, calculated from the known design conditions, be n_{11B} and Q_{11B} respectively and correspond to point B when plotted on the model turbine performance charcateristics, Figure 4.9 . It is clear that point B does not lie at the point of maximum efficiency if the model co-ordinate system of axes, denoted by n_{11m} and Q_{11m}, is used. In order to bring point B to the point of maximum efficiency a linear multiplying factor is applied to each of the axes. The factors required are the ratios of the prototype unit parameter values to the model unit parameter values, each taken at the point of maximum efficiency, which gives :-

$$\delta_n = \frac{n_{11B}}{n_{11A}} \quad \ldots\ldots\ldots\ldots\ldots \quad (4.4.12)$$

and

$$\delta_q = \frac{Q_{11B}}{Q_{11A}} \quad \ldots\ldots\ldots\ldots\ldots \quad (4.4.13)$$

where

δ_n = unit speed factor

δ_q = unit discharge factor

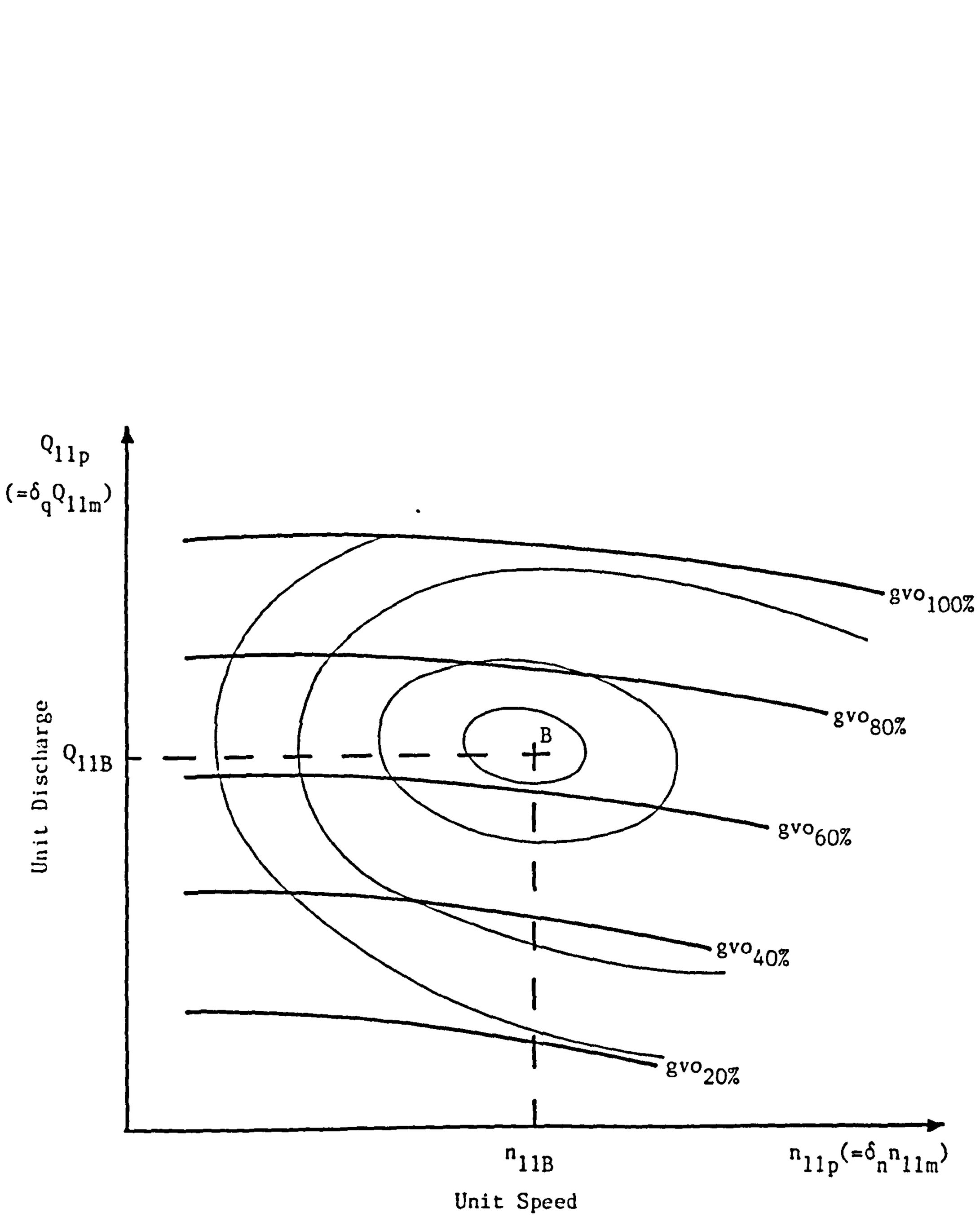

Figure 4.10 : Prototype point of maximum efficiency on mussel curve with factored axes.

By replacing the model performance characteristic axes, n_{11m} and Q_{11m}, by a new set of factored axes point B can be brought to the point of maximum efficiency. The new axes are denoted by n_{11p} and Q_{11p} which are calculated from :-

$$n_{11p} = \delta_n n_{11m} \qquad \ldots\ldots\ldots\ldots\ldots \quad (4.4.14)$$

and

$$Q_{11p} = \delta_q Q_{11m} \qquad \ldots\ldots\ldots\ldots\ldots \quad (4.4.15)$$

Applying these factored axes to the model performance charcateristics maps point B onto the point of maximum efficiency as shown in Figure 4.10.

The model performance characteristics require a majoration factor to be applied before they fully represent those of the prototype turbine, see Section 4.3.3. The relationship between the model and prototype efficiencies, from equation 4.3.13, gives :-

$$\xi_p = \xi_m + \Delta\xi \qquad \ldots\ldots\ldots\ldots\ldots \quad (4.4.16)$$

In terms of the prototype unit parameters, see equation 4.3.9, the efficiency majoration formula can be re-written as :-

$$\frac{M_{11p}\, n_{11p}\, 2\pi}{\rho g Q_{11p}\, 60} = \xi_m + \Delta\xi \qquad \ldots\ldots\ldots\ldots\ldots \quad (4.4.17)$$

Re-arranging and replacing the prototype unit speed and unit discharge using equations 4.4.14 and 4.4.15, respectively, leads to :-

$$M_{11p} = \frac{\delta_q Q_{11m}}{\delta_n n_{11m}} \frac{60\rho g}{2\pi} (\xi_m + \Delta\xi) \qquad \ldots\ldots\ldots\ldots\ldots \quad (4.4.18)$$

Equations 4.4.14, 4.4.15 and 4.4.18 give the prototype unit parameters as functions of the the model efficiency, unit speed, unit discharge and efficiency majoration factor. A model turbine performance characteristic, given as a mussel curve, of a similar specific speed can be utilised to represent those of a prototype turbine by using these three conversion formulae.

The model turbine performance characteristics in some cases may be given as a pair of complementary sets of curves; one giving the unit speed versus unit discharge relationship; the other giving the unit speed versus unit torque relationship. The method of transforming these curves to represent those of a prototype turbine of similar specific speed needs only slight modification from that described previously.

The unit speed and unit discharge axes are factored such that the prototype point of maximum efficiency corresponds to that of the model turbine by applying equations 4.4.12 and 4.4.13. The modified axes, n_{11p} and Q_{11p}, are given in equations 4.4.14 and 4.4.15. Again, an efficiency majoration factor is required between the model and prototype efficiencies, equation 4.4.16. Re-writing the majoration formula in terms of both the model and prototype unit parameters leads to :-

$$\frac{M_{11p}\, n_{11p}\, 2\pi}{\rho\, g\, Q_{11p}\, 60} = \frac{M_{11m}\, n_{11m}\, 2\pi}{\rho\, g\, Q_{11m}\, 60} + \Delta\xi \quad \ldots\ldots\ldots\ldots \quad (4.4.19)$$

The prototype unit torque , M_{11p} , therefore, is given by :-

$$M_{11p} = \frac{n_{11m}\, Q_{11p}}{n_{11p}\, Q_{11m}}\, M_{11m} + \frac{Q_{11p}}{n_{11p}}\, \frac{60\, \rho\, g\, \Delta\xi}{2\pi} \quad \ldots\ldots \quad (4.4.20)$$

Using equations 4.4.14 and 4.4.15 the prototype unit speed and unit discharge, n_{11p} and Q_{11p}, are eliminated to give :-

$$M_{11p} = \frac{\delta_q}{\delta_n}\left\{ M_{11m} + \frac{Q_{11m}}{n_{11m}}\, \frac{60\, \rho\, g\, \Delta\xi}{2\pi} \right\} \quad \ldots\ldots\ldots \quad (4.4.21)$$

The prototype unit torque is given as a function of the model turbine unit parameters and the efficiency majoration. The prototype unit speed and unit discharge are obtained from equations 4.4.14 and 4.4.15 respectively.

Two methods of utilising the performance characteristics of a model turbine of a similar specific speed have been demonstrated. The first method is applicable to performance characteristics given as a mussel curve and the second applies to the performance characteristics given as a pair of complementary unit parameter curves. These methods can also be applied to a prototype performance characteristic of similar specific speed. Under these circumstances the efficiency majoration factor is in general not required. The conversion formulae presented are still valid, therefore, if the efficiency majoration factor, $\Delta\xi$, is set to zero.

CHAPTER 5

REPRESENTATION OF TURBINE PERFORMANCE CHARACTERISTICS FOR USE IN HYDRAULIC TRANSIENT SIMULATIONS

5.1 INTRODUCTION

In hydraulic transient simulations of hydro-power stations the turbine or pump-turbine boundary is the most complex boundary condition to be encountered. Despite this there is a dearth of literature relating to methods of handling this boundary condition. This is particularly evident for the case of a reversible pump-turbine.

The primary input data for a turbine boundary are its performance characteristics. For use in a generalised hydraulic transient simulation program these must fulfil three main criteria :-

(a) they must be represented in a manner which is suitable for computer storage,

(b) their representation and storage must allow for the interpolation of the intermediate guide vane curves and

(c) the handling routine must be accurate whilst not being over complicated.

These criteria are discussed in detail in the following sections, with particular reference being made to the performance characteristics of a reversible pump-turbine.

5.2 INDIVIDUAL GUIDE VANE CURVE REPRESENTATION

5.2.1 Introduction

Turbine performance characteristics are constructed from a set of discrete operating conditions obtained from model turbine test studies. The complete performance characteristics are generally presented in graphical form but this does not provide a convenient method of storage in a digital computer. This is more readily achieved by reducing the graphical data to a set of discrete operating points, or co-ordinates, between which the graphical curves can be re-constructed or approximated. Hydraulic transient simulations require the location of the operating point within the performance characteristics to be identifiable for the full range of the turbines operating regions. Interpolation along each guide vane curve and between the guide vane curves themselves is, therefore, necessary. The method of representation of the individual guide vane curves must, therefore, be chosen to allow for this criterion.

Let the discrete operating points along a fixed guide vane curve be denoted by a set of co-ordinates (x_i, y_i) on the x-y plane. When referring to a turbine these would relate to either the unit speed versus unit discharge or unit speed versus unit torque planes. However, generalising the planes in this manner avoids the need to refer to these planes individually.

5.2.2 Polynomial Curve Fitting

Given a set of n+1 data points (x_i, y_i) where $0 \leq i \leq n$ a unique polynomial p(x) can be fitted to the points [55] such that :-

$$p(x_i) = y_i \qquad i=0,1,2,\ldots,n-1,n \qquad \ldots\ldots\ldots \qquad (5.2.1)$$

given that

$$x_0 < x_1 < x_2 < \ldots\ldots < x_{n-1} < x_n$$

The polynomial, p(x), takes the form :-

$$p(x) = a_n x^n + a_{n-1} x^{n-1} + \ldots\ldots + a_1 x + a_0 \qquad \ldots\ldots \qquad (5.2.2)$$

For a given value of x , within the range x_0 to x_n, a corresponding value of p(x) can be interpolated by substitution in equation 5.2.2.

This interpolation polynomial can also be written in its more usual form as a Lagrangian polynomial where the polynomial p(x) is given by :-

$$p(x) = \sum_{i=0}^{n} l_i(x)\, y_i \qquad \ldots\ldots\ldots\ldots\ldots \qquad (5.2.3)$$

where

$$l_i(x) = \frac{(x-x_0)\ldots\ldots(x-x_{i-1})(x-x_{i+1})\ldots\ldots(x-x_n)}{(x_i-x_0)\ldots(x_i-x_{i-1})(x_i-x_{i+1})\ldots(x_i-x_n)}$$

Again, for a given value of x a corresponding value of p(x) can be found by substitution in equation 5.2.3.

It must be noted that the polynomial, p(x), is an approximation to the actual relationship. At each of the discrete points the polynomial gives an exact value of y_i, equation 5.2.1, but at the intermediate points errors may occur. Also, if the guide vane curve is represented by a large number of data points an interpolating polynomial of a high degree will result.

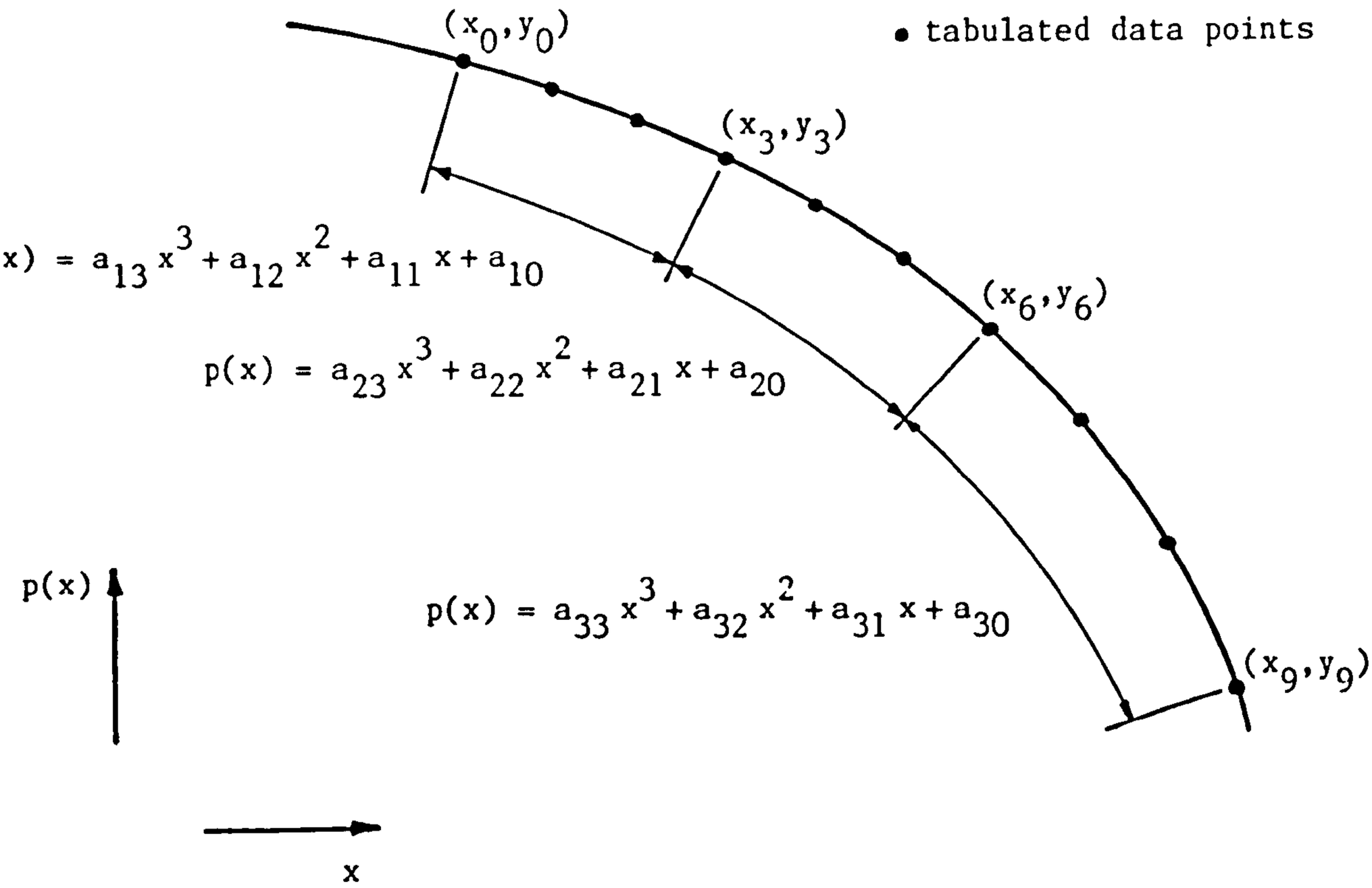

Figure 5.1 : Piecewise interpolation polynomials.

5.2.3 Piecewise Interpolation Polynomials

To avoid the need of high degree polynomials the guide vane curve can be separated into a number of sub-sections. A relatively low degree polynomial is then used to represent each sub-section. For example, if four data points are selected along each sub-section a cubic polynomial can be fitted to each of these. Referring to Figure 5.1 , an approximation of the guide vane relationship is given by :-

$$p(x) = \begin{cases} a_{13}x^3 + a_{12}x^2 + a_{11}x + a_{10} & x_0 \leq x \leq x_3 \\ a_{23}x^3 + a_{22}x^2 + a_{21}x + a_{20} & x_3 \leq x \leq x_6 \\ \text{etc.} \end{cases} \qquad (5.2.4)$$

Piecewise polynomials can be used as an effective alternative to global polynomials. One of their advantages is that for a given value of x only four polynomial constants, assuming a cubic is being used, need to be calculated to obtain the interpolating polynomial. This compares favourably with a global polynomial in which n+1, generally much greater than four, polynomial constants need to be found.

5.2.4 Cubic Splines

Cubic splines fitted between the discrete data points give a good approximation to the guide vane relationship with the following four conditions being met. The cubic spline must [56] :-

(a) pass through the data point at the start of the interval,

(b) pass through the data point at the end of the interval,

(c) agree with the previous spline in slope at the start of the interval, and

(d) agree with the previous spline in curvature at the start of the interval.

Since there are four constraints placed on the polynomial the lowest degree polynomial which will satisfy these constraints is a cubic polynomial, or cubic spline. Given a set of n+1 data points, (x_i, y_i), a cubic spline is fitted between each sub-interval, i to i+1, which gives continuity of smoothness. The full guide vane relationship, p(x), is given by :-

$$p(x) = \begin{cases} a_{13}x^3 + a_{12}x^2 + a_{11}x + a_{10} & x_0 \leq x \leq x_1 \\ a_{23}x^3 + a_{22}x^2 + a_{21}x + a_{20} & x_1 \leq x \leq x_2 \\ \vdots \quad \vdots \quad \vdots \quad \vdots & \\ a_{n3}x^3 + a_{n2}x^2 + a_{n1}x + a_{n0} & x_{n-1} \leq x \leq x_n \end{cases} \qquad (5.2.5)$$

Given a value of x the interpolated value of p(x) is found by firstly identifying the sub-interval then substituting the x value into the appropriate cubic spline from equation 5.2.5.

5.2.5 Linear Approximation

The simplest method of interpolating intermediate values along a guide vane relationship is found using linear approximation. The guide vane relationship is assumed to be linear between adjacent data points. The interpolating polynomial, p(x), is given by :-

$$p(x) = \frac{(x - x_{i+1})}{(x_i - x_{i+1})} y_i + \frac{(x - x_i)}{(x_{i+1} - x_i)} y_{i+1} \qquad (5.2.6)$$

between the i^{th} and $i+1^{th}$ data points. The linear approximation is effectively the piecewise interpolation polynomials taken to their extreme, a polynomial fitted between only two data points which gives the equation of a straight line.

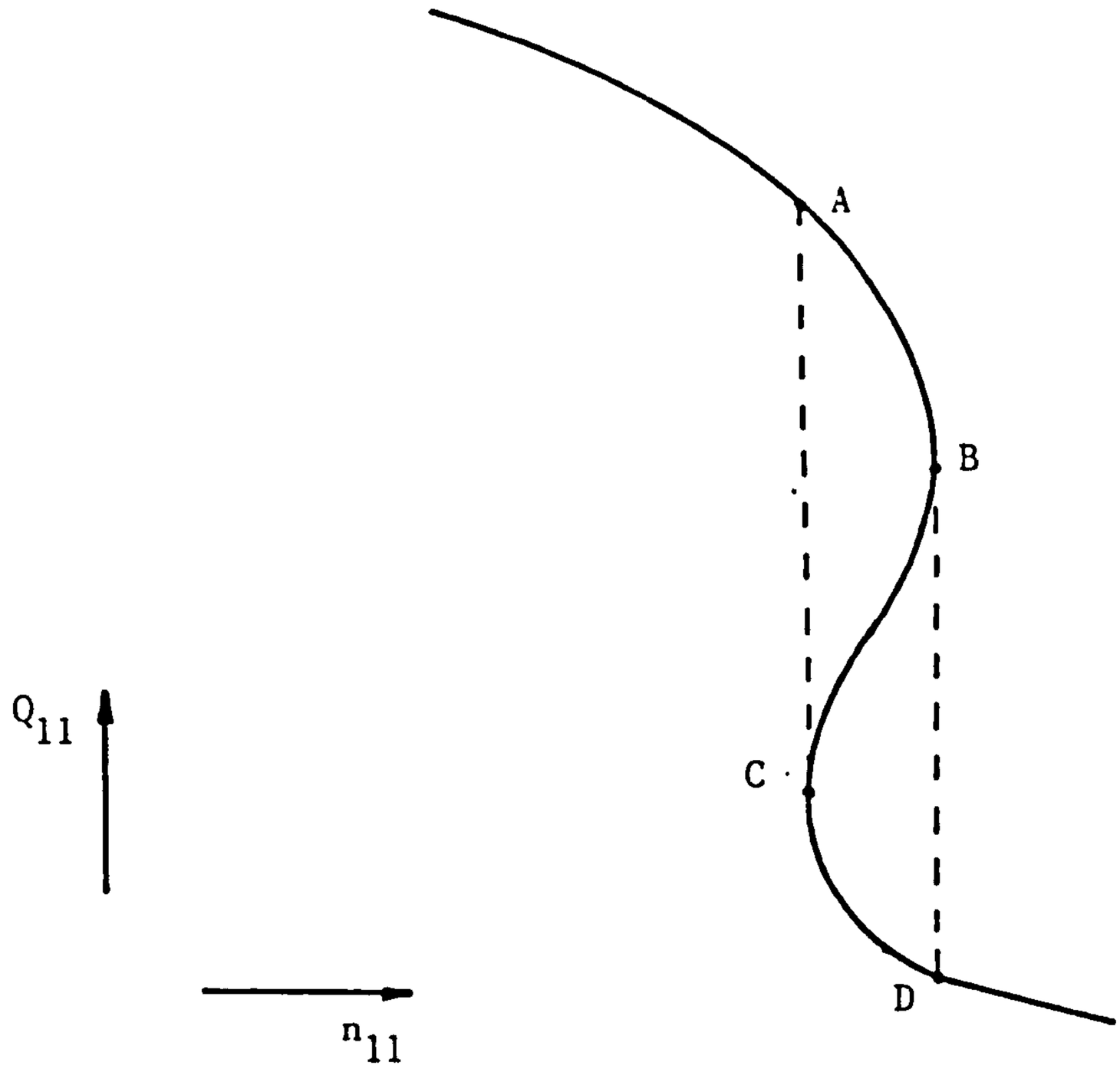

Figure 5.2 : Sub-division of the re-entant region of the performance characteristics for polynomial representation.

5.2.6 Selection of Guide Vane Representation

The different methods of representing the individual guide vane curves are assessed within their use in hydraulic transient simulations. The chosen method is required in a form suitable for storage in a computer data file and must allow for the solution of the machine boundary. In addition, it is desirable to have a representation which can be used for turbine and pump-turbine performance characteristics and which could have a generalised form that is independent of the performance characteristics in question.

Polynomial curve fitting, or Lagrangian polynomials, is based upon the assumption that the x values are unique and form a continuously increasing series. For a set of n+1 data points this requires that :-

$$x_0 < x_1 < \ldots\ldots < x_{n-1} < x_n \qquad \ldots\ldots\ldots\ldots \qquad (5.2.7)$$

Turbine performance characteristics generally adhere to this assumption but this is not necessarily true for pump-turbines. Pump-turbine performance characteristics can display guide vane curves which involve re-entrants, this is discussed further in section 5.3.5 . Figure 5.2 gives a schematic view of a re-entrant guide vane curve. It is clear from this diagram that the x values are neither unique nor adhere to equation 5.2.7 . For a given abscissa value there may be as many as three corresponding ordinate values. In cases where a re-entrant is present in the performance characteristics, therefore, a single polynomial cannot be fitted through the entire guide vane curve. One method of alleviating this problem is by using piecewise polynomials.

The re-entrant region of the guide vane curve is bounded at the extremeties by x values at points B and C, shown in Figure 5.2 . By dividing the curve into three distinct sections, A-B, B-C and C-D, an

individual polynomial can be derived for each section. Along each section there are no re-entrants and equation 5.2.7 is satisfied throughout. In fact, each section can be further subdivided without negating equation 5.2.7. Subdivision into these shorter sections reduces the number of data points along each section and, therefore, reduces the degree of the polynomial required to fit each section. The underlying problem in using piecewise polynomials is in trying to generalise the method. To stipulate a fixed number of data points along each sub-section could lead to a sub-section which lies partly within region B-C and partly outside. As already stated, this cannot be allowed as equation 5.2.7 is contravened. In the data input for such a method information would be required as to the number of points along each sub-section, the location of points B and C, and the total number of sub-sections. To generalise this approach, for use with turbines and pump-turbines,proves cumbersome as special cases are required to handle the re-entrants whereas other methods of representation do not need to distinquish between re-entrants and non re-entrants.

The use of cubic splines to represent the guide vane curve is similar to the piecewise polynomial approach. A spline is applied between each pair of adjacent data points. The slope and curvature of the curve is continuous, not the case for piecewise polynomials, and a good range of data points will give a good correlation to the curve. However, cubic splines are normally applied to data points which are separated by a fixed x interval [56]. This would lead to an unsatisfactory spread of data points along a guide vane curve for a pump-turbine, where the curves become predominately perpendicular to the x axis in certain regions. Their use with pump-turbine characteristics is therefore limited. The establishment of the spline equations is also relatively complex and whilst a good correlation can be achieved this must be considered against the accuracy of the performance characteristics themselves.

The simplest method of representing the guide vane curves is by linear approximation. For any pair of adjacent data points the guide vane relationship is approximated to the straight line joining the two points. The accuracy of the representation is dependent on the number of data points selected and the smoothness of the curves. Turbine performance characteristics are smooth and slow varying whereas pump-turbine performance characteristics show much more marked variations in slope. The latter will require a relatively greater number of data points in order to achieve a satisfactory correlation. A concentration of data points is needed in the areas where the slope of the curve varies rapidly if the true shape of the curve is to be depicted. A major advantage of this representation is that a fixed interval between the data points is not necessary. The data points, therefore, can be selected to suit the shape of the guide vane curve. A further advantage is also gained as the re-entrants do not form a special case. Since only two points are to be considered for each section of the curve the re-entrant merely manifests itself as a change in sign of the slope of the straight line. Linear approximation, therefore, can be used for both turbines and pump-turbines without the need to distinquish between them.

The most appropriate method of representing the guide vane curves, and the simplest, is by linear approximation. This method is independent of the shape of the performance characteristics and allows the data points to be selected by the user to suit their needs. Linear approximation, therefore, was selected as a basis for the guide vane represenation throughout the research.

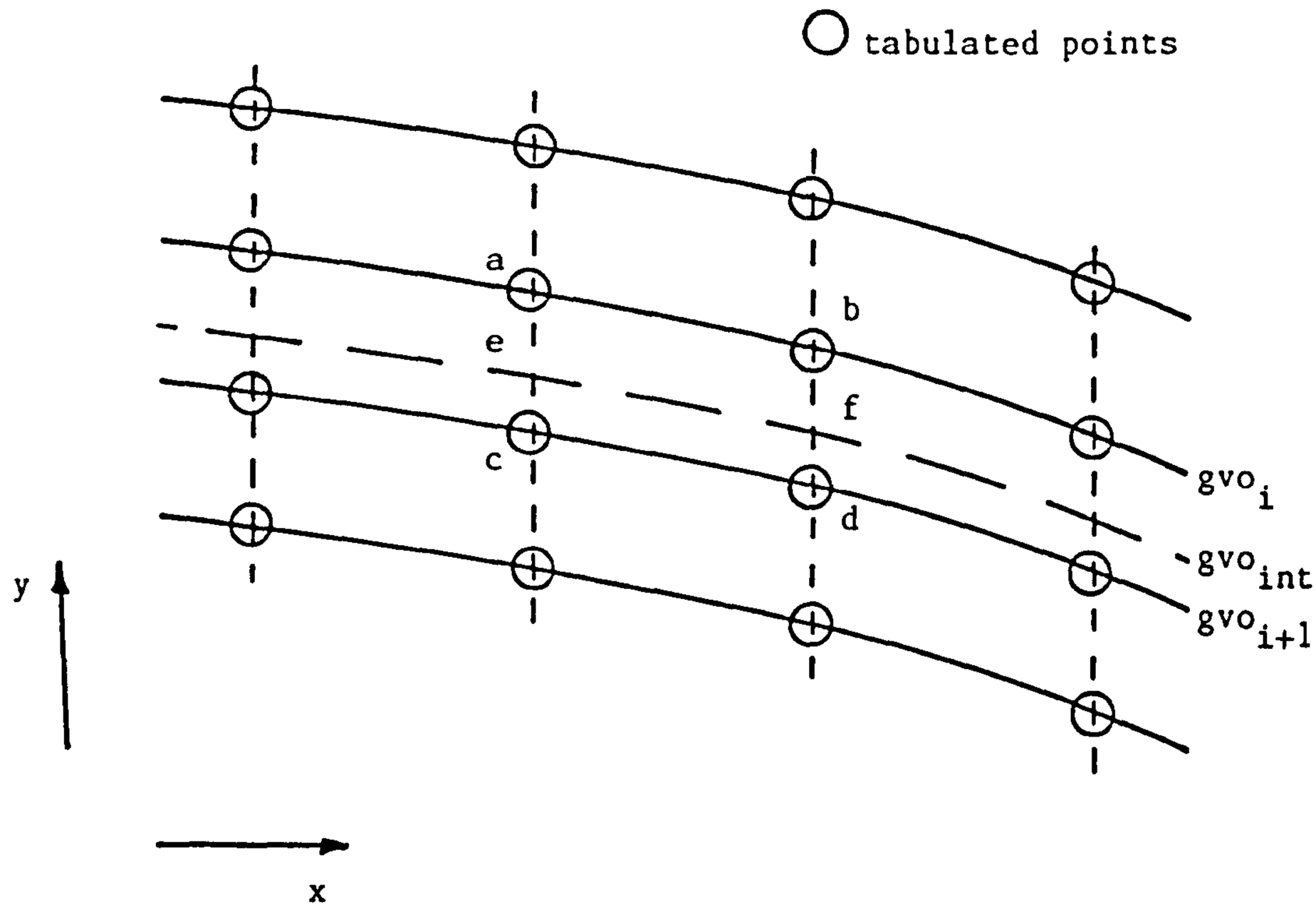

Figure 5.3 : Mesh generation with mesh lines parallel to y axis and the interpolation grid.

5.3 COMPLETE UNIT PARAMETER PERFOMANCE CHARACTERISTICS

5.3.1 Introduction

The individual guide vane curves are represented by a series of linear approximations between the adjacent tabulated points, see Section 5.2.6. In hydraulic transient simulations it is necessary to define both the tabulated and intermediate guide vane curves. For example, during a load rejection the turbine governor is designed to close the guide vanes at a predetermined rate. In terms of a computer simulation the guide vanes are assigned a specific opening for each time step of the calculation procedure. Invariably these openings do not correspond to one of the tabulated openings and the interpolation of the intermediate curves is required.

The method of representing the individual guide vane curves allows the tabulated data points to be selected by the user, providing a sufficient number of points are used to give a good approximation to the manufacturer's curve. Selecting the data points such that a mesh is formed enables the intermediate guide vane curves to be interpolated whilst ordering the data points into a convenient form for storage in a computer.

5.3.2 Curvilinear Mesh

One method of obtaining the intermediate guide vane curves was demonstrated by Chaudhry [35]. The turbine performance characteristics were divided into a mesh, using mesh lines perpendicular to the abscissa as shown in Figure 5.3 . Linear interpolation along the mesh lengths gave the points through which the intermediate guide vane curve would pass and a linear approximation between adjacent points was used to define the curve. The tabulated data points were selected at the intersection of

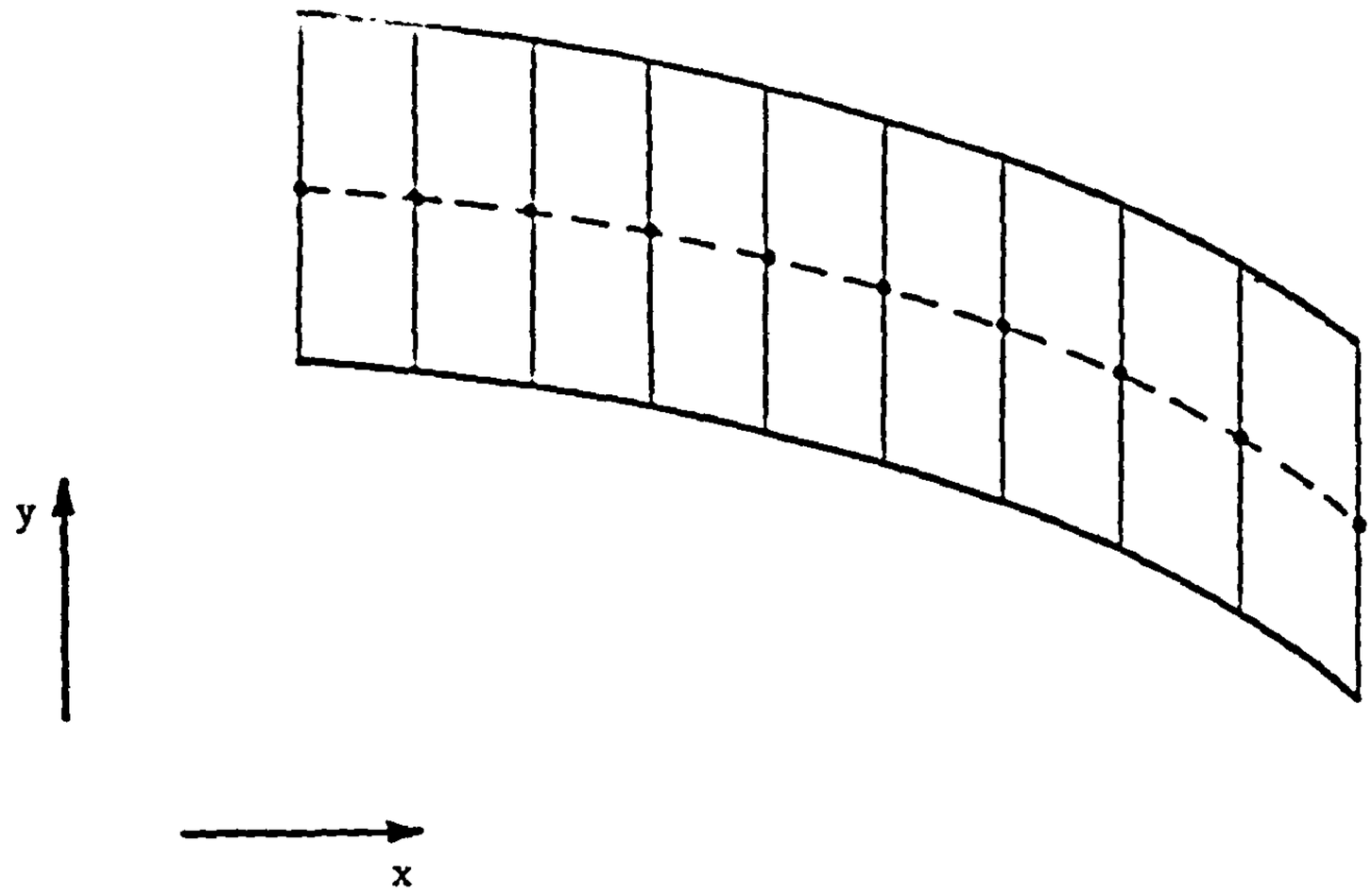

Satisfactory interpolation

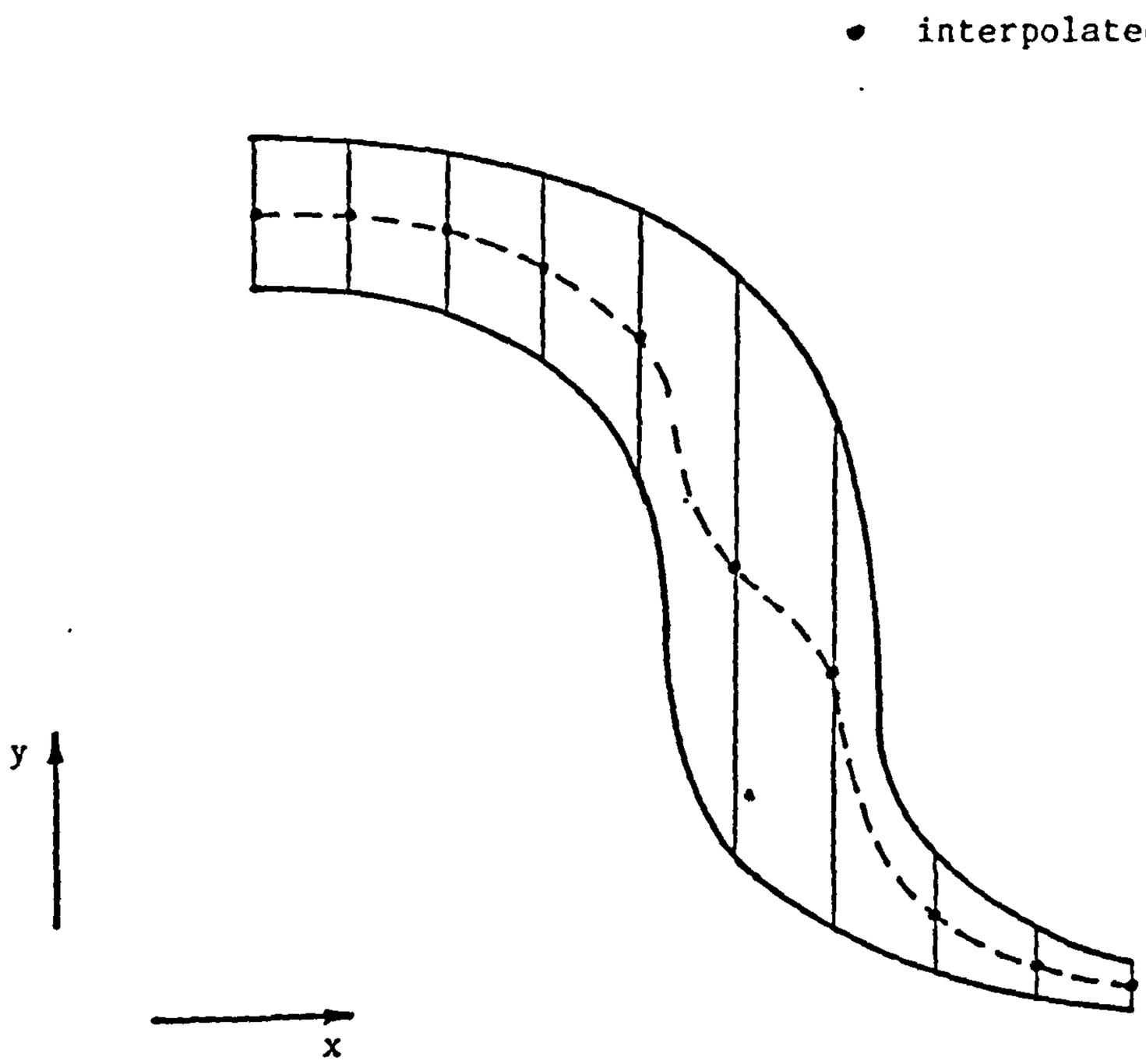

Unsatisfactory interpolation

Figure 5.4 : Linear interpolation of an intermediate guide vane curve with mesh lines parallel to the y axis

each mesh line and guide vane curve.

Consider the mesh given by a,b,c and d in Figure 5.3 . The intermediate guide vane curve is defined as the straight line which passes through points e and f, these being located by linear interpolation along the mesh lengths a-c and b-d, respectively. Linear interpolation gives :-

$$\frac{y_a - y_e}{y_a - y_c} = \frac{gvo_{i+1} - gvo_{int}}{gvo_{i+1} - gvo_i} \qquad \ldots\ldots\ldots\ldots \qquad (5.3.1)$$

therefore,

$$y_e = y_a - [y_a - y_c]\frac{[gvo_{i+1} - gvo_{int}]}{[\ gvo_{i+1} - gvo_i\ ]} \qquad \ldots\ldots\ldots \qquad (5.3.2)$$

along mesh length a-c. Similarly, along mesh length b-d the y co-ordinate of f is given by :-

$$y_f = y_b - [y_b - y_d]\frac{[gvo_{i+1} - gvo_{int}]}{[\ gvo_{i+1} - gvo_i\ ]} \qquad \ldots\ldots\ldots \qquad (5.3.3)$$

As the mesh lines are perpendicular to the x-axis the x co-ordinates of points e and f are :-

$$x_e = x_a = x_c \qquad \ldots\ldots\ldots\ldots \qquad (5.3.4)$$

and

$$x_f = x_b = x_d \qquad \ldots\ldots\ldots\ldots \qquad (5.3.5)$$

respectively. The intermediate guide vane curve, gvo_{int}, within the mesh is given by the straight line joining these two points, that is :-

$$y = m\,x + c \qquad \ldots\ldots\ldots\ldots \qquad (5.3.6)$$

where

$$m = \frac{y_e - y_f}{x_e - x_f}$$

and

$$c = y_e - m\,x_e = y_f - m\,x_f$$

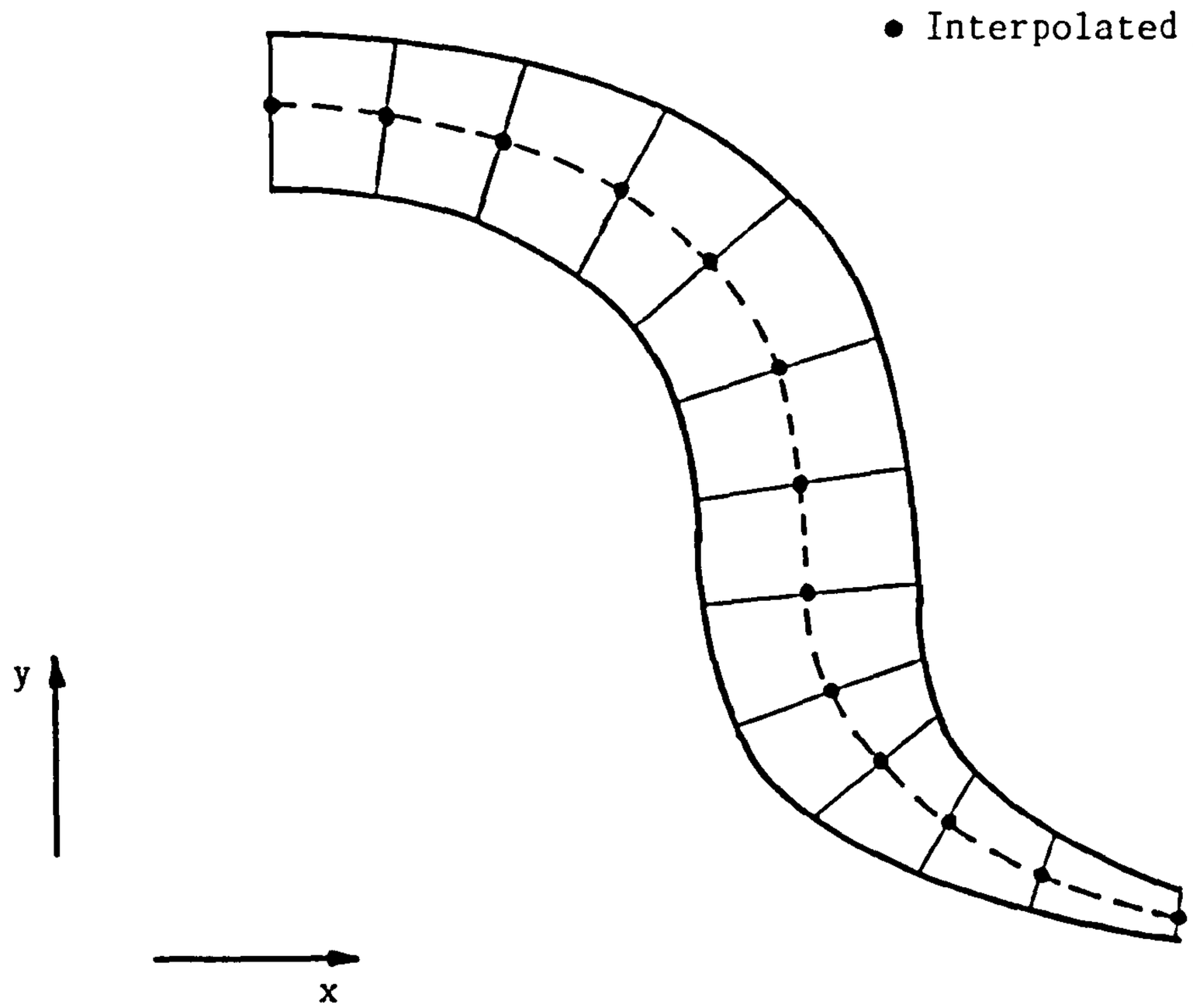

Figure 5.5 : Interpolation of intermediate guide vane curve based on an orthogonal curvilinear mesh.

This method of mesh generation and interpolation of the intermediate guide vane curves is acceptable for turbine performance characteristics which are predominately parallel to the x-axis, the unit speed axis. Its use with Francis and Kaplan turbines, therefore, presents no problems. However, pump-turbine performance characteristics do not adhere to this generalised rule. Their performance characteristics are more complex and contain regions where the guide vane curves become predominately perpendicular to the x-axis. This is demonstrated in the transition region between the turbining and reverse-pumping quadrants as shown schematically in Figure 5.4. Linear interpolations of the intermediate guide vane curves based upon mesh lines perpendicular to the x-axis produce unsatisfactory results, Figure 5.4. Boldy [36] overcame this problem by proposing that the mesh lines should intersect the guide vane curves orthogonally. An approximate curvilinear mesh is formed which gives a much more accurate representation of the intermediate guide vane curves, Figure 5.5 .

The simplest method of generating the approximate curvilinear mesh is by hand. With the turbine performance characteristics in a graphical form, as presented by the manufacturers, a series of mesh lines is superimposed manually. The mesh lines cut the guide vane curves at right angles to form an approximate curvilinear mesh. The points of intersection of the mesh lines and guide vane curves are then digitised and stored in a computer data file for use in the hydraulic transient studies. This method of generating the mesh is often laborious, particularly for complex performance characteristics, and is open to human errors. In order to alleviate these problems an automatic mesh generation algorithm has been developed as part of the research undertaken for this thesis. The algorithm is described in detail in Section 6.2 together with an example of its use with performance characteristics.

$n_{11}(1,1)$, $n_{11}(1,2)$, ... , $n_{11}(1,j)$, ... , $n_{11}(1,J)$

$Q_{11}(1,1)$, $Q_{11}(1,2)$, ... , $Q_{11}(1,j)$, ... , $Q_{11}(1,J)$

$n_{11}(2,1)$, $n_{11}(2,2)$, ... , $n_{11}(2,j)$, ... , $n_{11}(2,J)$

$Q_{11}(2,1)$, $Q_{11}(2,2)$, ... , $Q_{11}(2,j)$, ... , $Q_{11}(2,J)$

$n_{11}(i,1)$, $n_{11}(i,2)$, ... , $n_{11}(i,j)$, ... , $n_{11}(i,J)$

$Q_{11}(i,1)$, $Q_{11}(i,2)$, ... , $Q_{11}(i,j)$, ... , $Q_{11}(i,J)$

$n_{11}(I,1)$, $n_{11}(I,2)$, ... , $n_{11}(I,j)$, ... , $n_{11}(I,J)$

$Q_{11}(I,1)$, $Q_{11}(I,2)$, ... , $Q_{11}(I,j)$, ... , $Q_{11}(I,J)$

$n'_{11}(1,1)$, $n'_{11}(1,2)$, ... , $n'_{11}(1,j)$, ... , $n'_{11}(1,J)$

$M_{11}(1,1)$, $M_{11}(1,2)$, ... , $M_{11}(1,j)$, ... , $M_{11}(1,J)$

$n'_{11}(2,1)$, $n'_{11}(2,2)$, ... , $n'_{11}(2,j)$, ... , $n'_{11}(2,J)$

$M_{11}(2,1)$, $M_{11}(2,2)$, ... , $M_{11}(2,j)$, ... , $M_{11}(2,J)$

$n'_{11}(i,1)$, $n'_{11}(i,2)$, ... , $n'_{11}(i,j)$, ... , $n'_{11}(i,J)$

$M_{11}(i,1)$, $M_{11}(i,2)$, ... , $M_{11}(i,j)$, ... , $M_{11}(i,J)$

$n'_{11}(I,1)$, $n'_{11}(I,2)$, ... , $n'_{11}(I,j)$, ... , $n'_{11}(I,J)$

$M_{11}(I,1)$, $M_{11}(I,2)$, ... , $M_{11}(I,j)$, ... , $M_{11}(I,J)$

Figure 5.6 : Data matrix for turbine performance characteristics.

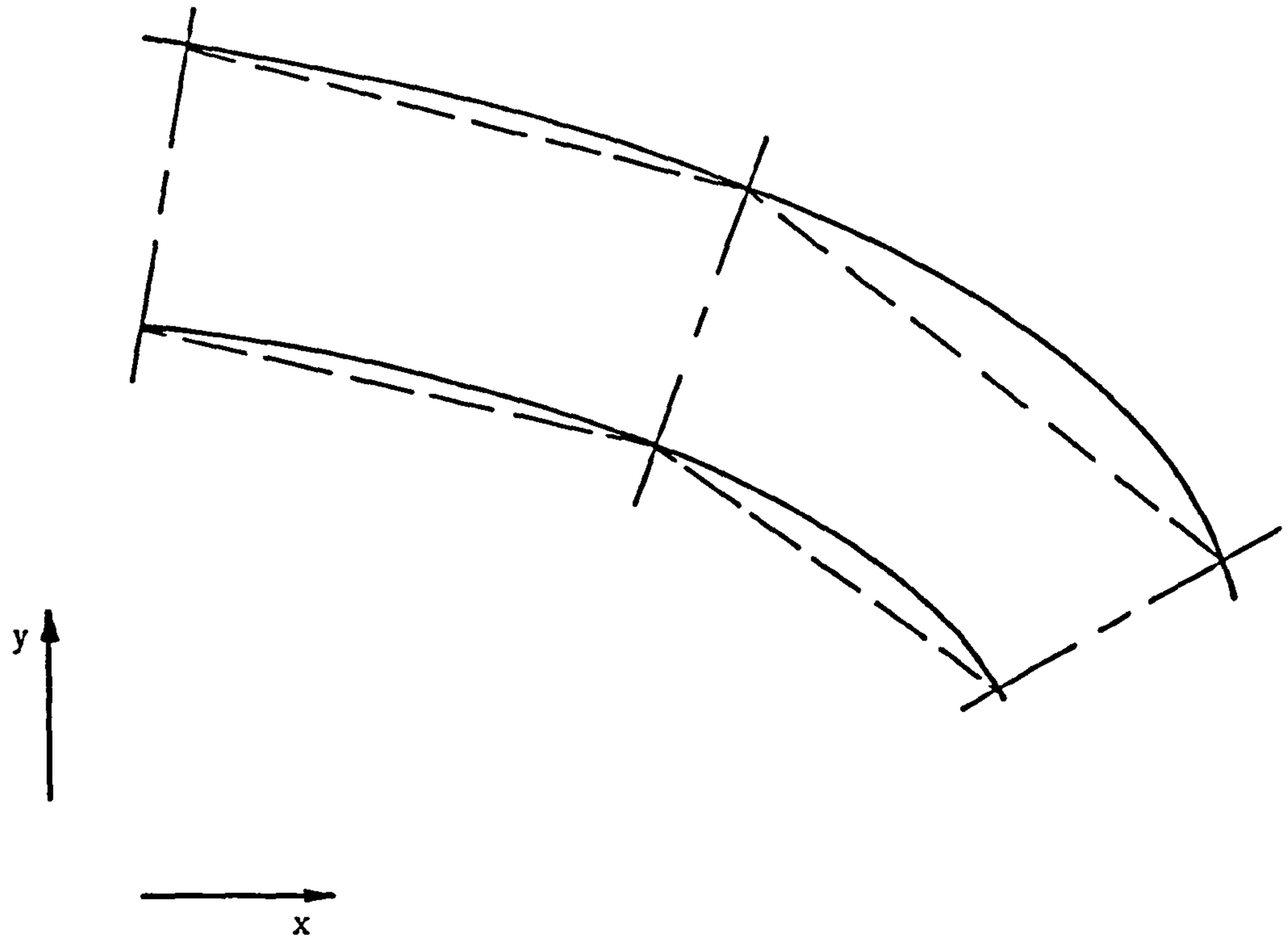

Unacceptable correlation with manufacturers curves.

Acceptable correlation with manufacturers curves.

Figure 5.7 : Selection of data points for correlation with manufacturers curves.

The digitised turbine performance characteristics are stored in a two dimensional array. Given a set of J guide vane curves superimposed with I mesh lines the points of intersection are given by :-

$$[n_{11}(i,j),Q_{11}(i,j)]$$

at the intersection of the i^{th} mesh line with the j^{th} guide vane curve on the unit speed versus unit discharge plane. Similarly, the co-ordinates on the unit speed versus unit torque plane are given by :-

$$[n'_{11}(i,j),M_{11}(i,j)]$$

where

$$1 \leq i \leq I$$

and

$$1 \leq j \leq J$$

The complete turbine performance characteristics are stored in array as shown in Figure 5.6 . It must be noted that the unit speed values for the unit discharge and unit torque curves do not correspond, as the mesh lines are superimposed independently for each set of curves, and are denoted as $n_{11}(i,j)$ and $n'_{11}(i,j)$ respectively.

The number of mesh lines selected to create the approximate curvilinear mesh is dependent on the shape of the guide vane curves. If the curves display only slight variations in slope, as for a Francis turbine , relatively few mesh lines are required. However, a sufficient number must be selected to ensure an acceptable correlation with the manufacturers curves, Figure 5.7 . The more complex the performance characteristics, as for a pump-turbine, the greater the number of mesh lines that are required to obtain an acceptable correlation, Figure 5.5 . A close correlation to the manufacturers curves makes possible an accurate linear interpolation of the intermediate guide vane curves.

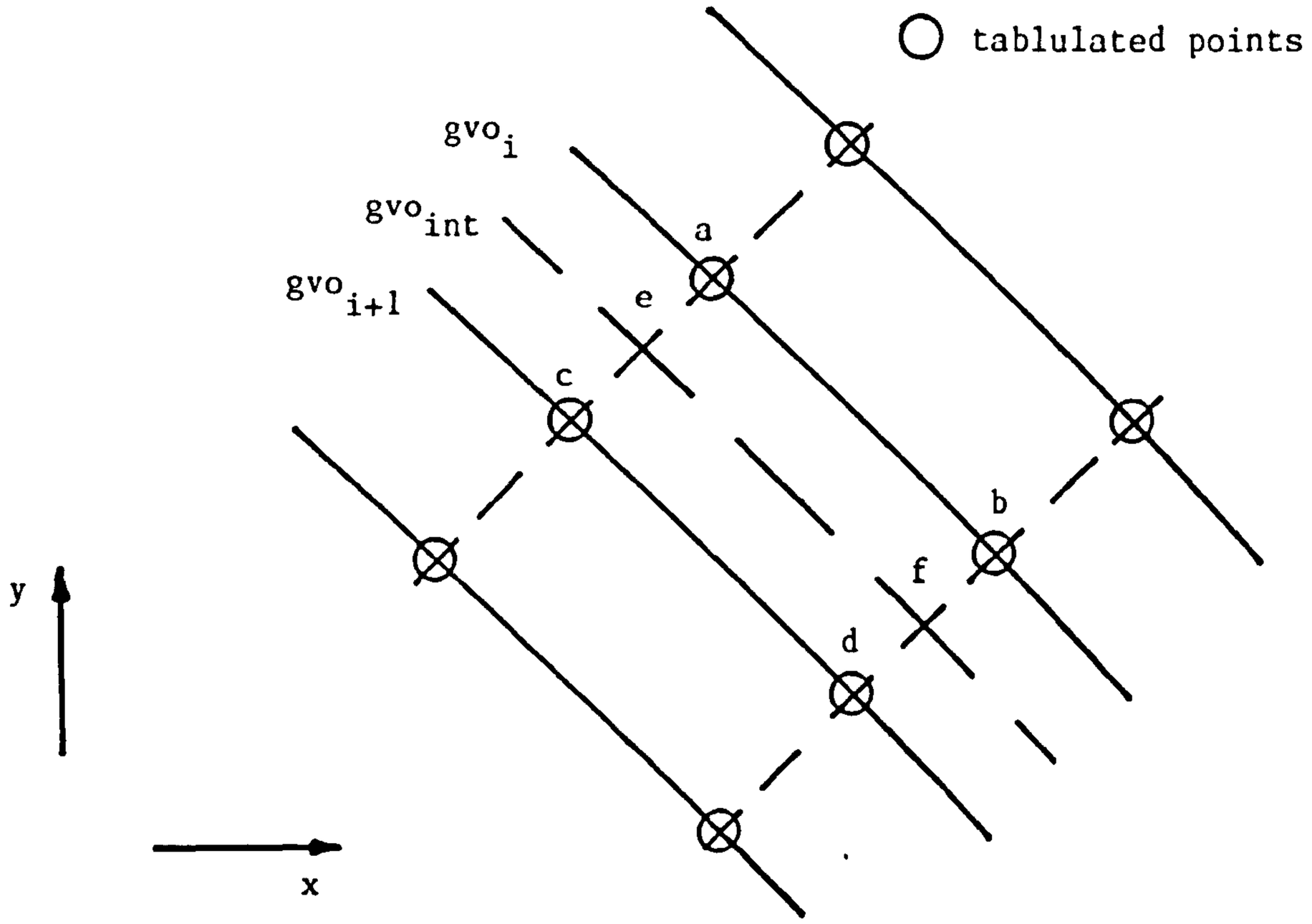

Figure 5.8 : Interpolation of intermediate guide vane curves within curvilinear mesh.

5.3.3 Interpolation of Intermediate Guide Vane Curves

An approximate curvilinear mesh superimposed on the turbine performance characteristics allows the intermediate guide vane curves to be interpolated. Linear interpolation along the mesh lengths between adjacent, tabulated, guide vane curves is used. Consider the mesh given by a,b,c and d in Figure 5.8 . Points a and b lie on the i^{th} guide vane curve and points c and d lie on the $(i+1)^{th}$ guide vane curve. The intermediate guide vane curve, gvo_{int}, passes through points e and f which are found by linear interpolation along the mesh lengths a-c and b-d respectively. The co-ordinates of these points are given by :-

$$\left.\begin{aligned} x_e &= x_a - [x_a - x_c]\frac{[gvo_i - gvo_{int}]}{[gvo_i - gvo_{i+1}]} \quad \cdots\cdots\cdots \\ y_e &= y_a - [y_a - y_c]\frac{[gvo_i - gvo_{int}]}{[gvo_i - gvo_{i+1}]} \quad \cdots\cdots\cdots \end{aligned}\right\} \quad (5.3.7)$$

and

$$\left.\begin{aligned} x_f &= x_b - [x_b - x_d]\frac{[gvo_i - gvo_{int}]}{[gvo_i - gvo_{int}]} \quad \cdots\cdots\cdots \\ y_f &= y_b - [y_b - y_d]\frac{[gvo_i - gvo_{int}]}{[gvo_i - gvo_{i+1}]} \quad \cdots\cdots\cdots \end{aligned}\right\} \quad (5.3.8)$$

The intermediate guide vane curve, gvo_{int}, within the mesh is given by the straight line joining points e and f, that is :-

$$y = m\,x + c \quad \cdots\cdots\cdots\cdots\cdots \quad (5.3.9)$$

where

$$m = \frac{y_e - y_f}{x_e - x_f}$$

and

$$c = y_e - m\,x_e = y_f - m\,x_f$$

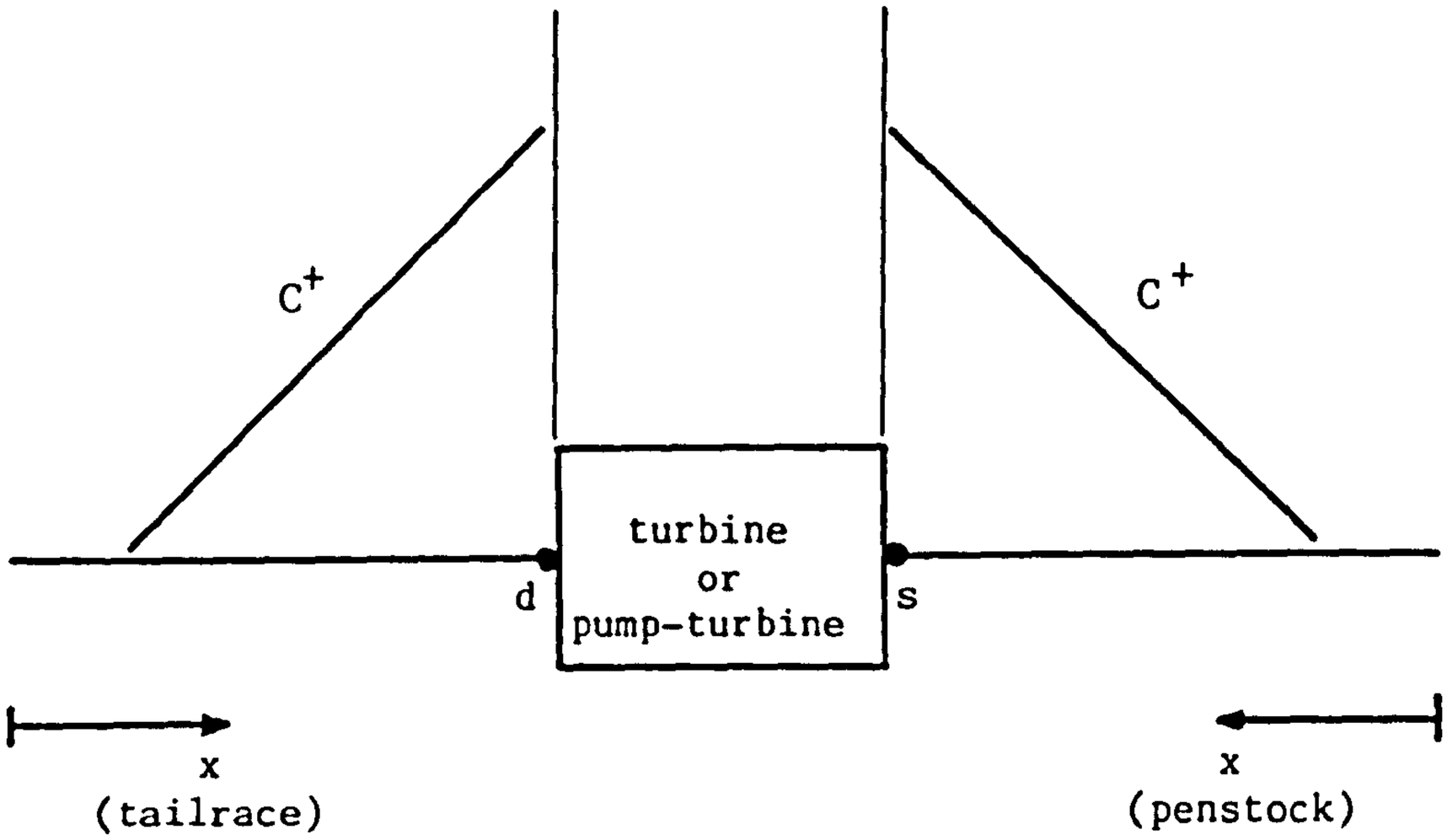

Figure 5.9 : Turbine or pump-turbine boundary condition

The advantages of linearly interpolating the intermediate guide vane curves are, firstly, its ease of application and secondly, the resulting linear equation can be utilised in the turbine solution algorithm. The interpolation algorithm is simple and involves only a few calculation steps. This helps to restrict overall computer program processor times for the complete hydraulic transient analysis as the procedure is performed at each calculation time step. The interpolation routine results in a pair of linear equations, one for the unit speed versus unit discharge relationship and one for the unit speed versus unit torque relationship. These have been fully utilised in the turbine solution algorithm such that the problem is reduced to a single variable, the net head, which is solved using a standard Newton-Raphson technique.

5.3.4 Turbine Boundary Solution Algorithm For Unit Parameter Representation

During the period of research an algorithm for the solution of the turbine boundary, using the unit parameter representation of the turbine performance characteristics, was developed. This was first reported in 1982 [49] and its use in hydraulic transient studies demonstrated.

The solution of the turbine boundary requires the simultaneous solution of the characteristic equations, one either side of the turbine, together with the turbine performance characteristics, Figure 5.9 . This is a multi-variable problem involving the turbine rotational speed, discharge,outof balance torque, net head, spiral entry head and draft tube exit head. The solution of such a problem generally requires a complex iterative procedure. However, by reducing the number of variables involved to one a standard Newton-Raphson technique can be used. Solution of this variable then leads to the solution of the other variables involved in the problem.

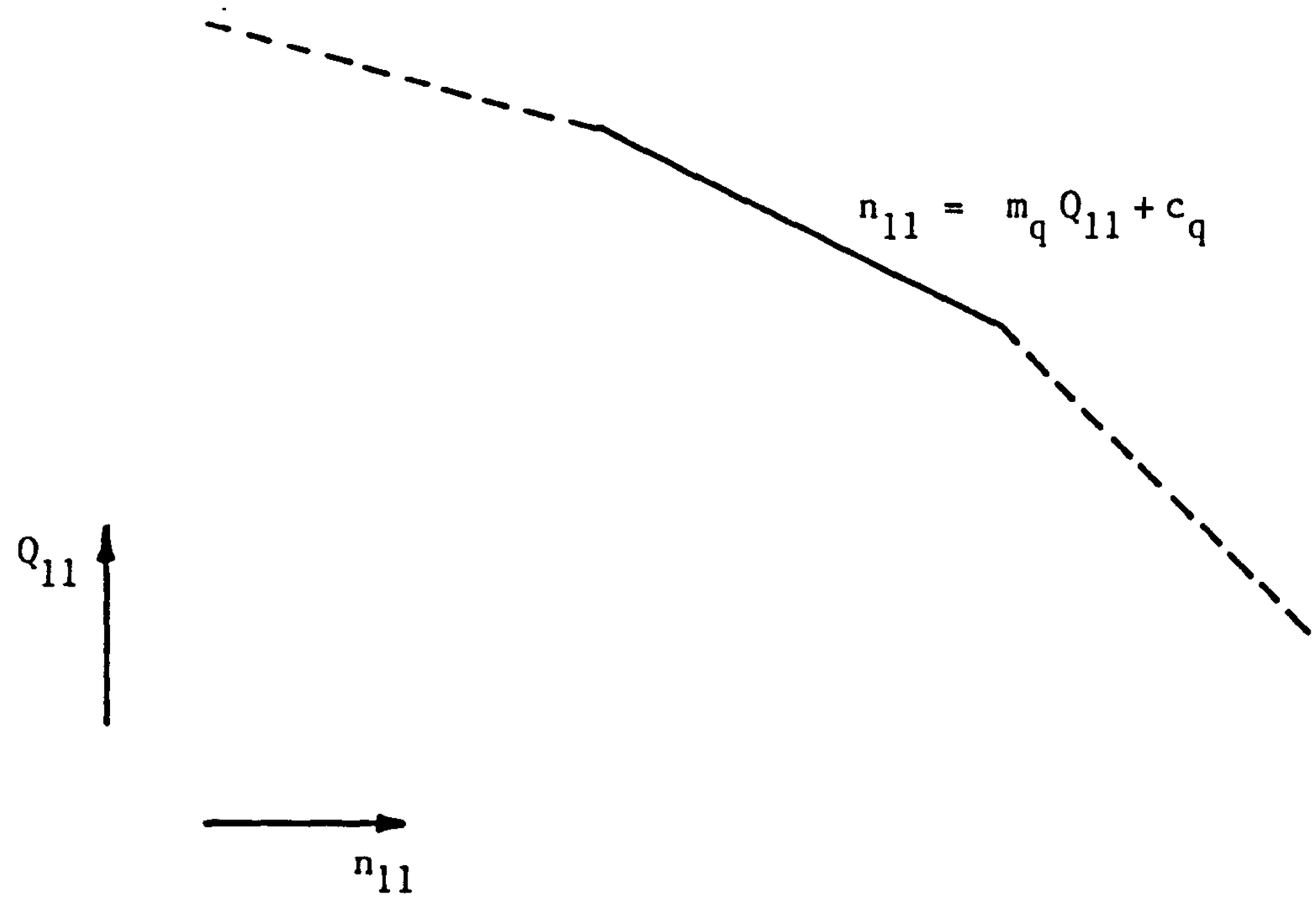

Figure 5.10 : Linear equation of guide vane section on the unit speed versus unit discharge plane.

On the unit speed versus unit discharge plane any section of a guide vane curve, tabulated or interpolated, is approximated by a straight line, Figure 5.10. The guide vane relationship is represented by the linear equation :-

$$n_{11} = m_q Q_{11} + c_q \qquad \text{..... (5.3.10)}$$

where

n_{11} = unit speed

Q_{11} = unit discharge

m_q = gradient

c_q = constant

therefore

$$\frac{n D}{\sqrt{H}} = \frac{m_q Q}{D^2 \sqrt{H}} + c_q \qquad \text{..... (5.3.11)}$$

where

n = rotational speed

Q = discharge

H = net head

D = runner diameter

The net head across the turbine at time $t+\Delta t$ is given by :-

$$H^{t+\Delta t} = H_s^{t+\Delta t} + \frac{[v_s^{t+\Delta t}]^2}{2g} - H_d^{t+\Delta t} - \frac{[v_d^{t+\Delta t}]^2}{2g} \qquad \text{.... (5.3.12)}$$

where

H_s = spiral inlet head

v_s = velocity at spiral inlet

H_d = draft tube exit head

v_d = velocity at draft tube exit

Equation 5.3.12 can be re-writen in terms of the velocity head across the turbine, ΔVH, to give :-

$$H^{t+\Delta t} = H_s^{t+\Delta t} - H_d^{t+\Delta t} + \Delta VH^{t+\Delta t} \qquad \text{..... (5.3.13)}$$

The velocity head across the turbine is a second order term which only varies slightly from one time step to the next. The net head across the turbine, therefore, can be approximated to :-

$$H^{t+\Delta t} = H_s^{t+\Delta t} - H_d^{t+\Delta t} + \Delta VH^t \quad \ldots\ldots\ldots\ldots\ldots \quad (5.3.14)$$

where ΔVH^t is the known velocity head across the turbine at time t.

The characteristic equations either side of the turbine boundary are in the form :-

$$H_s^{t+\Delta t} = a_1 Q_s^{t+\Delta t} + a_2 \quad \ldots\ldots\ldots\ldots\ldots \quad (5.3.15)$$

and

$$H_d^{t+\Delta t} = a_3 Q_d^{t+\Delta t} + a_4 \quad \ldots\ldots\ldots\ldots\ldots \quad (5.3.16)$$

where

Q_s = discharge at spiral inlet

Q_d = discharge at draft tube outlet

From continuity it is known that these two discharges are equal, that is :-

$$Q_s^{t+\Delta t} = -Q_d^{t+\Delta t} = Q^{t+\Delta t} \text{ (say)} \quad \ldots\ldots\ldots\ldots\ldots \quad (5.3.17)$$

where

Q = discharge through the turbine, positive in the turbining mode

Combining equations 5.3.14, 5.3.15, 5.3.16 and 5.3.17 gives a linear relationship between the net head across the turbine and the discharge through the turbine of the form :-

$$H^{t+\Delta t} = a_5 Q^{t+\Delta t} + a_6 \quad \ldots\ldots\ldots\ldots\ldots \quad (5.3.18)$$

with the known constants, a_5 and a_6, given by

$$a_5 = a_1 + a_3$$

$$a_6 = a_2 - a_4 + \Delta VH^t$$

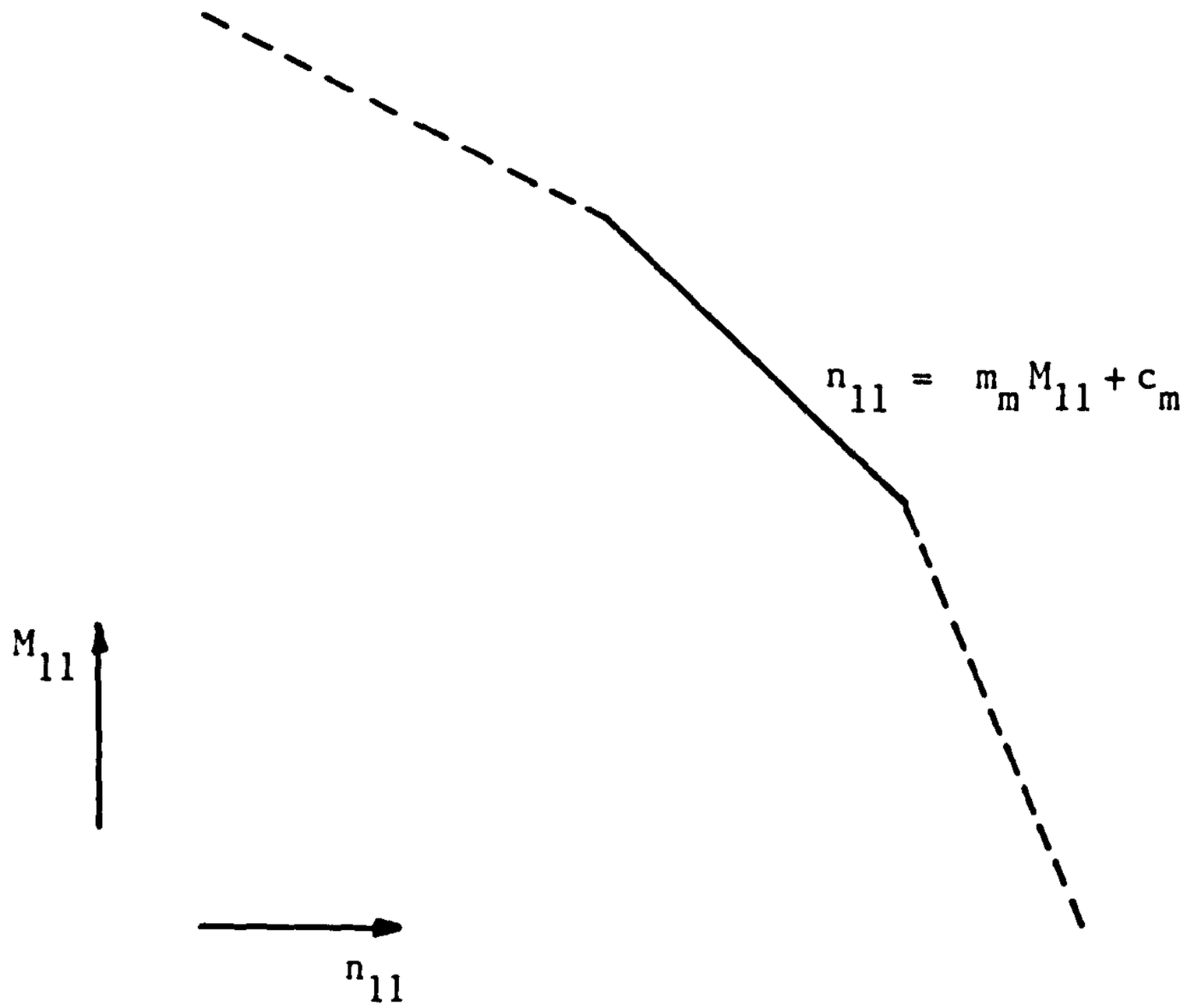

Figure 5.11 : Linear equation of guide vane section on the unit speed versus unit torque plane.

Eliminating the turbine discharge, Q, from equations 5.3.11 and 5.3.18 and re-arranging gives a relationship between the turbine speed, n, and net head, H, of the form :-

$$n^{t+\Delta t} = a_7 H^{t+\Delta t} + a_8 \sqrt{H}^{t+\Delta t} + a_9 \quad \ldots\ldots\ldots\ldots\ldots \quad (5.3.19)$$

where

$$a_7 = \frac{m_q}{D^3 a_5}$$

$$a_8 = \frac{c_q}{D}$$

$$a_9 = -\frac{m_q a_6}{D^3 a_5}$$

Adopting a similar approach for the unit speed versus unit torque curves a second relationship between the turbine speed and net head is established. On the unit speed versus unit torque plane any section of a guide vane curve is approximated by a straight line, Figure 5.11. This can be writen as :-

$$n_{11} = m_m M_{11} + c_m \quad \ldots\ldots\ldots\ldots\ldots \quad (5.3.20)$$

where

n_{11} = unit speed

M_{11} = unit torque

m_m = gradient

c_m = constant

therefore

$$\frac{n D}{\sqrt{H}} = \frac{m_m M}{D^3 H} + c_m \quad \ldots\ldots\ldots\ldots\ldots \quad (5.3.21)$$

where

M = out of balance torque

Since there is no external torque acting on the turbine following a load rejection the decelerating torque is the turbine torque, hence :-

$$M = -I\frac{d\omega}{dt} \qquad \ldots\ldots\ldots\ldots\ldots \quad (5.3.22)$$

where

I = polar moment of inertia of rotating parts

ω = angular velocity

By using an average value of the out of balance torque during the time step, equation 5.3.22 becomes :-

$$\frac{M^{t+\Delta t} + M^{t}}{2} = b_1[n^{t+\Delta t} - n^{t}] \qquad \ldots\ldots\ldots\ldots\ldots \quad (5.3.23)$$

where

$$b_1 = \frac{\pi GD^2}{120\, g\, \Delta t}$$

$$GD^2 = 4g\, I$$

Re-writing equation 5.3.23 gives :-

$$M^{t+\Delta t} = 2\, b_1\, n^{t+\Delta t} - 2\, b_1\, n^{t} - M^{t} \qquad \ldots\ldots\ldots\ldots\ldots \quad (5.3.24)$$

Applying equation 5.3.21 at time $t+\Delta t$ and substituting for $M^{t+\Delta t}$ from equation 5.3.24 gives :-

$$\frac{n^{t+\Delta t}\, D}{\surd H^{t+\Delta t}} = \frac{m_m\,[2b_1\, n^{t+\Delta t} - 2b_1\, n^{t} - M^{t}]}{D^3\, H^{t+\Delta t}} + c_m \qquad \ldots\ldots \quad (5.3.25)$$

which is re-arranged to give a function of the turbine speed and net head in the form :-

$$n^{t+\Delta t}[\surd H^{t+\Delta t} + b_2] + b_3\, H^{t+\Delta t} + b_4 = 0 \qquad \ldots\ldots \quad (5.3.26)$$

in which

$$b_2 = -\frac{2\, b_1\, m_m}{D^4}$$

$$b_3 = -\frac{c_m}{D}$$

$$b_4 = \frac{[2\,b_1\,n^t + M^t]\,m_m}{D^4}$$

Two equations, 5.3.19 and 5.3.26, have been derived which are functions of the turbine speed and net head at time $t+\Delta t$. By eliminating the turbine speed from these a function in a single variable, the net head, is established for the solution of the turbine boundary. This function is given by :-

$$[a_7 H^{t+\Delta t} + a_8 \sqrt{H}^{t+\Delta t} + a_9]\,[\sqrt{H}^{t+\Delta t} + b_2] + b_3 H^{t+\Delta t} + b_4 = 0 = f(H^{t+\Delta t}) \qquad (5.3.27)$$

A standard Newton-Raphson technique is used to solve for the net head, $H^{t+\Delta t}$, to within an acceptable tolerance. The remaining turbine parameters, speed, discharge and torque, are calculated by substituting the solution for the net head into equations 5.3.19, 5.3.18 and 5.3.24 respectively. The head and discharge at the spiral entry and draft tube outlet follow from equations 5.3.17, 5.3.15 and 5.3.16 .

The solution of equation 5.3.27 by a Newton-Raphson method relies on a good first estimate of the net head, H, for a rapid convergence to its solution. This first estimate is found by extrapolating values of the unit discharge from previous time intervals in order to get a good estimate of the discharge,at time $t+\Delta t$, and substitution into equation 5.3.18 leads to an estimate of the net head, at time $t+\Delta t$. Linear extrapolation of the discharge and unit discharge gives :-

$$Q_e^{t+\Delta t} = 2\,Q^t - Q^{t-\Delta t} \qquad \text{.....} \qquad (5.3.28)$$

and

$$Q_{11e}^{t+\Delta t} = 2\,Q_{11}^t - Q_{11}^{t-\Delta t} \qquad \text{.....} \qquad (5.3.29)$$

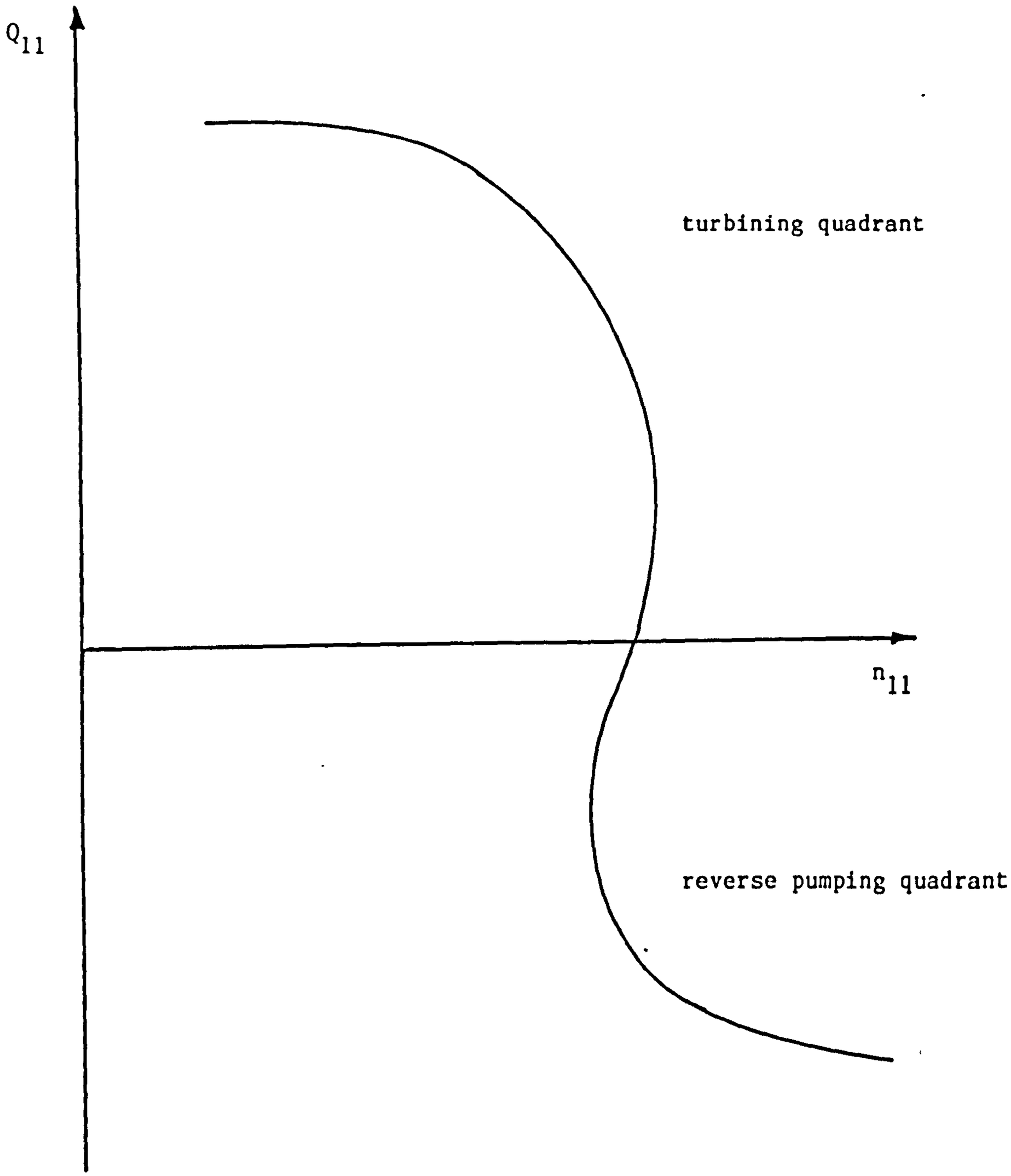

Figure 5.12 : Re-entrant guide vane curve

From the definition of unit discharge :-

$$Q_{11e}^{t+\Delta t} = \frac{Q^{t+\Delta t}}{D^2 \sqrt{H^{t+\Delta t}}} \qquad \text{.....} \qquad (5.3.30)$$

Replacing the net head term, using equation 5.3.18, and rearranging gives a function in terms of the discharge, Q, where :-

$$Q^{t+\Delta t^2} - Q_{11e}^{t+\Delta t} D^4 [a_5 Q^{t+\Delta t} + a_6] = 0 = f(Q^{t+\Delta t}) \qquad (5.3.31)$$

This function of the discharge, $f(Q^{t+\Delta t})$,is solved using a Newton-Raphson technique with the initial estimate of the discharge being $Q_e^{t+\Delta t}$ from equation 5.3.28. The solution of the function leads to a refined estimate of the discharge, $Q_e'^{t+\Delta t}$, and substitution into equation 5.3.18 gives an estimate of the net head, $H_e^{t+\Delta t}$, where :-

$$H_e^{t+\Delta t} = a_5 Q_e'^{t+\Delta t} + a_6 \qquad \text{.....} \qquad (5.3.32)$$

It was found from experience that obtaining the initial estimate of the net head in this manner created a rapid convergence towards the solution of the function given in equation 5.3.27 when compared to using an estimate found directly from equation 5.3.18.

5.3.5 Re-entrant Guide Vane Curves

An important feature of pump-turbine performance characteristics is the possible re-entrant, or 'S' shaped, guide vane curve. This may be found as the guide vane curves pass through the turbining quadrant and into the reverse pumping quadrant. A schematic view of this region is shown in Figure 5.12 on the unit discharge versus unit speed plane. The degree to which the re-entrants occur varies from one pump-turbine to another and not all pump-turbines display this feature. In general, however, where the re-entrant does occur in the performance characteristics it is much more marked in a pump-turbine of a low specific speed than one of a high specific speed.

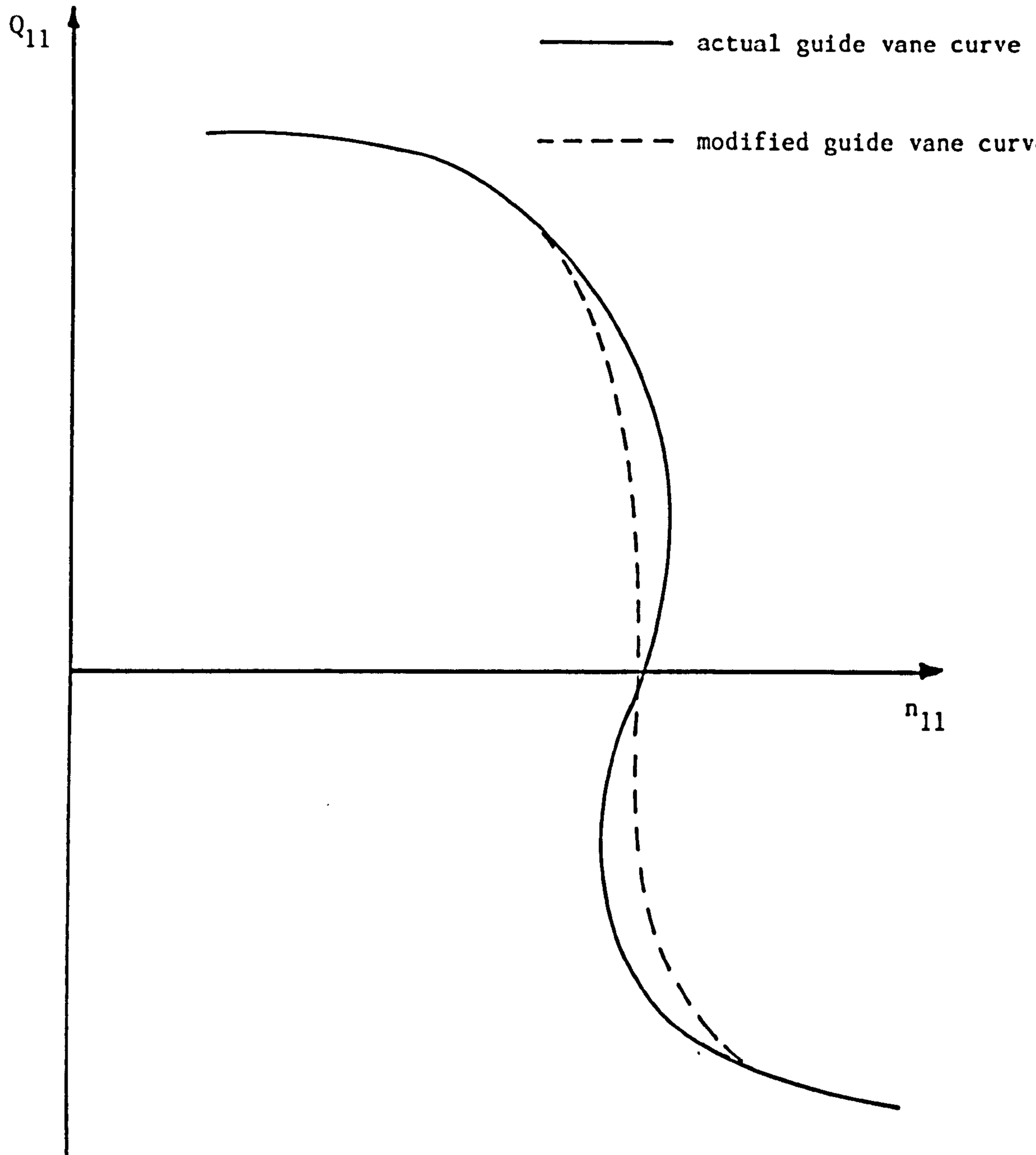

Figure 5.13 : Modification of guide vane curve, resulting in the guide vane curve being single valued.

The re-entrant of a guide vane curve is due to a recirculation of the flow at the runner crown which creates a vortex. This flow reversal is mainly due to centrifugal forces acting on the fluid ring at the runner crown. It is also aided by a poor angle of attack of the fluid as it enters the runner. The vortexing at the runner entrance acts as a partial blockage to the flow through the runner and this causes a reduction in the flow.

During the research described in this thesis an investigation of the re-entrant region of pump-turbine performance characteristics was undertaken and the interim results were published in 1982 [49]. The paper considered two hydraulic transient simulations of a typical pumped storage scheme. Each simulation modelled an identical pump-turbine trip, whilst operating in the turbining mode, with the only variation in the data being that for the performance characteristics. The initial simulation had the re-entrant regions of the guide vane curves replaced by a mean curve. This rendered the curves single valued, Figure 5.13, for a given unit speed value. The second simulation included the performance characteristics in their original form, as provided by the manufacturers. The results showed that for a given installation the re-entrant guide vane curves should be included in the performance characteristics and that any modification to the guide vane curves in this region had a marked effect on the simulation results.

The turbine or pump-turbine solution algorithm presented in Section 5.3.4 relies on the location of the guide vane sections within the vicinity of the operating point. Chaudhry [35] based the location of the appropriate guide vane section on an estimated unit speed value. His method of location, however, is based on the premise that the guide vane curves are single valued throughout. Pump-turbine performance characteristics

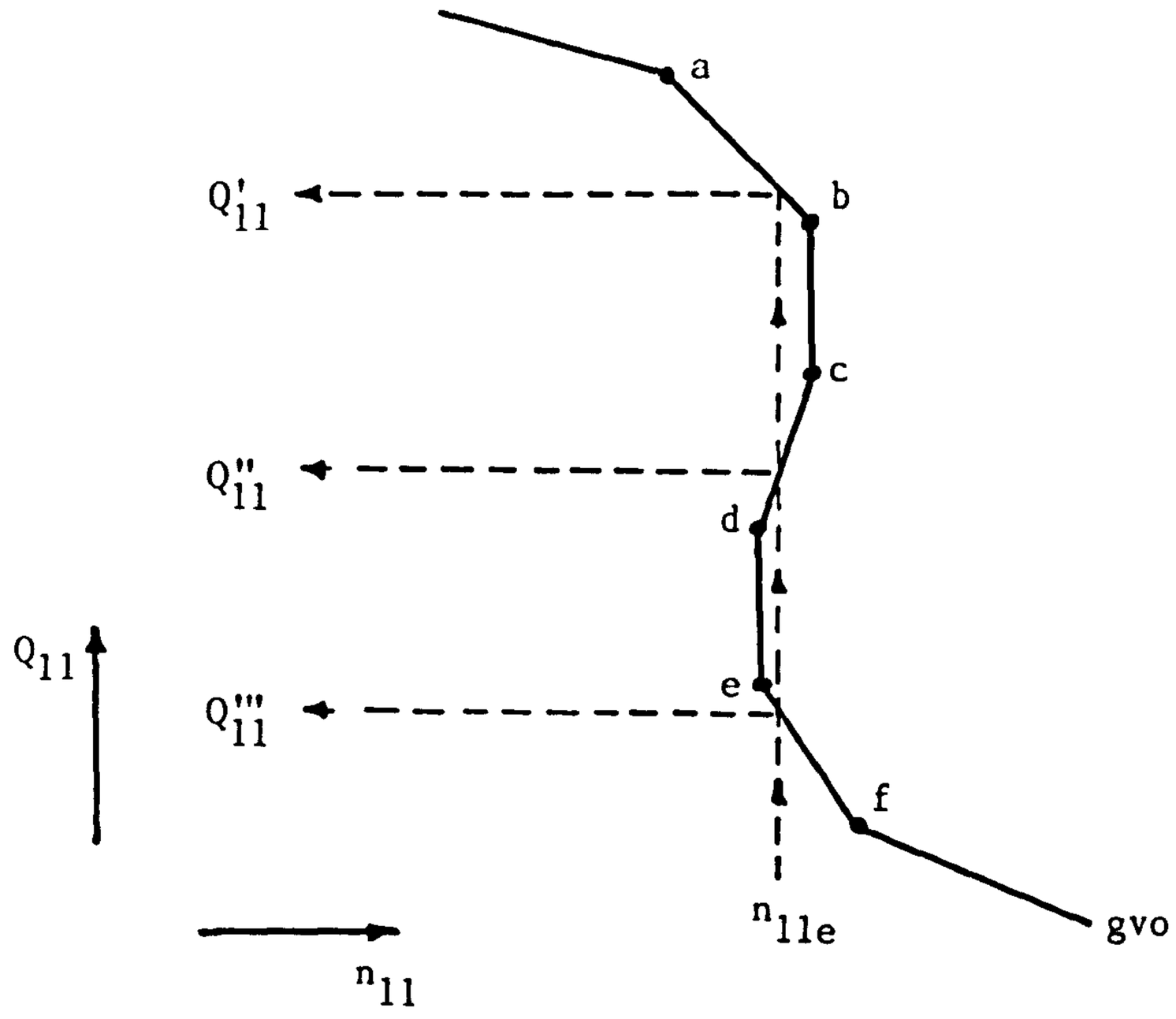

Figure 5.14 : Corresponding unit discharge values for a given unit speed value.

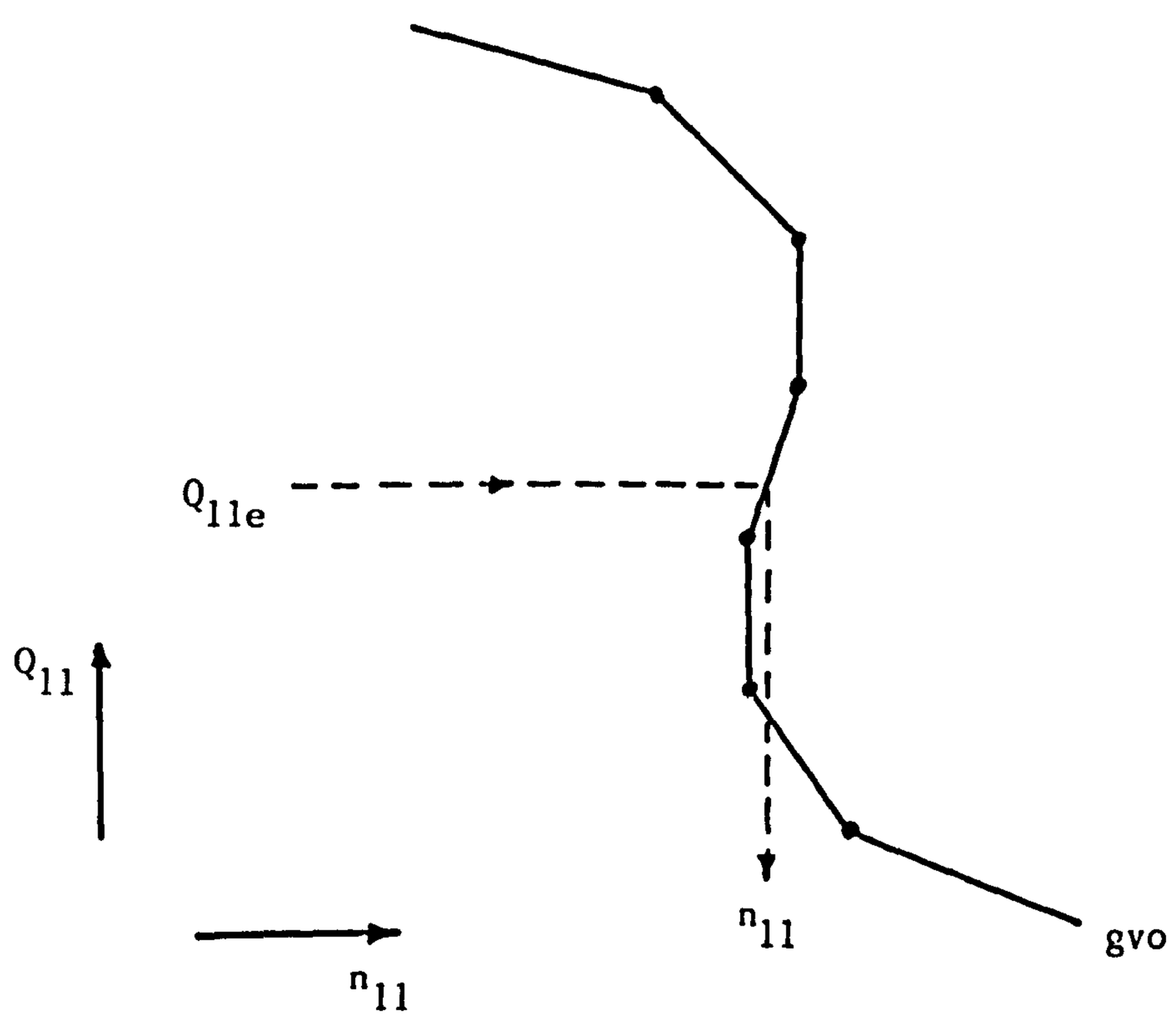

Figure 5.15 : Corresponding unit speed value for a given unit discharge value.

with re-entrant guide vane curves are multi-valued and a search procedure based purely on an estimated unit speed value will not suffice.

Figure 5.14 shows a re-entrant guide vane curve, $gvo^{t+\Delta t}$, on the unit speed versus unit discharge plane. For a given estimate of the unit speed, $n_{11e}^{t+\Delta t}$, at time $t+\Delta t$ there are three possible solutions for the unit discharge, $Q_{11}^{t+\Delta t}$. The guide vane sections along which the solutions lie are a-b, c-d and e-f. The location of the correct guide vane section, therefore, cannot be based purely on the estimated unit speed. This problem is overcome if the location of the sections is based on an estimated unit discharge value, $Q_{11e}^{t+\Delta t}$, as opposed to an estimated unit speed value. For a given unit discharge value, in the re-entrant region of the guide vane curves, there is a single corresponding guide vane section, Figure 5.15. The estimate of the unit discharge is based on a linear extrapolation of those at the previous two time intervals, to give :-

$$Q_{11e}^{t+\Delta t} = 2\,Q_{11}^{t} - Q_{11}^{t-\Delta t} \qquad \ldots\ldots\ldots\ldots \quad (5.3.33)$$

An additional constraint is also required to uniquely define the required guide vane section. The guide vane curves are not single valued for a given unit discharge value, see Figure 5.16 , but the corresponding unit speed values, in general, are of opposite sign. By introducing a constraint on the unit speed value, based on an estimated unit speed, the guide vane section is uniquely defined. An estimate of the unit speed at time $t+\Delta t$ is given by :-

$$n_{11e}^{t+\Delta t} = 2\,n_{11}^{t} - n_{11}^{t-\Delta t} \qquad \ldots\ldots\ldots\ldots \quad (5.3.34)$$

and the guide vane section located from the estimated unit discharge is bounded by an upper and lower limit of unit speed. If the estimated unit speed lies within these bounds then this corresponds to the correct guide vane section. Figure 5.17 shows the upper and lower limits, including an error margin, to which the estimated unit speed must correspond. The error

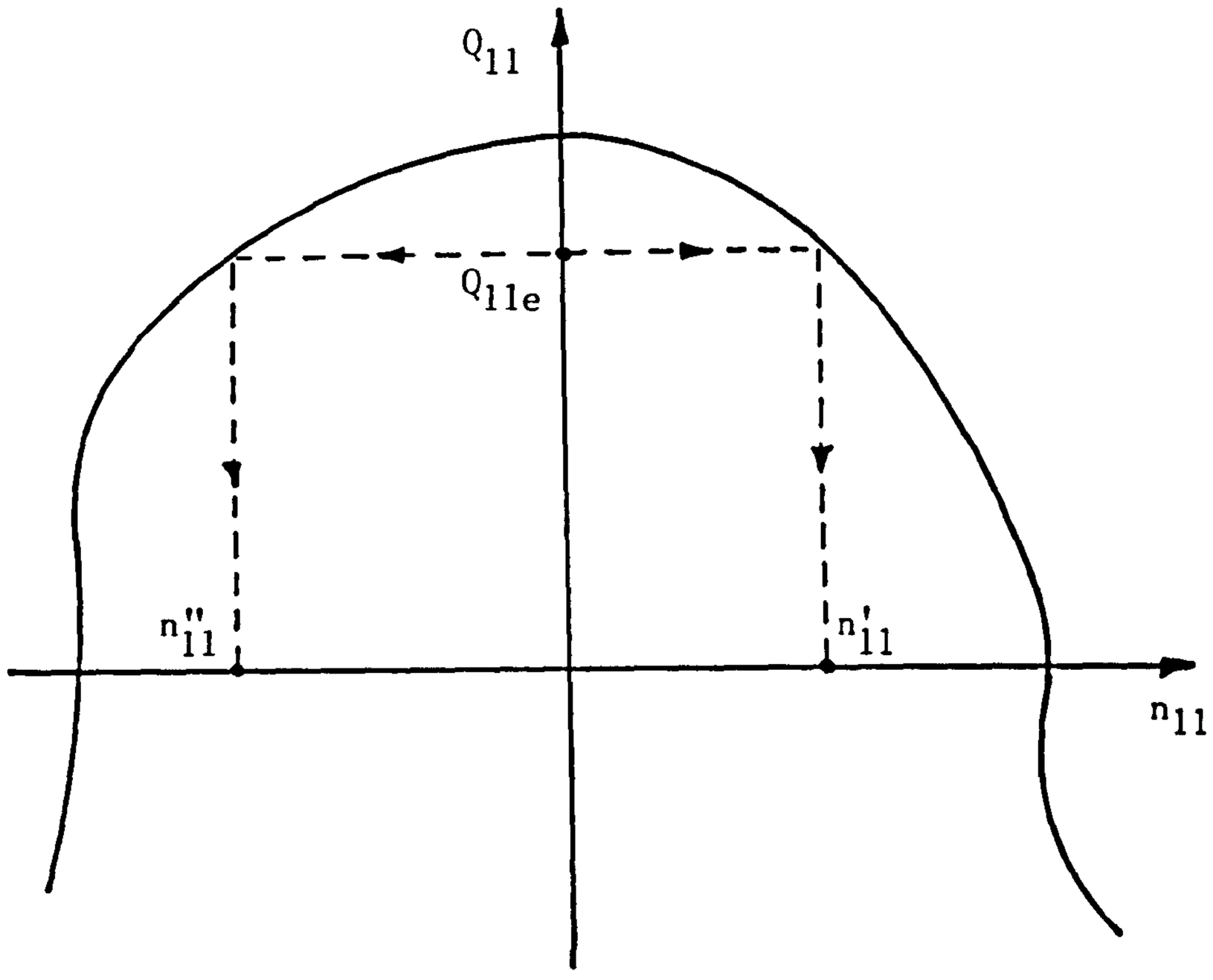

Figure 5.16 : Possible unit speed values for a given unit discharge value for four quadrant performance characteristics.

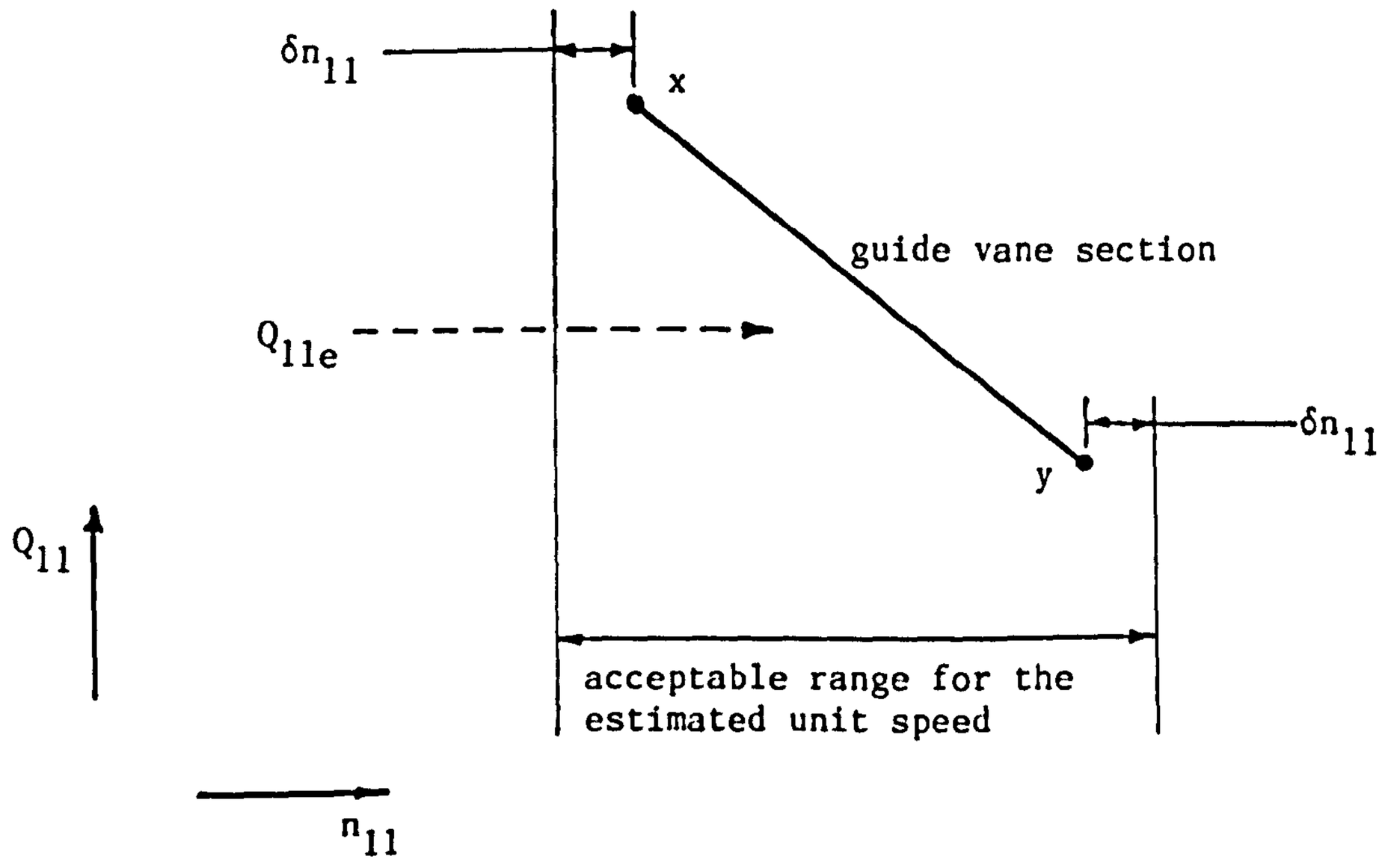

Figure 5.17 : Selection of guide vane section based on estimates of unit discharge and unit speed.

margins are introduced to allow for the error in the estimation of the unit speed. For any section of guide vane curve, x-y say, the estimated unit speed value must satisfy the following condition :-

$$n_{11x} - \delta n_{11} \leqq n_{11e}^{t+\Delta t} \leqq n_{11y} + \delta n_{11} \qquad \ldots\ldots\ldots \quad (5.3.35)$$

for a guide vane section with a negative slope, or

$$n_{11y} - \delta n_{11} \leqq n_{11e}^{t+\Delta t} \leqq n_{11x} + \delta n_{11} \qquad \ldots\ldots\ldots \quad (5.3.36)$$

for a guide vane section with a positive slope, in which

n_{11x} = unit speed at point x

n_{11y} = unit speed at point y

δn_{11} = error margin

A similar approach is adopted for the unit speed versus unit torque performance characteristics. The guide vane sections are located using an estimated unit torque value with the constraints applied to the unit speed, equation 5.3.35 or 5.3.36 still being applied.

5.4 ALTERNATIVE TURBINE PERFOMANCE CHARACTERISTIC REPRESENTATIONS

5.4.1 Introduction

It has been shown that the unit parameter representation of the turbine performance characteristics suffer from a number of drawbacks for use in hydraulic transient simulations. The multi-valued re-entrant, or 'S' characteristic, region of the performance characteristics must be handled with great care in order to correctly locate the operating point. An investigation of alternative representations was, therefore, undertaken to see if there was a viable alternative to the use of the unit parameter representation. The investigation concentrated on three main areas in assessing the alternative representations. These were the formation of a curvilinear mesh and the interpolation of the intermediate guide vane curves, the re-entrant region of the performance characteristics and whether the representation allowed the full range of operating conditions to be identified.

The operating range of a standard turbine is restricted to the turbining quadrant under normal modes of operation. During a load rejection the operating point may enter into the reverse pumping quadrant. These two quadrants provide the full operating range of a standard turbine needed for use in hydraulic transient studies. A reversible pump-turbine, however, operates over four quadrants. These are the pumping, braking or energy dissipation, turbining and reverse pumping quadrants which are defined as :-

Quad 1	n -ve	Q -ve	(pumping)
Quad 2	n -ve	Q +ve	(braking)
Quad 3	n +ve	Q +ve	(turbining)
Quad 4	n +ve	Q -ve	(reverse pumping)

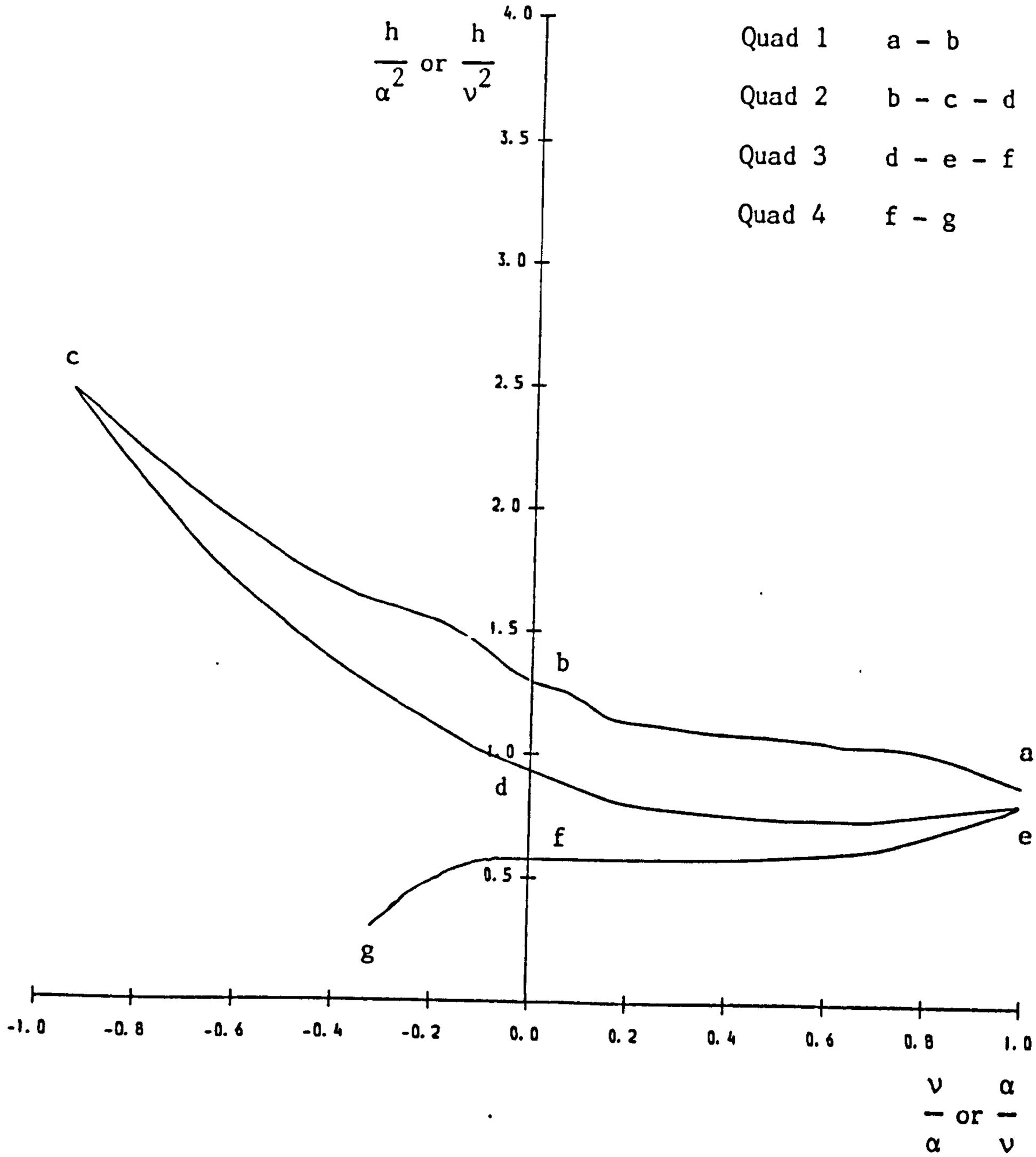

Figure 5.18 : Dimensionless homologous plane. Speed, head and discharge relationship for the maximum guide vane opening.

The operating range of a reversible pump-turbine covers those of a standard turbine together with an additional two quadrants. A pump-turbine, therefore, is a more generalised boundary condition and should be used when considering the development of a generalised hydraulic transient computer program. In assessing the alternative turbine performance characteristics those from a typical pump-turbine were used.

5.4.2 Dimensionless Homologous Plane

Dimensionless homologous relationships are used extensively for representing pump performance characteristics [57] and are given by :-

$$\frac{\nu}{\alpha} \quad \text{versus} \quad \frac{h}{\alpha^2} \quad \text{and} \quad \frac{\nu}{\alpha} \quad \text{versus} \quad \frac{\beta}{\alpha^2} \qquad \text{(A)}$$

or

$$\frac{\alpha}{\nu} \quad \text{versus} \quad \frac{h}{\nu^2} \quad \text{and} \quad \frac{\alpha}{\nu} \quad \text{versus} \quad \frac{\beta}{\nu^2} \qquad \text{(B)}$$

where the dimensionless ratios are :-

$$\alpha = \frac{n}{n_r} \quad , \quad \text{normalised speed}$$

$$\nu = \frac{Q}{Q_r} \quad , \quad \text{normalised discharge}$$

$$h = \frac{H}{H_r} \quad , \quad \text{normalised head}$$

$$\beta = \frac{M}{M_r} \quad , \quad \text{normalised torque}$$

in which subscript 'r' refers to the parameter values at the rated conditions.

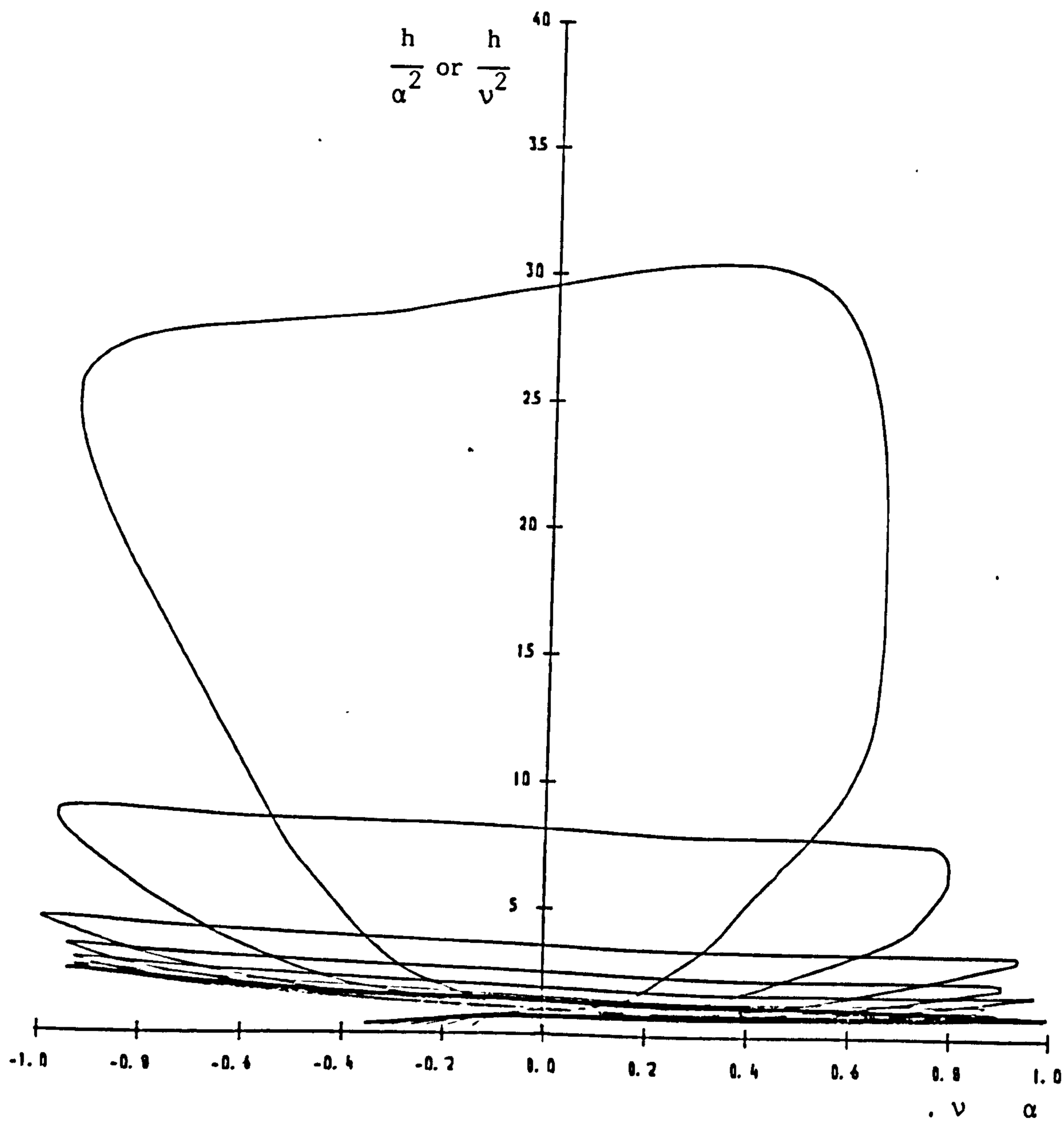

Figure 5.19 : Dimensionless homologous plane (speed, head and discharge relationship).

The full four quadrants of the performance characteristics are to be considered which means the normalised parameters may all change sign and pass through zero. This forces the dimensionless homologous relationships to infinity which presents difficulties from a computational viewpoint. By suggesting a combination of the two co-ordinate systems, A and B, Defazio [58] overcame this problem for pump performance characteristics. Co-ordinate system A is used for $-1 \leq \alpha/\nu \leq +1$ and co-ordinate system B is used for $-1 \leq \nu/\alpha \leq +1$. The absissa values each have limits of -1 and +1 imposed upon them, which correspond to the conditions where $|\alpha|$ equals $|\nu|$. Figure 5.18 shows the dual co-ordinate system for a single, the fully opened, guide vane curve. The sections of curve labelled a-b, b-c-d, d-e-f and f-g represent the ranges of operation in quadrants 1, 2, 3 and 4 respectively. The guide vane curve is smooth and continuous within the ranges of each abscissa but has a discontinuity of slope at the change over points of +1 and -1. Figure 5.19 gives the complete performance characteristics, minus the fully closed guide vane curve. This cannot be included as the ordinate values become infinite along this guide vane curve.when both α and ν equal zero.

5.4.3 Suter Plane

A method of representation which was developed from the dimensionless homologous relationships was proposed by Suter [34] in which the planes were given by :-

$$\frac{h}{\alpha^2 + \nu^2} \quad \text{versus} \quad \tan^{-1}\frac{\nu}{\alpha}$$

and

$$\frac{\beta}{\alpha^2 + \nu^2} \quad \text{versus} \quad \tan^{-1}\frac{\nu}{\alpha}$$

which are commonly referred to as the Suter plane.

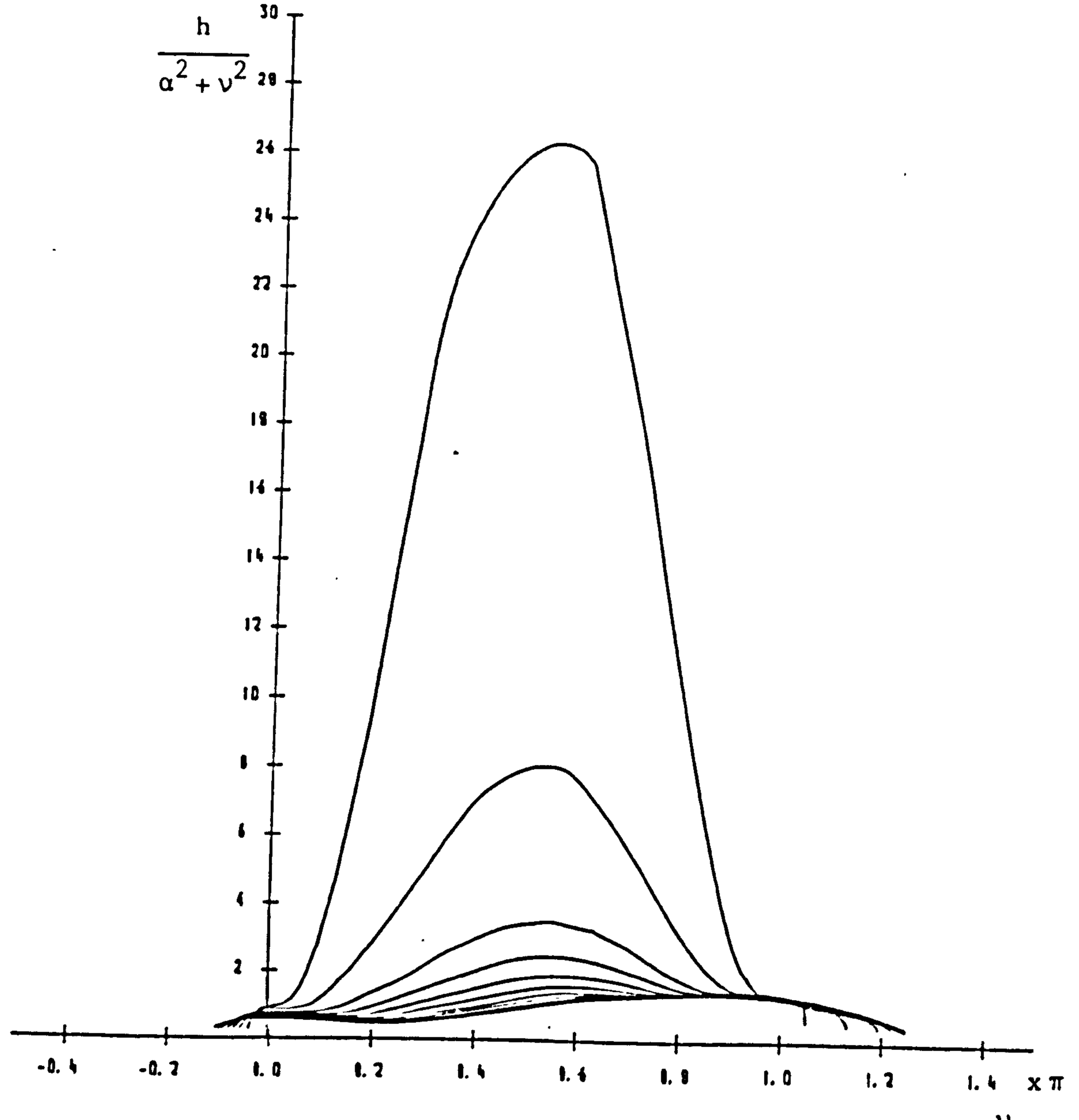

Figure 5.20 : Suter plane (speed, head and discharge relationship).

The use of a $\tan^{-1}$ function along the abscissa allows a single co-ordinate system to be used to represent the complete four quadrants of the performance characteristics. The function lies within finite bounds for all values of α and ν. However, in order to individually define each of the four quadrants it is necessary to define the range of the $\tan^{-1}$ function as follows :-

$$\text{Quad 1} \qquad \pi \leq \tan^{-1} \frac{\nu}{\alpha} \leq \frac{3\pi}{2}$$

$$\text{Quad 2} \qquad \frac{\pi}{2} \leq \tan^{-1} \frac{\nu}{\alpha} \leq \pi$$

$$\text{Quad 3} \qquad 0 \leq \tan^{-1} \frac{\nu}{\alpha} \leq \frac{\pi}{2}$$

$$\text{Quad 4} \qquad -\frac{\pi}{2} \leq \tan^{-1} \frac{\nu}{\alpha} \leq 0$$

in which the quadrants are as defined in Section 5.4.1. The head, speed and discharge relationship is shown in Figure 5.20. The guide vane curves are smooth and continuous throughout the four quadrants and there are no discontinuities in their slopes. The fully closed guide vane opening has been omitted from Figure 5.20. Given that both α and ν can be equal to zero, simultaneously, along this curve means the corresponding ordinate value will reach infinity and cannot, therefore, be depicted.

5.4.4 Exploded Unit Parameter Plane

In a discussion of DeFazio's paper [59] a method of opening out the unit parameter performance characteristics was proposed by Woznaik. A normalised guide vane factor was applied to the abscissa, or unit speed axes, which led to the following co-ordinate system :-

$$Q_{11} \qquad \text{versus} \qquad \frac{z}{z_f} n_{11}$$

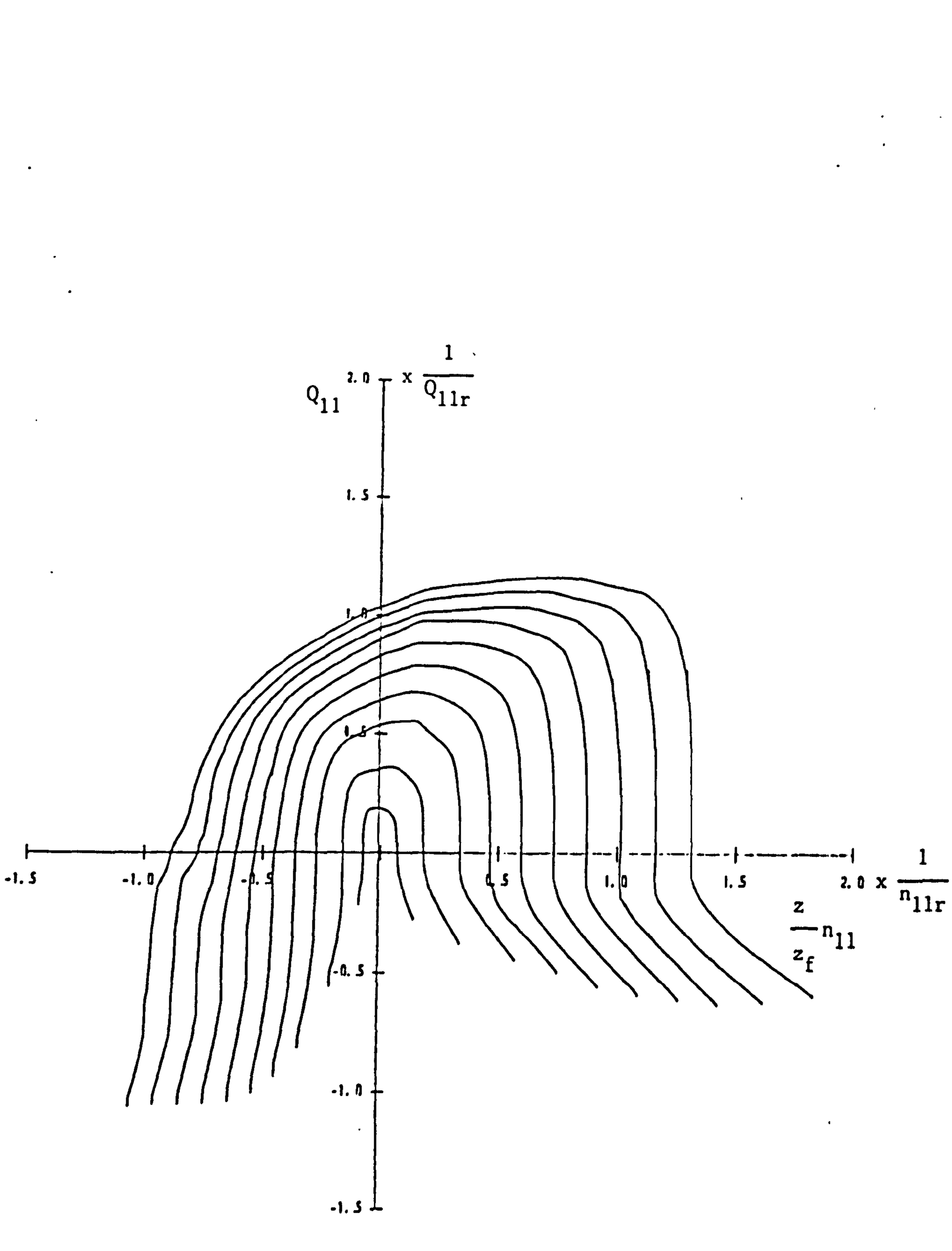

Figure 5.21 : Exploded unit parameter, normalised, plane (speed, head and discharge relationship).

and

$$M_{11} \quad \text{versus} \quad \frac{z}{z_f} n_{11}$$

where

z = actual guide vane opening

z_f = maximum guide vane opening

The effect of introducing the normalised guide vane opening can be seen in Figure 5.21 which gives the head, speed and discharge relationships. In Figure 5.21 the unit parameters have also been normalised by dividing them by the unit parameter values at the rated, in turbining mode, conditions. The subscript r is used to denote the parameter values at these conditions.

The introduction of the normalised guide vane opening has the effect of opening out the individual guide vane curves such that they become easily distinquishable. The curves are smooth and continuous throughout the full four quadrants and there are no discontinuities in their slopes. The full range of guide vane curves is depicted, including the fully closed guide vane curve. The normalised guide vane factor for this curve is equal to zero therefore, for the head, speed and discharge relationships this curve is reduced to a single point located at the origin. On the head, speed and torque realationships the fully closed guide vane curve forms part of the unit torque axis in the region of the origin.

5.4.5 Modified Suter Plane

The final representation was proposed by Martin [50] which involves a combination of opening out the performance characteristics, by the introduction of a normalised guide vane factor, and a transformation onto a modified Suter plane. The pair of co-ordinate systems which resulted

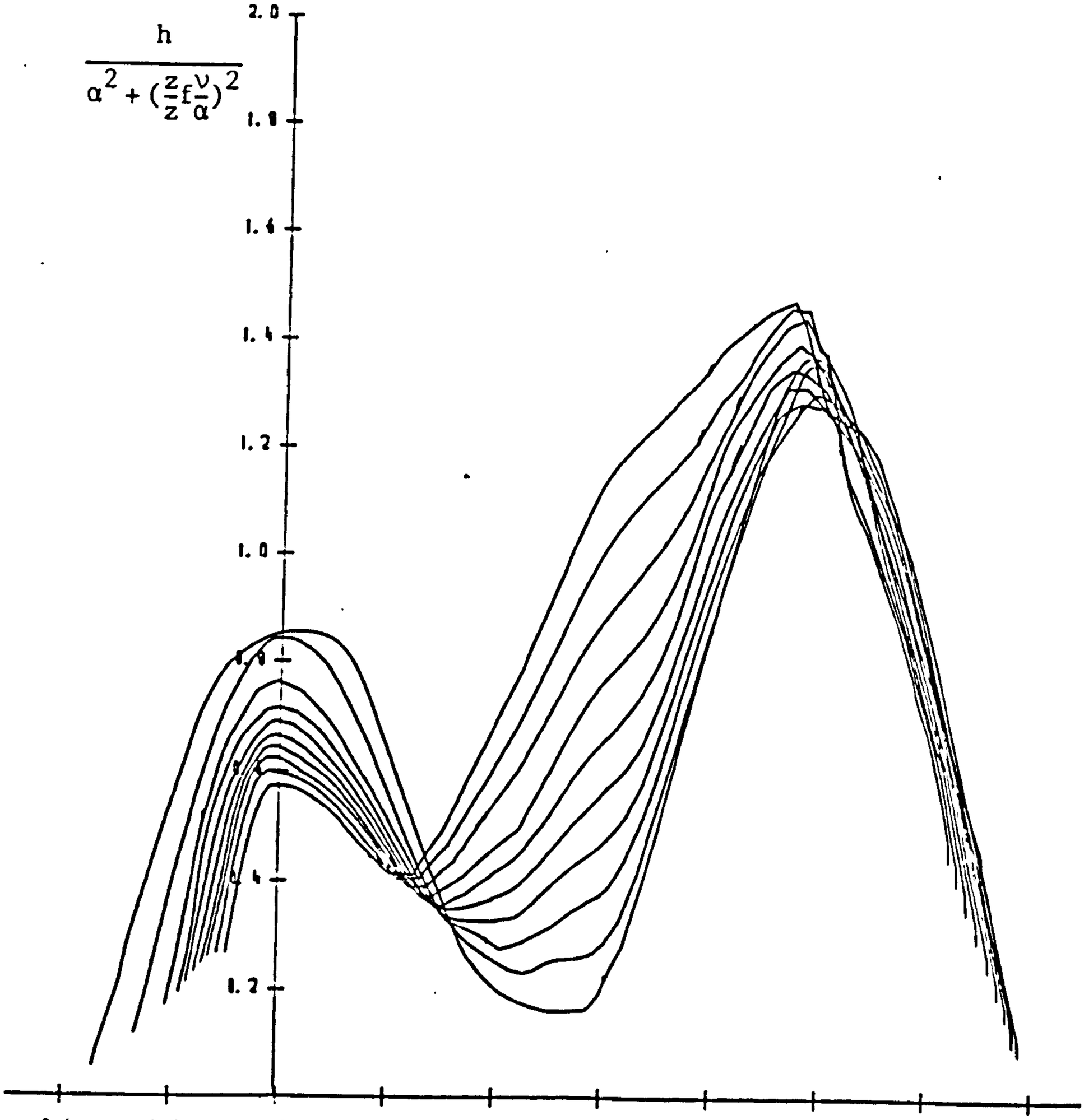

Figure 5.22 : Modified Suter plane (speed, head and discharge relationship).

were given by :-

$$\frac{h}{\alpha^2 + (\frac{z}{z_f}\frac{\nu}{\alpha})^2} \quad \text{versus} \quad \tan^{-1}\frac{z_f\nu}{z\ \alpha}$$

and

$$\frac{\beta}{\alpha^2 + \frac{z}{z_f}\nu^2} \quad \text{versus} \quad \tan^{-1}\frac{z_f\nu}{z\ \alpha}$$

A typical set of curves are shown in Figure 5.22 for the head,speed and discharge relationships. The curves are smooth and continuous with no discontinuities in their slopes being present. The curves are kept within finite bounds due to the $\tan^{-1}$ function used on the abscissa axes. However, along the ordinate the values can be infinite for the fully closed guide vane curve. Along this curve the normalised speed, α, and discharge, ν, can be zero, simultaneously, and the ordinate value becomes infinite. The fully closed guide vane curve, therefore, is not shown in Figure 5.22.

5.5 RECOMMENDATIONS

5.5.1 Selection Of Turbine Performance Characteristic Representation

Five different planes for the representation of turbine performance characteristics were presented in Sections 5.3 and 5.4. These were the unit parameter plane, the dimensionless homologous plane, the Suter plane, the exploded unit parameter plane and the modified Suter plane. Their individual merits and drawbacks, for use in hydraulic transient simulations, are to be discussed before a final recommendation is made. The principal areas of interest in their assessments are :-

(a) the formation of a curvilinear mesh,

(b) the interpolation of the intermediate guide vane curves,

(c) the multivalued, re-entrant, region of the guide vane curves, and

(d) the fully closed guide vane curve.

Turbine manufacturers generally present turbine performance characteristics on the unit parameter plane. If this plane is being used . a curvilinear mesh can be superimposed directly. The other planes of representation each require a transformation onto their respective planes before the mesh is superimposed. This requires the digitisation of the curves on the unit parameter plane for purposes of the transformation, the superimposing of mesh lines to form the curvilinear mesh and a second digitisation of the curves, at the intersection of each guide vane curve and mesh line. The latter digitised points are then arranged into an input data file for use in the hydraulic transient simulations. This procedure is laborious, if done by a hand method, particularly for complex performance characteristics such as those for a reversible pump-turbine. The

procedure can be considerably eased by using a computerised transformation and mesh generation algorithm. This is described in detail in Section 6.2. The turbine performance characteristics are digitised on the unit parameter plane and these points are used as the data input for the algorithm. The algorithm performs the necessary operations and produces an output file which is ready for use in the hydraulic transient simulations. The formation of a curvilinear mesh, therefore, presents no problems and is not dependent on the plane of representation.

The interpolation of the intermediate guide vane curves is performed within the curvilinear mesh, as described in Section 5.3.3. Linear interpolation is used along the sections of the mesh lines, between adjacent guide vane curves. Linear interpolation gives accurate results provided that the spacing between tabulated guide vane curves is regular. A number of the representations presented do not satisfy this criterion, namely the dimensionless homologous plane and the Suter plane. Their ordinate values become one or two orders of magnitude greater for the lower guide vane openings. This is due to the normalised speed and discharge values, α and ν, becoming relatively small in comparison with the normalised head and torque values, h and β. Interpolation routines of a higher order would be required for these representations to achieve a comparable degree of accuracy. The unit parameter plane and the modified Suter plane have less marked variations in the spacing of their guide vane curves and linear interpolation of the intermediate guide vane curves would give only slight errors. However, the expoloded unit parameter plane gives the most regular spacing of the curves and is, therefore, the most compatible with linear interpolation.

The re-entrant region of pump-turbine performance characteristics was described in Section 5.3.5. On the unit parameter plane the guide vane curves become multivalued. Care must be taken when locating the operating point in this region in order to identify the correct operating point. Although these problems can be overcome it is possible to avoid a re-entrant, multivalued, region altogether if an alternative representation is selected. The re-entrant region on the unit parameter plane is found to be single valued on the dimensionless homologous plane, the Suter plane and the modified Suter plane. The location of the operating points in the formerly multivalued region is, therefore, straightforward on these planes. The multivalued nature of the guide vane curves is, however, present on the exploded unit parameter plane. The use of this representation would require the turbine boundary handling routine to take account of the multivalued region.

When model testing turbines or pump-turbines data is recorded for the fully closed guide vane position. The fully closed guide vane curve is then presented on the performance characteristics together with the other tabulated openings. On transforming from the unit parameter plane to an alternative plane this information can be lost. The fully closed guide vane curve does not appear on the dimensioless homologous plane, the Suter plane or the modified Suter plane. The performance characteristics, therefore, cannot be used to simulate the final stages of a guide vane closure. Martin [50] noted this fact and suggested that the turbine or pump-turbine could be modelled as a valve during the final closure. In doing so, an additional boundary solution algorithm has to be used when the guide vane opening falls below its lowest tabulated value.

The five representations of turbine performance characteristics which have been discussed each have their merits and drawbacks for use in hydraulic transient studies. However, it is the exploded unit parameter representation which gives the most viable option. The formation of a curvilinear mesh can be achieved easily by using the automatic mesh generation algorithm, see Section 6.2 . The interpolation of the intermediate guide vane curves, within the curvilinear mesh, is particularly suited to the form the guide vane curves take in this plane. Their regular spacing means that linear interpolation along sections of the mesh lines will give accurate results in locating the intermediate curves. The exploded unit parameter plane also allows the full range of guide vane openings to be depicted,including the fully closed position. An alternative solution of the turbine boundary condition for the final closure of the guide vanes is not required. A single solution algorithm can, therefore, be used over the full range of guide vane movements. The main drawback of this representation is the re-entrant guide vane curves which can be present in pump-turbine performance characteristics. These render the curves multivalued and care must be exercised in order to locate the correct operating point in these regions. However, this problem is identical to that when using the unit parameter representation. The methods of alleviating this problem can, therefore, be taken directly from those discussed in Section 5.3.5 . In addition, the solution algorithm for use with the unit parameter plane, Section 5.3.4, can also be readily adapted for use with the exploded unit parameter plane.

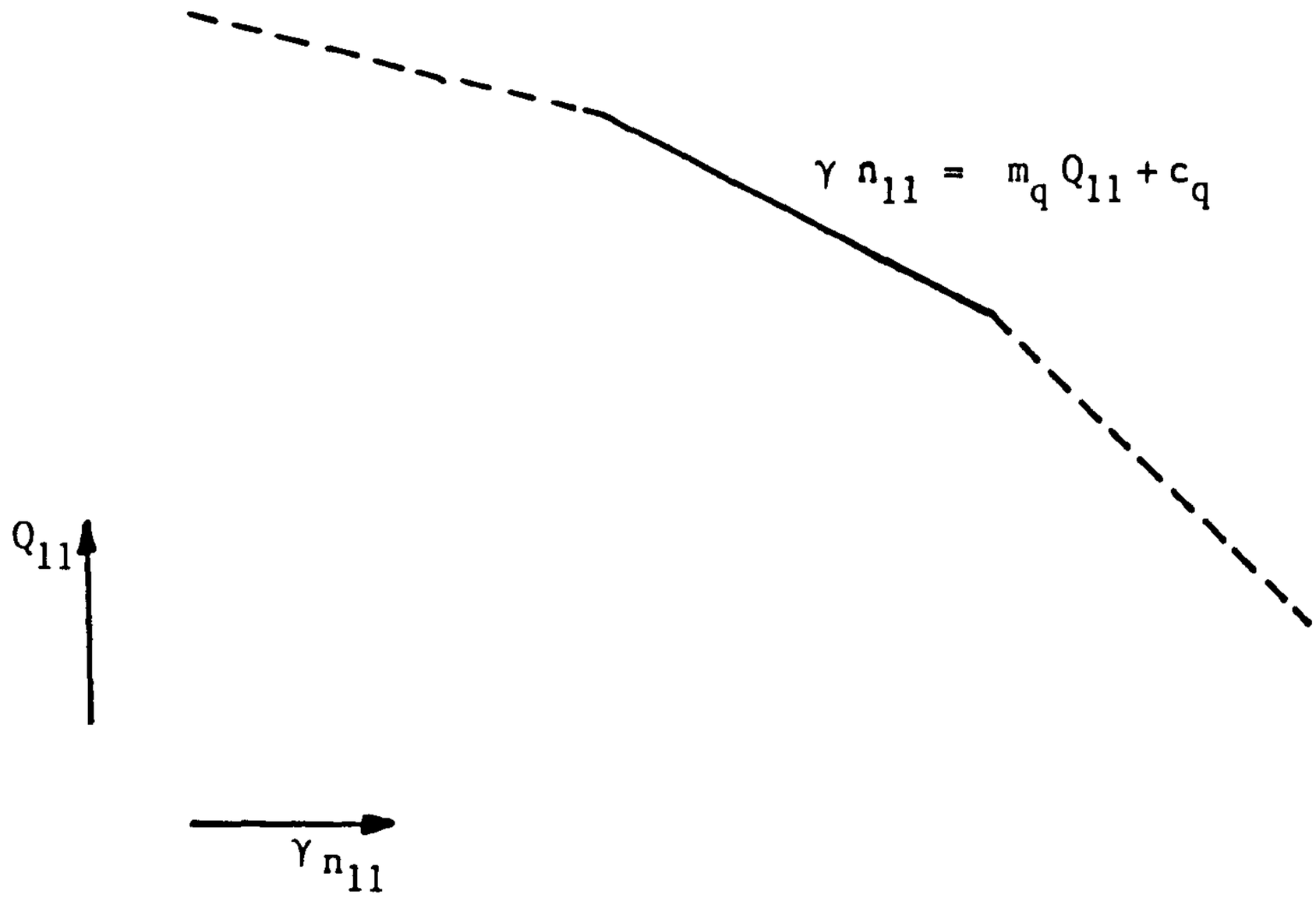

Figure 5.23 : Linear equation of guide vane section on the exploded unit speed versus unit discharge plane.

5.5.2 Turbine Boundary Solution Algorithm For Exploded Unit Parameter Representation

Any section of guide vane curve, tabulated or interpolated, on the exploded unit speed versus unit discharge plane is given by :-

$$\gamma n_{11} = m_q Q_{11} + c_q \qquad \text{.....} \qquad (5.5.1)$$

in which

γ = noramalised guide vane opening (z/z_f)

and is shown schematically in Figure 5.23. Re-writing equation 5.5.1 in terms of the turbine speed, head and discharge gives :-

$$\frac{\gamma n D}{\sqrt{H}} = \frac{m_q Q}{D^2 \sqrt{H}} + c_q \qquad \text{.....} \qquad (5.5.2)$$

A relationship between the head across the turbine and the discharge through the turbine is given in equation 5.3.18, for time $t+\Delta t$, which is :-

$$H^{t+\Delta t} = a_5 Q^{t+\Delta t} + a_6 \qquad \text{.....} \qquad (5.5.3)$$

where a_5 and a_6 are known constants. Eliminating the turbine discharge from equations 5.5.1 and 5.5.3 and re-arranging gives a relationship between the turbine speed and net head , at time $t+\Delta t$, of the form :-

$$\gamma n^{t+\Delta t} = a_7 H^{t+\Delta t} + a_8 \sqrt{H}^{t+\Delta t} + a_9 \qquad \text{.....} \qquad (5.5.4)$$

in which the constants a_7, a_8 and a_9 are as given in equation 5.3.19.

On the exploded unit speed versus unit torque plane any section of a guide vane curve is approximated by a straight line, Figure 5.24, which can be written as :-

$$\gamma n_{11} = m_m M_{11} + c_m \qquad \text{.....} \qquad (5.5.5)$$

Therefore

$$\frac{\gamma n D}{\sqrt{H}} = \frac{m_m M}{D^3 H} + c_m \qquad \text{.....} \qquad (5.5.6)$$

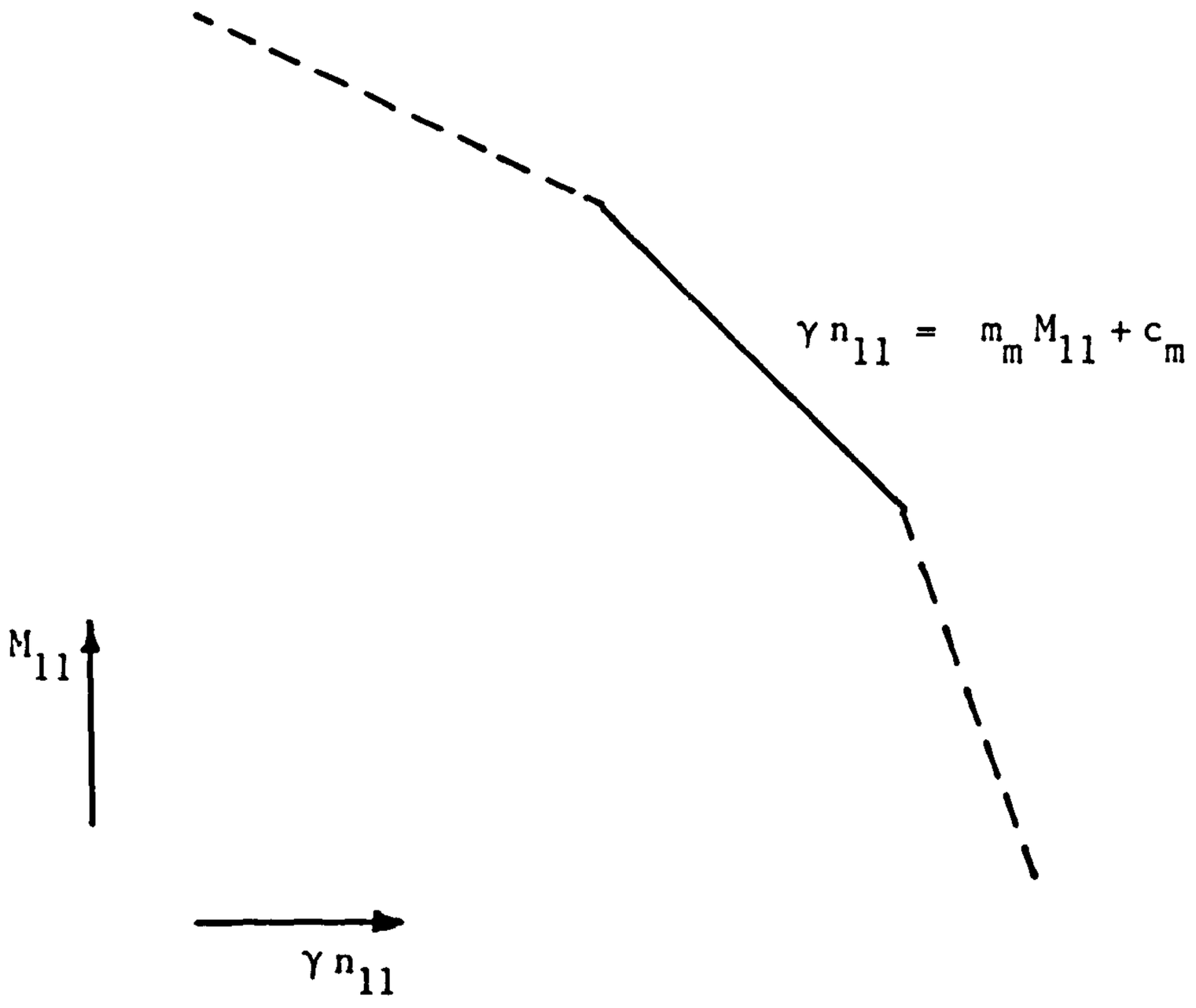

Figure 5.24 : Linear equation of guide vane section on the exploded unit speed versus unit torque plane.

From equation 5.3.24 the out of balance torque, at time $t+\Delta t$, is given by :-

$$M^{t+\Delta t} = 2 b_1 n^{t+\Delta t} - 2 b_1 n^t - M^t \quad \ldots\ldots\ldots\ldots \quad (5.5.7)$$

where b_1 is given in equation 5.3.23. Combining equations 5.5.6 and 5.5.7 to eliminate $M^{t+\Delta t}$ gives :-

$$\frac{\gamma n^{t+\Delta t} D}{\sqrt{H^{t+\Delta t}}} = \frac{m_m [2 b_1 n^{t+\Delta t} - 2 b_1 n^t - M^t]}{D^3 H^{t+\Delta t}} + c_m \quad \ldots\ldots \quad (5.5.8)$$

which is re-arranged to give a function of the turbine speed and net head of the form :-

$$n^{t+\Delta t} [\gamma \sqrt{H^{t+\Delta t}} + b_2] + b_3 H^{t+\Delta t} + b_4 = 0 \quad \ldots\ldots \quad (5.5.9)$$

in which b_2, b_3 and b_4 are given in equation 5.3.26.

Two equations, 5.5.4 and 5.5.9, have been derived as functions of the turbine speed and net head at time $t+\Delta t$. Multiplying equation 5.5.9 throughout by the normalised guide vane opening, γ, and replacing $\gamma n^{t+\Delta t}$ from equation 5.5.4 gives :-

$$[a_7 H^{t+\Delta t} + a_8 \sqrt{H^{t+\Delta t}} + a_9][\gamma \sqrt{H^{t+\Delta t}} + b_2]$$

$$+ \gamma b_3 H^{t+\Delta t} + \gamma b_4 = 0 = f(H^{t+\Delta t}) \quad (5.5.10)$$

The solution of the turbine boundary has been reduced to that of a single variable, $H^{t+\Delta t}$, which is solved using a standard Newton-Raphson technique. The solution of the remaining variables, turbine speed, discharge,torque, spiral head and draft tube head, then follows as given in Section 5.3.4. This solution is applicable to turbine or pump-turbine boundaries where the connecting pipes at the spiral entry and draft tube exit have an equivalent cross-sectional area to the spiral entry and draft tube exit respectively. If there is an expansion or contraction at either, or both, of these joints the spiral head and draft tube heads require a slight modification.

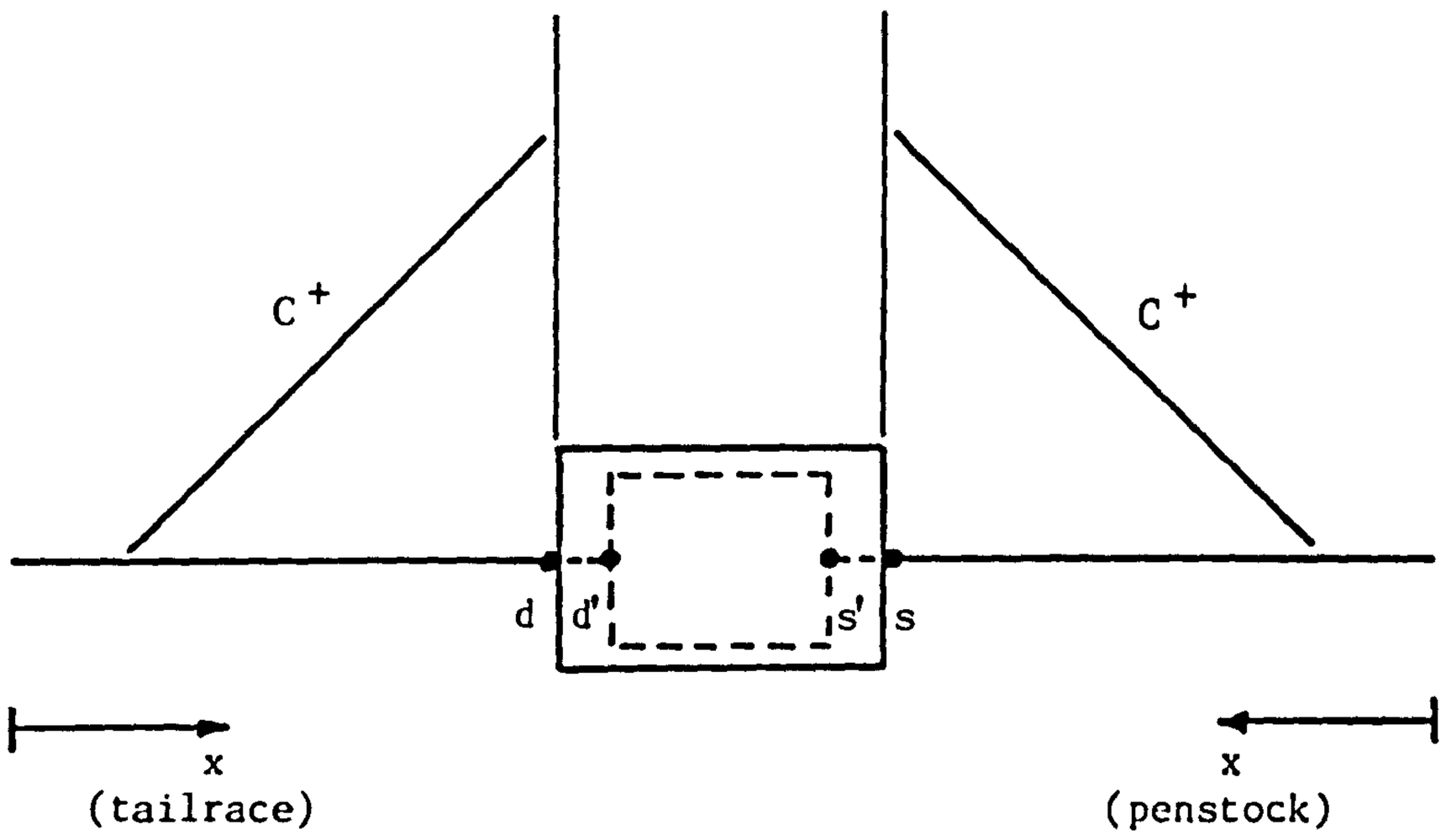

Figure 5.25 : Turbine or pump-turbine boundary condition with contraction or expansion joints at the spiral inlet and draft tube outlet.

The solution of equation 5.5.10 yields the net head across the turbine or pump-turbine, H, at time t+Δt. From Figure 5.25 let :-

A_s = cross-sectional area of pipe connected to the spiral entry

A_d = cross-sectional area of pipe connected draft tube exit

$A_{s'}$ = cross-sectional area of the spiral entry

$A_{d'}$ = cross-sectional area of the draft tube outlet

A common energy head exists at spiral entry and the draft tube exit which implies :-

$$H_s + \frac{v_s^2}{2g} = H_{s'} + \frac{v_{s'}^2}{2g} \qquad \text{.....} \quad (5.5.11)$$

and

$$H_d + \frac{v_d^2}{2g} = H_{d'} + \frac{v_{d'}^2}{2g} \qquad \text{.....} \quad (5.5.12)$$

From equation 5.5.3 the discharge at time t+Δt is given by :-

$$Q^{t+\Delta t} = \frac{H^{t+\Delta t} - a_6}{a_5} \qquad \text{.....} \quad (5.5.13)$$

Continuity of flow gives :-

$$Q^{t+\Delta t} = A_s v_s^{t+\Delta t} = A_{s'} v_{s'}^{t+\Delta t} = -A_d v_d^{t+\Delta t} = -A_{d'} v_{d'}^{t+\Delta t} \qquad (5.5.14)$$

therefore the discharge velocities at cross-sections s, s', d and d' can be calculated. The characteristic equations on either side of the boundary see equations 5.3.15 and 5.3.16, give the solutions for the heads at sections s and d, that is :-

$$H_s^{t+\Delta t} = a_1 Q_s^{t+\Delta t} + a_2 \qquad \text{.....} \quad (5.5.15)$$

and

$$H_d^{t+\Delta t} = a_3 Q_d^{t+\Delta t} + a_4 \qquad \text{.....} \quad (5.5.16)$$

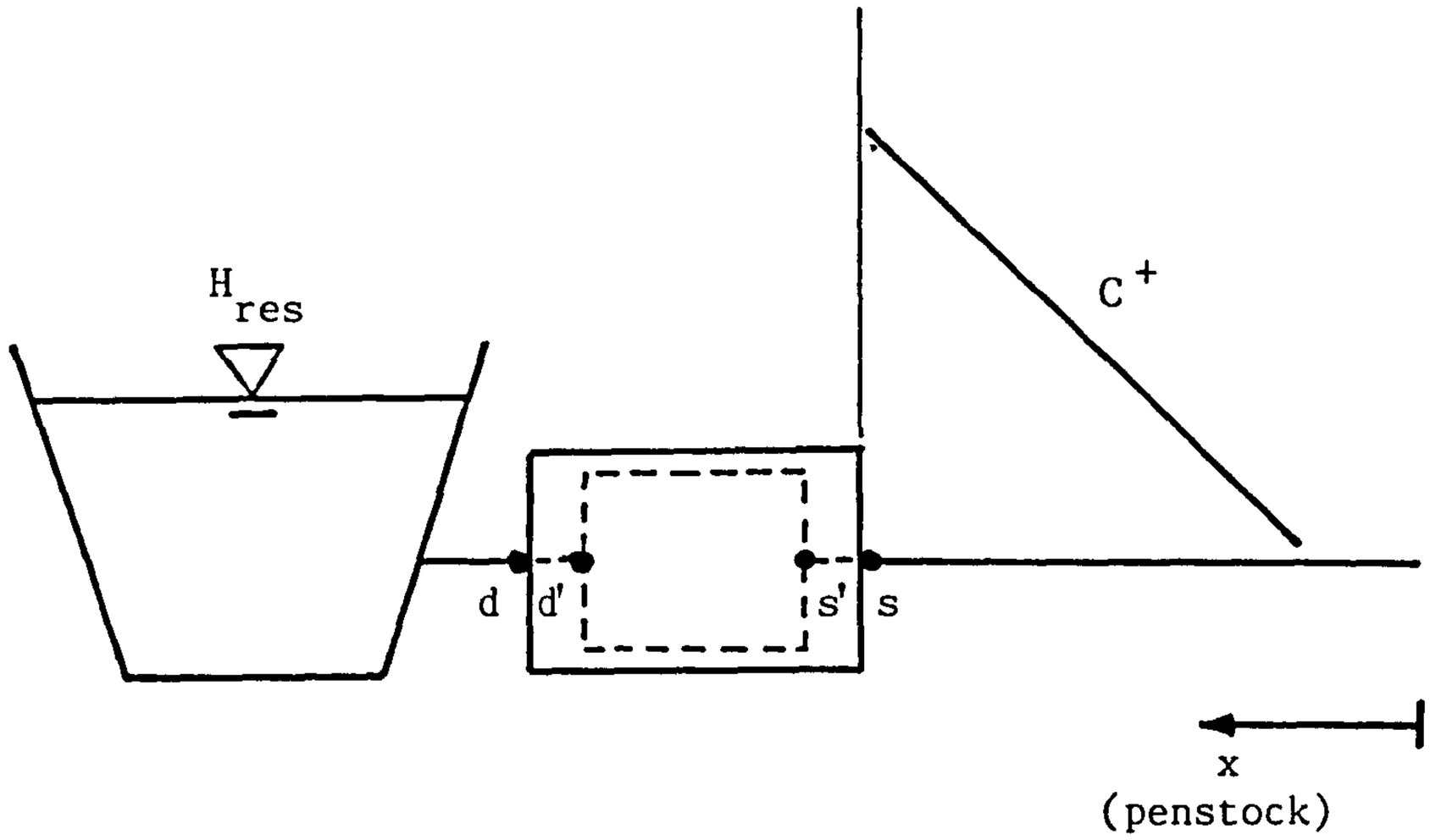

Figure 5.26 : Turbine or pump-turbine boundary condition for hydraulic system with no tailrace.

Therefore, rearranging equations 5.5.11 and 5.5.12, and taking all values to be at a time t+Δt, the heads at s' and d' are given by :-

$$H_{s'}^{t+\Delta t} = H_s^{t+\Delta t} + \frac{Q^{t+\Delta t^2}}{2g}\left\{\frac{1}{A_s^2} - \frac{1}{A_{s'}^2}\right\} \quad \ldots\ldots\ldots\ldots \quad (5.5.17)$$

and

$$H_{d'}^{t+\Delta t} = H_d^{t+\Delta t} + \frac{Q^{t+\Delta t^2}}{2g}\left\{\frac{1}{A_d^2} - \frac{1}{A_{d'}^2}\right\} \quad \ldots\ldots\ldots\ldots \quad (5.5.18)$$

The turbine, or pump-turbine, boundary solution algorithm given at present is for a hydraulic system which has a tailrace section. This leads to two characteristic equations, one either side of the machine. Installations with no tailrace section, however, are common. The solution algorithm for this variation is given below.

A single characteristic equation is available at the turbine boundary when there is no tailrace section, Figure 5.26, which is given by :-

$$H_s^{t+\Delta t} = a_1 Q_s^{t+\Delta t} + a_2 \quad \ldots\ldots\ldots\ldots \quad (5.5.19)$$

and the net head across the turbine, the tailrace head is equivalent to the head imposed by the reservoir, H_{res}, is given by :-

$$H^{t+\Delta t} = H_s^{t+\Delta t} - H_{res} + \Delta V H^t \quad \ldots\ldots\ldots\ldots \quad (5.5.20)$$

Combining equations 5.5.19 and 5.5.20 to eliminate the spiral head, H_s, gives :-

$$H^{t+\Delta t} = a_1 Q_s^{t+\Delta t} - H_{res} + \Delta V H^t + a_2 \quad \ldots\ldots\ldots\ldots \quad (5.5.21)$$

The discharge through the spiral inlet, Q_s, is equal to the discharge through the turbine, Q. Therefore :-

$$H^{t+\Delta t} = a_1 Q^{t+\Delta t} - H_{res} + \Delta V H^t + a_2 \quad \ldots\ldots\ldots\ldots \quad (5.5.22)$$

This is in the same form as equation 5.5.3 :-

$$H^{t+\Delta t} = a_5 Q^{t+\Delta t} + a_6 \qquad \text{.....} \quad (5.5.23)$$

providing

$$a_5 = a_1$$

$$a_6 = -H_{res} + \Delta V H^t + a_2$$

With the constants a_5 and a_6 established the solution of the turbine boundary for a hydraulic system with no tailrace section follows an identical algorithm to that given at the start of Section 5.5.2.

5.5.3 Turbine Boundary Solution Algorithm Including Relief Valve

Relief valves connected to the spiral casing are a common feature of turbines. The relief valves are used to control hydraulic transients and may also be used for irrigation purposes. Following a load rejection the relief valve is activated by the governor control. The relief valve opens at a predetermined rate whilst the the guide vanes are closing. Upon the full closure of the guide vanes the relief valve begin their closure. The advantages of using relief valves is that they allow a rapid closure of the guide vanes and this prevents damage to the turbine or generator due to over speeding. As the guide vanes close the discharge through the relief valve increases until the total discharge through the penstock is equivalent to the relief valve discharge. During the closure of the guide vanes a rapid deceleration, which would otherwise result in very large transient pressure waves being propagated, is avoided as the discharge is diverted through the relief valve. Once the turbine has been isolated from the rest of the system, by full closure of the guide vanes, the relief valve is used to arrest the flow through the penstock. The closure rate of the relief valve is, again, controlled by the governor and this is generally undertaken at a relatively slow rate. This is made possible

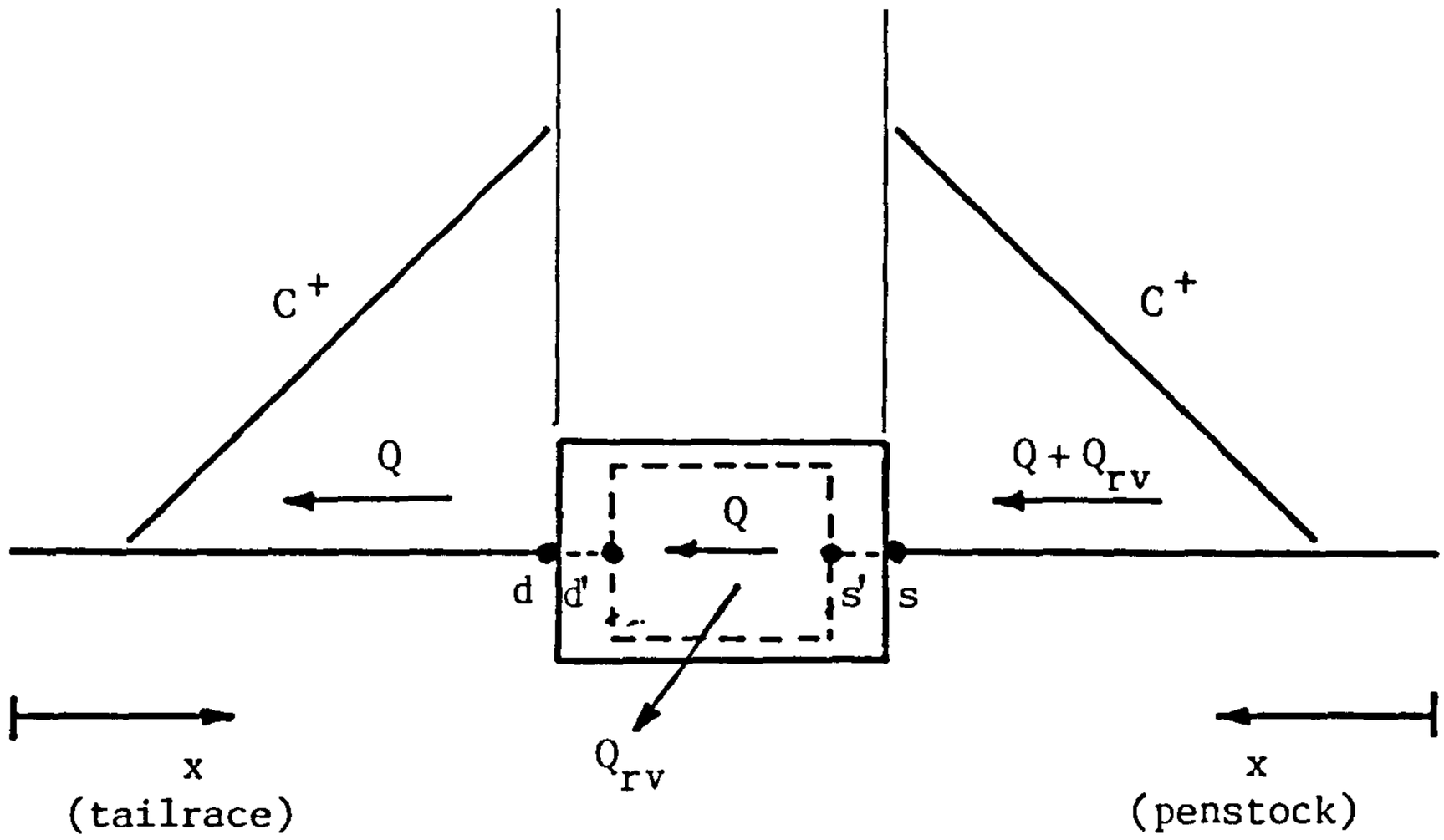

Figure 5.27 : Turbine boundary condition including relief valve.

due to the turbine being isolated and free from potential damage. A slow rate of closure for the relief valve is chosen so as to restrict the pressure rises in the system to within acceptable limits.

A turbine boundary condition including a relief valve is shown in Figure 5.27. The total flow through section s and s' is the sum of the flow through the turbine and the relief valve. The total flow then separates, between that through the relief valve and that through the turbine, the latter discharging through the draft tube outlet. The discharge through the relief valve can be expressed as :-

$$Q_{rv} = k_d A_{rv} [2g(H_{s'} - z_{rv})]^{0.5} \quad \ldots\ldots\ldots\ldots \quad (5.5.24)$$

in which

Q_{rv} = discharge through the relief valve

$H_{s'}$ = head at section s'

A_{rv} = full-bore cross-sectional area of the relief valve

k_d = relief valve discharge coefficient

z_{rv} = elevation of the relief valve

or

$$Q_{rv}^2 c_1 = H_{s'} - z_{rv} \quad \ldots\ldots\ldots\ldots \quad (5.5.25)$$

where

$$c_1 = \frac{1}{2 g k_d^2 A_{rv}^2}$$

Sections s and s' share a common energy head, that is :-

$$H_s + \frac{v_s^2}{2g} = H_{s'} + \frac{v_{s'}^2}{2g} \quad \ldots\ldots\ldots\ldots \quad (5.5.26)$$

In terms of the flow through sections s and s', $Q + Q_{rv}$, equation 5.5.26 becomes :-

$$H_{s'} = H_s + \frac{(Q+Q_{rv})^2}{2g} \left\{ \frac{1}{A_s^2} - \frac{1}{A_{s'}^2} \right\} \quad \ldots\ldots\ldots\ldots \quad (5.5.27)$$

or

$$H_s' = H_s + c_2(Q - Q_{rv})^2 \qquad \text{.....} \quad (5.5.28)$$

where

$$c_2 = \frac{1}{2g}\left\{\frac{1}{A_s^2} - \frac{1}{A_s'^2}\right\}$$

Combining equations 5.5.25 and 5.5.28 gives :-

$$Q_{rv}^2 c_1 = H_s + c_2(Q + Q_{rv})^2 - z_{rv} \qquad \text{.....} \quad (5.5.29)$$

The characteristic equation at the spiral inlet gives :-

$$H_s^{t+\Delta t} = a_1(Q^{t+\Delta t} + Q_{rv}^{t+\Delta t}) + a_2 \qquad \text{.....} \quad (5.5.30)$$

Taking equation 5.5.29 for time $t+\Delta t$ and substituting for H_s gives :-

$$Q_{rv}^{t+\Delta t\,2} c_3 + Q_{rv}^{t+\Delta t} c_4 + c_5 = 0 = f(Q_{rv}^{t+\Delta t}) \quad \text{....} \quad (5.5.31)$$

in which

$$c_3 = c_1 - c_2$$

$$c_4 = -[2 c_2 Q^{t+\Delta t} + a_1]$$

$$c_5 = z_{rv} - c_2 Q^{t+\Delta t\,2} - a_1 Q^{t+\Delta t} - a_2$$

The function of relief valve discharge, equation 5.5.31, can be solved using a Newton-Raphson technique provided that the constants c_3, c_4 and c_5 are known. This requires the machine discharge, Q, to be known at time $t+\Delta t$. An estimate of this discharge, linearly extrapolated from the known discharges at the previous two time intervals is given by :-

$$Q^{t+\Delta t} = 2Q^t - Q^{t-\Delta t} \qquad \text{.....} \quad (5.5.32)$$

Substituting the extrapolated machine discharge, Q, into the constants, c_3, c_4 and c_5, leads to the solution of the relief valve discharge, Q_{rv}, at time $t+\Delta t$.

The characteristic equation at the tailrace implies :-

$$H_d^{t+\Delta t} = a_3 Q_d^{t+\Delta t} + a_4 \qquad \text{.....} \quad (5.5.33)$$

The discharge through the draft tude exit is equal to minus the discharge through the turbine, therefore, equation 5.5.33 can be rewritten in terms of the turbine discharge, Q, to give :-

$$H_d^{t+\Delta t} = -a_3 Q^{t+\Delta t} + a_4 \qquad \text{.....} \quad (5.5.34)$$

The net head across the turbine, equation 5.3.14, is given by :-

$$H^{t+\Delta t} = H_s^{t+\Delta t} - H_d^{t+\Delta t} + \Delta VH^t \qquad \text{.....} \quad (5.5.35)$$

Substituting for H_s and H_d from the characteristic equations 5.5.30 and 5.5.34 leads to :-

$$H^{t+\Delta t} = a_1(Q^{t+\Delta t} + Q_{rv}^{t+\Delta t}) + a_2 + a_3 Q^{t+\Delta t} - a_4 + \Delta VH^t \quad (5.5.36)$$

which is in the form :-

$$H^{t+\Delta t} = a_5 Q^{t+\Delta t} + a_6 \qquad \text{.....} \quad (5.5.37)$$

where

$$a_5 = a_1 + a_3$$

$$a_6 = a_1 Q_{rv}^{t+\Delta t} + a_2 - a_4 + \Delta VH^t$$

The turbine net head is in the same form as that given by equation 5.5.3 and the solution of the net head follows that given in Section 5.5.2. Substituting the net head, H, into equation 5.5.37 leads to the turbine discharge, Q, at time $t+\Delta t$, and the heads at sections s and d follow from equations 5.5.30 and 5.5.34, respectively. Should there be a contraction or expansion at the the spiral inlet or draft tube exit joints the heads at sections s' and d' are calculated from equations 5.5.17 and 5.5.18, respectively.

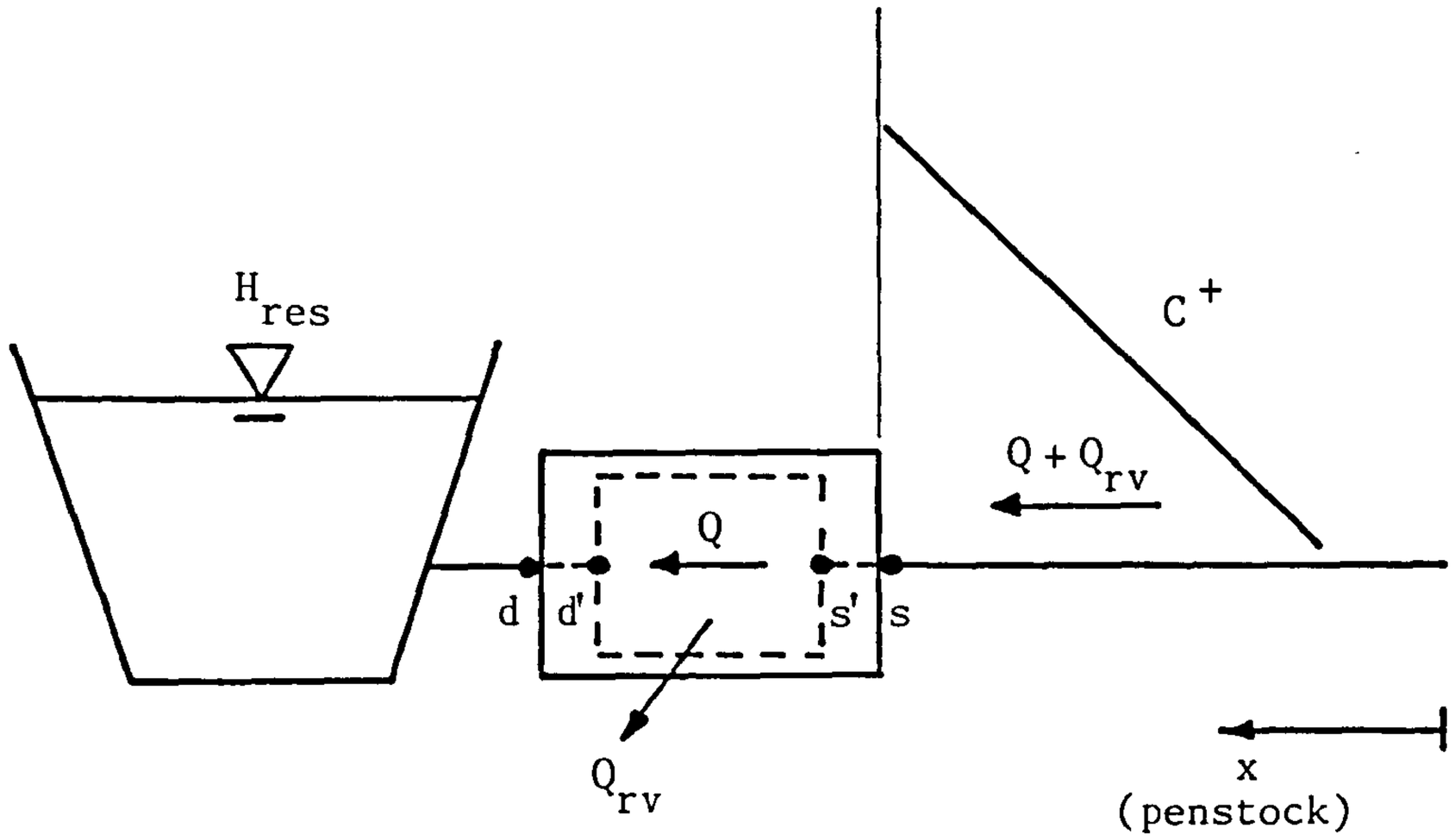

Figure 5.28 : Turbine boundary condition including relief valve for hydraulic system with no tailrace.

When a tailrace section is not present in the hydraulic system only one characteristic equation, for the penstock, is available, Figure 5.28 . The penstock characteristic equation implies :-

$$H_s^{t+\Delta t} = a_1 Q_s^{t+\Delta t} + a_2 \qquad \text{.....} \quad (5.5.38)$$

The discharge through the spiral entry, Q_s, is the sum of the discharges through the turbine and the relief valve, Q and Q_{rv}, therefore :-

$$H_s^{t+\Delta t} = a_1(Q^{t+\Delta t} + Q_{rv}^{t+\Delta t}) + a_2 \qquad \text{.....} \quad (5.5.39)$$

Substituting for the spiral head, H_s, in equation 5.5.20 the net head across the turbine is given by :-

$$H^{t+\Delta t} = a_1(Q^{t+\Delta t} + Q_{rv}^{t+\Delta t}) + a_2 - H_{res} + \Delta VH^t \qquad \text{....} \quad (5.5.40)$$

or

$$H^{t+\Delta t} = a_5 Q^{t+\Delta t} + a_6 \qquad \text{.....} \quad (5.5.41)$$

in which

$$a_5 = a_1$$

$$a_6 = a_2 - H_{res} + a_1 Q_{rv}^{t+\Delta t} + \Delta VH^t$$

Having established the constants a_5 and a_6 the solution of the turbine boundary, including a relief valve but without a tailrace section, follows that given in Section 5.5.2.

CHAPTER 6

HYDRAULIC TRANSIENT ANALYSIS AND RESULTS

6.1 INTRODUCTION

A computer program was developed to analyse the hydraulic transient response of hydro-power stations. The program incorporated the turbine performance characteristic representation recommended in Section 5.5 together with its solution algorithm. In order to demonstrate the operation of the computer program a number of hydraulic transient simulations were undertaken. Two hydro-power stations were selected for analysis which are referred to as Station A and Station B.

Station A is a pumped storage scheme incorporating 4x45 megawatt, Francis-type, pump-turbines. This scheme was selected for a number of reasons. The full hydraulic data was available for the hydraulic layout as were the pump-turbine performance characteristics. Therefore, all the necessary data input for a computer analysis were readily at hand. The pump-turbine performance characteristics also displayed re-entrants in their guide vane curves and this enabled the turbine boundary solution algorithm to be fully verified. In addition to the input data a trace taken during a full load rejection of all four pump-turbines, whilst operating in a turbining mode, was available. The results of the computer simulations could therefore be checked against these traces.

Station B is a 5x2.5 megawatt hydro-power station equipped with five Francis turbines. This station was selected to demonstrate the alternative mode of operation the computer program is able to handle and also to verify its use with a standard turbine installation. The simulation presented is typical of an early study needed to be carried

out during the feasibility stages of a hydro-power stations conception. The full hydraulic layout data was available for the analysis but no model test studies had been made on which to base the prototype performance characteristics. The turbine performance characteristics for the simulation, therefore, were obtained from the BUREC publication, as described in Section 4.4. Although Station B has not been completed to date, hence there are no site recordings available for comparison, the simulation demonstrates the use of the relief valve option.

The computer program was developed with versatility being a prime factor. Hydro-power station layouts vary greatly and care was taken to enable these to be simulated. In view of this, a study of the many variations in the layouts was undertaken to identify the requirements of a generalised hydraulic transients computer program. As a direct result of these investigations a novel method of representing the hydraulic layouts of a hydro-power station was developed. A simple code defines each pipe element and node, or boundary condition, in the system. The coded elements are manipulated into a matrix form, within the computer program, and this is used to order the calculation procedures during the steady state and transient analyses. The individual boundary condition solution algorithms incorporated in the computer program are summarised and presented in Section 6.4.

A listing of the program for the analysis of hydraulic transients in hydro-power plants, 'TRANSEX', is given in Appendix I.

6.2 MESH GENERATION ALGORITHM

In general, turbine and pump-turbine manufacturers present their performance characteristics on the unit parameter plane; unit speed versus unit discharge and unit speed versus unittorque. A typical set of performance characteristics from a reversible pump-turbine is shown in Figure 4.4 . For use in the hydraulic transients computer program these must undergo a number of modifications. The preparation of the performance characteristics requires :-

(a) digitisation of the manufacturer's unit parameter curves,

(b) transformation of the digitised points on to the exploded unit parameter plane,

(c) superimposing a curvilinear mesh on the transformed performance characteristics, and

(d) creation of a data file containing the points generated by the mesh.

The manufacturer's performance characteristics are given for a range of discrete guide vane openings. Each guide vane curve is digitised individually. A selection of points,along each curve, is chosen such that linear approximation between adjacent points gives a good correlation to the true curve. Simple, slow varying,curves require relatively few points, as for a standard turbine, where as a greater number of points are required for the more complex curves of a reversible pump-turbine. The number of points selected along each curve, however, is independent the number of points selected along the remaining curves.

The digitised unit performance characteristics are stored in a data array for use in the transformation on to the exploded unit parameter plane. The data array is given in a generalised form on the x-y plane. This

avoids the need to repeat the following procedures for the two cases of the unit speed versus unit discharge curves and the unit speed versus unit torque curves. In this generalised form the data array takes the form :-

$$x_{11} , x_{12} , \ldots\ldots , x_{1j} , \ldots\ldots , x_{1J_1}$$
$$y_{11} , y_{12} , \ldots\ldots , y_{1j} , \ldots\ldots , y_{1J_1}$$
$$\vdots \quad \vdots \qquad \vdots \qquad \vdots$$
$$x_{i1} , x_{i2} , \ldots\ldots , x_{ij} , \ldots\ldots , x_{iJ_i}$$
$$y_{i1} , y_{i2} , \ldots\ldots , y_{ij} , \ldots\ldots , y_{iJ_i}$$
$$\vdots \quad \vdots \qquad \vdots \qquad \vdots$$
$$x_{I1} , x_{I2} , \ldots\ldots , x_{Ij} , \ldots\ldots , x_{IJ_I}$$
$$y_{I1} , y_{I2} , \ldots\ldots , y_{Ij} , \ldots\ldots , y_{IJ_I}$$

in which

x_{ij} = x co-ordinate of the j^{th} point on the i^{th} guide vane curve

y_{ij} = y co-ordinate of the j^{th} point on the i^{th} guide vane curve

I = total number of guide vane curves

J_i = total number of points on the i^{th} guide vane curve

Having established the data array the digitised points are transformed from the unit parameter plane to the exploded unit parameter plane.by introducing a normalised guide vane factor. The planes of representation, from Section 5.4.4 , are given by :-

$$Q_{11} \quad \text{versus} \quad \frac{z}{z_f} n_{11} \quad \text{and} \quad M_{11} \quad \text{versus} \quad \frac{z}{z_f} n_{11}$$

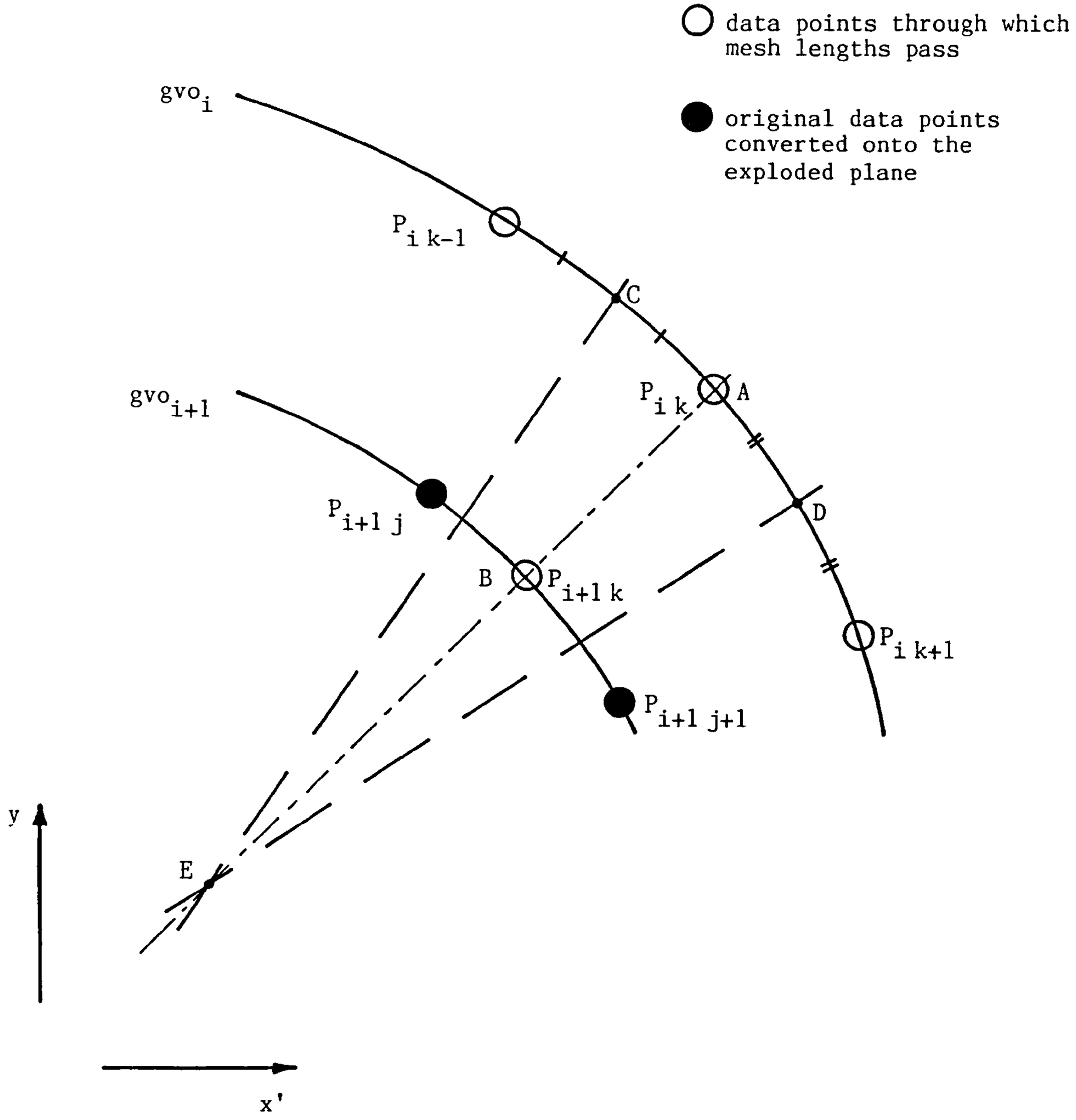

Figure 6.1 : Construction of mesh length A-B.

The transformed data array, on the generalised x-y plane, takes the form :-

$$\begin{array}{cccccc}
x'_{11} & , x'_{12} & , \ldots\ldots & , x'_{1j} & , \ldots\ldots & , x'_{1J_1} \\
y_{11} & , y_{12} & , \ldots\ldots & , y_{1j} & , \ldots\ldots & , y_{1J_1} \\
\vdots & \vdots & & \vdots & & \vdots \\
x'_{i1} & , x'_{i2} & , \ldots\ldots & , x'_{ij} & , \ldots\ldots & , x'_{iJ_i} \\
y_{i1} & , y_{i2} & , \ldots\ldots & , y_{ij} & , \ldots\ldots & , y_{iJ_i} \\
\vdots & \vdots & & \vdots & & \vdots \\
x'_{I1} & , x'_{I2} & , \ldots\ldots & , x'_{Ij} & , \ldots\ldots & , x'_{IJ_I} \\
y_{I1} & , y_{I2} & , \ldots\ldots & , y_{Ij} & , \ldots\ldots & , y_{IJ_I}
\end{array}$$

in which

$$x'_{ij} = x_{ij} \left\{ \frac{i^{th} \text{ guide vane opening}}{1^{st} \text{ guide vane opening}} \right\}$$

As described in Section 5.4.4 this transformation opens out the unit parameter guide vane curves on to the exploded unit parameter plane and it is on these curves that the curvilinear mesh is superimposed.

Consider the construction of a section of the mesh, A-B, as shown in Figure 6.1 . The mesh length A-B lies between the i^{th} and $i+1^{th}$ guide vane curves. The mesh length passes through point A, whose co-ordinates are given by (x'_{ik}, y_{ik}), which is a known data point and the point B, whose co-ordinates are given by (x'_{i+1k}, y_{i+1k}), is to be found such that the mesh length A-B forms an approximate curvilinear mesh with the i^{th} and $i+1^{th}$ guide vane curves. Let the data points on the i^{th} guide vane curve, either side of point A, be given by $(x'_{i\,k-1}, y_{i\,k-1})$ and $(x'_{i\,k+1}, y_{i\,k+1})$. The data points in close proximity to point B, on the $i+1^{th}$ guide vane curve are given by $(x'_{i+1\,j}, y_{i+1\,j})$ and $(x'_{i+1\,j+1}, y_{i+1\,j+1})$.

The data points on the i^{th} guide vane curve are calculated data points through which the $k-1^{th}$, k and $k+1^{th}$ mesh lengths pass. The data points on the $i+1^{th}$ guide vane curve are the original data points transformed onto the exploded unit parameter plane. Let the mid points along the guide vane sections either side of point A be given by points C and D where :-

$$x'_c = \frac{x'_{i\,k-1} - x'_{i\,k}}{2} \qquad \ldots\ldots\ldots\ldots \qquad (6.2.1)$$

$$y_c = \frac{y_{i\,k-1} - y_{i\,k}}{2} \qquad \ldots\ldots\ldots\ldots \qquad (6.2.2)$$

$$x'_d = \frac{x'_{i\,k+1} - x'_{i\,k}}{2} \qquad \ldots\ldots\ldots\ldots \qquad (6.2.3)$$

$$y_d = \frac{y_{i\,k+1} - y_{i\,k}}{2} \qquad \ldots\ldots\ldots\ldots \qquad (6.2.4)$$

The perpendicular bisectors of the guide vane sections, passing through points C and D, are given by :-

$$y = m_1 x' + c_1 \qquad \ldots\ldots\ldots\ldots \qquad (6.2.5)$$

and

$$y = m_2 x' + c_2 \qquad \ldots\ldots\ldots\ldots \qquad (6.2.6)$$

in which

$$m_1 = -\frac{x'_{i\,k-1} - x'_{i\,k}}{y_{i\,k-1} - y_{i\,k}}$$

$$m_2 = -\frac{x'_{i\,k+1} - x'_{i\,k}}{y_{i\,k+1} - y_{i\,k}}$$

$$c_1 = y_c - m_1 x'_c$$

$$c_2 = y_d - m_2 x'_d$$

The perpendicular bisectors intersect at point E where :-

$$x'_e = \frac{c_1 - c_2}{m_2 - m_1} \qquad \ldots\ldots\ldots\ldots \qquad (6.2.7)$$

$$y_e = m_1 x'_e + c_1 = m_2 x'_e + c_2 \qquad \ldots\ldots\ldots\ldots \qquad (6.2.8)$$

The mesh length lies along A-E which is given by the linear equation :-

$$y = m_3 x' + c_3 \qquad \ldots\ldots\ldots\ldots \qquad (6.2.9)$$

in which

$$m_3 = \frac{y_{i\,k} - y_e}{x'_{i\,k} - x'_e}$$

$$c_3 = y_{i\,k} - m_3 x'_{i\,k} = y_e - m_3 x'_e$$

and this intersects the guide vane section along the $i+1^{th}$ guide vane curve at point B, The linear equation of the guide vane section is :-

$$y = m_4 x' + c_4 \qquad \ldots\ldots\ldots\ldots \qquad (6.2.10)$$

in which

$$m_4 = \frac{y_{i+1\,j+1} - y_{i+1\,j}}{x'_{i+1\,j+1} - x'_{i+1\,j}}$$

$$c_4 = y_{i+1\,j+1} - m_4 x'_{i+1\,j+1} = y_{i+1\,j} - m_4 x'_{i+1\,j}$$

The co-ordinates of point B, therefore, are given by :-

$$x'_b = \frac{c_3 - c_4}{m_4 - m_3} \qquad \ldots\ldots\ldots\ldots \qquad (6.2.11)$$

$$y_b = m_3 x'_b + c_3 = m_4 x'_b + c_4 \qquad \ldots\ldots\ldots\ldots \qquad (6.2.12)$$

This procedure is repeated for each data point along the i^{th} guide vane curve to establish the full set of data points through which the mesh lengths pass on the $i+1^{th}$ guide vane curve. The calculated co-ordinates at point B are stored as $(x'_{i+1\,k}, y_{i+1\,k})$ at the intersection of the $i+1^{th}$ guide vane curve with the k^{th} mesh line. The calculated points on the $i+1^{th}$ guide vane curve are then used to calculate the data points on the $i+2^{th}$ guide vane curve through which the mesh lengths will pass.

This routine is repeated for each pair of adjacent guide vane curves and will conclude with the fully closed guide vane curve. The final data array becomes :-

$$\begin{matrix} x'_{11} , x'_{12} , \ldots\ldots , x'_{1k} , \ldots\ldots , x'_{1K} \\ y_{11} , y_{12} , \ldots\ldots , y_{1k} , \ldots\ldots , y_{1K} \\ \vdots \quad \vdots \qquad\qquad \vdots \qquad\qquad \vdots \\ x'_{i1} , x'_{i2} , \ldots\ldots , x'_{ik} , \ldots\ldots , x'_{iK} \\ y_{i1} , y_{i2} , \ldots\ldots , y_{ik} , \ldots\ldots , y_{iK} \\ \vdots \quad \vdots \qquad\qquad \vdots \qquad\qquad \vdots \\ x'_{I1} , x'_{I2} , \ldots\ldots , x'_{Ik} , \ldots\ldots , x'_{IK} \\ y_{I1} , y_{I2} , \ldots\ldots , y_{Ik} , \ldots\ldots , y_{IK} \end{matrix}$$

in which

K = total number of points along each guide vane curve

The total number of data points along each guide vane curve, K , is by default the number of data points along the first, or maximum, guide vane curve, J_1. These are taken as the initialising data points from which the mesh lengths eminate. It is particularly important, therefore, that an evenly distributed range of data points are taken during the initial tabulation of the guide vanes, from the unit parameter plane, along the maximum guide vane opening. It should also be noted that these data points remain unaltered on conversion to the exploded unit parameter plane as the normalising factor is the maximum guide vane opening itself. The spacing of the data points on the unit parameter plane, therefore, remains unaltered when converted onto the exploded unit parameter plane.

A listing of the mesh generation program 'SMESHJ', including the conversion from the unit parameter plane, is given in Appendix IV and

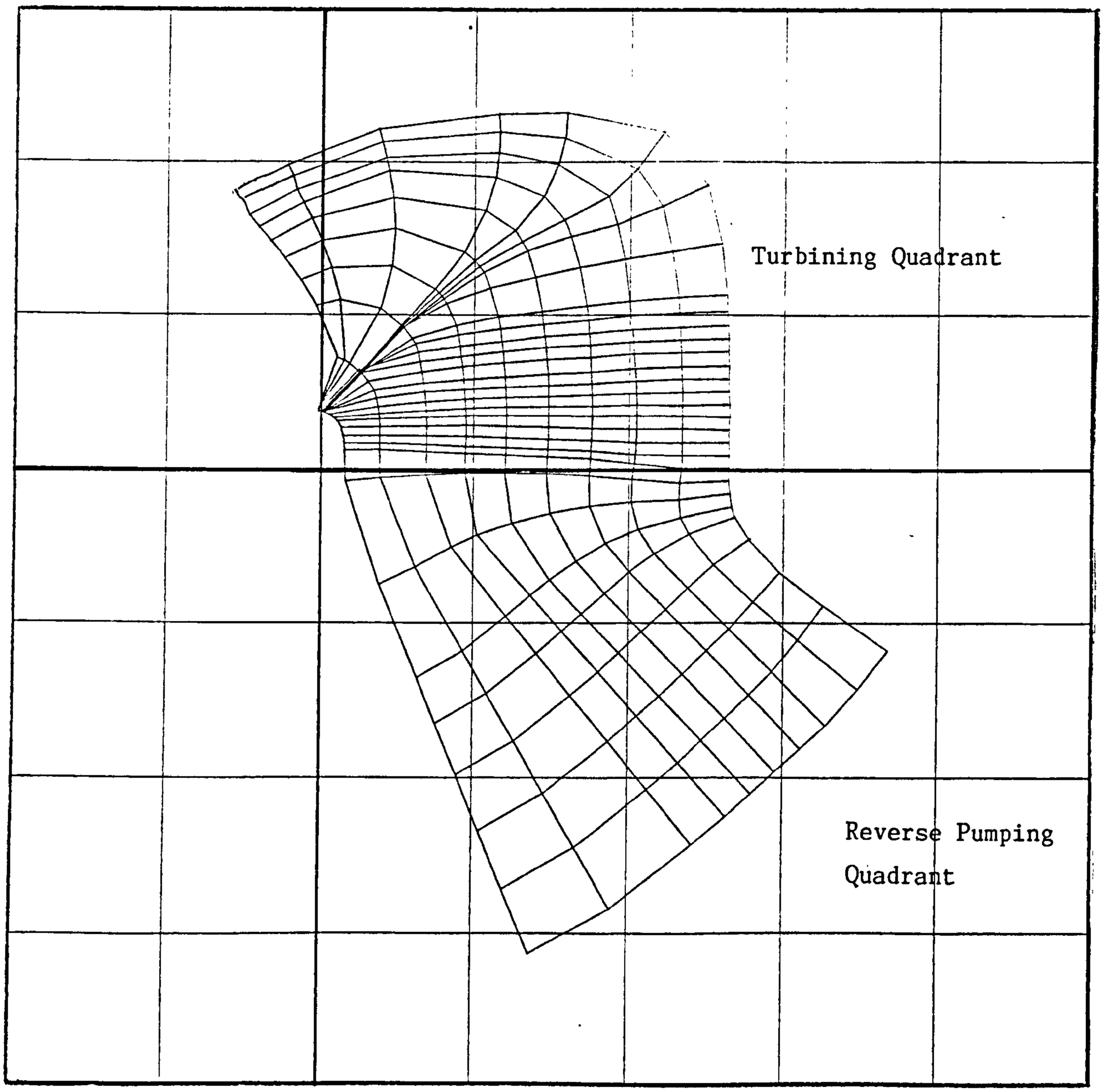

Figure 6.2 : Curvilinear mesh superimposed on the turbining and reverse pumping quadrants.

an example of its use with performance characteristics is shown in Figure 6.2. The curvilinear mesh is superimposed on the turbining and reverse pumping quadrants of a typical set of reversible, Francis-type, pump-turbine characteristics.

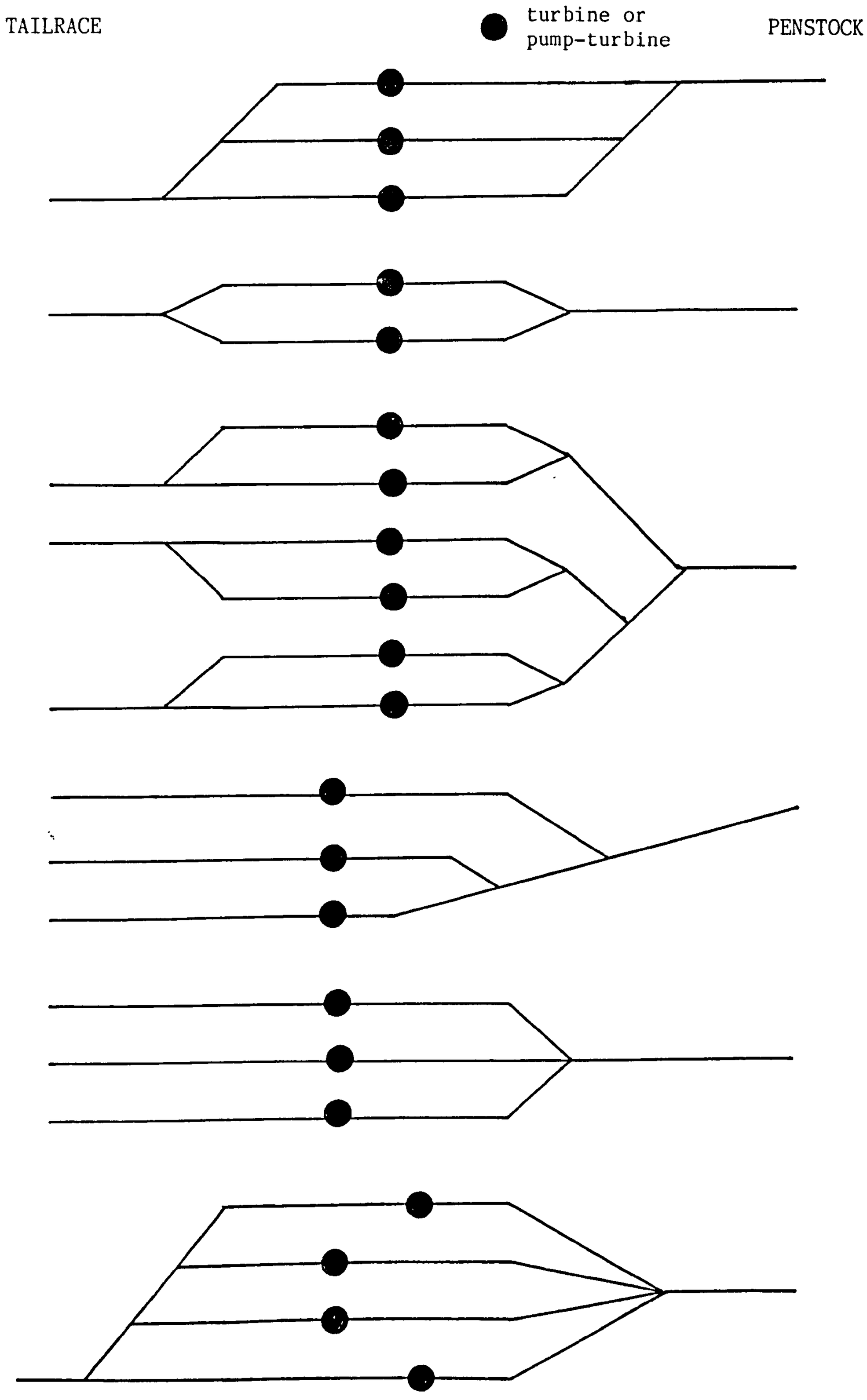

Figure 6.3 : Schematic layouts of a number of hydro-power plants

6.3 HYDRO-POWER PLANT LAYOUTS AND THEIR REPRESENTATION

6.3.1 Hydro-power Plant Layouts

A prime feature of hydro-power plants is their individuality, no two installations having identical hydraulic layouts or mechanical equipment. The development of a computer program for the analysis of hydraulic transients, therefore, requires an appraisal of the many varied layouts and the associated mechanical components, or boundary conditions.

This research was funded by the Science and Engineering Research Council (SERC) under a Collaborate Award in Science and Engineering (CASE) scheme. The collaborating body were Ewbank Preece Consultants of Brighton. Under this scheme a total of six months of the three year research period were undertaken whilst at Ewbank Preece's main Hydro Department offices. Advantage was taken during one of these study periods to carry out a study of hydro-power plant layouts. The aim of the study was to assess the needs of a generalised hydraulic transients computer program and to develop a a means of representing the various layouts within the program.

A number of sections from the layouts of hydro-power plants are shown schematically in Figure 6.3 . The principal feature of these layouts is that whilst a number of the layouts are symmetrical a large proportion are asymmetrical. A generalised hydraulic transients program must therefore be able to handle both classifications of layouts. The typical layouts also demonstrate some of the basic boundary conditions to be found in any layout; turbines or pump-turbines, pipe junctions and pipe branches. For a given laycut some of the following boundary conditions may also be included in the system ; reservoirs , main inlet valves, tailrace valves, and surge tanks. The algorithms for the solution of these boundary conditions and a method of simulating the many varied hydraulic layouts are presented in Section 6.3 and 6.4.

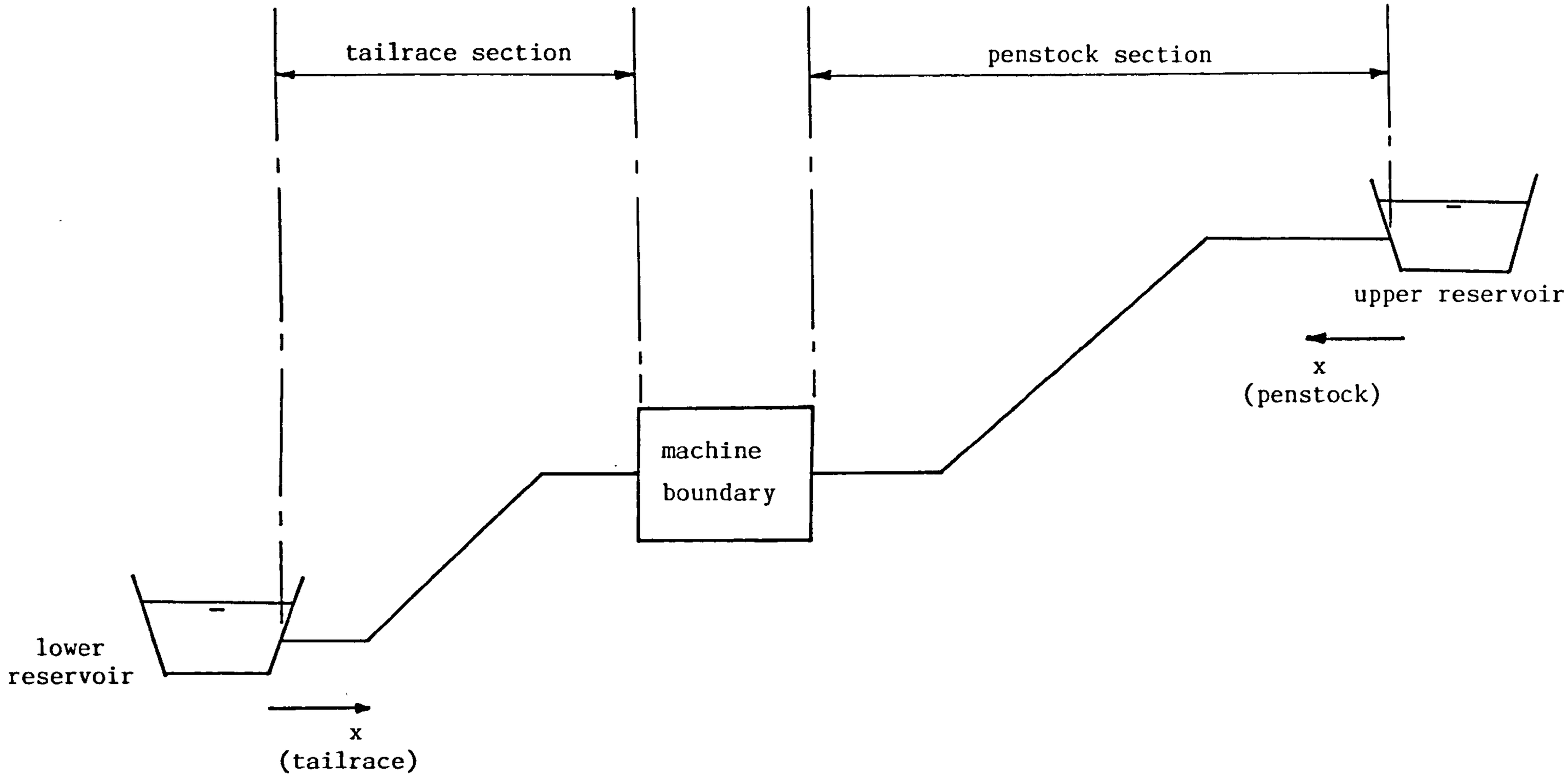

Figure 6.4 : Subdivision of the hydraulic system into a penstock and tailrace section.

6.3.2 Sign Convention

Hydro-power stations can be divided into two separate hydraulic systems with the turbine or pump-turbine serving as a common boundary. The upstream, or penstock, system comprises of the pipe elements and mechanical components between the upper reservoir and the machine boundary and the downstream, or tailrace, system is that from the lower reservoir to the machine boundary. The sub-division of the hydraulic layout is shown schematically in Figure 6.4 . The sign conventions for the two systems are also shown in Figure 6.4 . A positive x direction is that from the reservoir to the machine boundary, whether considering the penstock or tailrace. Positive flow in the two systems is also taken along these directions. However, when considering the turbine or pump-turbine boundary the machine discharge is defined as that when they operate in a turbining mode. This results in a positive flow in the positive x direction for the penstock and a positive flow in the negative x direction for the tailrace.

The advantage of using this sign convention is that the two systems can be analysed using the same solution algorithms. Generalised solution algorithms can be developed which do not need to distinguish between the tailrace and penstock systems. Within the hydraulic transient analysis program, 'TRANSEX', the generalised boundary conditions form subroutines. When a subroutine is called the relevant data is input into the subroutine, whether for the penstock or the tailrace, and output results are sent to directly into the result arrays, which are stored separately for the two systems. The calculation procedure performed in the subroutine, however, remains the same for both the tailrace and penstock systems.

6.3.3 System Identification

In Section 6.3.2 the sign convention adopted for the hydraulic transient studies was described. The hydraulic system is subdivided into two separate systems, the penstock system and the tailrace system. Each of these consists of a number of pipe reaches and their adjoining boundary elements. The arrangement of these elements within a hydro-power station varies from one station to another. In analysing their transient response it is therefore desirable to be able to identify the individual arrangements in a completely general manner. An original method, referred to as the System Identification Matrix or SIM, was developed as part of this research for representing hydro-power station layouts.

The SIM is generated during the during the initial input of data to the transients program and once established remains unchanged throughout the computational procedure. In the hydraulic transients analysis program, 'TRANSEX', the SIM is utilised during the steady state analysis and during the subsequent transient analysis. The SIM is used to order the calculation procedures in both cases and selects the subroutines needed for the solution of the boundary conditions and the internal nodes within the pipe reaches.

$\underline{X}$ = pipe number

X = node number

node number	node identification number
1	1
2	2
3	11
4	12
5	31
6	21
7	40
8	51

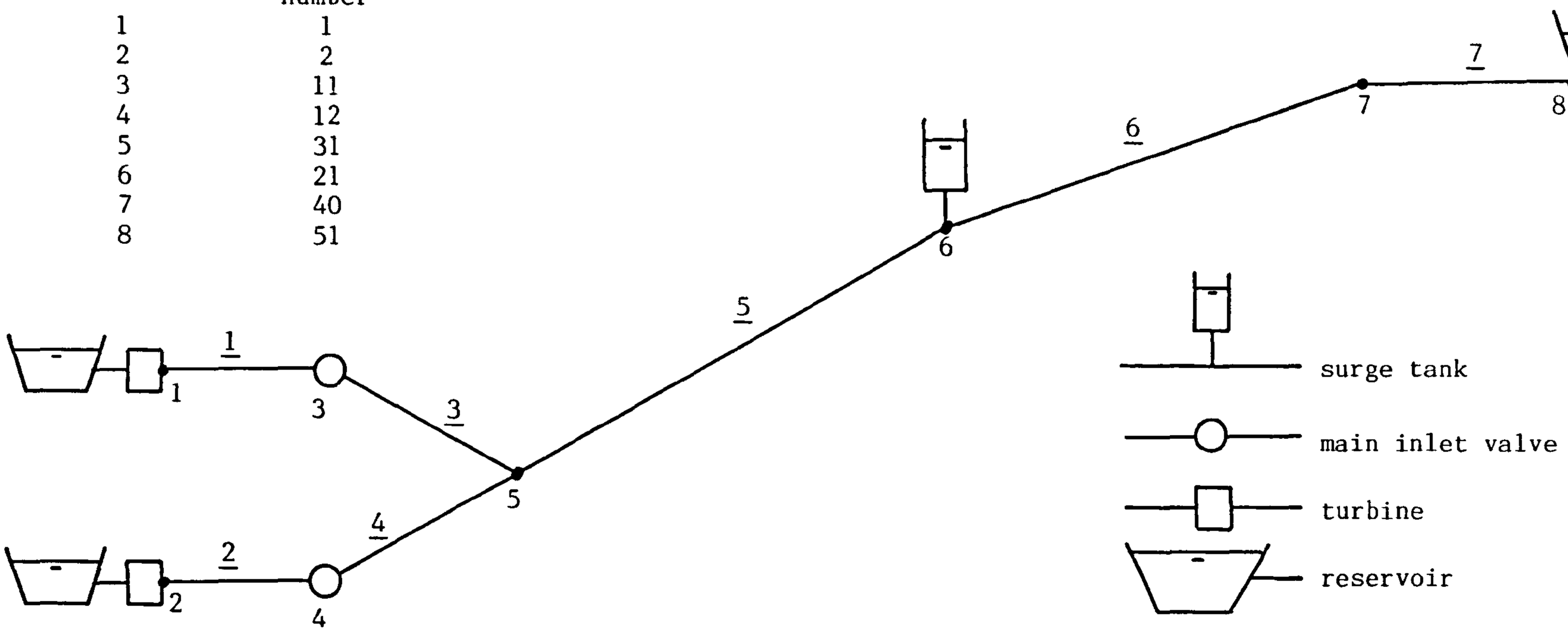

Figure 6.5 : Typical hydraulic system with pipe and node numbers applied.

6.3.4 System Identification Matrix (SIM)

The initial labelling of the hydraulic system is undertaken in the standard manner, as given in the principal texts [14]. To each pipe length within the system a pipe number is assigned and, similarly, to each boundary condition a node number is assigned. Figure 6.5 shows a typical hydraulic system, schematically, to which the pipe numbers and node numbers have been allocated. The system shown includes some typical hydropower plant boundary conditions such as turbines, main inlet valves, surge tanks, pipe branches, pipe junctions and reservoirs. Although a tailrace system is not included the formation of the SIM for the penstock system is identical to that for the tailrace system. In cases where a tailrace is included, therefore, a SIM is formed for both the penstock and tailrace systems.

The SIM allows the labelling of the pipe and node numbers, provided they are monotonically increasing, to be selected randomly except at the turbine boundary. At the turbine boundary the pipe and node numbers must correspond to the turbine number. Hence, turbine number one is connected to pipe number one and this junction occurs at node number one, as shown in Figure 6.5 . Likewise, turbine number two is connected to pipe number two at node number two, and so forth for each turbine in the hydraulic system. This restriction in the labelling of the pipe and node numbers is also applicable to the tailrace system, if one is present. In these cases pipe number one and node number one, in the tailrace, form the connecting pipe and junction with turbine number one respectively. Again, this is repeated for each turbine in the hydraulic system. The subsequent labelling of the pipe and node numbers, however, is arbitary provided the numbering is consecutive and follows from the highest pipe and node number to be found at a turbine boundary.

In addition to the node number of a boundary condition the SIM requires a node identification number. This identifies the type of boundary condition that is present at a particular node and specifies precisely which boundary condition of that type is being referenced. A numerical code is adopted for the node identification number which gives the necessary information.

The node identification number takes the form of a two digit number which in a generalised form is given by :-

$\underline{X}\,\underline{Y}$

where

$\underline{X}$ represents the type of boundary

$\underline{Y}$ represents the i^{th} boundary of this type

The code adopted for the type of boundary is as follows :-

$\underline{X}$ = 0 , turbine or pump-turbine

= 1 , main inlet, or in-line, valve

= 2 , surge tank

= 3 , 1-n pipe branch

= 4 , 1-1 pipe junction

= 5 , reservoir

A node identification number given as '13' therefore indicates the third main inlet valve in the hydraulic system and, similarly, one given as '01', which is abreviated to '1', indicates turbine number one. This method of coding permits a maximum of ten boundaries of the same type to be represented in both the penstock and tailrace systems. The one exception to this limitation is the 1-1 pipe junction. Due to the form the SIM takes it is unnecessary to identify each 1-1 pipe junction individually. The SIM itself indicates the pipes entering and leaving a junction and therefore only the type of boundary coding becomes relevant. This is important

as the number of 1-1 pipe junctions, particularly in a complex hydraulic system, will be greater than ten, the limit imposed on the remaining boundary conditions. However, the possibility of encountering more than ten of the latter boundary conditions in a penstock or tailrace system is extremely remote.

The SIM arranges the pipe numbers and node numbers, together with their node identification numbers, in a two dimensional array to give a numerical representation of the hydraulic system. This is then decoded in the computer program in order to identify the necessary elements which are needed to solve each boundary condition. The SIM is stored in an array given by :-

SYSP(I,J) for the penstock

and

SYST(I,J) for the tailrace

in which

I = 1 or 2

J = total number of elements in the array

The coded elements are introduced in to the array as given below.

Pipe elements require only their pipe number to distinquish them and these are entered into the SIM as :-

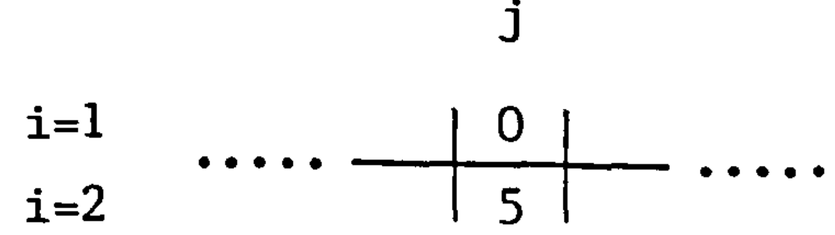

to represent pipe number five. In general, if SYSP(1,j) equals zero this indicates a pipe element and SYSP(2,j) gives the pipe number. Alternatively, a node, or boundary condition, requires its node number and node identification number to distinquish it. These are entered into the SIM

as follows :-

	j
i=1	5
i=2	11

where this represents node 5 at which there is main inlet valve and this is valve number one. In general, SYSP(1,j) gives the node number and SYSP(2,j) gives the node identification number.

The SIM elements are entered into the array in the order they occur in the hydraulic system if one travels from the turbine to the reservoir. The array is is initialised from turbine number one and proceeds until a 1-n pipe branch or reservoir is encountered. The initial elements of the hydraulic system given in Figure 6.5 are given by :-

1	0	3	0	5	.....
1	1	11	3	31	

upto the bifurcation. When a bifurcation is encountered the next element in the SIM is taken as the next turbine. The procedure is then repeated, travelling form the turbine towards the reservoir, until a 1-n pipe branch or a reservoir is encountered. In this example the SIM becomes :-

1	0	3	0	5	2	0	4	0	5	.....
1	1	11	3	31	2	2	12	4	31	

When each branching pipe has been included in the SIM the 1-n pipe branch is taken as the starting element and one travels from this towards the reservoir, inserting the elements in the SIM as they are encountered. When a reservoir boundary is entered into the SIM two courses of action can be taken. If all the turbines in the hydraulic system have been entered into the SIM the SIM is now complete, however, if not, the next turbine is entered and the above procedure repeated until all the elements have been included. The completed SIM for this hydraulic system, therefore, is given by :-

1	0	3	0	5	2	0	4	0	5	5	0	6	0	7	0	8
1	1	11	3	31	2	2	12	4	31	31	5	21	6	40	7	51

If the hydraulic layout of a hydro-power plant includes a tailrace system a second SIM needs to be established. The procedure followed to form the SIM is identical to that given for the example layout shown in Figure 6.5 but the coded elements are stored in a separate array as :-

$$SYST(I,J_t)$$

in which

I = 2

J_t = total number of elements in the array for the tailrace

6.4 BOUNDARY CONDITION SOLUTION ALGORITHMS

6.4.1 Introduction

The most important boundary condition to be found in a hydro-power plant is the turbine or pump-turbine boundary. An algorithm for the solution of this boundary condition was developed in Section 5.5.2. which included an option of having a relief valve connected to the spiral casing. In addition to the turbine or pump-turbine boundary, the analysis of hydraulic transients in hydro-power plants requires solution algorithms for the remaining boundary conditions.

Solution algorithms for the following boundary conditions are presented in this Section ; main inlet valves, surge tanks, 1-n pipe branches, reservoirs and 1-1 pipe junctions. In addition the solution of an internal node in a pipe reach is given. These solution algorithms correspond to subroutines in the transient analysis program, 'TRANSEX', as given below :-

main inlet valve	SUBROUTINE TRMV
surge tank	SUBROUTINE TRST
1-n pipe branch	SUBROUTINE TRBR
reservoir	SUBROUTINE TRRES
1-1 pipe junction	SUBROUTINE TRJN

The solution of the internal nodes within a pipe reach are solved for all the pipes in the hydraulic system, that is :-

internal nodes	SUBROUTINE NODE

The solution of the turbine or pump-turbine boundary condition in 'TRANSEX' precedes the solutions of the other boundary conditions, being calculated immediately after a new calculation time step has been initiated.

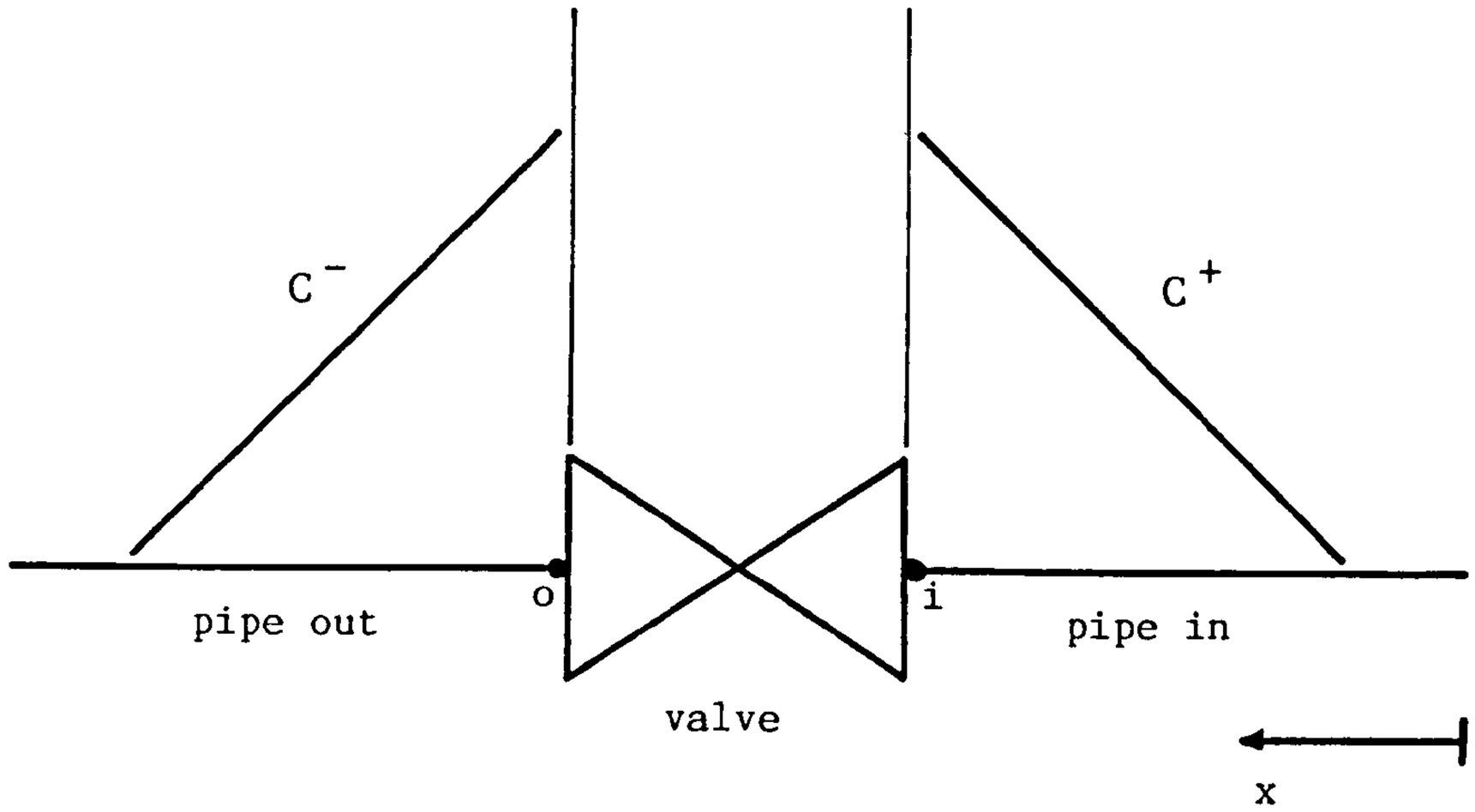

Figure 6.6 : Main inlet valve boundary condition

6.4.2 Main Inlet Valve

The characteristic equations either side of the main inlet valve, Figure 6.6 , give :-

$$C^+: \quad v_i^{t+\Delta t} = a_1 H_i^{t+\Delta t} + a_2 \qquad \ldots\ldots\ldots\ldots \qquad (6.4.1)$$

and

$$C^-: \quad v_o^{t+\Delta t} = a_3 H_o^{t+\Delta t} + a_4 \qquad \ldots\ldots\ldots\ldots \qquad (6.4.2)$$

in which

v_i = velocity at end of pipe in

H_i = head at end of pipe in

v_o = velocity at start of pipe out

H_o = head at start of pipe out

and a_1, a_2, a_3 and a_4 are known constants. From continuity of flow through the valve it follows that :-

$$Q^{t+\Delta t} = A_i v_i^{t+\Delta t} = A_o v_o^{t+\Delta t} \qquad \ldots\ldots\ldots\ldots \qquad (6.4.3)$$

in which

Q = discharge through the valve

A_i = cross-sectional area of pipe in

A_o = cross-sectional area of pipe out

The discharge through the valve can also be written in terms of the energy heads across the valve to give :-

$$Q = k_d A_v \left\{ 2g (H_i - H_o) + (v_i^2 - v_o^2) + \frac{Q^2}{A_v^2} \right\}^{0.5} \qquad \ldots\ldots \qquad (6.4.4)$$

in which

k_d = valve discharge coefficient

A_v = cross-sectional area of the valve

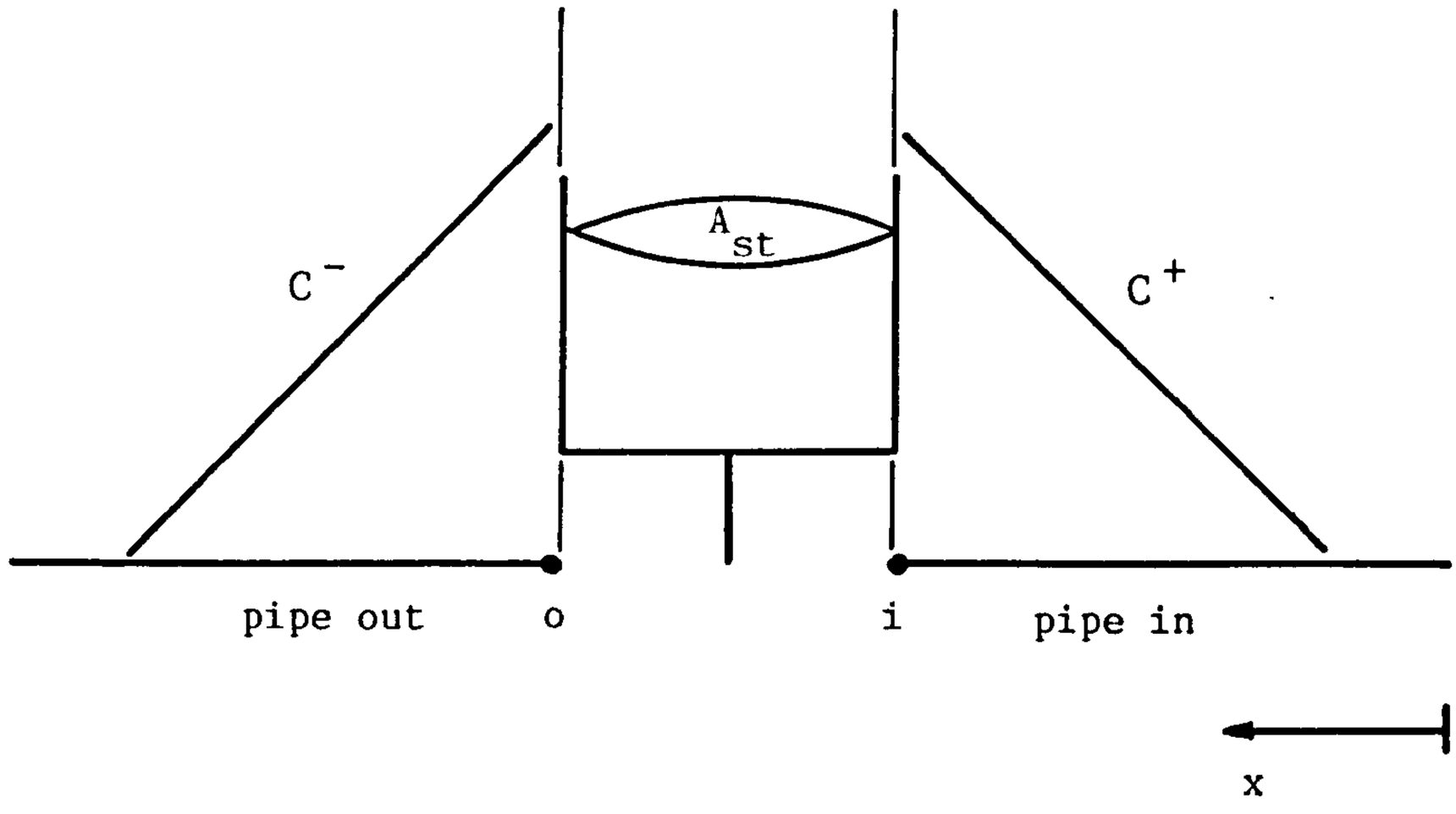

Figure 6.7 : Surge tank boundary condition.

Taking equation 6.4.4 at a time $t+\Delta t$ and combining this with characteristic and continuity equations, equations 6.4.1, 6.4.2 and 6.4.3 respectively, to eliminate the head terms, H_i and H_o, gives a quadratic function of the discharge through the valve, Q, of the form :-

$$f(Q^{t+\Delta t}) = b_1 Q^{t+\Delta t\,2} + b_2 Q^{t+\Delta t} + b_3 = 0 \quad \ldots\ldots \qquad (6.4.5)$$

in which

$$b_1 = \left\{ \frac{1}{k_d^{\,2}} - 1 \right\} \frac{1}{2 g A_v^{\,2}}$$

$$b_2 = \frac{1}{A_o a_3} - \frac{1}{A_i a_1}$$

$$b_3 = \frac{a_2}{a_1} - \frac{a_4}{a_3} - \Delta VH^t$$

The velocity head, ΔVH, is given as that for time t in the constant b_3 and this replaces the true velocity head which should be that at time $t+\Delta t$. The validity of this approximation has been previously discussed in Section 5.3.4.

The quadratic function, equation 6.4.5, is solved using a standard Newton-Raphson technique with the discharge through the valve at time t, Q^t , used as the initial estimate of the discharge. The velocities and heads at the valve inlet and outlet follow from the solution of equation 6.4.5 being substituted in eqvations 6.4.3, 6.4.1 and 6.4.2.

6.4.3 Surge Tank

The characteristic equations either side of the surge tank, Figure 6.7 give :-

$$C^+ : \quad v_i^{t+\Delta t} = a_1 H_i^{t+\Delta t} + a_2 \qquad \ldots\ldots\ldots\ldots \qquad (6.4.6)$$

and

$$C^- : \quad v_o^{t+\Delta t} = a_3 H_o^{t+\Delta t} + a_4 \qquad \ldots\ldots\ldots\ldots \qquad (6.4.7)$$

Continuity of flow implies :-

$$Q_i^{t+\Delta t} = Q_o^{t+\Delta t} + Q_{st}^{t+\Delta t} \qquad \text{.....} \qquad (6.4.8)$$

where

Q_i = discharge through the pipe in

Q_o = discharge through the pipe out

Q_{st} = discharge into the surge tank

The discharge into the surge tank varies only slightly between time steps and an estimate of this discharge is given by :-

$$Q_{st_e}^{t+\Delta t} = 2\,Q_{st}^{t} - Q_{st}^{t-\Delta t} \qquad \text{.....} \qquad (6.4.9)$$

where Q_{st}^{t} and $Q_{st}^{t-\Delta t}$ are the known discharges at the previous two time intervals. The corresponding head loss within the surge tank riser is given by :-

$$H_{st_{loss}}^{t+\Delta t} = K\,Q_{st}^{t+\Delta t}\,|Q_{st}^{t+\Delta t}| \qquad \text{.....} \qquad (6.4.10)$$

in which

$H_{st_{loss}}$ = riser head loss

K = riser head loss coefficient

An estimate of the surge tank water elevation at time $t+\Delta t$ based on the estimated discharge in to the surge tank is given by :-

$$z_{st_e}^{t+\Delta t} = z_{st}^{t} + Q_{st_e}^{t+\Delta t}\,\frac{\Delta t}{A_{st}} \qquad \text{.....} \qquad (6.4.11)$$

in which

z_{st_e} = estimated surge tank water elevation

z_{st} = calculated surge tank water elevation

A_{st} = surge tank cross-sectional area

Δt = time step interval

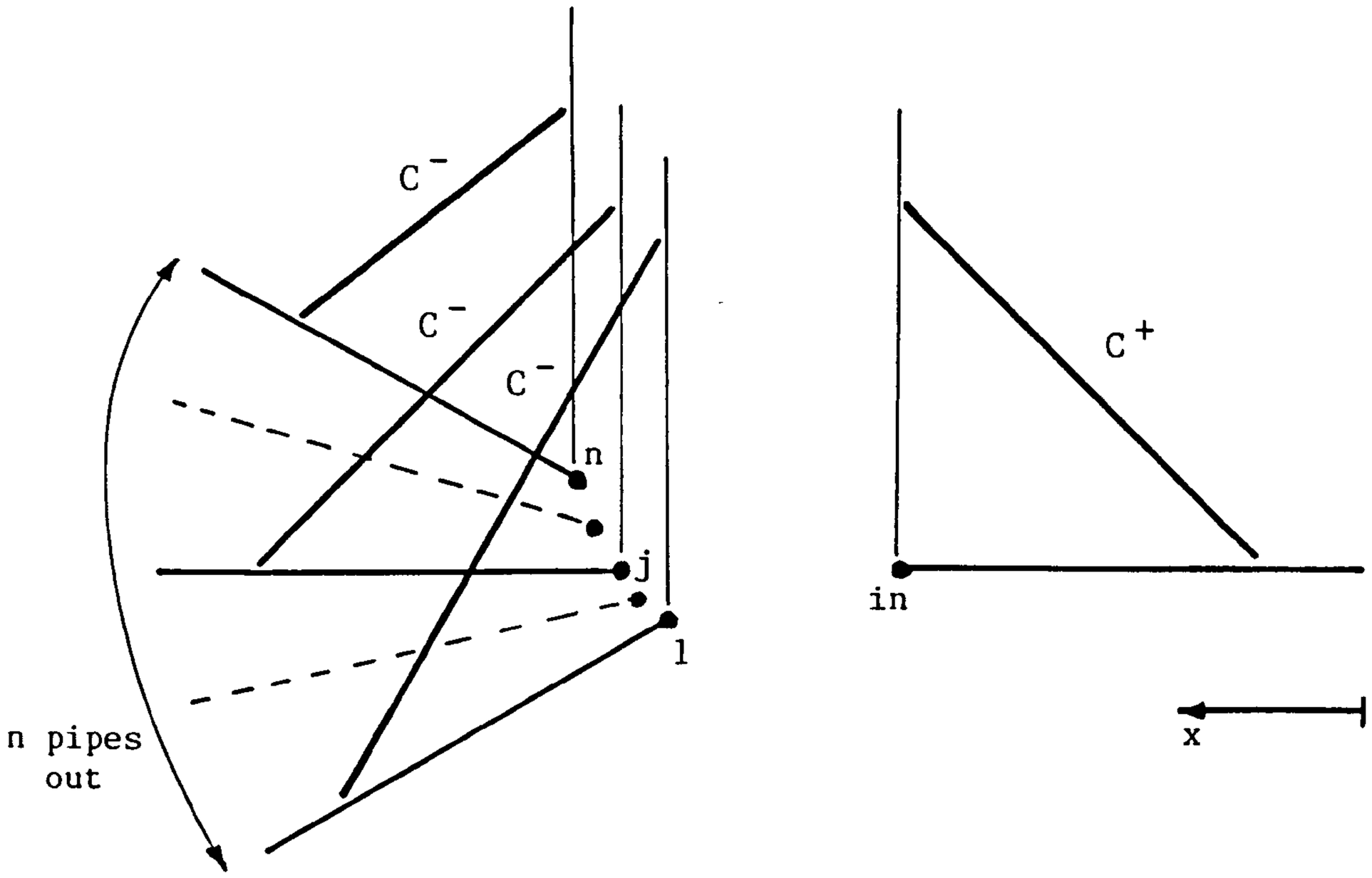

Figure 6.8 : 1-n pipe boundary condition.

The heads either side of the surge tank boundary are therefore given by :-

$$H_i^{t+\Delta t} = z_{st_e}^{t+\Delta t} + H_{st_{loss}}^{t+\Delta t} \qquad \text{.....} \quad (6.4.12)$$

and

$$H_o^{t+\Delta t} = z_{st_e}^{t+\Delta t} - \frac{v_o^t{}^2}{2g} \qquad \text{.....} \quad (6.4.13)$$

Substituting the calculated heads from equations 6.4.12 and 6.4.13 in to the charcteristic equations, equations 6.4.6 and 6.4.7, gives the respective flow velocities at the pipe junctions indicated by nodes i and o. The actual discharge in to the surge tank and its water elevation can then be calculated from :-

$$Q_{st}^{t+\Delta t} = Q_i^{t+\Delta t} - Q_o^{t+\Delta t} \qquad \text{.....} \quad (6.4.14)$$

and

$$z_{st}^{t+\Delta t} = z_{st}^{t} + Q_{st}^{t+\Delta t} \frac{\Delta t}{A_{st}} \qquad \text{.....} \quad (6.4.15)$$

respectively.

6.4.4 1-n Pipe Branch

The characteristic equation for the pipe in at the branch, Figure 6.8 gives :-

$$C^+ : \quad v_{in}^{t+\Delta t} = a_1 H_{in}^{t+\Delta t} + a_2 \qquad \text{.....} \quad (6.4.16)$$

and each of the characteristic equations of the branch pipes are given by :-

$$C^- : \quad v_j^{t+\Delta t} = a_{3j} H_j^{t+\Delta t} + a_{4j} \quad \text{for } j=1,n \quad \text{....} \quad (6.4.17)$$

Continuity of flow at the branch requires that :-

$$Q_{in}^{t+\Delta t} = Q_1^{t+\Delta t} + Q_2^{t+\Delta t} + \text{....} + Q_j^{t+\Delta t} + \text{....} + Q_n^{t+\Delta t} \qquad (6.4.18)$$

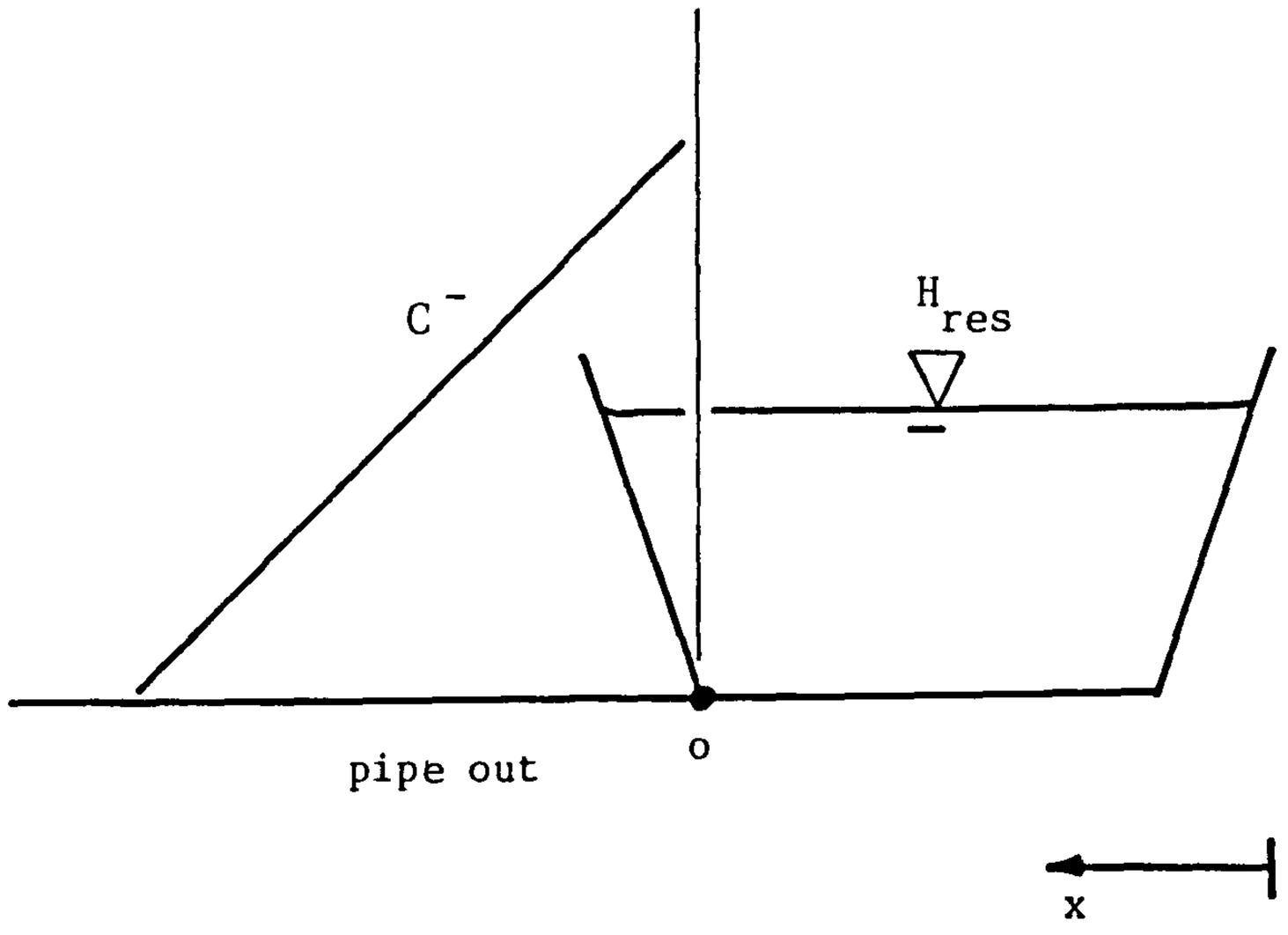

Figure 6.9 : Reservoir boundary condition.

At the branch there is also a common energy head, therefore :-

$$H_{in}^{t+\Delta t} = H_j^{t+\Delta t} + \Delta VH_j^{t+\Delta t} \qquad \text{for } j=1,n \qquad \ldots\ldots\ldots \quad (6.4.19)$$

in which

ΔVH = velocity head across the pipe in and the j^{th} pipe out, at time $t+\Delta t$

This velocity head term only varies slightly from one time step to the next and equation 6.4.19 can be re-written in terms of the known velocity head at time t, to give :-

$$H_{in}^{t+\Delta t} = H_j^{t+\Delta t} + \Delta VH_j^{t} \qquad \text{for } j=1,n \qquad \ldots\ldots\ldots \quad (6.4.20)$$

Combining equations 6.4.16, 6.4.17, 6.4.18 and 6.4.20 leads to the solution of the head at the end of the pipe in, where :-

$$H_{in}^{t+\Delta t} = \frac{A_{in}\, a_2 - \sum_{j=1}^{n} (A_j\, a_{3j}\, \Delta VH^t + A_j\, a_{4j})}{-A_{in}\, a_1 + \sum_{j=1}^{n} (A_j\, a_{3j})} \qquad \ldots\ldots\ldots \quad (6.4.21)$$

in which

A_{in} = cross-sectional area of pipe in

A_j = cross-sectional area of j^{th} pipe out

The corresponding value of $v_{in}^{t+\Delta t}$ is found by substituting the solution of equation 6.4.21 in equation 6.4.16. The head and velocity terms of the pipes out, $H_j^{t+\Delta t}$ and $v_j^{t+\Delta t}$ for j=1,n , follow from equations 6.4.20 and 6.4.17 respectively.

6.4.5 Reservoir

The single characteristic equation, Figure 6.9 , for the reservoir boundary is given by :-

$$C^- : \quad v_o^{t+\Delta t} = a_3 H_o^{t+\Delta t} + a_4 \qquad \ldots\ldots\ldots\ldots \quad (6.4.21)$$

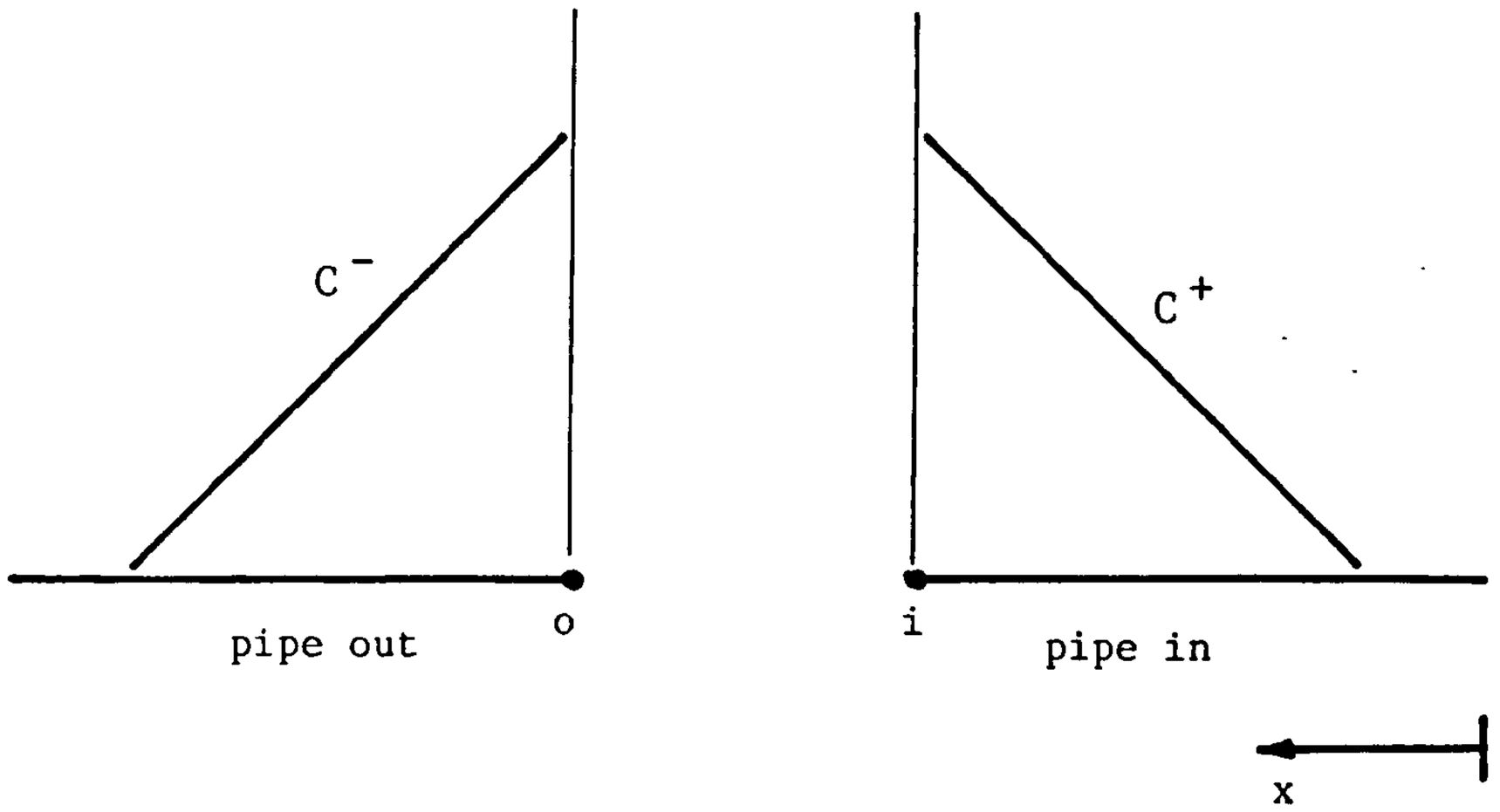

Figure 6.10 : 1-1 pipe junction boundary condition

The reservoir level is assumed to be constant and the head at the start of the pipe out is related to this by :-

$$H_o^{t+\Delta t} = H_{res} + L\frac{v_o^{t+\Delta t}{}^2}{2g} \qquad \text{.....} \quad (6.4.22)$$

in which

H_{res} = reservoir level

L = 0; for flow into the reservoir

L = -1; for flow out of the reservoir

This is further simplified, assuming the flow velocity varies only slightly between time steps, to give :-

$$H_o^{t+\Delta t} = H_{res} + L\frac{v_o^{t}{}^2}{2g} \qquad \text{.....} \quad (6.4.23)$$

The solution of equation 6.4.23 leads directly to the head at the start of the pipe out and substituting this in to equation 6.4.21 gives the corresponding velocity, v_o, at time $t+\Delta t$.

6.4.6 1-1 Pipe Junction

The characteristic equations, Figure 6.10, either side of the pipe to pipe junction are given by :-

$$C^+ : \quad v_i^{t+\Delta t} = a_1 H_i^{t+\Delta t} + a_2 \qquad \text{.....} \quad (6.4.24)$$

and

$$C^- : \quad v_o^{t+\Delta t} = a_3 H_o^{t+\Delta t} + a_4 \qquad \text{.....} \quad (6.4.25)$$

Continuity of flow at the pipe to pipe junction gives :-

$$Q_i^{t+\Delta t} = Q_o^{t+\Delta t} \qquad \text{.....} \quad (6.4.26)$$

or

$$A_i\, v_i^{t+\Delta t} = A_o\, v_o^{t+\Delta t} \qquad \text{.....} \quad (6.4.27)$$

where

A_i = cross-sectional area of the pipe in

A_o = cross-sectional area of the pipe out

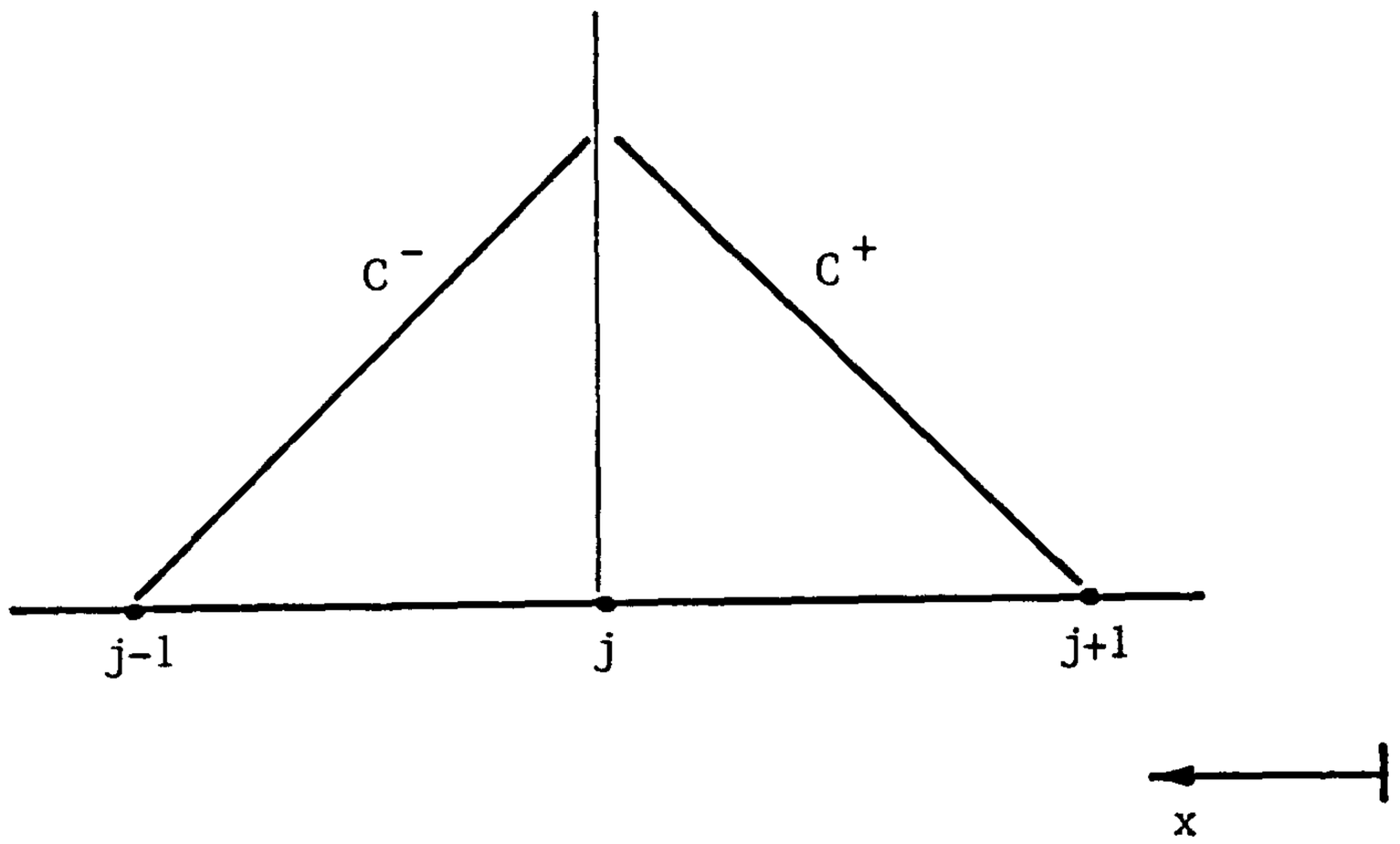

Figure 6.11 : Internal node solution

A common energy head is shared at the junction, giving :-

$$H_i^{t+\Delta t} = H_o^{t+\Delta t} + \Delta VH^{t+\Delta t} \qquad \ldots\ldots\ldots\ldots \quad (6.4.28)$$

which is simplified to be given as :-

$$H_i^{t+\Delta t} = H_o^{t+\Delta t} + \Delta VH^{t} \qquad \ldots\ldots\ldots\ldots \quad (6.4.29)$$

Combining equations 6.4.24, 6.4.25, 6.4.27 and 6.4.29, eliminating v_i, H_i and H_o, each at time $t+\Delta t$, leads to :-

$$v_o^{t+\Delta t} = \frac{\frac{a_2}{a_1} - \frac{a_4}{a_3} + \Delta VH^{t}}{\frac{A_o}{A_i a_1} - \frac{1}{a_3}} \qquad \ldots\ldots\ldots\ldots \quad (6.4.30)$$

The solutions to H_o, v_i and H_i, each at time $t+\Delta t$, follow directly from equations 6.4.25, 6.4.27 and 6.4.24, respectively.

6.4.7 Internal Node

The characteristic equations at an internal node, Figure 6.11, are given by :-

$$C^+ : \quad v_j^{t+\Delta t} = a_1 H_j^{t+\Delta t} + a_2 \qquad \ldots\ldots\ldots\ldots \quad (6.4.31)$$

and

$$C^- : \quad v_j^{t+\Delta t} = a_3 H_j^{t+\Delta t} + a_4 \qquad \ldots\ldots\ldots\ldots \quad (6.4.32)$$

The solution of the head and velocity at node j are, therefore, given by :-

$$H_j^{t+\Delta t} = \frac{a_2 - a_4}{a_3 - a_1} \qquad \ldots\ldots\ldots\ldots \quad (6.4.33)$$

and

$$v_j^{t+\Delta t} = a_1 H_j^{t+\Delta t} + a_2 = a_3 H_j^{t+\Delta t} + a_4 \qquad \ldots\ldots\ldots \quad (6.4.34)$$

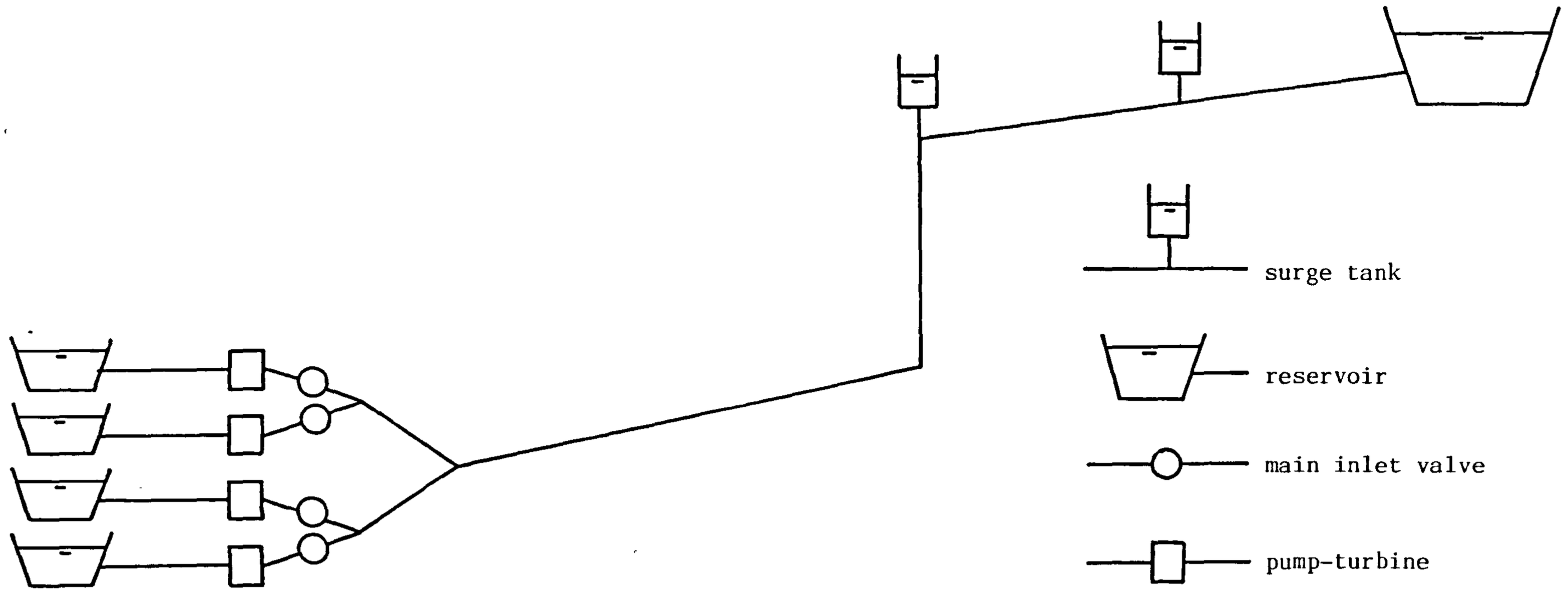

Figure 6.12 : Schematic layout of Station A.

6.5 COMPUTER PROGRAM ANALYSIS OF HYDRAULIC TRANSIENTS

6.5.1 Station A : Comparison with Site Recordings

Hydro-power station A is a typical pumped-storage scheme equipped with four reversible, Francis-type, pump-turbines. The hydraulic layout of the station is shown schematically in Figure 6.12. The upper reservoir leads into a 850 metre low pressure tunnel which is connected to 750 metre high pressure tunnel and penstock via the surge shaft. Upstream of the power house the penstock bifurcates into two sections. Each of these bifurcates again to supply the four pump-turbines. Immediately downstream of the power the 50 metre tailraces from each pump-turbine feed directly into the lower reservoir. Situated at the head of the surge shaft is a purpose built surge tank. There is also an access adit along the low pressure tunnel which acts as a second surge tank. The four pump-turbines are rated at 45 megawatts, turbining output, when operating under a 288 metre design head. At these conditions the discharge through each pump-turbine is approximately 19 cubic metres per second. Upstream of the power house the four pump-turbines are each equipped with their own main inlet valves.

The full hydraulic layout data for the scheme and the necessary data for each component in the scheme were available during this research. This included the pump-turbine performance characteristics which were given by the manufacturer in the unit speed versus unit discharge and unit speed versus unit torque form. In addition to this data a set of on-site recordings were also available. The hydraulic data is given in Appendix II.

The on-site recordings were taken during a simultaneous full load rejection of the four pump-turbines whilst operating in the turbining mode. These recordings were taken from pump-turbine number four and are

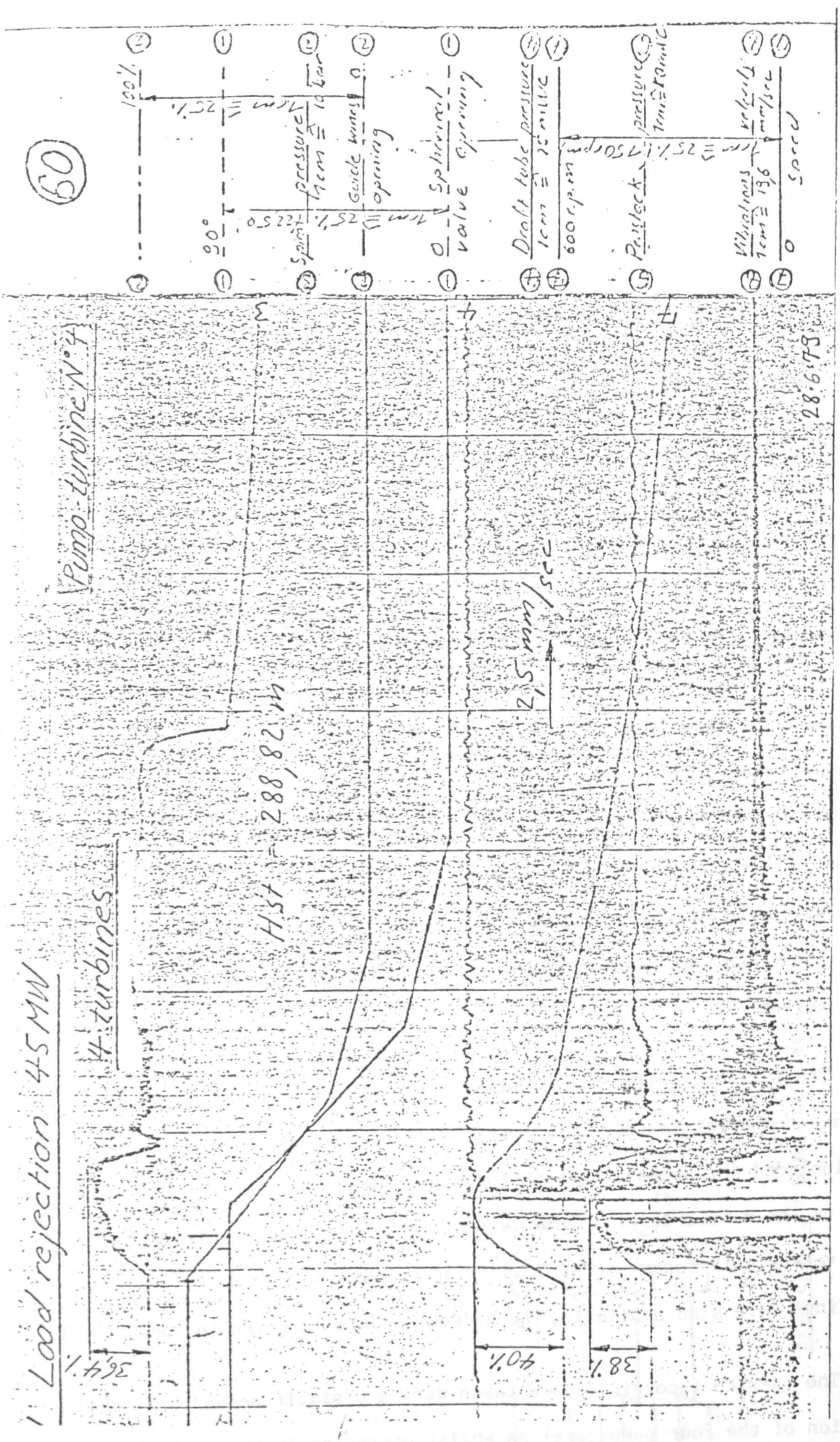

Figure 6.13: Site recordings for a full load rejection of all four pump-turbines. (Station A)

shown, to full scale, in Figure 6.13. The variables recorded during the load rejection are :-

(a) spiral pressure head,

(b) main inlet valve closing law,

(c) guide vane closing law,

(d) draft tube pressure,

(e) rotational speed,

(f) penstock pressure, and

(g) vibration velocity.

Of these seven traces the four which are significant for the hydraulic transient analysis of the scheme are; spiral pressure head, main inlet valve closing law, guide vane closing law and the rotational speed rise. The main inlet valve and guide vane closing laws are used as input data for the analysis whereas the spiral pressure and speed rise traces are what the analysis predicts. The latter two traces can therefore be used to assess the veracity of the transient analysis.

One of the problems in utilising the site recordings is in the accuracy to which they can be read. Figure 6.13 is shown to full scale and this only allows the spiral pressure and speed rise traces to be read within an accuracy of 2.5 metres and 5.0 r.p.m.,respectively. Therefore, in the assessment of the hydraulic analysis results this must be taken in to consideration. The traces also indicate the possibility of a time delay between the rejection of the load and the subsequent action taken by the governor to initiate the closure of the guide vanes. The time delay indicated, shown by the lateral shift between the start of the speed rise trace and that of the guide vane closure, is of the order of 0.5 seconds. However, although this discrepancy may be due to a non-alignment of the tracer pens a time delay in the response of the governor often occurs in practice and therefore it was incorporated in the transient analysis.

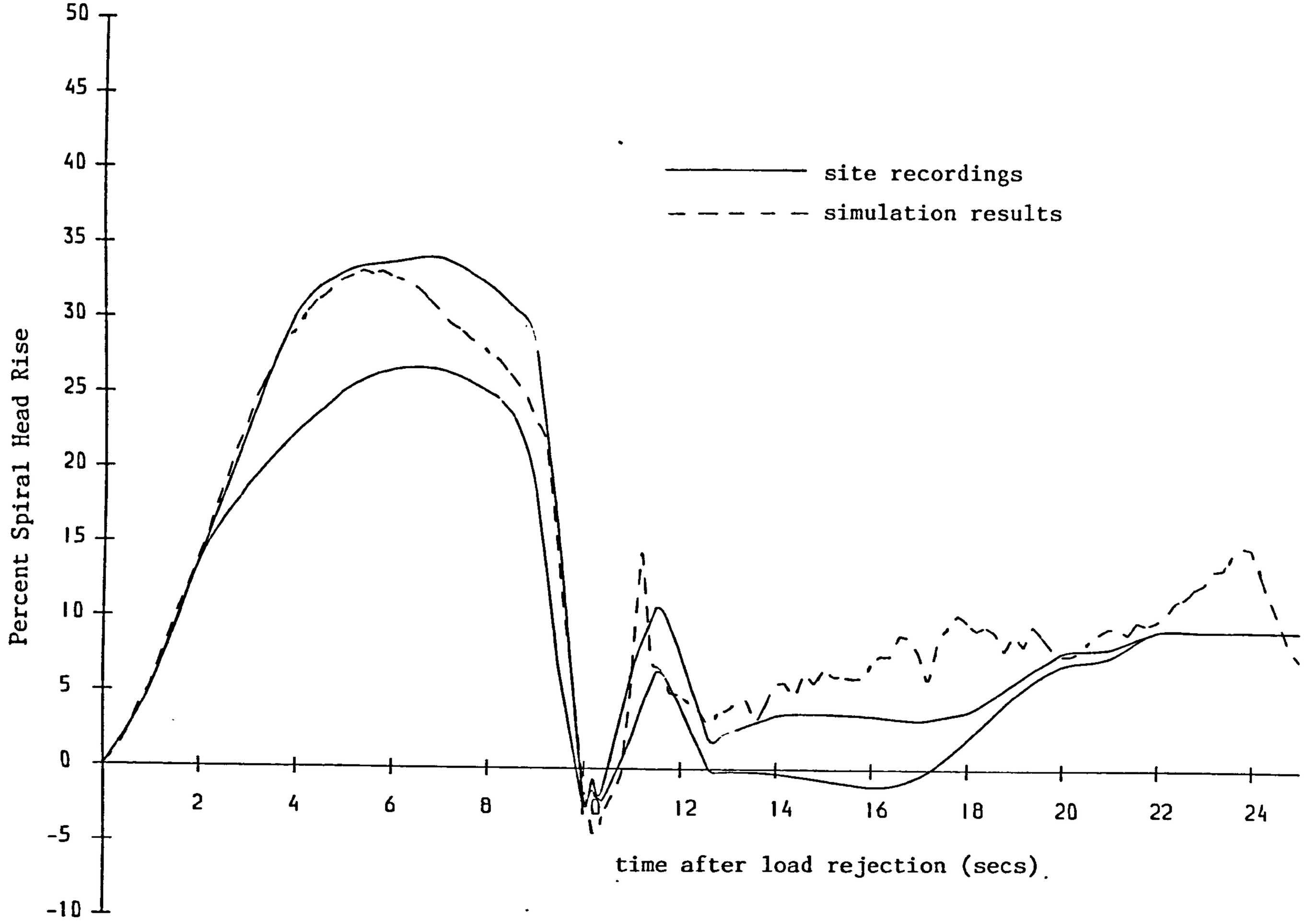

Figure 6.14 : Comparison of spiral head rise with site recordings.

The spiral pressure head trace, trace number three in Figure 6.13, displays a considerable fluctuation of the pressure head over the majority of the trace. These fluctuations lie within upper and lower bounds. For practical purposes these bounds were tabulated and these are the two traces indicated for the site recording spiral pressure head in Figure 6.14. The spiral pressure heads have also been converted to give the percent rise in spiral pressure. The percent speed rise and percent guide vane opening traces from the site recordings are shown in Figure 6.15.

Immediately after the load has been rejected the site recordings show a rapid increase in the spiral pressure. Between four and eight seconds after the rejection the spiral head levels off, reaching a maximum, around six seconds after the rejection, with a pressure rise in the order of thirty six percent. Eight to ten seconds after the rejection the spiral pressure head falls off rapidly to below the initial pressure head. This is followed immediately by a secondary rise in the pressure head which peaks between eleven and twelve seconds after the rejection. Following the secondary peak the pressure head levels off before rising steadily over the final closing stages of the guide vanes, complete closure coming twenty four seconds after the load rejection. Following the guide vane closure the spiral head trace indicates little variation in the pressure head.

The speed rise trace from the site recordings is reproduced in Figure 6.15 Following the load rejection the speed rises sharply and peaks at about a forty percent rise after six seconds. Subsequently the pump-turbine begins to decelerate and the speed rise is reduced. This initial reduction in the speed rise is a rapid one but becomes less marked over the final stages of the guide vane closure. Upon the full closure of the guide vanes the pump-turbine is rotating ten percent below the rated speed.

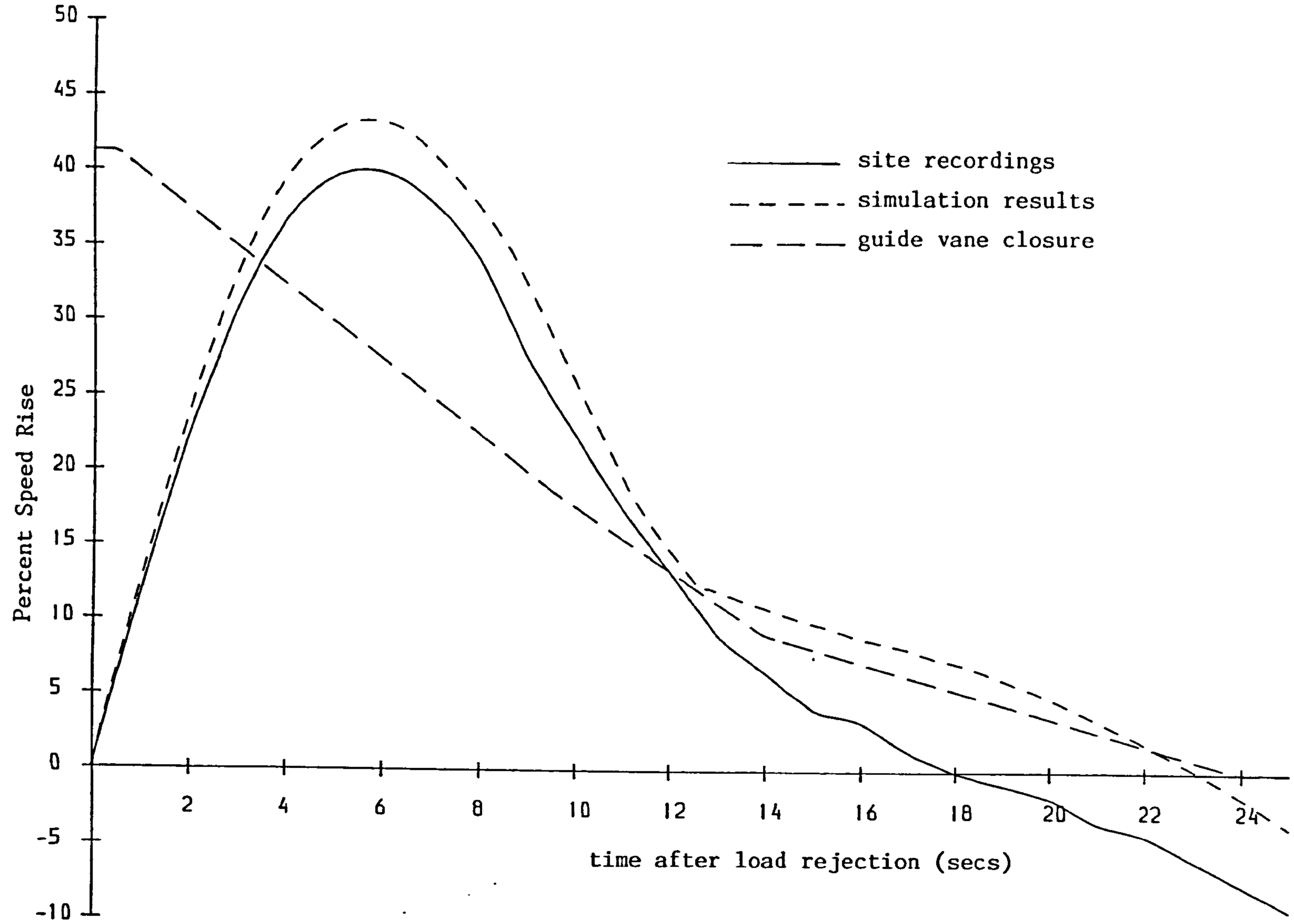

Figure 6.15 : Comparison of speed rise with site recordings.

The spiral pressure head results from the hydraulic transient simulation are shown in Figure 6.14 together with the site recordings. During the initial six seconds the calculated spiral pressure head shows a very good correlation with the site recordings. The maximum pressure rise is depicted to within one percent and the results follow closely to those of the upper limit of the pressure head. Between six and ten seconds the results lie within the upper and lower limit traces and the marked fall off of the pressure head has been picked up. The results have also picked up the secondary pressure head peak although the peak value is slightly over estimated by three to four percent. Subsequent to the secondary peak the results give the general trend of the site recordings, a steady increase in the pressure head to around ten percent above the steady state conditions. However, during the final closure of the guide vanes the pressure head continues to rise and then falls after the guide vanes have closed. In fact the spiral pressure is moving in to a period of oscillatory motion. This would generally be the expected case following the closure of the guide vanes. Once closed the pressure waves continue to propagate through the hydraulic system, between the spiral inlet and the upper reservoir or the spiral inlet and the main inlet valve should this also be closed. These oscillations would continue for many minutes before being fully damped by the friction in the system. It remains unclear why such oscillations are not shown on the site recordings.

The corresponding results for the speed rise are shown in Figure 6.15 Throughout the period of the simulation the results for the speed rise have been over estimated. The results over the initial six seconds closely follow those from the site recordings and the peak speed rise is depicted to within four percent. Over the subsequent six seconds the results once again give a good correlation with those from the site recordings. The results

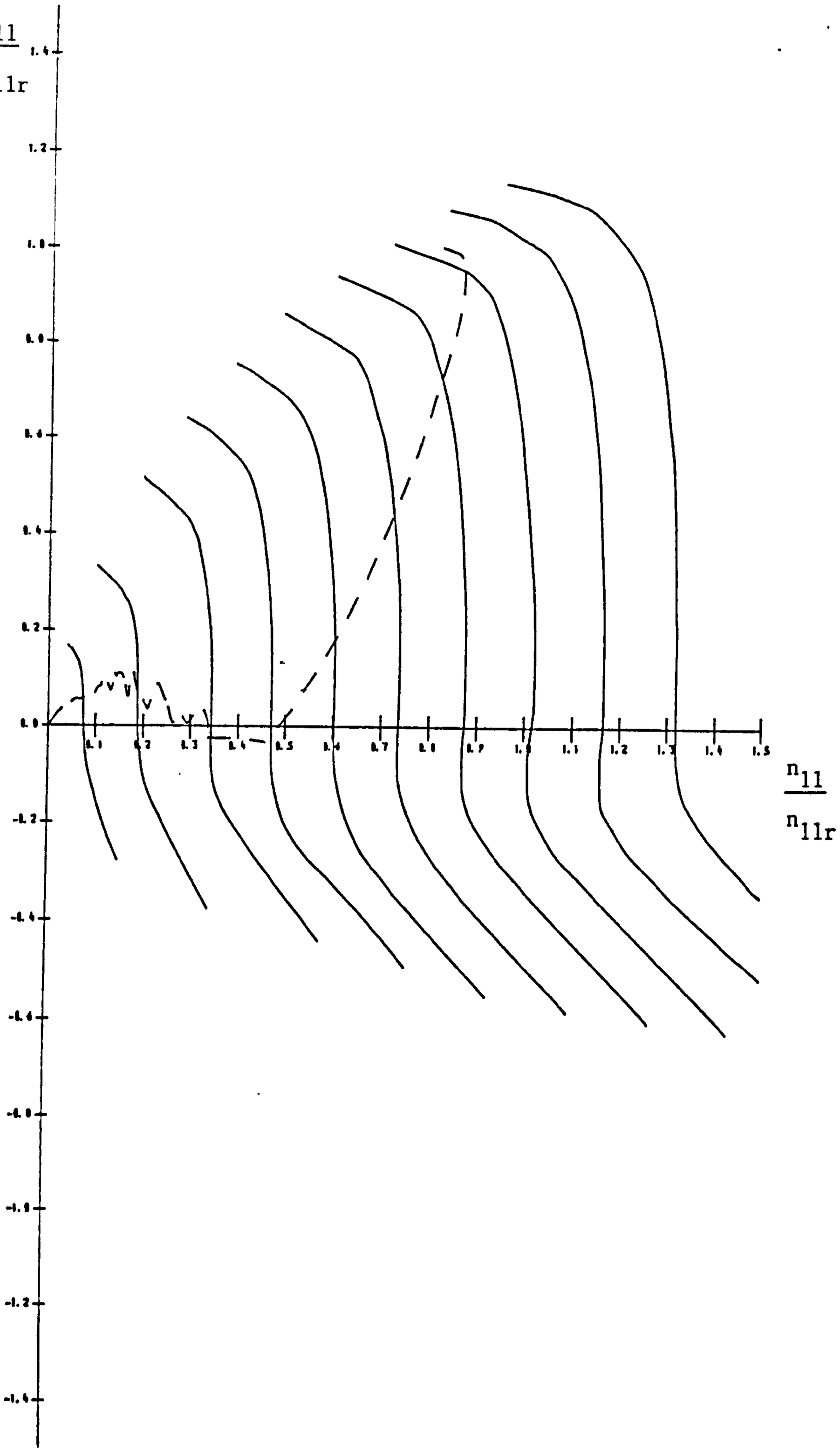

Figure 6.16 : Locus of operating point through the exploded unit speed versus unit discharge performance characteristics.

after twelve seconds lie within two percent of the site recordings. After twelve seconds the speed rise gives the general trend of those from the site recordings but with the speed rise being calculated approximately eight percent higher. The simulation results indicate a less marked deceleration of the pump-turbine than that given in the site recordings. during the period between twelve and twenty seconds and this accounts for the discrepancy in the speed rise over the final closure of the guide vanes.

The computer simulation results show a satisfactory correlation with the site recordings and have served as a verification of the program's operation. The results were able to depict the maximum spiral pressure head and rotational speed rises to within one and four percent, respectively. These results are particularly important as the design of a hydro-power plant is dependent on withstanding these maximum pressure and speed rises. Simulations must be able to predict these accurately and the degree of accuracy found in the simulation of station A has proved itself to be acceptable.

The locus of the operating point for the hydraulic transient analysis is shown in Figure 6.16 on the exploded unit speed versus unit discharge plane. It is clear that the operating point passes in to the reverse pumping quadrant and that a reversal of flow occurred during the full load rejection. Whilst passing through the reverse pumping quadrant the operating point is within the re-entrant region of the guide vane curves. There are no discontinuities in the locus in this region and this shows that the handling routines for the location of the guide vane sections in the re-entrant region were successful.

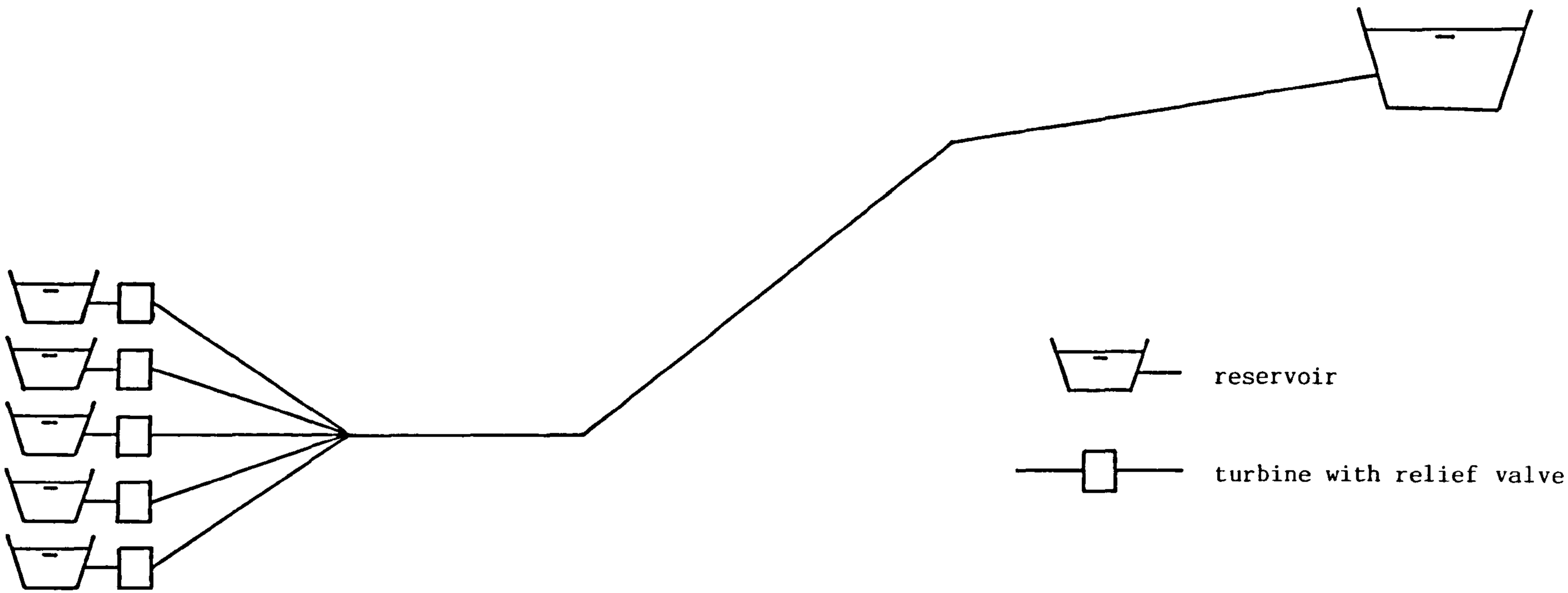

Figure 6.17 : Schematic layout of Station B

6.5.2 Station B : Alternative Mode of Operation

Station B is a typical hydro-power plant equipped with five Francis turbines each rated at 2.5 megawatts. The schematic layout of Station B is shown in Figure 6.17. The upper reservoir leads into a single penstock which is 470 metres long. The penstock branches 34 metres upstream of the power house, with a seperate branch for each of the five turbines. The turbine draft tubes are not connected to a tailrace system but feed directly into the lower reservoir. The turbines are designed to operate under a net head of 32 metres at 500 r.p.m. which delivers a discharge in the order of 8.7 cubic metres per second. The full hydraulic data for Station B is given in Appendix III.

The five Francis turbines have relief valves connected to their spiral casings. Following the full load rejection of the turbines the relief valves are designed to open in the same time as the guide vanes close. The relief valve opening is a two stage opening, over a period of 8 seconds, and their subsequent closure is a single stage closure. The full closure of the relief valve is achieved 32 seconds after the rejection of the load. The guide vane and relief valve opening laws are shown in Figure 6.18.

The hydraulic transient analysis of Station B simulates a full load rejection. The load is rejected from all five turbine simultaneously and the subsequent guide vane and relief valve movements are identical for each turbine. The hydraulic layout for Station B is symmetrical. This together with the identical operation of each turbine produces the same simulation results for each turbine. The results from a single turbine, therefore, only need to be discussed.

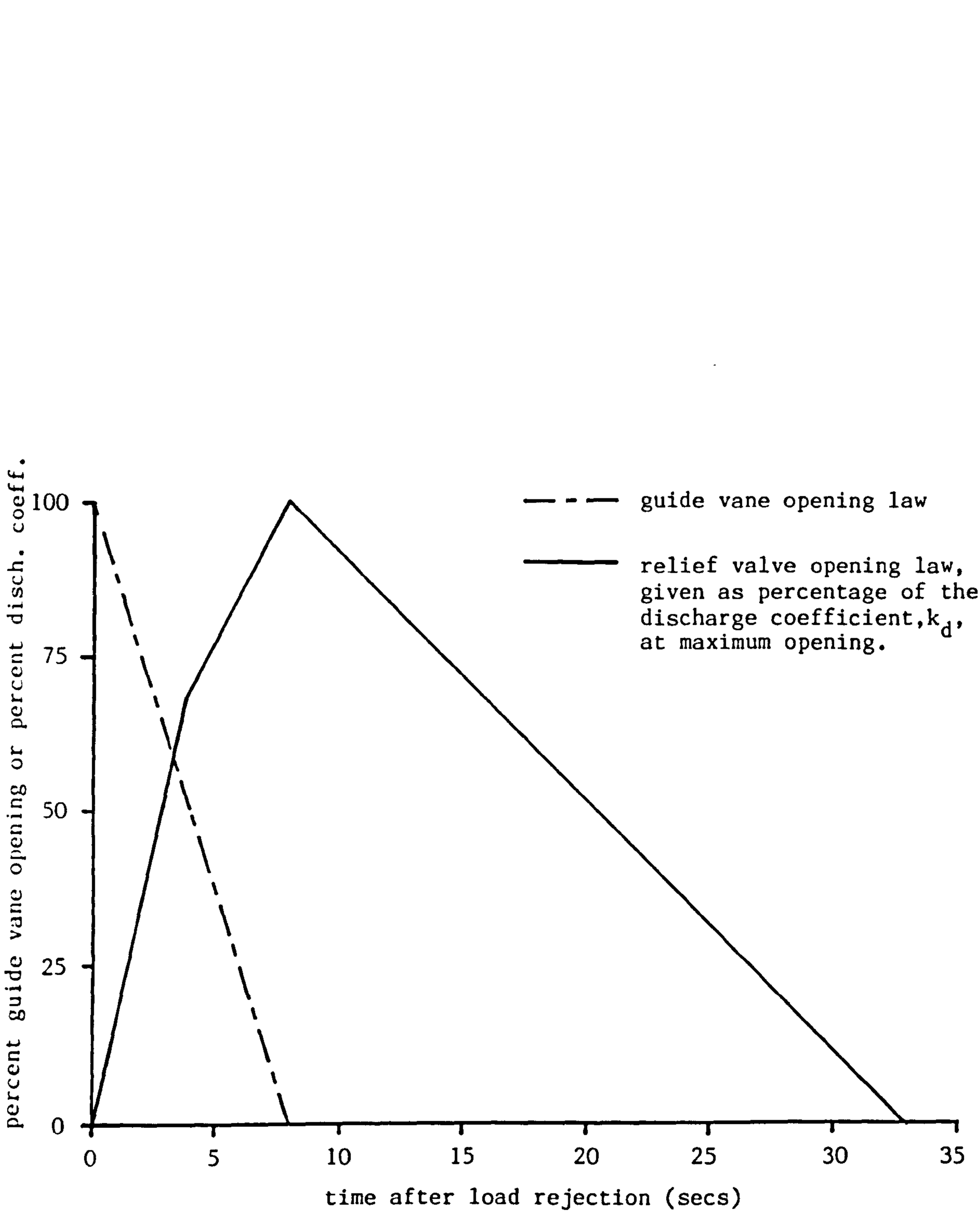

Figure 6.18 : Guide vane and relief valve opening laws for Station B.

The simulation results for Station B are shown in Figure 6.19 . The traces of prime importance are the spiral head rise and the speed rise. In addition to these traces Figure 6.19 indicates the guide vane closure law, the turbine discharge and the relief valve discharge. The relief valve discharge is given as a percentage of initial turbine discharge. The spiral head and speed rises are given as percentages of their initial values, at time zero. The load rejection occurs at time zero and the abscissa indicates the time after the load rejection.

In the first second after the load rejection the spiral head falls slightly before rising to an initial peak of 9.3 percent after 5 seconds. The final closing stages of the guide vanes initiate a second rise in the spiral head which rises steadily throughout the subsequent closure of the relief valve. The spiral head rises to maximum of 16.0 percent upon the complete closure of the relief valve, 32 seconds after the rejection of the load. Following the closure of the relief valve the spiral head shows an oscillatory motion as the pressure waves continue to propagate between the spiral inlet and the upper reservoir. The oscillatory motion will continue until the friction in the system damps out the pressure waves.

The speed rises sharply following the load rejection and reaches a a peak value of 34.1 percent after 4.0 seconds. After the peak speed rise the turbine decelerates and the speed rise falls to 19.5 percent as the guide vanes close, 8 seconds after the load rejection. The speed rise continues to fall throughout the subsequent closure of the relief valve, falling below the initial speed, at time zero, after 15.6 seconds. It should be noted that the speed rise results given here are those for a retardation of the turbine without the aid of mechanical breaking.

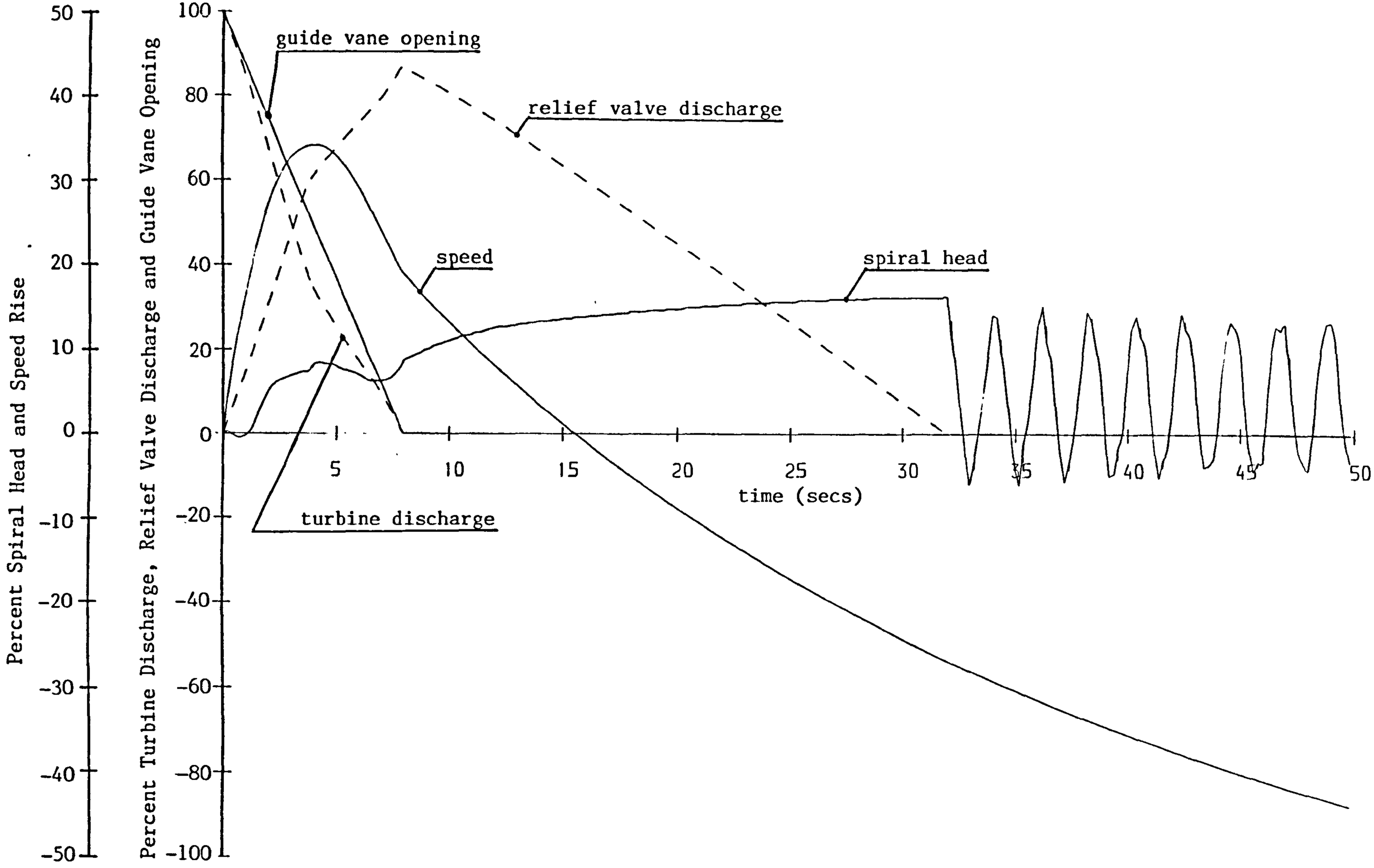

Figure 6.19 : Simulation results for Station B.

The relief valve operation is indicated in Figure 6.19 by the relief valve discharge results. The relief valve discharge rises throughout the closure of the guide vanes. The initial fall off of the spiral head, in the first second, indicates that the sum of the turbine and relief valve dicharges during this period is slightly greater than the initial turbine discharge at time zero. Subsequently the combination of guide vane closure and relief valve opening results in an overall reduction in the discharge through the penstock. At the full guide vane closure the relief valve discharge reaches a maximum, 87.5 percent of the initial turbine discharge. As the relief valve closes the discharge is reduced, approximately linearly, and falls to zero on the final closure of the relief valve, 32 seconds after the load rejection.

The hydraulic transient simulation presented in this Section is for a relief valve of a fixed full bore cross-sectional area operating under a predetermined open and closure rate. By repeating the simulations for a range of cross-sectional areas and movement rates an optimisation of the required characteristics of the relief valve can be made. The characteristics of the relief valve will be dependent on the limitations imposed on the spiral head and speed rises.

Although no site recordings are available for comparison with the simulation results the results themselves suggest that the turbine boundary with relief valve is functioning properly. This is indicated by the smooth change of flow from the turbine to the relief valve and the steady rise in pressure as the relief valve is closed.

CHAPTER 7

SUGGESTIONS FOR FURTHER RESEARCH

The development of prototype performance characteristics from alternative sources, as opposed to model testing, provides opportunities for further research. Some of the areas that can be pursued are :-

(i) the comparison of prototype performance characteristics, obtained from model test studies on a hydraulically similar turbine, with those obtained from the alternative sources.

(ii) the comparison with prototype performance characteristics, as above, but covering a wide range of specific speeds in order to assess their eligibility over a range of different specific speeds.

(iii) the hydraulic transient analysis of a hydro-power station using actual prototype performance characteristics and correlating the results with those using the alternative sources of turbine performance characteristics.

The algorithm for the solution of the turbine or pump-turbine boundary can be developed further :-

(iv) to include operation under governor control for the analysis of response to changes in load and utilising the linear relationships between the unit parameters which results from the method of guide vane curve representation.

(v) to include an optimisation procedure for the relief valve, with the relief valve characteristics being determined by limits imposed on the speed or spiral head rises.

CHAPTER 8

CONCLUSIONS

(i) Two methods of obtaining turbine performance characteristics from alternative sources, other than from the testing of a hydraulically similar model turbine, have been developed. The first is based on the published performance characteristics of typical reaction turbines and the second method is based on the performance characteristics of a turbine with a similar specific speed.

(ii) Investigations of the problems associated with the use of unit parameter, four quadrant, reversible pump-turbine performance characteristics in hydraulic transient analyses led to the development of a solution algorithm based on a modified unit parameter plane. The solution algorithm reduces the multi-variable boundary problem to one in a single variable.

(iii) A computer program for the analysis of hydraulic transients in hydro-power stations, incorporating the machine boundary solution algorithm, was developed. Simulation results were compared with a set of on-site recordings and the operation of the program verified.

(iv) In conjunction with the transient analysis program an automatic mesh generation program, to facilitate the interpolation of intermediate guide vane curves in turbine or pump-turbine performance characteristics, was verified by the comparison of the simulation results with the on-site recordings.

(v) The machine boundary solution algorithm was extended to incorporate a relief valve option. Despite a lack of on-site recordings for purposes of comparison the simulation results suggest that the algorithm was successful.

REFERENCES

1. Joukowski, N., "Waterhammer," Translated by O.Simin, Proc. Amer. Water Works Assoc., vol.24,1904, pp.341-424.

2. Allievi, L., "Theory of Waterhammer," Translated by E.E. Halmos, Ricardo Garoni, Rome, 1925.

3. Lowy, R., Druckscckwankungen in Druckrohrleitungen, Springer, 1928.

4. Schnyder, O., "Comparisons Between Calculated and Test Results on Waterhammer in Pumping Plants," Trans. ASME, vol.59, No.8, Nov..1937, pp.695-700.

5. Bergeron, L., Waterhammer in Hydraulics and Wave Surges in Electricity, John Wiley and Sons, Inc., New York, 1961.

6. Angus, R.W., "Simple Graphical Solutions for Pressure Rise and Pump Discharge Lines," Jour. Engineering Institute of Canada, Feb. 1935, pp.72-81.

7. Angus, R.W., "Waterhammer Pressure in Compound and Branched Pipes," Proc. ASCE, Jan. 1938, pp.340-401.

8. Lupton, H.R., "Graphical Analysis of Pressure Surges in Pumping Systems," Jour. Inst. Water Engrs., vol.7, No.2, March 1953, pp.87-156.

9. Strowger, E.B., "Waterhammer Problems in Connection With the Design of Hydroelectric Plants," Trans. ASME, July 1945,pp.377-392.

10. Gray, C.A.M., "The Analysis of the Dissipation of Energy in Waterhammer," Proc. ASCE, vol.119, Paper 274, 1953, pp.1176-1194.

11. Streeter, V.L. and Lai, C., "Waterhammer Analysis Including Fluid Friction," J. Hyd. Div., ASCE, vol.88, No.HY3, May 1962, pp.79-112.

12. Streeter, V.L., "Waterhammer Analysis of Pipelines," J. Hyd. Div., ASCE, vol.90, No.HY4, July 1964, pp.151-172.

13. Streeter, V.L., "Valve Stroking for Complex Piping Systems," J. Hyd. Div., ASCE, vol.93, No.HY3, May 1967, pp.81-98.

14. Wylie, E.B. and Streeter, V.L., "Fluid Transients," McGraw-Hill Book Co. Ltd., New York, 1978.

15. Courant, R. and Friedrichs, K.O., "Supersonic Flow and Shock Waves," Interscience, New York, 1948.

16. Lister, M., "The Numerical solutions of Hyperbolic Partial Differential Equations by the Method of Characteristics," A.Ralston and H.S.Wilf (eds.), Numerical Methods for Digital Computers, John Wiley and Sons Inc., New York 1960.

17. Vardy, A.E., "On the use of the Method of Characteristics for the Solution of Unsteady Flows in Networks," Second Int. Conf. on Pressure Surges, BHRA, London, Paper H2, Sept. 1976.

18. Streeter, V.L., "Waterhammer Analysis," J. Hyd. Div., ASCE, vol.95 No.HY6, No.HY6, Nov. 1969, pp.1959-1971.

19. Evangelisti, G., et al, "Some Applications of Waterhammer Analysis by the Method of Characteristics," L'Energia Elettrica, Nos.1 and 6, 1973, pp.1-12, 309-324.

20. Fox, J.A., "Pressure Transients in Pipe Networks - a Computer Solution," Int. Conf. on Pressure Surges,BHRA,Kent,Paper B1, Sept. 1972.

21. Amien, M. and Chu, H.L., "Implicit Numerical Modelling of Unsteady Flows," J. Hyd. Div., ASCE, vol.101, No.HY6, June 1975, pp.717-731.

22. Perkins, F.E., Tedrow, A.C., Eagleson, P.S. and Ippen, A.T., "Hydro-Power Plant Transients," Hydrodynamic Lab. Report No.71, Dept. of Civil Engineering, Massachusetts Institute of Technology, Sept. 1964.

23. Watt, C.S., "Analysis of Hydraulic Transients," Thesis presented to Sunderland Polytechnic, England, in partial fulfillment of the requirements for the degree of Ph.D., Feb. 1982.

24. Jaeger, C., "The Theory of Resonance in Hydropower Systems. Discussion of Incidents and Accidents Occurring in Pressure Systems," Trans. ASME, vol 85, J. of Basic Eng., Series D, Dec. 1963, pp631-640.

25. Wylie, E.B., "Resonance in Pressurised Piping Systems," J. Basic Eng., Trans. ASME, vol. 87, Series D, No.4, Dec. 1965, pp.960-966.

26. Wylie, E.B. and Streeter, V.L., "Resonance in Bersimis No.2 Piping System," J. Basic Eng., Trans. ASME, vol.87, Series D, No.4, Dec. 1965, pp.925-931.

27. Chaudhry, M.H., "Resonance in Pressurised Piping Systems," J. Hyd. Div., Procs. ASCE, vol.98, No.HY9, Sept. 1970, pp.1819-1839.

28. Strowger, E.B. and Kerr, S.L., "Speed Changes of Hydraulic Turbines for Sudden Changes of Load," Trans. ASME, vol.48, No.2009, 1926, pp.209-262.

29. Kitteridge, C.P., "Centrifugal Pumps Operated Under Abnormal Conditions," Power, vol.73, June 1931, pp.881-884.

30. Knapp, R.T., "Complete Characteristics of Centrifugal Pumps and Their Use in the Prediction of Transient Behaviour," Trans. ASME, vol.59, No.8, Nov. 1937, pp.683-689.

31. Donsky, B., "Complete Pump Characteristics and the Effects of Specific Speeds on Hydraulic Transients," J. of Basic Eng., Trans. ASME, Dec. 1961, pp.685-699.

32. Parmakian, J., "Waterhammer Analysis," Dover Publications, New York, 1963.

33. Harding, D.A., "A Method for Programming Graphical Surge Analysis for Medium Speed Computers," Symp. on Surges in Pipelines, Inst. Mech. Eng., London, vol.180, Part 3E, Nov. 1965, pp.83-97

34. Marchal, M., Flesch, G. and Suter, P., "The Calculation of Waterhammer Problems by Means of Digital Computer," Int. Symp. on Waterhammer in Pumped Storage Projects, ASME, Chicago, Nov. 1965, pp.168-188.

35. Chaudhry, M.H., "Applied Hydraulic Transients," Van Nostrand Reinhold Company, New York, 1979.

36. Boldy, A.P., "Waterhammer Analysis in Hydroelectric Pumped Storage Installations," Second Int. Conf. on Pressure Surges, BHRA, London, Paper B6, Sept. 1976.

37. Enever, K.J. and Hassan, J.M., "Transients Caused by Changes in Load on a Turbogenerator Set Governed by a P.I.D. Governor," Fourth Int. Conf. on Pressure Surges, BHRA, Kent, Paper G3, Sept. 1983.

38. Portfors, E.A. and Chaudhry, M.H., "Analysis and Prototype Verification of Hydraulic Transients in Jordan River Power Plant," First Int. Conf. on Pressure Surges, BHRA, Kent, Paper E4, Sept. 1972.

39. Hornberger, R.G. and Rodriguez, S., "Hydraulic Transient Studies for Taum Sauk Pumped-Storage Plant," Int. Symp. on Waterhammer in Pumped Storage Projects, ASME, Chicago, Nov 1965, pp.8-23.

40. Bovet, G.A. and Tschumy, A.S., "The Calculation of Pressure Surges in Pumped Storage Schemes Equipped with Isogyre Pump-Turbines," Int. Symp. on Waterhammer in Pumped Storage Projects, ASME, Chicago, Nov. 1965, pp.85-95.

41. Borel, L. and Mamin, M., "Transients in Pump-Turbine Installations," Int. Symp. on Waterhammer in Pumped Storage Projects, ASME, Chicago, Nov. 1965, pp.34-60.

42. Malamet, S., "Operation of Pumped Storage Schemes," Int. Conf. on Waterhammer in Pumped Storage Projects, ASME, Chicago, Nov. 1965, pp.201-213.

43. Kerensky, G., "Adapting Pump Storage Plant to Meet Grid Emergencies," Int. Conf. on Waterhammer in Pumped Storage Projects, ASME, Chicago, Nov. 1965, pp.24-33.

44. Yamabe, M., "Hysteresis Characteristics of Francis Pump-Turbines when Operated as a Turbine," J. Basic Eng., Trans. ASME, March 1971, pp.80-84.

45. Yamabe, M., "Improvement of Hysteresis Characteristics of Francis Pump-Turbines when Operated as a Turbine," J. Basic Eng., Trans. ASME, Sept. 1972, pp.581-585.

46. Whippen, W.G. and Chen, T.Y.W., "Turbine Runaway, Hysteresis and Thoma's Sigma Characteristics of Francis Pump-Turbines," Joint Symp. on Design and Operation of Fluid Machinery, ASCE-IAHR-ASME, June 1978.

47. Taulan, J.P., "Pressure Surges in Hydroelectric Installations. Peculiar Effects of Low Specific Speed Turbine Characteristics," Fourth Int. Conf. on Pressure Surges, Paper H2 , Bath, England, Sept. 1983.

48. Pejovic, S., Krsmanovic, L., Jemcov, R, and Crnkovic, P., "Unstable Operation of High-Head Reversible Pump-Turbines," Symp. on Problems of Hydraulic Machinery - Hydraulic Structure Interactions, IAHR, vol.1, Paper III-2, Leningrad, 1976, pp.283-295.

49. Boldy, A.P. and Walmsley, N., "Performance Characteristics of Reversible Pump-Turbines," Procs. Eleventh Symp. of the Section on Hydraulic Machinery, Equipment and Cavitation,IAHR, vol.3, Paper 60, Amsterdam, Sept. 1982.

50. Martin, C.S., "Transformation of Pump-Turbine Characteristics for Hydraulic Transient Analysis," Procs. Eleventh Symp. of the Section on Hydraulic Machinery, Equipment and Cavitation, IAHR, vol.2, Paper 30, Amsterdam, Sept. 1982.

51. Boldy, A.P. and Walmsley, N., "Representation of the Characteristics of Reversible Pump-Turbines for use in Waterhammer Simulations," Fourth Int. Conf. on Pressure Surges, BHRA, Bath, Paper G1, Sept. 1983.

52. Pejovic, S., Krsmanovic, L. and Gajic, A., "Kaplan Turbine Accidents and Reverse Waterhammer," Third Int. Conf. on Pressure Surges, BHRA, Kent, Paper H2, March 1980, pp.391-399.

53. "I.E.C. International Code for Model Acceptance Tests of Hydraulic Turbines," I.E.C. Pub. 193, International Electrotechnical Commission, Geneva, 1965.

54. "Selecting Hydraulic Reaction Turbines," Eng. Monograph No.20, United States Department of the Interior, Bureau of Reclamation (BUREC), Washington, 1976.

55. Dodes, I.A., "Numerical Analysis for Computer Science," North-Holland, New York, 1978.

56. Ralston, A. and Rabinowitz, P., "A First Course in Numerical Analysis" McGraw-Hill Book Co., New York, 1978.

57. Martin, C.S., "Representation of Pump Characteristics for Transient Analysis," Procs. Winter Annual Meeting of the ASME, Performance Characteristics of Hydraulic Turbines and Pumps,Fluids Eng. Div.,vol.6, Boston, Nov. 1983, pp.1-13.

58. DeFazio, F.G., "Transient Analysis of Variable-Pitch Pump-Turbines," J. Eng. for Power, Trans. ASME,Oct. 1967, pp.547-557.

59. Woznaik, L., Discussion of Reference 58, J. Eng. for Power, Trans. ASME, Oct. 1967, p.556.

APPENDICES

APPENDIX I Listing of Program 'TRANSEX' for the Analysis of Hydraulic Transients in Hydro-Power Plants.

APPENDIX II Hydraulic Data for Station A.

APPENDIX III Hydraulic Data for Station B.

APPENDIX IV Listing of Program 'SMESHJ' for the Automatic Generation of a Curvilinear Mesh.

APPENDIX V Published Papers. (Co-author with Dr. A.P. Boldy)

"Performance Characteristics of Reversible Pump-Turbines," Procs. 11th Symp. of the Section on Hydraulic Machinery,Equipment and Cavitation, IAHR, vol.3, Paper 60, Amsterdam, Sept. 1982.

"Representation of the Characteristics of Reversible Pump-Turbines for use in Waterhammer Simulations," 4th Int. Conf. on Pressure Surges, BHRA, Paper G1, Bath England, Sept. 1983.

APPENDIX 1: Listing of Program 'TRANSEX' for the Analysis of Hydraulic Transients in Hydro-Power Plants

```
C PROGRAM TRANSEX. TRANSIENT ANALYSIS WITH EXPLODED M/C CHAR
      DIMENSION IIP(10,30),BBP(30,20),IIT(10,30),BBT(30,20),
     1          IMVP(3,10),RMVP(30,11),IMVT(3,10),RMVT(30,11),
     1          ISTP(3,10),RSTP(20,14),ISTT(3,10),RSTT(20,14),
     1          IBRP(15,10),IBRT(15,10),ITB(4,10),RTB(70,14),
     1          HP(30,20),VP(30,20),HT(30,20),VT(30,20),
     1           QN11(10,60,15),Q11(10,60,15),
     1             TN11(10,60,15),T11(10,60,15),
     1          GVO(10,15),NGVO(10),NS(10)
     1           ,FX(10),FY(10),N11R(10),Q11R(10),M11R(10)
      INTEGER SYSP(2,100),SYST(2,100),PIN,POUT
      OPEN(UNIT=1,FILE='DATA')
      OPEN(UNIT=2,FILE='WQDATA')
      OPEN(UNIT=3,FILE='RESULTS',FORM='FORMATTED')
      OPEN(UNIT=4,FILE='GRAFRST',FORM='FORMATTED')
C
C     ***************************************************************
C
C                                                    READ DATA IN
C
C     ***************************************************************
C
      TT=0.0
      NTIME=0
      CALL TITLE
      READ(1,*)DT,TL,OT
      ITIME=INT(OT/DT+0.0001)
      READ(1,*)URES,XLRES
      READ(1,*)IIP(1,1)
      IF(IIP(1,1).NE.0)CALL DATPP(IIP,BBP,DT)
      READ(1,*)IMVP(1,1)
      IF(IMVP(1,1).NE.0)CALL DATMV(IMVP,RMVP)
      READ(1,*)ISTP(1,1)
      IF(ISTP(1,1).NE.0)CALL DATST(ISTP,RSTP)
      READ(1,*)IBRP(1,1)
      IF(IBRP(1,1).NE.0)CALL DATBR(IBRP)
      CALL DATTB(ITB,RTB,QN11,Q11,TN11,T11,GVO,NGVO,NS)
      READ(1,*)IIT(1,1)
      IF(IIT(1,1).EQ.0)GOTO 10
      CALL DATPP(IIT,BBT,DT)
      READ(1,*)IMVT(1,1)
      IF(IMVT(1,1).NE.0)CALL DATMV(IMVT,RMVT)
      READ(1,*)ISTT(1,1)
      IF(ISTT(1,1).NE.0)CALL DATST(ISTT,RSTT)
      READ(1,*)IBRT(1,1)
      IF(IBRT(1,1).NE.0)CALL DATBR(IBRT)
10    CALL SYSTEM(SYSP,NSYSP,IIP,IMVP,ISTP,IBRP,ITB)
      IF(IIT(1,1).NE.0)CALL SYSTEM(SYST,NSYST,IIT,IMVT,ISTT,IBRT,ITB)
C
C     ***************************************************************
C
C                                                    CALCULATE STEADY STATE
C
C     ***************************************************************
C
```

```
      ICOUNT=0
99    CALL SSFLOW(SYSP,NSYSP,IIP,BBP,VP,ITB,RTB,IBRP,-1)
      JJ=NSYSP
100   IF(JJ.LE.1)GOTO 190
      IF(SYSP(1,JJ).EQ.SYSP(1,JJ-1))JJ=JJ-1
      NTYPE=INT((SYSP(2,JJ)+9)/10)
      NUMBER=SYSP(2,JJ)+10-NTYPE*10
      GOTO(101,102,103,104,105,106)NTYPE
101   JJ=JJ-1
      GOTO 100
102   CALL SSMV(RMVP,NUMBER,IIP,BBP,SYSP,JJ,HP,VP,-1)
      GOTO 100
103   CALL SSST(RSTP,NUMBER,IIP,BBP,SYSP,JJ,HP,VP,-1)
      GOTO 100
104   CALL SSBR(IBRP,NUMBER,IIP,BBP,SYSP,JJ,HP,VP,-1)
      GOTO 100
105   CALL SSRES(URES,IIP,BBP,SYSP,JJ,HP,VP,-1)
      GOTO 100
106   CALL SSJN(IIP,BBP,SYSP,JJ,HP,VP,-1)
      GOTO 100
190   CONTINUE
      IF(IIT(1,1).EQ.0)GOTO 210
      CALL SSFLOW(SYST,NSYST,IIT,BBT,VT,ITB,RTB,IBRT,0)
      JJ=NSYST
200   IF(JJ.LE.1)GOTO 220
      IF(SYST(1,JJ).EQ.SYST(1,JJ-1))JJ=JJ-1
      NTYPE=INT((SYST(2,JJ)+9)/10)
      NUMBER=SYST(2,JJ)+10-NTYPE*10
      GOTO(201,202,203,204,205,206)NTYPE
201   JJ=JJ-1
      GOTO 200
202   CALL SSMV(RMVT,NUMBER,IIT,BBT,SYST,JJ,HT,VT,0)
      GOTO 200
203   CALL SSST(RSTT,NUMBER,IIT,BBT,SYST,JJ,HT,VT,0)
      GOTO 200
204   CALL SSBR(IBRT,NUMBER,IIT,BBT,SYST,JJ,HT,VT,0)
      GOTO 200
205   CALL SSRES(XLRES,IIT,BBT,SYST,JJ,HT,VT,0)
      GOTO 200
206   CALL SSJN(IIT,BBT,SYST,JJ,HT,VT,0)
      GOTO 200
210   IF(ICOUNT.EQ.1)GOTO 250
220   CONTINUE
      ICOUNT=ICOUNT+1
      DO 240 I=1,ITB(1,1)
         IF(IIT(1,1).EQ.0)HT(I,1)=XLRES
         IF(IIT(1,1).EQ.0)VT(I,1)=4.0*(VP(I,1)*BBP(I,6))/
     1                                (3.142*RTB(I,6)**2)
         H=HP(I,1)-HT(I,1)+(VP(I,1)**2-VT(I,1)**2)/(2.0*9.806)
         RTB(I,8)=RTB(I,1)*RTB(I,11)/SQRT(H)
         ZZQN11=RTB(I,8)*RTB(20+I,1)/GVB(I,1)
         RTB(I,9)=RTB(I,2)/(RTB(I,11)*RTB(I,11)*SQRT(H))
         RTB(I,10)=100.0
         CALL FIND(QN11,Z11,NGVB,NS,GVB,I,RTB(20+I,1),
     1                                   ZZQN11,RTB(I,9),AAX,AAY,BBX,BBY)
```

```
            RTB(I,2)=RTB(I,9)*RTB(I,11)*RTB(I,11)*SQRT(H)
240   CONTINUE
      IF(ICOUNT.GE.2)GOTO 250
      GOTO 99
250   DO 260 I=1,ITB(1,1)
            H=HP(I,1)-HT(I,1)+(VP(I,1)**2-VT(I,1)**2)/(2.0*9.806)
            RTB(I,8)=RTB(I,1)*RTB(I,11)/SQRT(H)
            ZZTN11=RTB(I,8)*RTB(20+I,1)/GVO(I,1)
            CALL FIND(TN11,T11,NGVO,NS,GVO,I,RTB(20+I,1),
     1                                    ZZTN11,RTB(I,10),AAX,AAY,BBX,BBY
            RTB(I,3)=H
            RTB(I,4)=RTB(I,10)*RTB(I,3)*RTB(I,11)*RTB(I,11)*RTB(I,11)
            RTB(I+10,5)=-(4.0*RTB(I,2)/(3.142*RTB(I,5)**2))**2
            RTB(I+10,5)=RTB(I+10,5)/(2.0*9.806)+HP(I,1)
            RTB(I+10,5)=RTB(I+10,5)+VP(I,1)**2/(2.0*9.806)
            RTB(I+10,6)=-(4.0*RTB(I,2)/(3.142*RTB(I,6)**2))**2
            RTB(I+10,6)=RTB(I+10,6)/(2.0*9.806)+HT(I,1)
            RTB(I+10,6)=RTB(I+10,6)+VT(I,1)**2/(2.0*9.806)
            IF(IIT(1,1).EQ.0)RTB(I+10,6)=XLRES
            RTB(I+10,7)=RTB(I+20,1)
260   CONTINUE
C
C     ****************************************************************
C
C                                                    WRITE DATA OUT
C
C     ****************************************************************
C
      WRITE(3,310)DT,TL,DT
310   FORMAT(//5X,'TIME INCREMENTS',/5X,'***************',///
     1       'TIME STEP FOR CALCULATIONS',T35,'=',5X,F5.2,//
     1       'TIME LIMIT FOR CALCULATIONS',T35,'=',5X,F5.2,//
     1     'TIME STEP FOR OUTPUT',T35,'=',5X,F5.2,////)
      WRITE(3,320)URES,XLRES
320   FORMAT(//5X,'RESERVOIR DATA',/5X,'**************',///
     1       'UPPER RESERVOIR LEVEL',T35,'=',5X,F5.1,//
     1       'LOWER RESERVOIR LEVEL',T35,'=',5X,F5.1,////)
      WRITE(3,330)
330   FORMAT(//'********',//T44,'PENSTOCK DATA',//'********',////)
      IF(IIP(1,1).NE.0)CALL OUTPP(IIP,BBP,HP,VP)
      IF(IMVP(1,1).NE.0)CALL OUTMV(IMVP,RMVP)
      IF(ISTP(1,1).NE.0)CALL OUTST(ISTP,RSTP)
      IF(IBRP(1,1).NE.0)CALL OUTBR(IBRP)
      WRITE(3,340)
340   FORMAT(//'********',//T44,'TURBINE DATA',//'********',////)
      CALL OUTTB(ITB,RTB)
      WRITE(3,350)
350   FORMAT(//'********',//T44,'TAILRACE DATA',//'********',////)
      IF(IIT(1,1).EQ.0)GOTO 360
      CALL OUTPP(IIT,BBT,HT,VT)
      IF(IMVT(1,1).NE.0)CALL OUTMV(IMVT,RMVT)
      IF(ISTT(1,1).NE.0)CALL OUTST(ISTT,RSTT)
      IF(IBRT(1,1).NE.0)CALL OUTBR(IBRT)
      GOTO 370
360   WRITE(3,380)
```

```
380   FORMAT(//T44,'NO TAILRACE',////)
370   CONTINUE
      CALL INIT(ITB,RTB,ISTP,RSTP,ISTT,RSTT,IIP,BBP,IIT,BBT,VP,HP,VT,
      CALL HDGRST
      CALL OUTRST(ITB,RTB,TT)
C     ********************************************************************
C
C                                                    TRANSIENT CALCULATION
C
C     ********************************************************************
400   TT=TT+DT
      IF(TT.GT.TL)GOTO 2000
      DO 410 I=1,ITB(1,1)
            ZZ=RTB(I+10,7)/GVO(I,1)
            D2=RTB(I,11)*RTB(I,11)
            D3=D2*RTB(I,11)
            D4=D3*RTB(I,11)
            IF(ITB(I,4).EQ.0)GOTO 461
            RVQ=RTB(50+I,12)
            CALL CPLUS(I,BBP,DT,AS,BS)
            DO 464 J=1,ITB(4,I)
                  FX(J)=RTB(40+I,J)
                  FY(J)=RTB(50+I,J)
464         CONTINUE
            CALL INTERP(FX,FY,TT,RTB(50+I,13),ITB(4,I))
            KD=RTB(50+I,13)
            IF(KD.GT.0.0001)GOTO 466
            RTB(50+I,12)=0.0
            GOTO 461
466         EQ=2.0*RTB(I,2)-RTB(I+10,2)
            C1=1.0/(2.0*9.806*KD*KD*RTB(40+I,11)*RTB(40+I,11))
            C2=3.142*RTB(I,5)*RTB(I,5)/4.0
            C2=(1.0/(C2*C2)-1.0/(BBP(I,6)*BBP(I,6))/(2.0*9.806)
            C3=2.0*EQ*C2-1.0/(AS*BBP(I,6))
            C4=EQ*EQ*C2+BS/AS-EQ/(AS*BBP(I,6))+RTB(40+I,12)
            ICOUNT=1
472         FQ=RVQ*RVQ*(C1+C2)+RVQ*C3+C4
            IF(ABS(FQ).LT.0.001)GOTO 468
            ICOUNT=ICOUNT+1
            IF(ICOUNT.LT.20)GOTO 470
468         RTB(50+I,12)=RVQ
            GOTO 461
470         DFQ=2.0*RVQ*(C1+C2)+C3
            RVQ=RVQ-FQ/DFQ
            GOTO 472
461         CALL CPLUS(I,BBP,DT,AS,BS)
            IF(IIT(1,1).EQ.0)GOTO 414
            CALL CPLUS(I,BBT,DT,AD,BD)
            DD=1.0/(BBP(I,6)*AS)+1.0/(BBT(I,6)*AD)
            EE=BD/AD-BS/AS+(BBP(I,11)*BBP(I,11)-BBT(I,11)*BBT(I,11))
     1                    /(2.0*9.806)+RTB(50+I,12)/(AS*BBP(I,6))
            GOTO 416
414         DD=1.0/(BBP(I,6)*AS)
            EE=VP(I,1)**2/(2.0*9.806)-BS/AS-HT(I,1)
            EE=EE-VT(I,1)**2/(2.0*9.806)+RTB(50+I,12)/(AS*BBP(I,6))
```

```
416         CK=3.142*RTB(I,7)/(120.0*9.806*DT)
            EN=2.0*RTB(I,1)-RTB(I+10,1)
            EQ=2.0*RTB(I,2)-RTB(I+10,2)
            EM=2.0*CK*(EN-RTB(I,1))-RTB(I,4)
            EQ11=2.0*RTB(I,9)-RTB(I+10,9)
            EM11=2.0*RTB(I,10)-RTB(I+10,10)
            A1=1.0
            A2=-(EQ11**2*D4)*DD
            A3=-(EQ11**2*D4)*EE
421         FQ=A1*EQ*EQ+A2*EQ+A3
            IF(ABS(FQ).LT.ABS(EQ/1000.0))GOTO 422
            DFQ=2.0*A1*EQ+A2
            EQ=EQ-FQ/DFQ
            GOTO 421
422         HH=DD*EQ+EE
            RTB(I+10,1)=RTB(I,1)
            RTB(I+10,2)=RTB(I,2)
            RTB(I+10,4)=RTB(I,4)
            RTB(I+10,9)=RTB(I,9)
            RTB(I+10,10)=RTB(I,10)
            EN11=EN*RTB(I,11)/SQRT(HH)
            EQ11=EQ/(D2*SQRT(HH))
            DO 420 J=1,ITB(3,I)
                FX(J)=RTB(30+I,J)
                FY(J)=RTB(20+I,J)
420         CONTINUE
            CALL INTERP(FX,FY,TT,RTB(I+10,7),ITB(3,I))
            CALL YYFIND(Q11,QN11,NGVO,NS,GVO,I,RTB(I+10,7),EQ11,
     1                                  RTB(I,8),AAX,AAY,BBX,BBY)
            IF(AAX.EQ.BBX)GOTO 455
            SL1=(AAY-BBY)/(AAX-BBX)
            CO1=BBY-SL1*BBX
            CALL YYFIND(T11,TN11,NGVO,NS,GVO,I,RTB(I+10,7),EM11,
     1                                  RTB(I,8),AAX,AAY,BBX,BBY)
            IF(AAX.EQ.BBX)GOTO 455
            SL2=(AAY-BBY)/(AAX-BBX)
            CO2=BBY-SL2*BBX
            ITER=0
            A1=SL1/(DD*D3)
            A2=CO1/RTB(I,11)
            A3=-(SL1*EE)/(DD*D3)
            A4=-(2.0*CK*SL2)/(D4)
            A5=-CO2/RTB(I,11)
            A6=(2.0*CK*RTB(I,1)+RTB(I,4))*SL2/(D4)
450         FH=(A1*HH+A2*SQRT(HH)+A3)*(ZZ*SQRT(HH)+A4)
            FH=FH+ZZ*A5*HH+ZZ*A6
            IF(ABS(FH).LT.0.001)GOTO 460
            DFH=(A1+A2/(2.0*SQRT(HH)))*(ZZ*SQRT(HH)+A4)
            DFH=DFH+(A1*HH+A2*SQRT(HH)+A3)*(ZZ/(2.0*SQRT(HH)))
            DFH=DFH+ZZ*A5
            HH=HH-FH/DFH
            ITER=ITER+1
            IF(ITER.GT.20)GOTO 455
            GOTO 450
460         RTB(I,3)=HH
```

```
      RTB(I,2)=(RTB(I,3)-EE)/DD
      RTB(I,1)=(A1*RTB(I,3)+A2*SQRT(RTB(I,3))+A3)/ZZ
      GOTO 456
455   RTB(I,1)=EN
      RTB(I,2)=EQ
      RTB(I,3)=DD*EQ+EE
      EN11=RTB(I,1)*RTB(I,11)/SQRT(RTB(I,3))*ZZ
      CALL FIND(TN11,T11,NGVO,GVO,I,RTB(I+10,7),
     1                  EN11,EM11,AAX,AAY,BBX,BBY)
      DN=EM11*D3*RTB(I,3)/(2.0*CK)
      RTB(I,1)=RTB(I+10,1)+DN
456   RTB(I,4)=2.0*CK*(RTB(I,1)-RTB(I+10,1))-RTB(I+10,4)
      RTB(I,8)=RTB(I,1)*RTB(I,11)/SQRT(RTB(I,3))
      RTB(I,9)=RTB(I,2)/(D2*SQRT(RTB(I,3)))
      RTB(I,10)=0.5*(RTB(I,4)+RTB(I+10,4))/
     1                                  (D3*RTB(I,3))
      VP(I,1)=(RTB(I,2)+RTB(50+I,12))/BBP(I,6)
      IF(IIT(1,1).NE.0)VT(I,1)=-RTB(I,2)/BBT(I,6)
      IF(IIT(1,1).EQ.0)VT(I,1)=-4.0*RTB(I,2)/(3.142*RTB(I,6)**2)
      HP(I,1)=VP(I,1)/AS-BS/AS
      IF(IIT(1,1).NE.0)HT(I,1)=VT(I,1)/AD-BD/AD
      IF(IIT(1,1).EQ.0)HT(I,1)=XLRES
      RTB(I+10,5)=-(4.0*(RTB(I,2)+RTB(50+I,12))/
     1                                (3.142*RTB(I,5)**2))**2
      RTB(I+10,5)=RTB(I+10,5)/(2.0*9.806)+HP(I,1)
      RTB(I+10,5)=RTB(I+10,5)+VP(I,1)**2/(2.0*9.806)
      RTB(I+10,6)=-(4.0*RTB(I,2)/(3.142*RTB(I,6)**2))**2
      RTB(I+10,6)=RTB(I+10,6)/(2.0*9.806)+HT(I,1)
      RTB(I+10,6)=RTB(I+10,6)+VT(I,1)**2/(2.0*9.806)
      IF(IIT(1,1).EQ.0)RTB(I+10,6)=XLRES
410   CONTINUE
      CALL TRNODE(IIP,BBP,DT,HP,VP)
      JJ=0
500   JJ=JJ+1
      IF(JJ.GT.NSYSP)GOTO 700
      IF(SYSP(1,JJ).EQ.SYSP(2,JJ).AND.SYSP(2,JJ).LE.10)GOTO 500
      IF(SYSP(1,JJ).EQ.0)GOTO 500
      IF(SYSP(2,JJ).GE.31.AND.SYSP(2,JJ).LE.40)GOTO 510
      GOTO 520
510   IF(SYSP(2,JJ).NE.SYSP(2,JJ-1))GOTO 500
520   NTYPE=INT((SYSP(2,JJ)-1)/10)
      NUMBER=SYSP(2,JJ)-NTYPE*10
      GOTO(601,602,603,604,605)NTYPE
601   PIN=SYSP(2,JJ+1)
      POUT=SYSP(2,JJ-1)
      CALL TRMV(PIN,POUT,NUMBER,IMVP,RMVP,TT,IIP,BBP,DT,HP,VP)
      GOTO 500
602   PIN=SYSP(2,JJ+1)
      POUT=SYSP(2,JJ-1)
      CALL TRST(PIN,POUT,NUMBER,ISTP,RSTP,IIP,BBP,DT,HP,VP)
      GOTO 500
603   PIN=SYSP(2,JJ+1)
      CALL TRBR(PIN,NUMBER,IBRP,IIP,BBP,DT,HP,VP)
      GOTO 500
604   POUT=SYSP(2,JJ-1)
```

```
      CALL TRRES(POUT,URES,IIP,BBP,DT,HP,VP,-1)
      GOTO 500
605   PIN=SYSP(2,JJ+1)
      POUT=SYSP(2,JJ-1)
      CALL TRJN(PIN,POUT,IIP,BBP,DT,HP,VP)
      GOTO 500
700   IF(IIT(1,1).EQ.0)GOTO 900
      CALL TRNODE(IIT,BBT,DT,HT,VT)
      JJ=0
710   JJ=JJ+1
      IF(JJ.GT.NSYST)GOTO 900
      IF(SYST(1,JJ).EQ.SYST(2,JJ).AND.SYST(2,JJ).LE.10)GOTO 710
      IF(SYST(1,JJ).EQ.0)GOTO 710
      IF(SYST(2,JJ).GE.31.AND.SYST(2,JJ).LE.40)GOTO 720
      GOTO 730
720   IF(SYST(2,JJ).NE.SYST(2,JJ-1))GOTO 710
730   NTYPE=INT((SYST(2,JJ)-1)/10)
      NUMBER=SYST(2,JJ)-NTYPE*10
      GOTO(801,802,803,804,805)NTYPE
801   PIN=SYST(2,JJ+1)
      POUT=SYST(2,JJ-1)
      CALL TRMV(PIN,POUT,NUMBER,IMVT,RMVT,TT,IIT,BBT,DT,HT,VT)
      GOTO 710
802   PIN=SYST(2,JJ+1)
      POUT=SYST(2,JJ-1)
      CALL TRST(PIN,POUT,NUMBER,ISTT,RSTT,IIT,BBT,DT,HT,VT)
      GOTO 710
803   PIN=SYST(2,JJ+1)
      CALL TRBR(PIN,NUMBER,IBRT,IIT,BBT,DT,HT,VT)
      GOTO 710
804   POUT=SYST(2,JJ-1)
      CALL TRRES(POUT,XLRES,IIT,BBT,DT,HT,VT,0)
      GOTO 710
805   PIN=SYST(2,JJ+1)
      POUT=SYST(2,JJ-1)
      CALL TRJN(PIN,POUT,IIT,BBT,DT,HT,VT)
      GOTO 710
900   NTIME=NTIME+1
      IF(NTIME.EQ.ITIME)CALL OUTRST(ITB,RTB,TT)
      IF(NTIME.EQ.ITIME)NTIME=0
      CALL UPDATE(IIP,BBP,HP,VP)
      IF(IIT(1,1).NE.0)CALL UPDATE(IIT,BBT,HT,VT)
      GOTO 400
2000  STOP
      END
C     ********
C
C     TITLE
C
C     ********
C
C
C
C
      SUBROUTINE TITLE
C
```

```
C
C
C
      WRITE(3,10)
10    FORMAT(T41,'*********************************************************
     1          T41,'*
     1          T41,'* UNIV. OF WARWICK                    ENGINEERING DEPT.
     1          T41,'*
     1          T41,'*
     1          T41,'*                    WATERHAMMER CALCULATIONS
     1          T41,'*
     1          T41,'*
     1          T41,'*                              BY
     1          T41,'*
     1          T41,'*                        NIGEL WALMSLEY
     1          T41,'*
     1          T41,'*********************************************************
     1          //////////)
      CONTINUE
      RETURN
      END
C     ***************
C
C          HDGRST
C
C     ***************
C
C
      SUBROUTINE HDGRST
      WRITE(3,10)
10    FORMAT(//'*******'//T48,'RESULTS OF WATERHAMMER CALCULATIONS',
     1       //'*******'////)
      WRITE(3,20)
20    FORMAT('  TIME',T10,'  MACHINE',T20,
     1       '  TURBINE',T30,'  TURBINE',T40,'  TURBINE',T50,
     1       'GUIDE VANE',T60,'    UNIT',T70,'    UNIT',T80,'    UNIT',T
     1       '  SPIRAL',T100,'  D/TUBE',/
     1       T10,'  NUMBER',T20,'    SPEED',T30,' DISCHARGE',T40,
     1       ' NET HEAD',T50,'  OPENING',T60,'    SPEED',T70,
     1       ' DISCHARGE',T80,'  TORQUE',T90,'    HEAD',T100,'    HEAD',
     1       '  (SECS)',T20,' (R.P.M.)',T30,' (CUMECS)',T40,
     1       '    (M)',T90,'     (M)',T100,'     (M)',//)
      RETURN
      END
C     ***************
C
C          DATPP
C
C     ***************
C
C
      SUBROUTINE DATPP(II,BB,DT)
C
      DIMENSION II(10,30),BB(30,20)
      DO 10 I=1,II(1,1)
```

```
20          READ(1,*)BB(I,1),BB(I,2),BB(I,3),BB(I,5),BB(I,4),BB(I,6),
     1                   II(3,I),II(5,I),II(4,I),II(6,I)
            BB(I,6)=3.142*BB(I,2)*BB(I,2)/4.0
            BB(I,7)=ARSIN((BB(I,4)-BB(I,8))/BB(I,1))
            II(2,I)=INT((BB(I,1)/(DT*BB(I,3)))+0.5)
            II(7,I)=II(2,I)+1
            BB(I,9)=BB(I,1)/(DT*II(2,I))
10      CONTINUE
        RETURN
        END
C       ***********
C
C          DATMV
C
C       ***********
C
C
      SUBROUTINE DATMV(IMV,RMV)
C
      DIMENSION IMV(3,10),RMV(30,11)
      DO 10 I=1,IMV(1,1)
            READ(1,*)IMV(2,I)
            READ(1,*)RMV(I,11)
            READ(1,*)IMV(3,I)
            DO 20 J=1,IMV(3,I)
                  READ(1,*)RMV(I,J),RMV(10+I,J),RMV(20+I,J)
20          CONTINUE
10      CONTINUE
        RETURN
        END
C       ***********
C
C          DATST
C
C       ***********
C
C
      SUBROUTINE DATST(IST,RST)
C
      DIMENSION IST(3,10),RST(20,14)
      DO 10 I=1,IST(1,1)
            READ(1,*)IST(2,I)
            READ(1,*)RST(I,11),RST(I,12)
            READ(1,*)IST(3,I)
            DO 20 J=1,IST(3,I)
                  READ(1,*)RST(I,J),RST(10+I,J)
20          CONTINUE
10      CONTINUE
        RETURN
        END
C       ***********
C
C          DATER
C
C       ***********
```

```
C
C
      SUBROUTINE DATBR(IBR)
C
      DIMENSION IBR(15,10)
      DO 10 J=1,IBR(1,1)
            READ(1,*)IBR(2,J)
            READ(1,*)IBR(3,J)
            READ(1,*)IBR(4,J)
            READ(1,*)(IBR(4+I,J),I=1,IBR(4,J))
            IBR(15,J)=0
10    CONTINUE
      RETURN
      END
C     ***********
C
C        SYSTEM
C
C     ***********
C
C
C
      SUBROUTINE SYSTEM(SYS,NSYS,II,IMV,IST,IBR,ITB)
C
      INTEGER II(10,30),IMV(3,10),IST(3,10),
     1          IBR(15,10),ITB(4,10),NBR(3,10),
     1          SYS(2,100),NT
      K=0
      NT=0
100   NT=NT+1
      DO 10 I=1,II(1,1)
            IF((II(6,I)).NE.NT)GOTO 10
            NODE=II(4,I)
            GOTO 20
10    CONTINUE
20    DO 30 I=1,II(1,1)
            IF (II(4,I).NE.NODE)GOTO 30
            K=K+1
            SYS(1,K)=II(4,I)
            SYS(2,K)=II(6,I)
            K=K+1
            SYS(1,K)=0
            SYS(2,K)=I
            IF(II(5,I).NE.50)GOTO 40
            K=K+1
            SYS(1,K)=II(3,I)
            SYS(2,K)=II(5,I)
            IF(NT.NE.ITB(1,1))GOTO 100
            GOTO 50
40          NODE=II(3,I)
            IF(II(5,I).NE.40)GOTO 90
            K=K+1
            SYS(1,K)=II(3,I)
            SYS(2,K)=II(5,I)
            DO 60 J=1,IBR(1,1)
                  IF(IBR(2,J).EQ.II(3,I))GOTO 70
```

```
60              CONTINUE
70              IBR(15,J)=IBR(15,J)+1
                IF(IBR(15,J).EQ.IBR(4,J))GOTO 80
                GOTO 100
80              NODE=II(3,I)
                GOTO 90
30      CONTINUE
90      GOTO 20
50      NSYS=K
        DO 200 I=1,NSYS
                IF(SYS(1,I).EQ.0)GOTO 200
                NTYPE=INT((SYS(2,I)+9)/10)
                GOTO(210,220,230,240)NTYPE
210             GOTO 200
220             CALL NODENO(SYS,I,IMV)
                GOTO 200
230             CALL NODENO(SYS,I,IST)
                GOTO 200
240             DO 242 KK=1,3
                        DO 244 JJ=1,IBR(1,1)
                                NBR(KK,JJ)=IBR(KK,JJ)
244                     CONTINUE
242             CONTINUE
                CALL NODENO (SYS,I,NBR)
                GOTO 200
200     CONTINUE
        RETURN
        END
C       ************
C
C           NODENO
C
C       ************
C
C
C
        SUBROUTINE NODENO(SYS,I,ITYPE)
C
        INTEGER SYS(2,100),ITYPE(3,10)
        DO 10 J=1,ITYPE(1,1)
                IF(ITYPE(2,J).NE.SYS(1,I))GOTO 10
                SYS(2,I)=SYS(2,I)-10+J
10      CONTINUE
        RETURN
        END
C       ************
C
C           DATTB
C
C       ************
C
C
C
        SUBROUTINE DATTB(ITB,RTB,QN11,Q11,TN11,T11,GVO,NGVO,NS)
C
        DIMENSION ITB(4,10),RTB(70,14),
     1            QN11(10,60,15),Q11(10,60,15),TN11R(10),Q11R(10),
```

```
     1          TN11(10,60,15),T11(10,60,15),M11R(10),
     1          GVO(10,15),NGVO(10),NS(10)
      READ(1,*)ITB(1,1)
      DO 10 I=1,ITB(1,1)
            READ(1,*)RTB(I,1),RTB(I,2)
            READ(1,*)RTB(I,5),RTB(I,6)
            READ(1,*)RTB(I,7)
            READ(1,*)RTB(I,11)
            READ(1,*)ITB(2,I)
            READ(1,*)ITB(3,I)
            DO 20 J=1,ITB(3,I)
                  READ(1,*)RTB(20+I,J),RTB(30+I,J)
 20         CONTINUE
            READ(1,*)ITB(4,I)
            IF(ITB(4,I).EQ.0)GOTO 30
            DO 30 J=1,ITB(4,I)
                  READ(1,*)RTB(40+I,J),RTB(50+I,J),RTB(60+I,J)
 30         CONTINUE
 10   CONTINUE
      DO 40 I=1,ITB(1,1)
            READ(2,*)N11R(I),Q11R(I),M11R(I)
            READ(2,*)NGVO(I),NS(I)
            READ(2,*)(GVO(I,K),K=1,NGVO(I))
            DO 50 J=1,NS(I)
                  READ(2,*)(QN11(I,J,K),K=1,NGVO(I))
                  READ(2,*)(Q11(I,J,K),K=1,NGVO(I))
 50         CONTINUE
            DO 60 J=1,NS(I)
                  READ(2,*)(TN11(I,J,K),K=1,NGVO(I))
                  READ(2,*)(T11(I,J,K),K=1,NGVO(I))
 60         CONTINUE
 40   CONTINUE
      RETURN
      END
C     ************
C
C        SSFLOW
C
C     ************
C
C
      SUBROUTINE SSFLOW(SYS,NSYS,II,BB,V,ITB,RTB,IBR,L)
C
      DIMENSION II(10,30),BB(30,20),V(30,20),
     1          ITB(4,10),RTB(70,14),IBR(15,10)
      INTEGER SYS(2,100),PIPE,POUT
      DO 10 I=1,NSYS
            IF(SYS(1,I).EQ.SYS(2,I).AND.SYS(2,I).LE.10)GOTO 20
            IF(SYS(1,I).NE.0)GOTO 10
            IF(I.LE.2)GOTO 70
            IF(SYS(1,I-1).EQ.SYS(1,I-2))GOTO 30
 70         PIPE=SYS(2,I)
            V(PIPE,1)=-1.0*(1.0+2.0*L)*QQ/BB(PIPE,6)
            GOTO 10
 20         QQ=RTB(SYS(2,I),2)
```

```
      GOTO 10
30    PIPE=SYS(2,I)
      K=SYS(2,I-1)-30
      QQ=0.0
      DO 40 J=1,IBR(4,K)
            POUT=IBR(J+4,K)
            QQ=QQ+V(POUT,1)*BB(POUT,6)
40    CONTINUE
      V(PIPE,1)=-1.0*(1.0+2.0*L)*QQ/BB(PIPE,6)
10    CONTINUE
      DO 50 I=1,II(1,1)
            RE=(ABS(V(I,1)*BB(I,2)*1000000.0/1.5))
            BB(I,10)=(RE**0.145*BB(I,5)*12.1*BB(I,2)**5.0)/BB(I,1)
            DO 60 J=1,II(7,I)
                  V(I,J)=V(I,1)
60          CONTINUE
50    CONTINUE
      RETURN
      END
C     ***************
C
C           SSMV
C
C     ***************
C
C
      SUBROUTINE SSMV(RMV,ND,II,BB,SYS,JJ,H,V,L)
C
      DIMENSION RMV(30,11),II(10,30),BB(30,20),H(30,20),
     1          V(30,20)
      INTEGER SYS(2,100),PIN,POUT
      PIN=SYS(2,JJ+1)
      POUT=SYS(2,JJ-1)
      J=II(7,POUT)
      H(POUT,J)=-(BB(POUT,5)*V(POUT,1))**2*(1.0/(RMV(10+ND,1)**2)
     1                                                    -1.
      H(POUT,J)=H(POUT,J)/(2.0*9.806*RMV(ND,11)*RMV(ND,11))
      H(POUT,J)=H(POUT,J)+H(PIN,1)+V(PIN,1)**2/(2.0*9.806)
      H(POUT,J)=H(POUT,J)-V(POUT,1)**2/(2.0*9.806)
      CALL SSHEAD(II,BB,H,V,POUT,L)
      JJ=JJ-2
      RETURN
      END
C     ***************
C
C           SSST
C
C     ***************
C
C
C
      SUBROUTINE SSST(RST,ND,II,BB,SYS,JJ,H,V,L)
C
      DIMENSION RST(20,14),II(10,30),BB(30,20),H(30,20),V(30,20)
      INTEGER SYS(2,100),PIN,POUT
      PIN=SYS(2,JJ+1)
```

```
      POUT=SYS(2,JJ-1)
      J=II(7,POUT)
      H(POUT,J)=H(PIN,1)+(V(PIN,1)**2-V(POUT,1)**2)/(2.0*9.806)
      RST(NO,13)=H(PIN,1)
      RST(NO,14)=0.0
      RST(NO+10,14)=RST(NO,14)
      CALL SSHEAD(II,BB,H,V,POUT,L)
      JJ=JJ-2
      RETURN
      END
C     ***********
C
C          SSBR
C
C     ***********
C
C
      SUBROUTINE SSBR(IBR,NO,II,BB,SYS,JJ,H,V,L)
C
      DIMENSION IBR(15,10),II(10,30),BB(30,20),H(30,20),V(30,20)
      INTEGER SYS(2,100),PIN,POUT
      NJ=SYS(2,JJ)-30
      PIN=IBR(3,NO)
      POUT=SYS(2,JJ-1)
      J=II(7,POUT)
      H(POUT,J)=H(PIN,1)+(V(PIN,1)**2-V(POUT,1)**2)/(2.0*9.806)
      CALL SSHEAD(II,BB,H,V,POUT,L)
      JJ=JJ-2
      RETURN
      END
C     ***********
C
C          SSRES
C
C     ***********
C
C
      SUBROUTINE SSRES(HRES,II,BB,SYS,JJ,H,V,L)
C
      DIMENSION II(10,30),BB(30,20),H(30,20),V(30,20)
      INTEGER SYS(2,100),POUT
      POUT=SYS(2,JJ-1)
      J=II(7,POUT)
      H(POUT,J)=HRES+(L*V(POUT,1)**2)/(2.0*9.806)
      CALL SSHEAD(II,BB,H,V,POUT,L)
      JJ=JJ-2
      RETURN
      END
C     ***********
C
C          SSJN
C
C     ***********
C
C
```

```
      SUBROUTINE SSJN(II,BB,SYS,JJ,H,V,L)
C
      DIMENSION II(10,30),BB(30,20),H(30,20),V(30,20)
      INTEGER SYS(2,100),PIN,POUT
      PIN=SYS(2,JJ+1)
      POUT=SYS(2,JJ-1)
      J=II(7,POUT)
      H(POUT,J)=H(PIN,1)+(V(PIN,1)**2-V(POUT,1)**2)/(2.0*9.806)
      CALL SSHEAD(II,BB,H,V,POUT,L)
      JJ=JJ-2
      RETURN
      END
C     ************
C
C        SSHEAD
C
C     ************
C
C
      SUBROUTINE SSHEAD(II,BB,H,V,I,L)
C
      DIMENSION II(10,30),BB(30,20),H(30,20),V(30,20)
      REAL KQQ
      KQQ=(BB(I,5)*(V(I,1)*BB(I,6))**2)/II(2,I)
      DO 10 K=2,II(7,I)
         KK=II(7,I)+1-K
         H(I,KK)=H(I,II(7,I))+(2.0*L+1)*(K-1)*KQQ
10    CONTINUE
      RETURN
      END
C     ************
C
C        OUTPP
C
C     ************
C
C
      SUBROUTINE OUTPP(II,BB,H,V)
C
      DIMENSION II(10,30),BB(30,20),H(30,20),V(30,20)
      WRITE(3,10)
10    FORMAT(//5X,'PIPELINE DATA',/5X,'*************',///)
      WRITE(3,20)
20    FORMAT('   PIPE',T10,'          START',T30,'         FINISH',T50,
     1       '   PIPE',T60,'   PIPE',T70,'   WAVE',T80,
     1       '      ELEVATION',T100,'   ANGLE',T110,' FRICTION',/
     1       ' NUMBER',T10,'          NODE',T30,'          NODE',T50,
     1       ' LENGTH',T60,' DIAMETER',T70,' VELOCITY',T80,
     1       '   START',T90,'  FINISH',T100,' TO HORZ.',T110,'   CONST
     1      /T10,'  NUMBER',T20,'    TYPE',T30,'  NUMBER',T40,
     1       '    TYPE',T50,'     (M)',T60,'     (M)',T70,
     1       '   (M/S)',T80,' (M.A.D.)',T90,' (M.A.D.)',T100,
     1       ' (RADS)',T110,'     (K)',//)
      DO 30 I=1,II(1,1)
         WRITE(3,40)I,II(3,I),II(5,I),II(4,I),II(6,I),
```

```
     1                    BB(I,1),BB(I,2),BB(I,3),
     1                    BB(I,4),BB(I,6),BB(I,7),BB(I,5)
40        FORMAT(I6,T10,I6,T20,I6,T30,I6,T40,I6,
     1          T50,F8.1,T60,F8.2,T70,F8.2,T80,F8.2,
     1          T90,F8.2,T100,F8.4,T110,F8.6)
30    CONTINUE
      WRITE(3,50)
50    FORMAT(//'   PIPE',T10,'   MEAN',T20,'  NUMBER',T30,
     1       'CALCULATED',T40,
     1       '       NET HEADS',T60,' FRICTION',/
     1       '  NUMBER',T10,' VELOCITY',T20,'    OF',T30,
     1       '   WAVE',T40,
     1       '   START',T50,'  FINISH',T60,'  COEFF.',/
     1       T10,'   (M/S)',T20,' DIVISIONS',T30,' VELOCITY',T40,
     1       ' (M.A.D.)',T50,' (M.A.D.)',T60,'   (FK)',//)
      DO 60 I=1,II(1,1)
      WRITE(3,70)I,V(I,1),II(2,I),BB(I,9),H(I,II(7,I)),H(I,1),
     1                                                  BB(I,1
70        FORMAT(I6,T10,F8.2,T20,I6,T30,F8.2,T40,F8.2,T50,F8.2,
     1                                                T60,F8.3)
60    CONTINUE
      RETURN
      END
C     ***********
C
C
C        OUTMV
C
C        ************
C
C
C
      SUBROUTINE OUTMV(IMV,RMV)
C
      DIMENSION IMV(3,10),RMV(30,11)
      WRITE(3,10)
10    FORMAT(//5X,'MAIN VALVE DATA',/5X,'**************************',///)
      WRITE(3,20)
20    FORMAT('  M.I.V.',T10,'   NODE',T20,'   VALVE',T30,'  OPENING',
     1       T40,'   LOSS',T50,'   TIME',/
     1       '  NUMBER',T10,'  NUMBER',T20,'    AREA',T30,/
     1    T20,'  (SQ.M)',T30,'     (%)',T40,'    (CD)',T50,'  (SECS)',/
      DO 30 I=1,IMV(1,1)
         WRITE(3,40)I,IMV(2,I),RMV(I,11)
40       FORMAT(/I5,T10,I6,T20,F8.2)
         DO 50 J=1,IMV(3,I)
            WRITE(3,60)RMV(I,J),RMV(10+I,J),RMV(20+I,J)
60          FORMAT(1H+,T30,F8.2,T40,F8.2,T50,F8.2)
50       CONTINUE
30    CONTINUE
      RETURN
      END
C     ***************
C
C        OUTST
C
C     ************
```

```
C
C
      SUBROUTINE OUTST(IST,RST)
C
      DIMENSION IST(3,10),RST(20,14)
      WRITE(3,10)
10    FORMAT(//5X,'SURGE TANK DATA',/5X,'**************',///)
      WRITE(3,20)
20    FORMAT('   SURGE',T10,'   NODE',T20,'     LOSS COEFF.',T40,
     1       '   INITIAL',T50,'      SURGE TANK',/
     1       '   TANK',T10,'  NUMBER',T20,'   FLOW',T30,'    FLOW',T40,
     1      'WATER ELEV',T50,'   ELEV',T60,'   AREA',/T20,'     IN',T3
     1       '    OUT',T40,' (M.A.D.)',T50,' (M.A.D.)',T60,'  (SQ.M)',/
      DO 30 I=1,IST(1,1)
         WRITE(3,40)I,IST(2,I),RST(I,11),RST(I,12),RST(I,13)
40       FORMAT(/I6,T10,I6,T20,F8.6,T30,F8.5,T40,F8.2)
         DO 50 J=1,IST(3,I)
            WRITE(3,60)RST(I,J),RST(10+I,J)
60          FORMAT(1H+,T50,F8.2,T60,F8.2)
50       CONTINUE
30    CONTINUE
      RETURN
      END
C     ************
C
C        OUTBR
C
C     ************
C
C
      SUBROUTINE OUTBR(IBR)
C
      DIMENSION IBR(15,10)
      WRITE(3,10)
10    FORMAT(//5X,'BRANCH DATA',/5X,'***********',///)
      WRITE(3,20)
20    FORMAT('   BRANCH',T10,'    NODE',T20,'    PIPE',T30,'    PIPES',/
     1       '    NUMBER',T10,'   NUMBER',T20,'      IN',T30,'     OUT',/)
      DO 30 J=1,IBR(1,1)
         WRITE(3,40)J,IBR(2,J),IBR(3,J)
40       FORMAT(/I6,T10,I6,T20,I6)
         DO 50 I=1,IBR(4,J)
            WRITE(3,60)IBR(I+4,J)
60          FORMAT(1H+,T30,I6)
50       CONTINUE
30    CONTINUE
      RETURN
      END
C     ****************
C
C        OUTTB
C
C     ****************
C
C
```

```
      SUBROUTINE OUTTB(ITB,RTB)
C
      DIMENSION ITB(4,10),RTB(70,14)
      WRITE(3,10)
10    FORMAT('     M/C',T10,' OPERATION',T20,'    TOTAL',T30,
     1       '          INITIAL',T50,' GUIDE VANE MOVEMENT',/
     1       '  NUMBER',T10,'    CODE',T20,'    G*D*D',T30,' DISCHARGE',
     1      T40,'    SPEED',T50,'      GVO',T60,'    TIME',/
     1       T20,'(KG.SQ.M.)',T30,' (CUMECS)',T40,' (R.P.M.)',T60,
     1       '   (SECS)',/)
      DO 20 I=1,ITB(1,1)
      WRITE(3,30)I,ITB(2,I),RTB(I,7),RTB(I,2),RTB(I,1)
30          FORMAT(/4X,I2,T10,4X,I2,T21,F8.1,T31,F8.2,T41,F8.1)
            DO 50 J=1,ITB(3,I)
                  WRITE(3,40)RTB(20+I,J),RTB(30+I,J)
40                FORMAT(1H+,T51,F8.2,T61,F8.2)
50          CONTINUE
20    CONTINUE
      RETURN
      END
C     ********************
C
C         FIND
C
C     ********************
C
C
      SUBROUTINE FIND(XX,YY,NGVO,NS,GVO,I,GVOT,EX,EY,AAX,AAY,BBX,BBY)
C
      DIMENSION XX(10,60,15),YY(10,60,15),NGVO(10),NS(10),GVO(10,15)
      DO 10 K=1,NGVO(I)
            IF(GVO(I,K).LE.GVOT)GOTO 20
10    CONTINUE
20    K=K-1
      DO 30 J=1,NS(I)
            BBX=(GVOT-GVO(I,K+1))*(XX(I,J,K)-XX(I,J,K+1))
            BBX=BBX/(GVO(I,K)-GVO(I,K+1))+XX(I,J,K+1)
            IF(J.EQ.1)AAX=-1000.0
            IF(BBX.GE.EX.AND.AAX.LE.EX)GOTO 50
            IF(BBX.LE.EX.AND.AAX.GE.EX)GOTO 50
            AAX=BBX
            GOTO 30
50          BBY=(GVOT-GVO(I,K+1))*(YY(I,J,K)-YY(I,J,K+1))
            BBY=BBY/(GVO(I,K)-GVO(I,K+1))+YY(I,J,K+1)
            AAY=(GVOT-GVO(I,K+1))*(YY(I,J-1,K)-YY(I,J-1,K+1))
            AAY=AAY/(GVO(I,K)-GVO(I,K+1))+YY(I,J-1,K+1)
            DELTAY=ABS(BBY-AAY)
            IF(BBY.GT.AAY)GOTO 60
            YMIN=BBY-DELTAY
            YMAX=AAY+DELTAY
            IF(YMAX.GE.EY.AND.YMIN.LE.EY)GOTO 70
            GOTO 30
60          YMAX=BBY+DELTAY
            YMIN=AAY-DELTAY
            IF(YMAX.GE.EY.AND.YMIN.LE.EY)GOTO 70
```

```
            GOTO 30
20      CONTINUE
70      IF(AAX.EQ.BBX)AAX=AAX-0.000001
        EY=AAY+(EX-AAX)*(BBY-AAY)/(BBX-AAX)
        RETURN
        END
C       ***********
C
C           CPLUS
C
C       ***********
C
C
C
        SUBROUTINE CPLUS(PIPE,BB,DT,ACP,BCP)
C
        DIMENSION BB(30,20)
        INTEGER PIPE
        BCP=BB(PIPE,13)
        F=FRIC(BCP,BB(PIPE,2),BB(PIPE,10))
        F=0.5*F*ABS(BCP)*BCP*DT/BB(PIPE,2)
        BCP=(9.806*(BB(PIPE,14)-BCP*DT*BB(PIPE,7))/BB(PIPE,9))+BCP-F
        ACP=-9.806/BB(PIPE,9)
        RETURN
        END
C       ***********
C
C           CMINUS
C
C       ***********
C
C
C
        SUBROUTINE CMINUS(PIPE,BB,DT,CCM,DCM)
C
        DIMENSION BB(30,20)
        INTEGER PIPE
        DCM=BB(PIPE,15)
        F=FRIC(DCM,BB(PIPE,2),BB(PIPE,10))
        F=0.5*F*ABS(DCM)*DCM*DT/BB(PIPE,2)
        DCM=(9.806*(BB(PIPE,7)*DT*DCM-BB(PIPE,16))/BB(PIPE,9))+DCM-F
        CCM=9.806/BB(PIPE,9)
        RETURN
        END
C       ***********
C
C           FRIC
C
C       ***********
C
C
C
        FUNCTION FRIC(V,D,FK)
C
        RE=ABS(V)*D*1000000.0/1.5
        IF(RE.GT.0.1)GOTO 10
        FRIC=640.0
        RETURN
```

```
10      IF(RE.GT.1900.0)GOTO 20
        FRIC=64.0/RE
        RETURN
20      FRIC=FK/(RE**0.145)
        RETURN
        END
C       ***********
C
C         TRNODE
C
C       ***********
C
C
C
        SUBROUTINE TRNODE(II,BB,DT,H,V)
C
        DIMENSION II(10,30),BB(30,20),H(30,20),V(30,20),HC(20),VC(20)
        DO 10 I=1,II(1,1)
        IF(II(2,I).LE.1)GOTO 10
              DO 20 J=2,II(2,I)
                    VA=V(I,J+1)
                    HA=H(I,J+1)
                    F=FRIC(VA,BB(I,2),BB(I,10))
                    F=0.5*F*ABS(VA)*VA*DT/BB(I,2)
                    HA=(9.806*(HA-VA*DT*BB(I,7))/BB(I,9))-F+VA
                    VB=V(I,J-1)
                    HB=H(I,J-1)
                    F=FRIC(VB,BB(I,2),BB(I,10))
                    F=0.5*F*ABS(VB)*VB*DT/BB(I,2)
                    HB=(9.806*(VB*DT*BB(I,7)-HB)/BB(I,9))-F+VB
                    HC(J)=0.5*BB(I,9)*(HA-HB)/9.806
                    VC(J)=0.5*(HA+HB)
20            CONTINUE
              DO 30 J=2,II(2,I)
                    V(I,J)=VC(J)
                    H(I,J)=HC(J)
30            CONTINUE
10      CONTINUE
        RETURN
        END
C       ***********
C
C         TRMV
C
C       ***********
C
C
C
        SUBROUTINE TRMV(PIN,POUT,NOMV,IMV,RMV,TT,II,BB,DT,H,V)
C
        DIMENSION IMV(3,10),RMV(30,11),II(10,30),BB(30,20),
     1                                  FX(10),FY(10),H(30,20),V(30,20)
        INTEGER PIN,POUT
        REAL KD
        CALL CPLUS(PIN,BB,DT,ACP,BCP)
        CALL CMINUS(POUT,BB,DT,CCM,DCM)
        DO 30 J=1,IMV(3,NOMV)
```

```
            FX(J)=RMV(20+NOMV,J)
            FY(J)=RMV(10+NOMV,J)
30      CONTINUE
        CALL INTERP(FX,FY,TT,KD,IMV(3,NOMV))
        EQ=BB(PIN,6)*V(PIN,1)
        AAA=(1.0/(KD**2)-1.0)/(2.0*9.806*RMV(NOMV,11)**2)
        BBB=1.0/(BB(POUT,5)*CCM)-1.0/(BB(PIN,6)*ACP)
        CCC=BCP/ACP-DCM/CCM
        CCC=CCC-(BB(PIN,11)**2-BB(POUT,17)**2)/(2.0*9.806)
20      FQ=AAA*EQ**2+BBB*EQ+CCC
        DFQ=2.0*AAA*EQ+BBB
        IF(ABS(FQ).LT.ABS(EQ/1000.0))GOTO 10
        EQ=EQ-FQ/DFQ
        GOTO 20
10      V(PIN,1)=EQ/BB(PIN,6)
        H(PIN,1)=V(PIN,1)/ACP-BCP/ACP
        J=II(7,POUT)
        V(POUT,J)=BB(PIN,6)*V(PIN,1)/BB(POUT,6)
        H(POUT,J)=V(POUT,J)/CCM-DCM/CCM
        RETURN
        END
C       ***************
C
C           TRST
C
C       ***********
C
C
C
        SUBROUTINE TRST(PIN,POUT,NOST,IST,RST,II,BB,DT,H,V)
C
        DIMENSION IST(3,10),RST(20,14),II(10,30),BB(30,20),
     1                                              H(30,20),V(30,20)
        INTEGER PIN,POUT
        REAL KQQ
        CALL CPLUS(PIN,BB,DT,ACP,BCP)
        CALL CMINUS(POUT,BB,DT,CCM,DCM)
        DO 10 J=1,IST(3,NOST)
            IF(RST(NOST,13).LT.RST(NOST,J))GOTO 20
10      CONTINUE
20      AREA=RST(NOST+10,J-1)
        EQST=2.0*RST(NOST,14)-RST(NOST+10,14)
        RST(NOST+10,14)=RST(NOST,14)
        IF(EQST.GE.0.0)KQQ=RST(NOST,11)
        IF(EQST.LT.0.0)KQQ=RST(NOST,12)
        EZST=RST(NOST,13)+EQST*DT/AREA
        H(PIN,1)=EZST+KQQ*EQST*ABS(EQST)
        H(POUT,II(7,POUT))=EZST-BB(POUT,17)**2/(2.0*9.806)
        V(PIN,1)=ACP*H(PIN,1)+BCP
        V(POUT,II(7,POUT))=CCM*H(POUT,II(7,POUT))+DCM
        RST(NOST,14)=BB(PIN,6)*V(PIN,1)-BB(POUT,6)*V(POUT,II(7,POUT))
        RST(NOST,13)=RST(NOST,13)+RST(NOST,14)*DT/AREA
        RETURN
        END
C       ***************
C
```

```
C
C          TRBR
C
C     ***************
C
C
C
      SUBROUTINE TRBR(PIN,NOBR,IBR,II,BB,DT,H,V)
C
      DIMENSION IBR(15,10),II(10,30),BB(30,20),H(30,20),V(30,20),
     1                                                C(10),D(10)
      REAL NUM
      INTEGER PIN,POUT
      SNUM=0.0
      SDEN=0.0
      CALL CPLUS(PIN,BB,DT,ACP,BCP)
      DO 10 I=1,IBR(4,NOBR)
            POUT=IBR(I+4,NOBR)
            CALL CMINUS(POUT,BB,DT,CCM,DCM)
            C(I)=CCM
            D(I)=DCM
            NUM=BB(POUT,6)*CCM*(BB(PIN,11)**2-BB(POUT,17)**2)/
     1                                                (2.0*9.806)
            NUM=NUM+BB(POUT,6)*DCM
            DEN=BB(POUT,6)*CCM
            SNUM=SNUM+NUM
            SDEN=SDEN+DEN
10    CONTINUE
      NUM=BB(PIN,6)*BCP-SNUM
      DEN=SDEN-BB(PIN,6)*ACP
      H(PIN,1)=NUM/DEN
      V(PIN,1)=H(PIN,1)*ACP+BCP
      DO 20 I=1,IBR(4,NOBR)
            POUT=IBR(I+4,NOBR)
            J=II(7,POUT)
            H(POUT,J)=(BB(PIN,11)**2-BB(POUT,17)**2)/(2.0*9.806)
            H(POUT,J)=H(POUT,J)+H(PIN,1)
            V(POUT,J)=C(I)*H(POUT,J)+D(I)
20    CONTINUE
      RETURN
      END
C     ***********
C
C          TRRES
C
C     ***********
C
C
C
      SUBROUTINE TRRES(POUT,HRES,II,BB,DT,H,V,L)
C
      DIMENSION II(10,30),BB(30,20),H(30,20),V(30,20)
      INTEGER POUT
      CALL CMINUS(POUT,BB,DT,CCM,DCM)
      H(POUT,II(7,POUT))=HRES+(L*BB(POUT,17)**2)/(2.0*9.806)
      V(POUT,II(7,POUT))=CCM*H(POUT,II(7,POUT))+DCM
      RETURN
      END
```

```
C     ***********************
C
C           TRJN
C
C     ***********************
C
C
      SUBROUTINE TRJN(PIN,POUT,II,BB,DT,H,V)
C
      DIMENSION II(10,30),BB(30,20),H(30,20),V(30,20)
      REAL NUM
      INTEGER PIN,POUT
      CALL CPLUS(PIN,BB,DT,ACP,BCP)
      CALL CMINUS(POUT,BB,DT,CCM,DCM)
      NUM=BCP/ACP-DCM/CCM+(BB(POUT,17)**2-BB(PIN,11)**2)/
     1                                                (2.0**9.806)
      DEN=BB(POUT,6)*(1.0/(BB(PIN,6)*ACP)-1.0/(BB(POUT,6)*CCM))
      V(POUT,II(7,POUT))=NUM/DEN
      H(POUT,II(7,POUT))=V(POUT,II(7,POUT))/CCM-DCM/CCM
      V(PIN,1)=V(POUT,II(7,POUT))*BB(POUT,6)/BB(PIN,6)
      H(PIN,1)=V(PIN,1)/ACP-BCP/ACP
      RETURN
      END
C     ***********************
C
C          INTERP
C
C     ***********************
C
C
      SUBROUTINE INTERP(FX,FY,CX,CY,NPTS)
C
      DIMENSION FX(10),FY(10)
      DO 10 I=2,NPTS
           IF(FX(I).LE.CX)GOTO 10
           GOTO 20
10    CONTINUE
20    CY=FY(I)+(CX-FX(I))*(FY(I-1)-FY(I))/(FX(I-1)-FX(I))
      RETURN
      END
C     ***********************
C
C          INIT
C
C     ***********************
C
C
      SUBROUTINE INIT(ITB,RTB,ISTP,RSTP,ISTT,RSTT,IIP,BBP,IIT,BBT,
     1                                                VP,HP,VT,HT)
C
      DIMENSION ITB(4,10),RTB(70,14),IIP(10,30),BBP(30,20),
     1          IIT(10,30),BBT(30,20),
     1          ISTP(3,10),RSTP(20,14),ISTT(3,10),RSTT(20,14),
     1          VP(30,20),HP(30,20),VT(30,20),HT(30,20)
      DO 10 I=1,ITB(1,1)
```

```
                RTB(I+10,1)=RTB(I,1)
                RTB(I+10,2)=RTB(I,2)
                RTB(I+10,4)=RTB(I,4)
                RTB(I+10,6)=RTB(I,6)
                RTB(I+10,9)=RTB(I,9)
                RTB(I+10,10)=RTB(I,10)
10          CONTINUE
            DO 20 I=1,IIP(1,1)
                BBP(I,7)=SIN(BBP(I,7))
                BBP(I,11)=VP(I,1)
                BBP(I,12)=HP(I,1)
                BBP(I,13)=VP(I,2)
                BBP(I,14)=HP(I,2)
                BBP(I,15)=VP(I,IIP(7,I)-1)
                BBP(I,16)=HP(I,IIP(7,I)-1)
                BBP(I,17)=VP(I,IIP(7,I))
                BBP(I,18)=HP(I,IIP(7,I))
20          CONTINUE
            DO 25 I=1,ISTP(1,1)
                RSTP(I+10,13)=RSTP(I,13)
25          CONTINUE
            IF(IIT(1,1).EQ.0)GOTO 40
            DO 30 I=1,IIT(1,1)
                BBT(I,7)=SIN(BBT(I,7))
                BBT(I,11)=VT(I,1)
                BBT(I,12)=HT(I,1)
                BBT(I,13)=VT(I,2)
                BBT(I,14)=HT(I,2)
                BBT(I,15)=VT(I,IIT(7,I)-1)
                BBT(I,16)=HT(I,IIT(7,I)-1)
                BBT(I,17)=VT(I,IIT(7,I))
                BBT(I,18)=HT(I,IIT(7,I))
30          CONTINUE
            DO 35 I=1,ISTT(1,1)
                RSTT(I+10,13)=RSTT(I,13)
35          CONTINUE
40          CONTINUE
            RETURN
            END
C           ***************
C
C               UPDATE
C
C           ***************
C
C
            SUBROUTINE UPDATE(II,BB,H,V)
C
            DIMENSION II(10,30),BB(30,20),H(30,20),V(30,20)
            DO 10 I=1,II(1,1)
                BB(I,11)=V(I,1)
                BB(I,12)=H(I,1)
                BB(I,13)=V(I,2)
                BB(I,14)=H(I,2)
                BB(I,15)=V(I,II(7,I)-1)
```

```
                BB(I,16)=H(I,II(7,I)-1)
                BB(I,17)=V(I,II(7,I))
                BB(I,13)=H(I,II(7,I))
10      CONTINUE
        RETURN
        END
C       ***************
C
C          OUTRST
C
C       ***************
C
C
C
        SUBROUTINE OUTRST(ITB,RTB,TT)
C
        DIMENSION ITB(4,10),RTB(70,14)
        WRITE(3,10)TT
10      FORMAT(F8.2)
        DO 20 I=1,ITB(1,1)
              WRITE(3,30)I,RTB(I,1),RTB(I,2),RTB(I,3),RTB(I+10,7),
     1              RTB(I,8),RTB(I,9),RTB(I,10),RTB(I+10,5),RTB(I+10,6)
20      CONTINUE
30      FORMAT(T10,I6,T20,F8.2,T30,F8.3,T40,F8.2,T50,F8.2,T60,F8.2,
     1        T70,F8.3,T80,F8.1,T90,F8.2,T100,F8.2)
        RETURN
        END
C       ***************
C
C          YYFIND
C
C       ***************
C
C
C
        SUBROUTINE YYFIND(XX,YY,NGVO,NS,GVO,I,GVOT,EX,EY,AAX,AAY,BBX,BB
C
        DIMENSION XX(10,60,15),YY(10,60,15),NGVO(10),NS(10),GVO(10,15)
        DO 10 K=1,NGVO(I)
              IF(GVO(I,K).LE.GVOT)GOTO 20
10      CONTINUE
20      K=K-1
        DO 30 J=1,NS(I)
              BBX=(GVOT-GVO(I,K+1))*(XX(I,J,K)-XX(I,J,K+1))
              BBX=BBX/(GVO(I,K)-GVO(I,K+1))+XX(I,J,K+1)
              IF(J.EQ.1)AAX=1000.0
              IF(BBX.LE.EX.AND.AAX.GE.EX)GOTO 50
              AAX=BBX
              GOTO 30
50            BBY=(GVOT-GVO(I,K+1))*(YY(I,J,K)-YY(I,J,K+1))
              BBY=BBY/(GVO(I,K)-GVO(I,K+1))+YY(I,J,K+1)
              AAY=(GVOT-GVO(I,K+1))*(YY(I,J-1,K)-YY(I,J-1,K+1))
              AAY=AAY/(GVO(I,K)-GVO(I,K+1))+YY(I,J-1,K+1)
              DELTAY=ABS(BBY-AAY)
              IF(BBY.GT.AAY)GOTO 60
              YMIN=BBY-DELTAY
              YMAX=AAY+DELTAY
```

```
            IF(YMAX.GE.EY.AND.YMIN.LE.EY)GOTO 70
            GOTO 30
60          YMAX=BBY+DELTAY
            YMIN=AAY-DELTAY
            IF(YMAX.GE.EY.AND.YMIN.LE.EY)GOTO 70
            GOTO 30
20      CONTINUE
70      IF(AAX.EQ.BBX)AAX=AAX-0.000001
        EY=AAY+(EX-AAX)*(BBY-AAY)/(BBX-AAX)
        RETURN
        END
```

UNIV. OF WARWICK ENGINEERING DEPT.

WATERHAMMER CALCULATIONS

BY

NIGEL WALMSLEY

TIME INCREMENTS

TIME STEP FOR CALCULATIONS	=	0.01
TIME LIMIT FOR CALCULATIONS	=	25.00
TIME STEP FOR OUTPUT	=	0.20

RESERVOIR DATA

UPPER RESERVOIR LEVEL	=	369.6
LOWER RESERVOIR LEVEL	=	80.8

PENSTOCK DATA

PIPELINE DATA

PIPE NUMBER	START NODE NUMBER	START NODE TYPE	FINISH NODE NUMBER	FINISH NODE TYPE	PIPE LENGTH (M)	PIPE DIAMETER (M)	WAVE VELOCITY (M/S)	ELEVATION START (M.A.D.)	ELEVATION FINISH (M.A.D.)	ANGLE TO HORZ. (RADS)	FRICTION CONST. (K)
1	8	20	1	1	10.0	1.30	1200.00	52.00	52.00	0.0000	0.001964
2	7	20	2	2	10.0	1.30	1200.00	52.00	52.00	0.0000	0.001964
3	6	20	3	3	10.0	1.30	1200.00	52.00	52.00	0.0000	0.001964
4	5	20	4	4	10.0	1.30	1200.00	52.00	52.00	0.0000	0.001964
5	10	40	7	20	10.0	1.30	1200.00	52.00	52.00	0.0000	0.001964
6	10	40	8	20	10.0	1.30	1200.00	52.00	52.00	0.0000	0.001964
7	9	40	5	20	10.0	1.30	1200.00	52.00	52.00	0.0000	0.001964
8	9	40	6	20	10.0	1.30	1200.00	52.00	52.00	0.0000	0.001964
9	11	40	9	40	47.7	2.30	1200.00	88.00	52.00	0.8552	0.001964
10	11	40	10	40	47.7	2.30	1200.00	88.00	52.00	0.8552	0.001964
11	12	60	11	40	58.2	3.42	1200.00	110.20	88.00	0.3916	0.000135
12	13	60	12	60	93.5	3.53	1200.00	127.45	110.20	0.1856	0.000180
13	14	60	13	60	93.5	3.53	1200.00	144.93	127.45	0.1881	0.000180
14	15	60	14	60	110.1	3.54	1200.00	185.93	144.93	0.3816	0.000212
15	16	60	15	60	67.9	3.86	1200.00	185.93	185.93	0.0000	0.000084
16	17	60	16	60	67.9	3.86	1200.00	185.93	185.93	0.0000	0.000084
17	18	60	17	60	90.7	5.70	1200.00	194.00	185.93	0.0891	0.000025
18	19	60	18	60	90.7	5.70	1200.00	202.20	194.00	0.0905	0.000025
19	20	60	19	60	90.7	5.70	1200.00	210.40	202.20	0.0905	0.000025
20	21	60	20	60	59.2	6.40	1200.00	269.64	210.40	1.5705	0.000041
21	22	30	21	60	59.2	6.40	1200.00	328.88	269.64	1.5708	0.000041
22	23	60	22	30	100.0	4.50	1200.00	331.06	328.80	0.0226	0.000058
23	24	60	23	60	100.0	4.50	1200.00	333.24	331.06	0.0218	0.000058
24	25	60	24	60	100.0	4.50	1200.00	335.82	333.24	0.0258	0.000058
25	26	60	25	60	111.7	4.50	1200.00	338.25	335.82	0.0218	0.000064
26	27	60	26	60	111.7	4.50	1200.00	340.68	338.25	0.0218	0.000064
27	28	30	27	60	111.7	4.50	1200.00	343.11	340.68	0.0218	0.000064
28	29	60	28	30	75.0	4.50	1200.00	344.74	343.11	0.0217	0.000043
29	30	60	29	60	75.0	4.50	1200.00	346.37	344.74	0.0217	0.000043
30	31	50	30	60	75.0	4.50	1200.00	348.00	346.37	0.0217	0.000043

PIPE NUMBER	MEAN VELOCITY (M/S)	NUMBER OF DIVISIONS	CALCULATED WAVE VELOCITY	NET HEADS START (M.A.D.)	NET HEADS FINISH (M.A.D.)	FRICTION COEFF. (FK)

1	14.46	1	1000.00	346.30	345.58	0.094
2	14.46	1	1000.00	346.30	345.58	0.094
3	14.46	1	1000.00	346.30	345.58	0.094
4	14.46	1	1000.00	346.30	345.58	0.094
5	14.46	1	1000.00	347.03	346.30	0.094
6	14.46	1	1000.00	347.03	346.30	0.094
7	14.46	1	1000.00	347.03	346.30	0.094
8	14.46	1	1000.00	347.03	346.30	0.094
9	9.24	4	1192.50	356.23	353.34	0.349
10	9.24	4	1192.50	356.23	353.34	0.349
11	8.36	5	1163.20	357.82	357.03	0.149
12	7.35	8	1168.75	359.31	358.25	0.144
13	7.35	8	1168.75	360.37	359.31	0.144
14	7.30	9	1223.33	361.65	360.40	0.146
15	6.56	6	1132.17	363.06	362.56	0.143
16	6.56	6	1132.17	363.55	363.06	0.143
17	3.01	8	1134.00	365.43	365.29	0.209
18	3.01	8	1134.00	365.58	365.43	0.209
19	3.01	8	1134.00	365.72	365.58	0.209
20	2.39	5	1184.80	366.14	365.89	0.933
21	2.39	5	1184.80	366.38	366.14	0.933
22	4.33	8	1250.00	365.82	365.48	0.141
23	4.33	8	1250.00	366.16	365.82	0.141
24	4.33	8	1250.00	366.51	366.16	0.141
25	4.33	9	1240.78	366.89	366.51	0.141
26	4.33	9	1240.78	367.27	366.89	0.141
27	4.33	9	1240.78	367.65	367.27	0.141
28	4.33	6	1250.00	367.90	367.65	0.141
29	4.33	6	1250.00	368.16	367.90	0.141
30	4.33	6	1250.00	368.41	368.16	0.141

MAIN VALVE DATA
****

M.I.V. NUMBER	NODE NUMBER	VALVE AREA (SQ.M)	OPENING (%)	LOSS (CO)	TIME (SECS)
1	8	1.33			
+			100.00	1.00	0.00
+			100.00	1.00	5.00
+			94.00	0.98	6.70
+			89.00	0.89	7.60
+			77.50	0.65	9.35
+			66.00	0.46	11.10
+			44.00	0.21	14.50
+			19.00	0.07	18.40
+			0.00	0.00	33.00
+			0.00	0.00	50.00
2	7	1.33			

+			100.00	1.00	0.00
+			100.00	1.00	5.80
+			94.00	0.98	6.70
+			89.00	0.89	7.60
+			77.50	0.65	9.35
+			66.00	0.46	11.10
+			44.00	0.21	14.60
+			19.00	0.07	18.40
+			0.00	0.00	33.00
+			0.00	0.00	50.00
	3	6	1.33		
+			100.00	1.00	0.00
+			100.00	1.00	5.80
+			94.00	0.98	6.70
+			89.00	0.89	7.60
+			77.50	0.65	9.35
+			66.00	0.46	11.10
+			44.00	0.21	14.60
+			19.00	0.07	18.40
+			0.00	0.00	33.00
+			0.00	0.00	50.00
	4	5	1.33		
+			100.00	1.00	0.00
+			100.00	1.00	5.80
+			94.00	0.98	6.70
+			89.00	0.89	7.60
+			77.50	0.65	9.35
+			66.00	0.46	11.10
+			44.00	0.21	14.60
+			19.00	0.07	18.40
+			0.00	0.00	33.00
+			0.00	0.00	50.00

SURGE TANK DATA
****

SURGE TANK	NODE NUMBER	LOSS COEFF. FLOW IN	LOSS COEFF. FLOW OUT	INITIAL WATER ELEV (M.A.D.)	SURGE TANK ELEV (M.A.D.)	SURGE TANK AREA (SQ.M)
1	28	0.000000	0.00000	367.65		
+					350.00	15.90
+					372.00	15.90
+					400.00	1000.00
+					500.00	1000.00
2	22	0.001058	0.00165	365.48		
+					335.00	7.00
+					371.00	78.54

+		380.00	314.16
+		380.00	500.00

BRANCH DATA

BRANCH NUMBER	NODE NUMBER	PIPE IN	PIPES OUT
1	10	10	
+			5
+			6
2	9	9	
+			7
+			8
3	11	11	
+			9
+			10

TURBINE DATA

M/C NUMBER	OPERATION CODE	TOTAL G*D*D (KG.SQ.M.)	INITIAL DISCHARGE (CUMECS)	INITIAL SPEED (R.P.M.)	GUIDE VANE MOVEMENT GVO	GUIDE VANE MOVEMENT TIME (SECS)
1	1	355000.0	19.20	600.0		
+					33.00	0.00
+					33.00	0.50
+					15.00	9.50
+					7.30	14.00
+					0.00	24.00
+					0.00	50.00
2	1	355000.0	19.20	600.0		
+					33.00	0.00
+					33.00	0.50
+					15.00	9.50
+					7.30	14.00
+					0.00	24.00
+					0.00	50.00

	3	1	355000.0	19.20	600.0		
+						33.00	0.00
+						33.00	0.50
+						15.00	9.50
+						7.30	14.00
+						0.00	24.00
+						0.00	50.00
	4	1	355000.0	19.20	600.0		
+						33.00	0.00
+						33.00	0.50
+						15.00	9.50
+						7.30	14.00
+						0.00	24.00
+						0.00	50.00

******

TAILRACE DATA

******

PIPELINE DATA
****

PIPE NUMBER	START NODE NUMBER	START NODE TYPE	FINISH NODE NUMBER	FINISH NODE TYPE	PIPE LENGTH (M)	PIPE DIAMETER (M)	WAVE VELOCITY (M/S)	ELEVATION START (M.A.D.)	ELEVATION FINISH (M.A.D.)	ANGLE TO HORZ. (RADS)	FRICTION CONST. (K)
1	8	50	1	1	45.6	3.00	1200.00	70.15	50.00	0.4580	0.001110
2	7	50	2	2	45.6	3.00	1200.00	70.15	50.00	0.4580	0.001110
3	6	50	3	3	45.6	3.00	1200.00	70.15	50.00	0.4580	0.001110
4	5	50	4	4	45.6	3.00	1200.00	70.15	50.00	0.4580	0.001110

PIPE NUMBER	MEAN VELOCITY (M/S)	NUMBER OF DIVISIONS	CALCULATED WAVE VELOCITY	NET HEADS START (M.A.D.)	NET HEADS FINISH (M.A.D.)	FRICTION COEFF. (FK)
1	-2.72	4	1139.25	80.75	81.16	0.679
2	-2.72	4	1139.25	80.75	81.16	0.679
3	-2.72	4	1139.25	80.75	81.16	0.679
4	-2.72	4	1139.25	80.75	81.16	0.679

UNIV. OF WARWICK ENGINEERING DEPT.

WATERHAMMER CALCULATIONS

BY

NIGEL WALMSLEY

TIME INCREMENTS

TIME STEP FOR CALCULATIONS	=	0.04
TIME LIMIT FOR CALCULATIONS	=	50.00
TIME STEP FOR OUTPUT	=	0.20

RESERVOIR DATA

UPPER RESERVOIR LEVEL	=	61.0
LOWER RESERVOIR LEVEL	=	26.5

PENSTOCK DATA

PIPELINE DATA
****

PIPE NUMBER	START NODE NUMBER	START NODE TYPE	FINISH NODE NUMBER	FINISH NODE TYPE	PIPE LENGTH (M)	PIPE DIAMETER (M)	WAVE VELOCITY (M/S)	ELEVATION START (M.A.D.)	ELEVATION FINISH (M.A.D.)	ANGLE TO HORZ. (RADS)	FRICTION CONST. (K)
1	6	40	1	1	34.0	1.75	1000.00	27.50	26.30	0.0353	0.004550
2	6	40	2	2	34.0	1.75	1000.00	27.50	26.30	0.0353	0.004550
3	6	40	3	3	34.0	1.75	1000.00	27.50	26.30	0.0353	0.004550
4	6	40	4	4	34.0	1.75	1000.00	27.50	26.30	0.0353	0.004550
5	6	40	5	5	34.0	1.75	1000.00	27.50	26.30	0.0353	0.004550
6	7	60	6	40	50.0	4.00	1000.00	27.63	27.50	0.0026	0.000096
7	8	60	7	60	70.0	4.00	1000.00	27.80	27.63	0.0024	0.000135
8	9	60	8	60	150.0	4.00	1000.00	28.18	27.80	0.0025	0.000289
9	10	60	9	60	200.0	4.00	1000.00	28.68	28.18	0.0025	0.000385

PIPE NUMBER	MEAN VELOCITY (M/S)	NUMBER OF DIVISIONS	CALCULATED WAVE VELOCITY	NET HEADS START (M.A.D.)	NET HEADS FINISH (M.A.D.)	FRICTION COEFF. (FK)
1	3.62	1	850.00	58.61	58.27	0.243
2	3.62	1	850.00	58.61	58.27	0.243
3	3.62	1	850.00	58.61	58.27	0.243
4	3.62	1	850.00	58.61	58.27	0.243
5	3.62	1	850.00	58.61	58.27	0.243
6	3.47	1	1250.00	58.35	58.67	0.244
7	3.47	2	875.00	59.11	58.85	0.245
8	3.47	4	937.50	59.66	59.11	0.244
9	3.47	5	1000.00	60.39	59.66	0.244

BRANCH DATA
****

BRANCH NUMBER	NODE NUMBER	PIPE IN	PIPES OUT
1	0	0	
			1
			2
			3
			4

TURBINE DATA

M/C NUMBER	OPERATION CODE	TOTAL GD**D (KG.SQ.M.)	INITIAL DISCHARGE (CUMECS)	INITIAL SPEED (R.P.M.)	GUIDE VANE MOVEMENT GVO	GUIDE VANE MOVEMENT TIME (SECS)
1	1	18000.0	8.71	500.0		
					82.00	0.00
					0.00	8.00
					0.00	50.00
					0.000	0.00
					0.957	3.80
					1.400	8.00
					0.000	32.00
					0.000	100.00
2	1	18000.0	8.71	500.0		
					82.00	0.00
					0.00	8.00
					0.00	50.00
					0.000	0.00
					0.957	3.80
					1.400	8.00
					0.000	32.00
					0.000	100.00
3	1	18000.0	8.71	500.0		
					82.00	0.00
					0.00	8.00
					0.00	50.00
					0.000	0.00
					0.957	3.80
					1.400	8.00
					0.000	32.00
					0.000	100.00
4	1	18000.0	8.71	500.0		
					82.00	0.00
					0.00	8.00
					0.00	50.00
					0.000	0.00
					0.957	3.80
					1.400	8.00
					0.000	32.00

+								0.000	100.00
	5	1	18000.0	8.71	500.0				
+						82.00	0.00		
+						0.00	8.00		
+						0.00	50.00		
+								0.000	0.00
+								0.957	3.80
+								1.400	8.00
+								0.000	32.00
+								0.000	100.00

TAILRACE DATA

NO TAILRACE

APPENDIX IV: Listing of Program 'SMESHJ' for the Automatic Generation of a Curvilinear Mesh

```
      DIMENSION GV0(15),XX(60,15),YY(60,15),QN11(60,15),Q11(60,15),
     *          PX(60,15),PY(60,15),NS(15)
      REAL K0,K1,K2,K3,MAX,MIN
      INTEGER PT,NGV0,NS,NSM,COUNT,NPTS,PPTS,NPTS1
      OPEN(UNIT=1,FILE='MCDATA')
      OPEN(UNIT=2,FILE='SMJRST')
      READ(1,*)XXR,YYR
      READ(1,*)NGV0
      READ(1,*)(GV0(I),I=1,NGV0)
      DO 10 J=1,NGV0
            READ(1,*)NS(J)
            NPTS=NS(J)
            DO 15 I=1,NPTS
                  READ(1,*)XX(I,J),YY(I,J)
                  XX(I,J)=XX(I,J)/XXR*GV0(J)/GV0(1)
                  YY(I,J)=YY(1,J)/YYR
15          CONTINUE
10    CONTINUE
      NPTS1=NS(1)
      DO 50 I=1,NPTS1
            PX(I,1)=XX(I,1)
            PY(I,1)=YY(I,1)
50    CONTINUE
      NGV01=NGV0-1
      DO 60 J=1,NGV01
            NPTS=NS(1)-1
            DO 70 K=2,NPTS
                  IF(PX(K,J).EQ.PX(K-1,J))PX(K-1,J)=PX(K-1,J)-0.00001
                  IF(PX(K,J).EQ.PX(K+1,J))PX(K+1,J)=PX(K+1,J)-0.00001
                  ANG5=ATAN((PY(K-1,J)-PY(K,J))/(PX(K-1,J)-PX(K,J)))
                  ANG6=ATAN((PY(K,J)-PY(K+1,J))/(PX(K,J)-PX(K+1,J)))
                  S5=SIN(ANG5)/COS(ANG5)
                  IF(S5.EQ.0.0)S5=S5-0.00001
                  S6=SIN(ANG6)/COS(ANG6)
                  IF(S6.EQ.0.0)S6=S6-0.00001
                  A1=(PX(K-1,J)+PX(K,J))/2.0
                  B1=(PY(K-1,J)+PY(K,J))/2.0
                  S1=-1.0/S5
                  S2=-1.0/S6
                  A2=(PX(K,J)+PX(K+1,J))/2.0
                  B2=(PY(K,J)+PY(K+1,J))/2.0
                  C1=B1-S1*A1
                  C2=B2-S2*A2
                  IF(S1.EQ.S2)S1=S1-0.00001
                  A3=-(C1-C2)/(S1-S2)
                  B3=S1*A3+C1
                  IF(A3.EQ.PX(K,J))A3=A3-0.00001
                  SLP8=(B3-PY(K,J))/(A3-PX(K,J))
                  CON8=PY(K,J)-(SLP8*PX(K,J))
                  RMIN=1000000.
                  PPTS=NS(J+1)-1
      DO 80 PT=1,PPTS
                  X1=XX(PT,J+1)
                  Y1=YY(PT,J+1)
                  X2=XX(PT+1,J+1)
```

```
      Y2=YY(PT+1,J+1)
      IF(X1.EQ.X2.AND.Y1.EQ.Y2)GOTO 80
      IF(X1.EQ.X2)X2=X2-0.0001
      SLP1=(Y1-Y2)/(X1-X2)
      CON1=Y1-(SLP1*X1)
      IF(SLP1.EQ.SLP8)SLP1=SLP1-0.00001
      CROX=(CON1-CON8)/(SLP8-SLP1)
      CROY=SLP1*CROX+CON1
      IF(PT.EQ.PPTS)GOTO 75
            IF(X1.GE.X2)XMAX=X1+0.0001
            IF(X1.LT.X2)XMAX=X2+0.0001
            IF(X1.GE.X2)XMIN=X2-0.0001
            IF(X1.LT.X2)XMIN=X1-0.0001
            IF(CROX.GT.XMAX)GOTO 80
            IF(CROX.LT.XMIN)GOTO 80
            IF(Y1.GE.Y2)YMAX=Y1+0.0001
            IF(Y1.LT.Y2)YMAX=Y2+0.0001
            IF(Y1.GE.Y2)YMIN=Y2-0.0001
            IF(Y1.LT.Y2)YMIN=Y1-0.0001
            IF(CROY.GT.YMAX)GOTO 80
            IF(CROY.LT.YMIN)GOTO 80
75          RR=(PX(K,J)-CROX)**2
            RR=RR+(PY(K,J)-CROY)**2
            IF(RR.GT.RMIN)GOTO 80
                  RMIN=RR
                  PX(K,J+1)=CROX
                  PY(K,J+1)=CROY
80                CONTINUE
      IF(PX(K-1,J).EQ.PX(K-1,J+1))PX(K-1,J)=PX(K-1,J)-0.0001
      SLP2=(PY(K-1,J)-PY(K-1,J+1))/(PX(K-1,J)-PX(K-1,J+1))
      IF(SLP1.EQ.SLP2)SLP1=SLP1-0.00001
      CON2=PY(K-1,J)-SLP2*PX(K-1,J)
      CROX1=(CON2-CON1)/(SLP1-SLP2)
      CROY1=SLP1*CROX1+CON1
      RR1=(PX(K-1,J)-CROX1)**2
      RR1=RR1+(PY(K-1,J)-CROY1)**2
      IF(RR1.GT.RMIN)GOTO 70
      PX(K,J+1)=PX(K-1,J+1)
      PY(K,J+1)=PY(K-1,J+1)
70          CONTINUE
60    CONTINUE
      NPTS1=NS(1)
      DO 200 I=2,NPTS1-1
            WRITE(2,100)(PX(I,J),J=1,NGVO)
            WRITE(2,100)(PY(I,J),J=1,NGVO)
200   CONTINUE
100   FORMAT(1X,10(F6.3,2X),F6.3)
      STOP
      END
```

APPENDIX V: Published Papers

IAHR AIRH

Operating Problems of Pump Stations and Power Plants

PERFORMANCE CHARACTERISTICS OF REVERSIBLE PUMP TURBINES

CARACTERISTIQUES DU RENDEMENT DES TURBINES DE POMPE REVERSIBLES

DR. A.P. BOLDY LECTURER UNIVERSITY OF WARWICK, COVENTRY, ENGLAND.
MR. N. WALMSLEY RESEARCH STUDENT UNIVERSITY OF WARWICK, COVENTRY, ENGLAND.

SUMMARY

The paper presents a method of representation of the four quadrant performance characteristics of reversible pump turbines such that acceptable interpolations are obtained between adjacent guide vane curves.

Problems associated with the performance characteristics used in the simulation of the transient performance of a Pumped Storage Scheme are discussed. A revised calculation procedure designed to alleviate the problems is presented and the simulated results compared with prototype site recordings.

RESUME

Cette communication présente une méthode pour représenter les caractéristiques due rendement des quatre secteurs des turbines de pompe réversibles qui permet des interpolations entre les courbes de palettes-guides adjacentes.

Des problèmes relevant des caractéristiques du rendement utilisées dans la simulation du rendement transitoire d'un projet d'emmagasinement sont discutés. Une méthode de calcul modifiée pour réduire les problèmes est présentée, et les résultats simulés sont comparés à des enregistrements directs du prototype.

INTRODUCTION

During the last 10 years the principal author has developed a suite of computer programs to analyse the transient response of hydroelectric installations. The calculations are based on the well known explicit finite difference method of characteristics to solve the governing quasi-linear hyperbolic partial differential equations of momentum and continuity [1,2,3,4]. The variant of the method used is "specified time intervals", which produces values of piezometric head and volumetric mean velocity at regular, specified, values of position and time. The programs have been used extensively in connection with a number of hydroelectric installations (e.g. Cruachan, Foyers, Planicie Banderita, El Chocon, Steenbras, Dinorwic, Victoria and Lungga). The results produced by the programs have been validated against site recordings taken during commissioning of various installations, notably Cruachan, Foyers and Steenbras.

A schematic layout of a typical pumped storage scheme is shown in Figure 1. The boundary conditions normally encountered are; (a) constant head reservoir, (b) surge tank, (c) pipe branch, (d) main inlet valve, and (e) reversible pump turbine. Various methods for simulating the boundary conditions (a), (b), (c) and (d) above are in common use and adequately documented [1,2,5,6].Conventional Francis and Kaplan hydroelectric turbine performance characteristics are so shaped as to present no major difficulties for computer simulation, Chaudbry [5] explains such a method although the authors question Chaudbry's philosophy of extrapolating the net head across the turbine. The authors suggest it is more accurate to extrapolate the turbine discharge and combine this with the upstream and downstream characteristic equations in order to obtain an estimation of the turbine net head for the given time interval.

The predominant boundary condition which must be considered when simulating the transient behaviour of a reversible pump storage installation is the four quadrant performance characteristics of the pump turbine. In this paper the problems associated with the representation and interpolation (between guide vane curves) of the performance characteristics are discussed. The limitations of a technique developed by the principal author [3] are explained followed by suggestions, which are under investigation by the second author, for overcoming these limitations. The site recordings taken during the load rejection commissioning tests of a pumped storage scheme are used as a basis for evaluation of the various techniques.

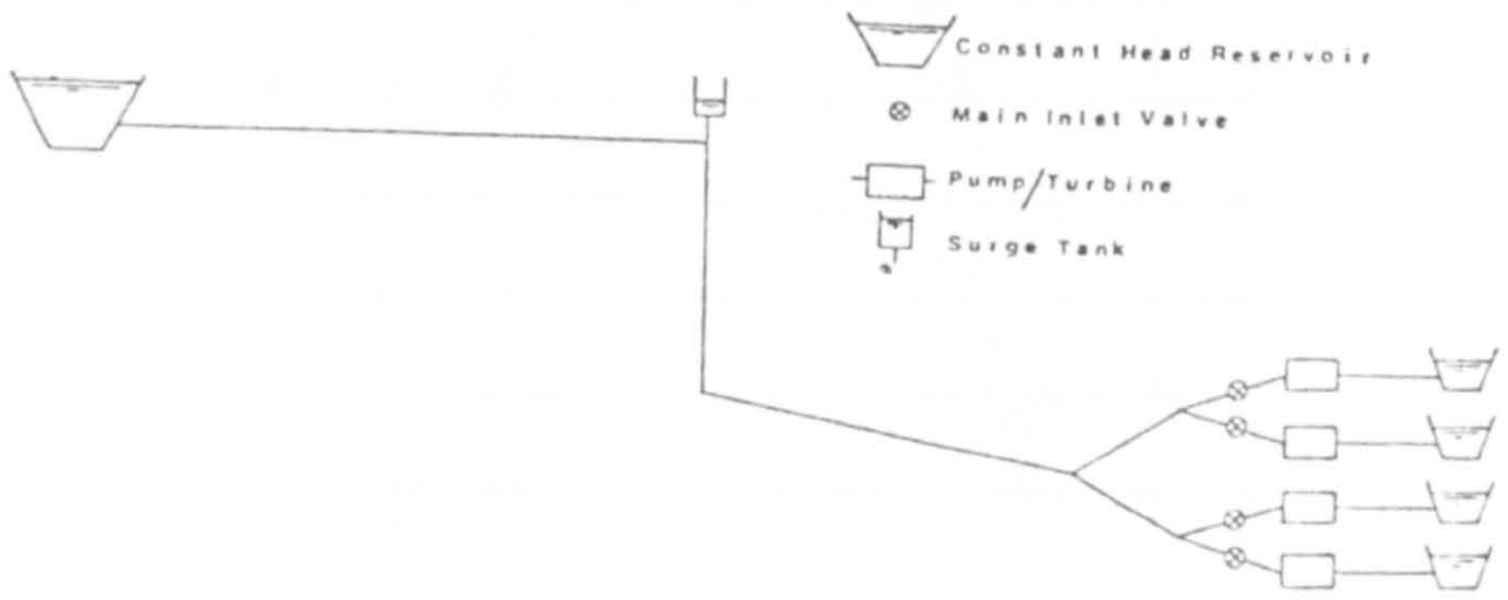

Fig. 1. Schematic layout of a pumped storage scheme

FOUR QUADRANT CHARACTERISTICS OF REVERSIBLE PUMP TURBINES

Definitions

Figure 2 shows the general shape of the performance characteristics of a typical reversible pump turbine. These curves show the variation of unit discharge against unit speed and the variation of unit torque against unit speed, both for the range of guide vane openings. These unit parameters are defined as follows:

$$\text{unit speed} \quad n_{11} = \frac{nD}{\sqrt{H}}$$

$$\text{unit discharge} \quad Q_{11} = \frac{Q}{D^2\sqrt{H}}$$

$$\text{unit torque} \quad M_{11} = \frac{M}{D^3 H}$$

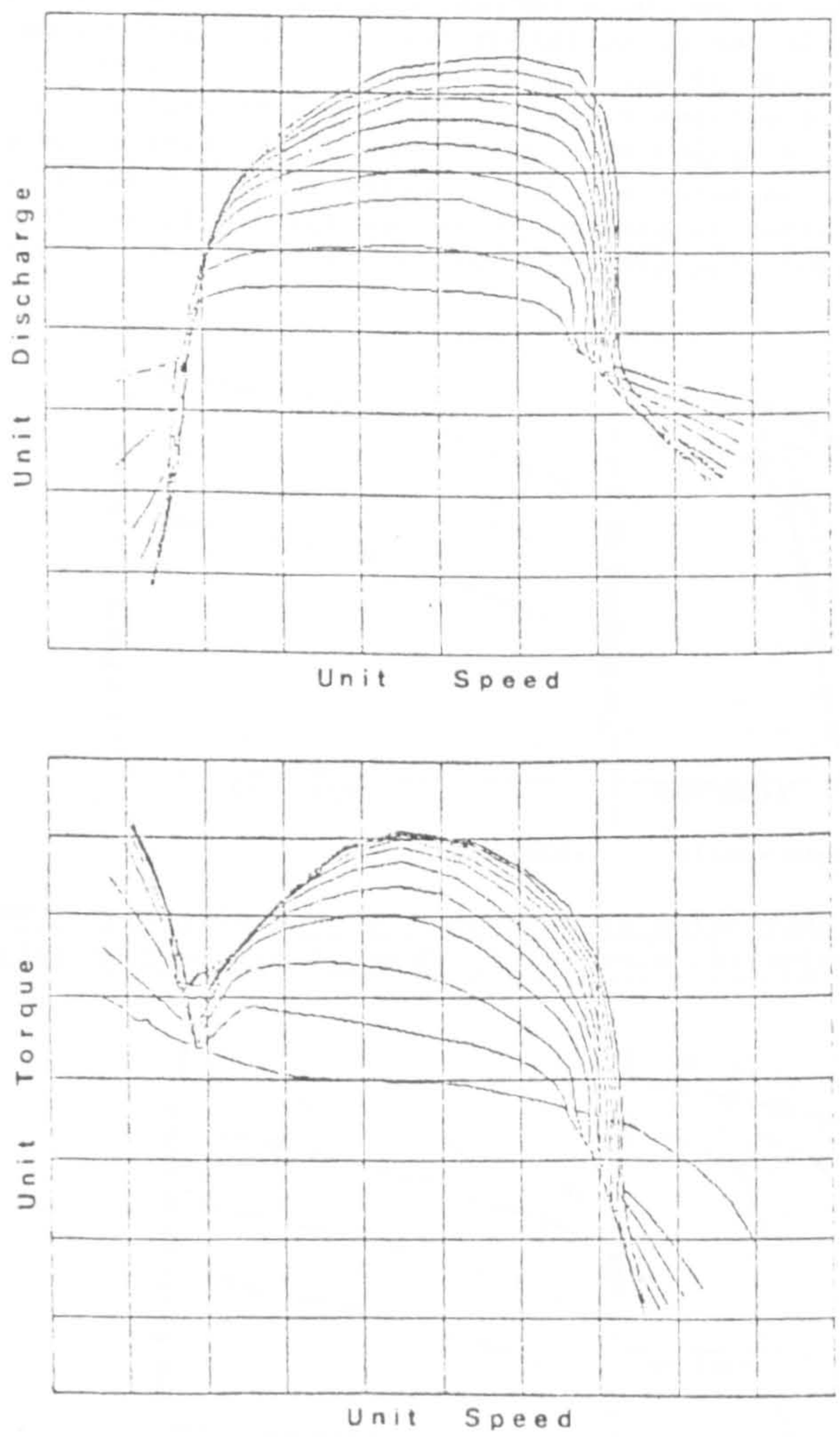

Fig. 2. Four-quadrant performance characteristics of a reversible pump turbine.

where n is the pump turbine speed

Q is the pump turbine discharge

D is the turbine runner throat diameter

H is the net head across the machine

M is the pump turbine torque

Representation and Interpolation

It is convenient to represent (and store in a computer data bank) the above characteristics by a series of points such that a given guide value relationship may be assumed to be a series of straight lines connecting adjacent points. The problem is then to obtain accurate interpolation between successive guide vane curves, over the whole domain of the curves. Consider, for example, the turbining quadrant of the unit discharge against unit speed relationship, linear interpolation between successive guide vane curves produces an intermediate guide vane curve as shown in Figure 3. The interpolation is satisfactory in the region where the guide vane curves are predominately parallel to the unit speed axis but produces unsatisfactory results when the curve becomes predominately parallel to the unit discharge axis. A technique for overcoming this problem, developed by the principal another [3], is based on the principle of a curvilinear mesh obtained by drawing a series of 'S' curves through points of corresponding gradient on each guide vane curve. This produces acceptable interpolations as shown in Figure 4.

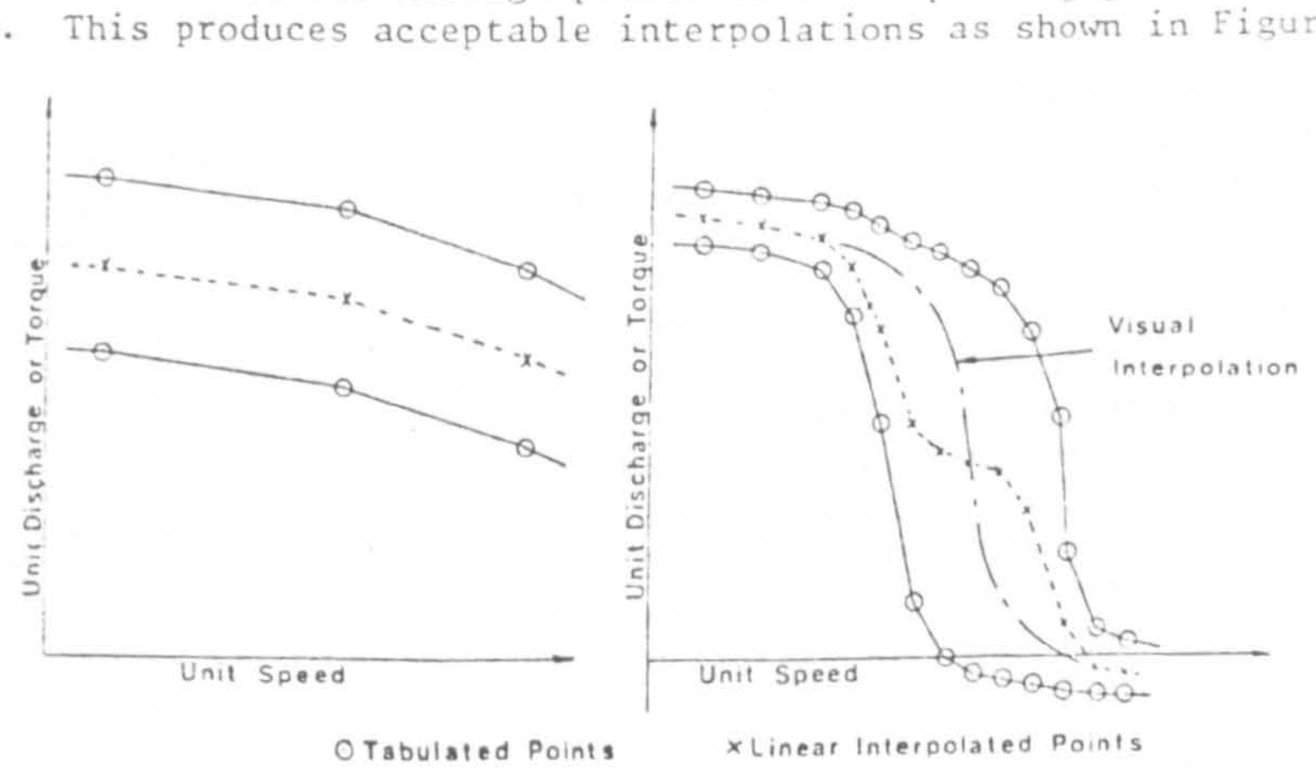

Fig. 3. Linear interpolation for intermediate guide vane curve based on cartesian representation of performance characteristics shown in Fig. 2.

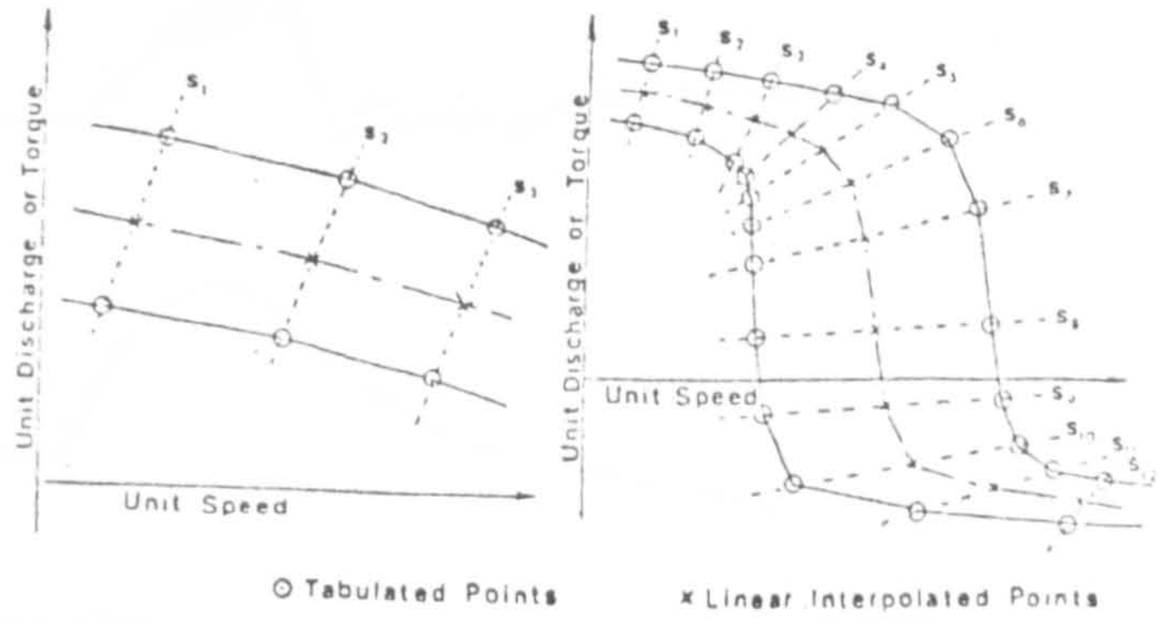

Fig. 4. Linear interpolation for intermediate guide vane curve based on orthogonal curvilinear representation of performance characteristics shown in Fig. 2.

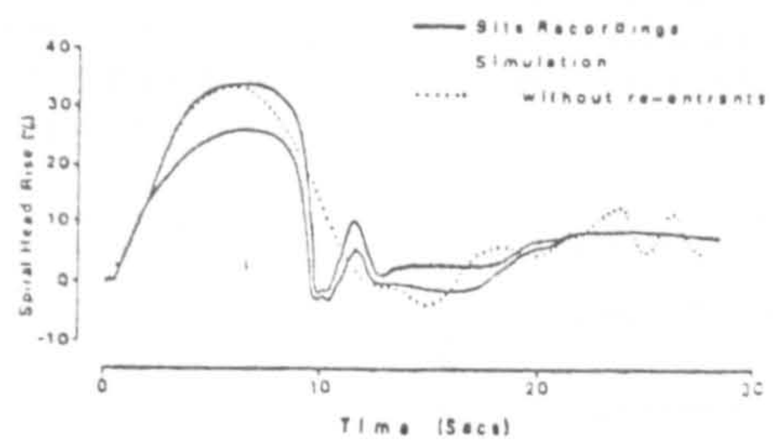

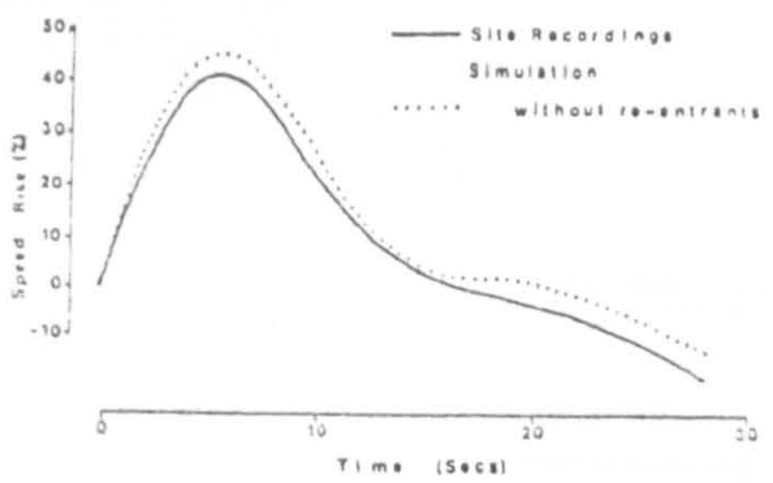

Fig. 5. Comparison of computer simulation and site recordings for load rejection

Figure 5 shows the results of a computer simulation, incorporating the above interpolation procedure, of a load rejection test taken during the commissioning of a Pumped Storage Scheme. Overall the simulation results are satisfactory. The depiction of the maximum values of turbine speed and spiral piezometric head are particularly good, especially considering the accuracy with which values may be obtained from the site recordings. A typical example is reproduced in Figure 6. It is questionable whether the value of the spiral head can be read to within 5 m and the speed to within 7.5 rpm. The area which gives most concern in the comparison shown in Figure 5 is the lack of correlation in the piezometric head in the time interval between approximately 9 and 12 seconds after the load rejection. For this simulation the pump turbine performance characteristics were represented by a series of points such that for a specified value of unit speed a unique value of unit discharge (or unit torque) was obtained for a given value of guide vane opening. In general this is not true in the region where the guide vane curves are predominately parallel to the unit discharge (or torque) axis in

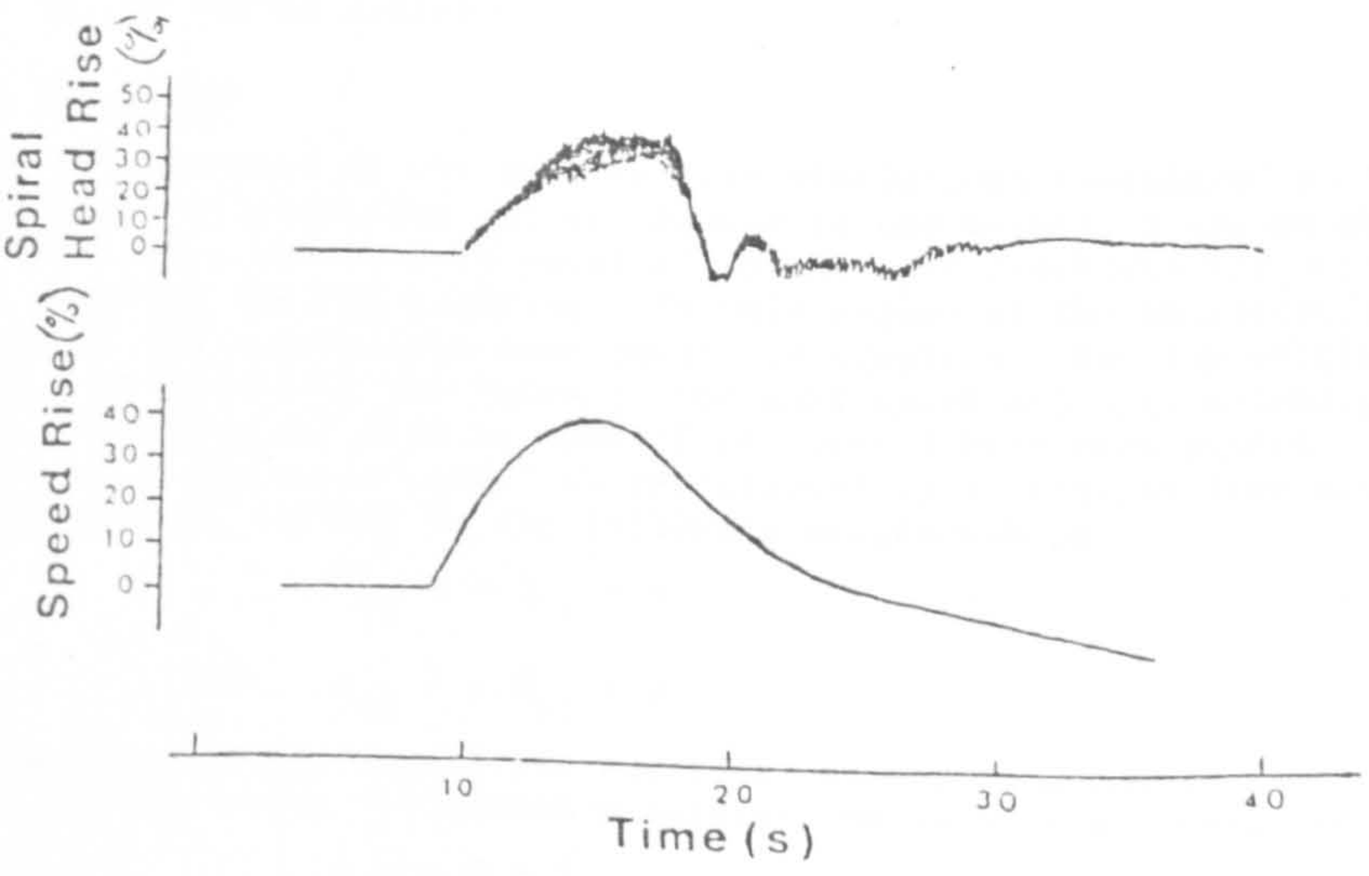

Fig. 6. Typical site recording of load rejection

both the pumping and turbining quadrants. The 'true' shape of the characteristic in these areas involves 're-entrants' as shown schematically in Figure 7 where three values of unit discharge (or torque) are possible for a given value of unit speed and guide vane opening.

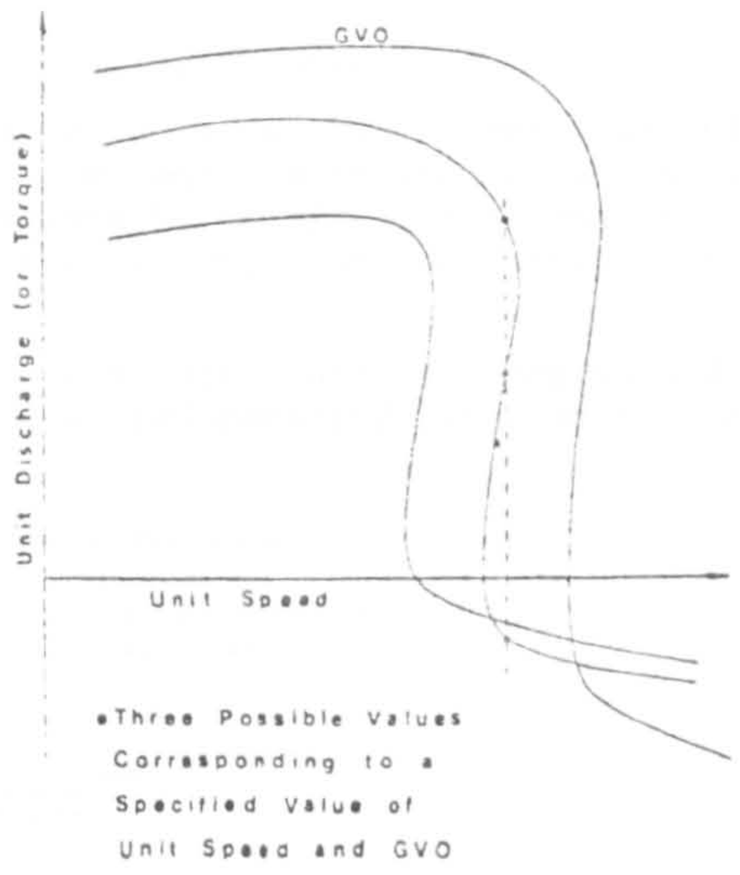

Fig. 7. 'True' shape of pump turbine performance characteristics including 're-entrants'.

Incorporation of 're-entrant' sections of characteristics

The multivalued nature of the characteristics occurring in the region where the curves are predominately parallel to the unit discharge (or unit torque) axis, as shown in Figure 7, creates problems in defining the appropriate value of unit discharge (or unit torque) corresponding to given values of unit speed and guide vane opening. By extrapolating calculated values of turbine discharge and speed from previous time intervals and combining the pipe characteristic equations upstream and downstream of the turbine it is possible to identify the appropriate operating point on the turbine performance characteristic. If this point does not satisfy the turbine boundary condition a revised estimate of unit speed is required. Slight variations in the value of unit speed are accentuated in this region when interpolating the value of unit discharge (or torque) and this caused instabilities in the calculations. In order to overcome these problems a new algorithm has been devised by the second author.

Revised Algorithm

For the purposes of the turbine trip simulations considered in this paper the pump turbine characteristic may be reduced to the turbining region where the guide vane curves are predominately parallel to the unit discharge (or unit torque) axis and the reversed pumping quadrant. In this region of the characteristic the selection of the appropriate mesh square is simplified and the multivalued problem eliminated by reversing the roles of the unit speed and unit discharge (or unit torque). Full use may also be made of the curvilinear mesh system. The interpolated guide vane 'curve' is represented by a straight line within the 'mesh square' and defined by the following relationships.

$$n_{11} = a\, Q_{11} + b \qquad (1)$$

and

$$n_{11} = c\, M_{11} + d \qquad (2)$$

Combining the pipe characteristic equation upstream and downstream of the turbine produces the following relationship between the turbine net head and discharge

$$H = e\, Q + f \qquad (3)$$

Since there are four variables (net head, turbine discharge, speed and to) to be evaluated a fourth equation is required. This is provided by equating th mean out of balance torque to the rate of change of turbine speed

$$M = - I \frac{d\omega}{dt} \qquad (4)$$

where I is the moment of inertia of the rotating masses.

In the above equations (1) to (4) a, b, c, d, e and f are constants for given time interval and the equations may be combined to produce a function of ne variable which can be solved using a standard Newton-Raphson technique. Rapid convergence is obtained since a 'good' first estimate of the variable is available from the extrapolation procedure.

The algorithm described above was incorporated into the program and Figure 8 shows the results of the turbine trip simulation compared with the site results and the simulation shown in Figure 5.

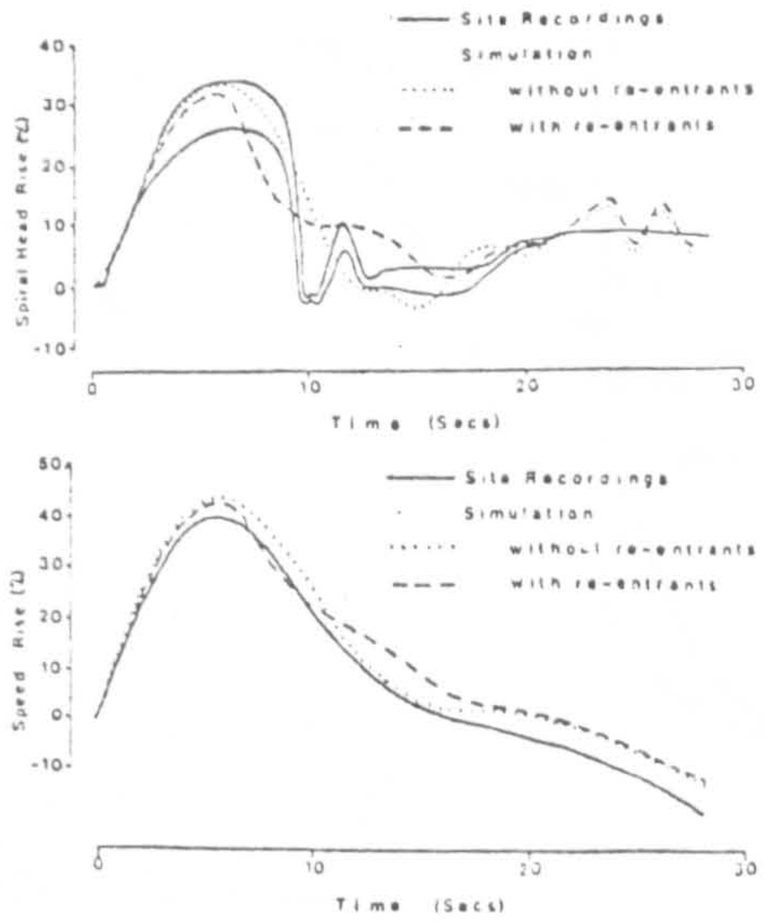

Fig. 8. Comparison of computer simulations and site recording for load rejection

DISCUSSION

The sensitivity of the simulated results upon the shape of the pump turbine performance characteristics is shown in Fig. 9.

The calculated values of unit discharge and unit speed are plotted on the appropriate region of the turbine characteristic which includes the 're-entrant' shaped guide vane relationships. This shows the considerable effect caused by slight variations in the shape of the turbine characteristics. Such a variation probably exists between the model and prototype pump turbine characteristics and this should be considered when comparing simulated and site results. The authors are of the opinion that the 're-entrant' part of the pump turbine characteristics is in fact a mean curve 'drawn' through a hysteresis loop similar to that observed by Yamabe [7]. This area requires further research during the model testing of pump turbines in order to provide more 'accurate' performance characteristics.

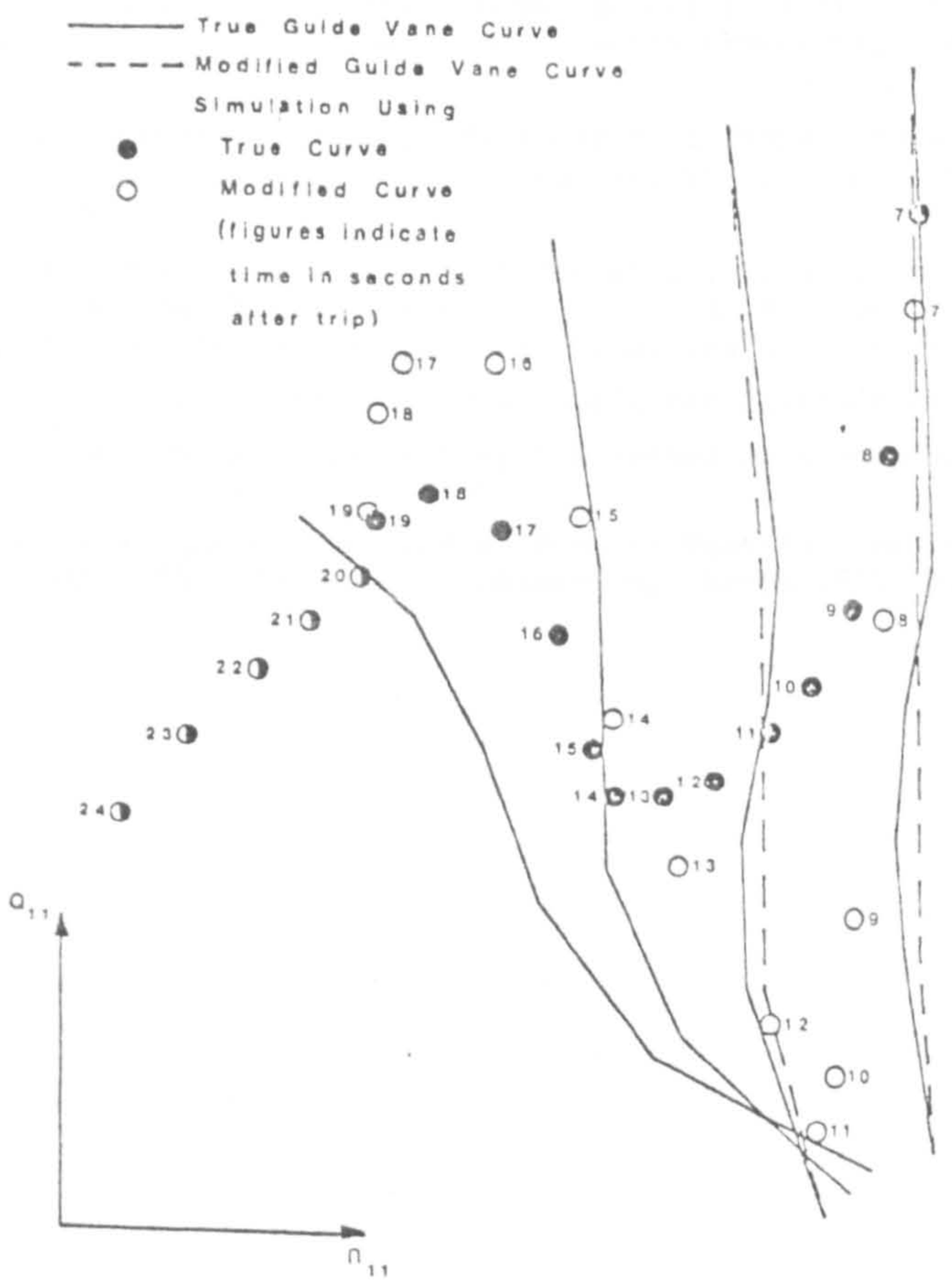

Fig. 9. Computer simulated results superimposed on pump turbine performance characteristics.

ACKNOWLEDGEMENTS

The research described in the paper by the second author is one area under investigation as part of a CASE (Collaborative Award in Science and Engineering) studentship financed by SERC (Science and Engineering Research Council) and Preece Cardew & Rider, Consulting Engineering, Brighton, England.

The basis for the research described in the paper is founded on work commenced by the principal author approximately 10 years ago whilst employed in the Hydroelectric Department of Merz and McLellan, Consulting Engineers, Newcastle-Upon-Tyne, England.

REFERENCES

1. E.B. Wylie and V.L. Streeter. "Fluid Transients", McGraw-Hill Book Co. 1978.

2. A.P. Boldy, "Analysis of Waterhammer in Hydroelectric Installations", Toward Real-Time Simulation, Part 1, Simulation Councils Proceedings Series, Vol. 6, No. 1, June 1976, p. 29.

3. A.P. Boldy, "Waterhammer Analysis in Hydroelectric Pumped Storage Installations" Second Int. Conf. on Pressure Surges. Organised by B.H.R.A. City University, England. Sept. 1976.

4. M. Lister. "The numerical solution of hyperbolic partial differential equations by the method of characteristics". In. A. Ralston and H.S. Wilf. editors, "Mathematical Methods for Digital Computers", Wiley 1962, p. 165.

5. M.H. Chaudbry. "Applied Hydraulic Transients", Van Nostrand Reinhold Co. 1979.

6. G. Evangelistic "Waterhammer analysis by the method of characteristics (III)" L'Energia Elettrica No. 12-1969, p. 839.

7. M. Yamabe "Hysteresis Characteristics of Francis Pump-Turbines when operated as Turbine", Trans. ASME. Jul. Basic Engineering, March 1971, p.80.

4th International Conference on
Pressure Surges
September 21-23, 1983

PAPER G1

REPRESENTATION OF THE CHARACTERISTICS OF REVERSIBLE PUMP TURBINES FOR USE IN WATERHAMMER SIMULATIONS

Dr. A. P. Boldy* and N. Walmsley**

* Lecturer, University of Warwick, Coventry, England

** Research Student, University of Warwick, Coventry, England

Summary

An increasing number of pumped storage schemes are being commissioned to handle the problems of frequency control and peak-load power generation of large electrical networks. Computer simulations of waterhammer phenomenon are nowadays accepted as an integral part of the design of these installations and are used as a "tool" to aid the Engineer when making decisions concerning optimum operation, construction and protection measures. It is essential, therefore, that the simulations are accurate and reliable.

The theory behind waterhammer simulations is well established and most of the boundary conditions encountered are well documented, along with their handling routines. However, the boundary condition which is often ignored is that of the reversible pump turbine. In order to simulate this boundary it is necessary to represent the machine characteristics in a form suitable for computer storage. The paper describes the merits and drawbacks of various representations of the performance characteristics with particular reference to the multivalued, instability regions and their associated interpolation problems.

A method of manipulating the basic data obtained from performance model tests of the pump turbine into a suitable form for transient analysis is presented in the paper.

Held at the University of Bath, England.
Organised and sponsored by BHRA, The Fluid Engineering Centre.

NOMENCLATURE

D [m] = diameter of impeller

H [m] = pressure head across pump turbine

M [Nm] = out of balance torque

n [r.p.m.] = rotational speed

Q [m^3/s] = discharge

Z [mm] = guide vane opening (gvo).

Z_F [mm] = maximum guide vane opening

Dimensionless ratios

$\alpha = \frac{n}{n_R}$ normalised speed

$\beta = \frac{M}{M_R}$ normalised torque

$h = \frac{H}{H_R}$ normalised pressure head

$v = \frac{Q}{Q_R}$ normalised discharge

where suffix R refers to rated conditions.

1. INTRODUCTION

Transient simulation of hydro-electric installations are based upon the simultaneous consideration of the dynamic equilibrium and continuity equations describing the fluid motion within the system together with the governing equations or performance characteristics of each boundary condition. This paper is devoted to the four quadrant performance characteristics of a reversible pump turbine describing the machine boundary of a pumped storage scheme. Due to the complexity of this machine, the number of variables involved and the diverse modes of operation, empirical formulae cannot adequately describe the performance of the machine. Instead, information must be collected from scale model tests and presented in the form of performance characteristics, which relate the rotational speed (n), discharge (Q), pressure head across the machine (H) and the out of balance torque (M) for a range of guide vane openings, over the range of operating conditions. When considering a pumped storage scheme, employing a reversible Francis-type pump turbine, the operating conditions cover the full four quadrants which may be defined as follows;

Quad 1	n - ve	Q - ve	(pumping)
Quad 2	n - ve	Q + ve	(braking)
Quad 3	n + ve	Q + ve	(turbining)
Quad 4	n + ve	Q - ve	(reverse pumping)

A review of various co-ordinate systems used to represent the pump turbine performance characteristics is presented and their advantages and disadvantages, for use in transient simulations, are discussed. Recommendations of the most appropriate forms to use are made and an algorithm presented which will superimpose a curvilinear mesh upon the performance characteristics, in order to facilitate interpolation for the intermediate guide vane curves, independent of the co-ordinate system selected.

2. PUMP TURBINE PERFORMANCE CHARACTERISTICS

The scale model test results are generally presented in graphical form but the co-ordinate systems used may vary from one turbine manufacturer to another. They may need to be transformed when adapting them for use in transient simulations where problems relating to computer storage, interpolation of intermediate guide vane curves and the handling routines must be taken into account. It was demonstrated by Boldy (Ref 1) that interpolation of the intermediate guide vane curves was only valid if the interpolation was performed within a curvilinear mesh system. This mesh is generated by superimposing a series of 'S' curves onto the guide vane curves. It has been assumed, therefore, that this mesh system is required for each of the co-ordinate systems described later and that linear interpolation along sections of the 'S' curves should be used where possible in locating the position of an intermediate guide vane curve. A further consideration is the form in which the instability regions (Ref 2) take in the co-ordinate system as this may complicate the handling routines. Fig 1 shows part of the performance characteristics plotted as discharge against pressure head, with the speed constant. For a certain range of values of the pressure head there may be as many as three possible values for the corresponding discharge. Correct location of the operating point in these regions is difficult and has been discussed elsewhere, (Ref 3).

In order to save space only the speed, discharge and pressure head relationships will be discussed in this paper. The same arguments are equally applicable to the speed, torque and pressure head relationships.

2.1 REPRESENTATION 1

A natural choice for the co-ordinate system to be used for the performance characteristics would be the dimensionless homologous relationships:

$$\frac{h}{\alpha^2} \text{ versus } \frac{v}{\alpha} \quad \text{and} \quad \frac{\beta}{\alpha^2} \text{ versus } \frac{v}{\alpha} \quad \text{-A}$$

$$\text{or} \quad \frac{h}{v^2} \text{ versus } \frac{\alpha}{v} \quad \text{and} \quad \frac{\beta}{v^2} \text{ versus } \frac{\alpha}{v} \quad \text{-B}$$

Because the full four quadrants are to be considered both v and α can be equal to zero forcing the dimensionless ratios to tend to infinity. This is highly undesirable and in order to allieviate this problem DeFazio (Ref 5) recommended a combination of the two co-ordinate systems, A and B. System A is used for $-1 \leq v/\alpha \leq +1$ and system B for the range $-1 \leq \alpha/v \leq +1$. Limits of + 1 and - 1 are imposed on the absisca corresponding to the points where the switching of the coordinate system occurs. Fig 2 shows the form of this representation for a single, (the fully open) guide vane curve. It is always an advantage to have the quadrants individually defined but it is clear from Fig 2 that this is not the case. Up to three ordinate values are possible for a given absisca value, two of which refer to a single quadrant. Problems will be found in locating the correct operating point particularly in the region of the extremities, + 1 and - 1. Furthermore, Fig 2 only shows a single guide vane curve. The full range of guide vane openings is shown in Fig 3. Note how the ordinate values become at least one order of magnitude larger for the lower guide vane openings compared with the fully open position. This is due to v and α becoming small with respect to h and creates difficulties when interpolating intermediate guide vane curves, linear interpolation becoming unsuitable. Also, the curves do not lend themselves easily to a curvilinear mesh and the authors consider that this representation is inappropriate for the full four quadrants of a reversible pump turbine.

2.2 REPRESENTATION 2

Perhaps the most widely adopted representation of machine performance characteristics used by pump-turbine manufacturers is based on the unit parameters. The information is presented by two sets of complementary curves with the following co-ordinate systems

$$Q_{11} \text{ versus } n_{11}$$
$$M_{11} \text{ versus } n_{11}$$

where the unit parameters are defined as;

$$\text{unit speed, } n_{11} = nD/\sqrt{H}$$

$$\text{unit discharge } Q_{11} = Q/D^2\sqrt{H}$$

$$\text{unit torque } M_{11} = M/D^3H$$

Fig 4 shows a typical set of curves for the Q_{11} against n_{11} relationship. Because the curves are smooth and continuous they are easily approximated by a series of points joined by straight lines, as shown, providing a sufficient number of points are taken. Superimposing a series of 'S' curves to form a curvilinear presents no problems providing care is taken where the curves intersect and overlap. Fig 5 shows such a mesh, the 'S' curves being overlayed by hand but employing the algorithm described later, greater accuracy and a greater number of 'S' curves, producing a finer grid, is possible. One of the drawbacks of the representation is the form in which the instability region occur. In the unit plane they appear as re-entrants, Fig 6, causing the curves to become multivalued. The general handling routine of a machine boundary involves estimating the operating point on the performance characteristics before using an iterative process to find the true operating point, which must satisfy the conditions imposed by the hydraulic system. If the operating point lies within the multivalued region an incorrect solution will develop unless great care is taken to identify the correct operating point. Representations which are single valued, therefore, have a distinct advantage over representations which include re-entrants.

2.3 REPRESENTATION 3

A method of avoiding some of the problems associated with Representation 1 was put forward by Marchal et al (Ref 4) where the following planes were suggested;

$$\frac{h}{\alpha^2 + v^2} \text{ versus } \tan^{-1}(v/\alpha)$$

and

$$\frac{\beta}{\alpha^2 + v^2} \text{ versus } \tan^{-1}(v/\alpha)$$

These are commonly known as a form of the Suter representation. Introducing the $\tan^{-1}$ function considerably collapses the data. However, in order to individually define each of the four quadrants it is necessary to define the range of the $\tan^{-1}$ function as follows:

Quad 1 $\quad \pi \leq \tan^{-1}\left(\frac{V}{\alpha}\right) \leq 3\pi/2$

Quad 2 $\quad \pi/2 \leq \tan^{-1}\left(\frac{V}{\alpha}\right) \leq \pi$

Quad 3 $\quad 0 \leq \tan^{-1}\left(\frac{V}{\alpha}\right) \leq \pi/2$

Quad 4 $\quad -\pi/2 \leq \tan^{-1}\left(\frac{V}{\alpha}\right) \leq 0$

Fig 7 shows the $h/(V^2+\alpha^2)$ against $\tan^{-1}(V/\alpha)$ representation. The main problem with the representation arise from the range of values the ordinate takes for various guide vane opening. For the smaller guide vane openings it is possible for $h \gg (V^2+\alpha^2)$ resulting in ordinate values which are at least one order of magnitude greater than those for the fully open guide vane position. Linear interpolation would lead to incorrect positioning of the intermediate guide vane curves and therefore to errors in the location of the operating point. Although this representation renders the curves single valued, even in the instability regions, it is not recommended for use when the full four quadrants are required, as for a pump-turbine.

2.4 REPRESENTATION 4

In the discussion of DeFazio's paper (Ref 5) Waznaik proposed a method of opening out the unit parameter performance characteristics by the introduction of a normalised guide vane opening factor leading to

$$Q_{11} \text{ versus } (Z/Z_F)\, n_{11}$$
$$M_{11} \text{ versus } (Z/Z_F)\, n_{11}$$

where Z = actual guide vane opening.
Z_F = maximum guide vane opening.

The effect of introducing this factor can be seen in Fig 8, showing the performance characteristics on the Q_{11} against $(Z/Z_F)\, n_{11}$ plane. The individual guide vane curves become easily distinguishable and would present no problems in superimposing a series of 'S' curves to form a curvilinear mesh. The regularity of the spacing of the curves suggest linear interpolation within the mesh squares would be quite adequate and would lead to very good approximations of the intermediate guide vane curves. The main disadvantage of this system is that, as with Representation 2, the instability regions occur in the form of re-entrants. But, providing care is taken when the locus of the operating point passes through these regions in order to define the correct operating point, this representation is acceptable. The smooth, continuous shape of the curves reduces the number of points required to depict the true shape, a curvilinear mesh is easily envisaged and presents no problems whether superimposed by hand or by the algorithm described later and linear interpolation is acceptable.

2.5 REPRESENTATION 5

The final representation was proposed by Martin (Ref 6) and involves a combination of opening out the performance characteristics by introducing a normalised guide vane opening factor and transforming this to a modified Suter plane, leading to

$$\frac{h}{\alpha^2 + \left(\frac{Z_F}{Z}\frac{V}{\alpha}\right)^2} \text{ versus } \tan^{-1}\left(\frac{Z_F}{Z}\frac{V}{\alpha}\right)$$

and

$$\frac{\beta}{\alpha^2 + Z/Z_F V^2} \text{ versus } \tan^{-1}\left(\frac{Z_F}{Z}\frac{V}{\alpha}\right)$$

co-ordinate systems. A typical set of curves is shown in Fig 9. This representation suffers because the zero guide vane opening curve is undefined and an additional handling routine is therefore required for the final closure of the guide vanes. Such a routine can be found in Ref 6. The representation essentially opens out the individual guide vane curves, whilst collapsing the numerical ranges between maximum and minimum guide vane openings, but creates much overlapping in some areas. However, providing a curvilinear mesh can be superimposed then linear interpolation of the intermediate guide vane curves can be carried out accurately. As the curves are

single valued throughout there are no problems when finding the operating point in the instability regions and it is felt this advantage outweighs the disadvantages.

3. SUPERIMPOSING A CURVILINEAR MESH

Preparation of the performance characteristics into the form use in transient simulations will normally require transforming the manufacturers' data into the co-ordinate system chosen : then superimposing a curvilinear mesh and, finally, creating a data file containing the co-ordinates of the intersections of guide vane curves and 'S' curves. This is a very tedious and time consuming process if done by hand so an algorithm has been developed to carry out this process automatically.

Consider the construction of a section of an 'S' curve, as shown in Fig 10, which passes from the i^{th} to the $(i+1)^{th}$ guide vane opening through points $P_{i,j}$ and $P_{i+1,j}$.

Let $P_{i,j-1}$, $P_{i,j}$ and $P_{i,j+1}$ be three adjacent data points on the i^{th} guide vane curve and $P_{i+1,k-1}$, $P_{i+1,k}$ and $P_{i+1,k+1}$ be three adjacent points on the $(i+1)^{th}$ guide vane curve. Each of the above points has a corresponding (x, y) co-ordinate. The two sections of guide vane curves may be approximated by two quadratic functions, say

$$y = Ax^2 + Bx + C \text{ along } i^{th} \text{ curve}$$
$$y = ax^2 + bx + c \text{ along } (i+1)^{th} \text{ curve}$$

A true curvilinear mesh requires that the angle subtended between the guide vane curve and the 'S' curves is a right angle but this is not possible if the 'S' curve is approximated by a series of straight lines.

The best approximation to a true curvilinear mesh occurs when

$$\phi_1 = \phi_2 \qquad -1$$

or
$$\pi - (\theta_1 + \theta_2) = (\theta_1 + \theta_3) \qquad -2$$

where
$$\theta_1 = \tan^{-1}\left[\frac{y_{i,j} - y_{i+1,j}}{x_{i,j} - x_{i+1,j}}\right] \qquad -3$$

but along $(i+1)^{th}$ guide vane curve

$$y_{i+1,j} = a x_{i+1,j}^2 + b x_{i+1,j} + c$$

$$\therefore \quad \theta_1 = \tan^{-1}\left[\frac{y_{i,j} - (a x_{i+1,j}^2 + b x_{i+1,j} + c)}{(x_{i,j} - x_{i+1,j})}\right] \qquad -4$$

Differentiation of the quadratic approximations leads to

$$\theta_2 = \tan^{-1}\left[2Ax_{i,j} + B\right] \qquad -5$$
$$\theta_3 = \tan^{-1}\left[2a x_{i+1,j} + b\right] \qquad -6$$

Combining equations 2, 4, 5 and 6 produces a function of one variable, $x_{i+1,j}$, which may be solved using a standard Newton-Raphson technique. Knowing $x_{i+1,j}$, $y_{i+1,j}$ is found by simply substituting back into $y = ax^2 + bx + c$.

This procedure is repeated for each point along the i^{th} guide vane curve before repeating between the $(i+1)^{th}$ and $(i+2)^{th}$ guide vane curves, noting that the new set of data points, through which the 'S' curves pass, has been created along the $(i+1)^{th}$ guide vane opening. A complete array of data points which form a curvilinear mesh can be built up by merely repeating the above process.

4. CONCLUSIONS

Although all the representations of the performance characteristics have certain drawbacks, when used in transient simulations, it is clear that some are better suited than others.

Representation 4 is ideally suited to the curvilinear mesh system and to linear interpolation of the intermediate guide vane curves within the mesh. The only drawback is the multivalued nature of the curves in the instability regions but this problem can be overcome.

Representation 5, whilst overcoming the multivalued problem suffers slightly from the fully closed guide vane opening being undefined in this plane. A separate handling routine is required for the final closing stages of the guide vanes but a method of achieving this is described by Martin (Ref 6). Superimposing a curvilinear mesh would prove difficult by a hand method in this plane but introducing the algorithm described herein this problem is alleviated.

The algorithm also ensures that an accurate mesh system will be attained, independent of the co-ordinate system chosen, resulting in better interpolation of the intermediate guide vane curves and greater accuracy in locating the operating point, which will, therefore, lead to greater accuracy in the final results.

5. REFERENCES

1. Boldy, A.P.: "Waterhammer Analysis in Hydroelectric Pumped Storage Installations". Second International Conference on Pressure Surges, BHRA, London, 1976, Paper B1.

2. Yamabe, M.: "Hysteresis Characteristics of Francis Pump Turbines when Operated as a Turbine". Trans. ASME J. of Basic Engineering, March 1971, p. 80.

3. Boldy, A.P. and Walmsley, N.: "Performance Characteristics of Reversible Pump Turbines". Proceedings, Eleventh Symposium of the Section on Hydraulic Machinery, Equipment and Covitation, IAHR, Amsterdam, 1982, Paper 60.

4. Marchal, M., Flesh, G. and Suter, P.: "The Calculation of Waterhammer Problems by Means of the Digital Computer". Proceedings, International Symposium on Waterhammer in Pumped Storage Projects, ASME, Chicago, 1965.

5. DeFazio, F.G.: "Transient Analysis of Variable Pitch Pump Turbines". Trans ASME, J. of Dynamic Systems, Measurement and Control, Vol. 94, 1972, pp 198 - 205.

6. Martin, C.S.: "Transformation of Pump Turbine Characteristics for Hydraulic Transient Analysis". Proceedings, Eleventh Symposium of the Section on Hydraulic Machinery, Equipment and Cavitation, IAHR, Amsterdam, 1982, Paper 30.

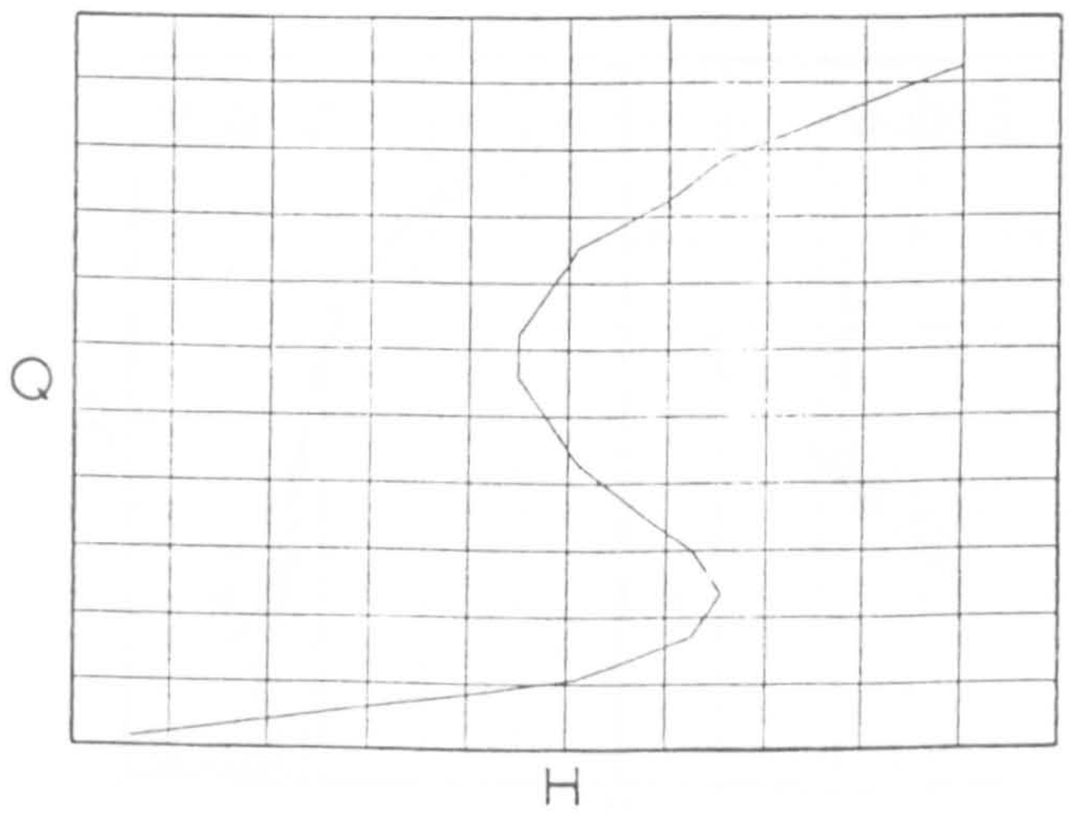

Fig. 1 Typical instability region represented in the discharge against pressure head plane.

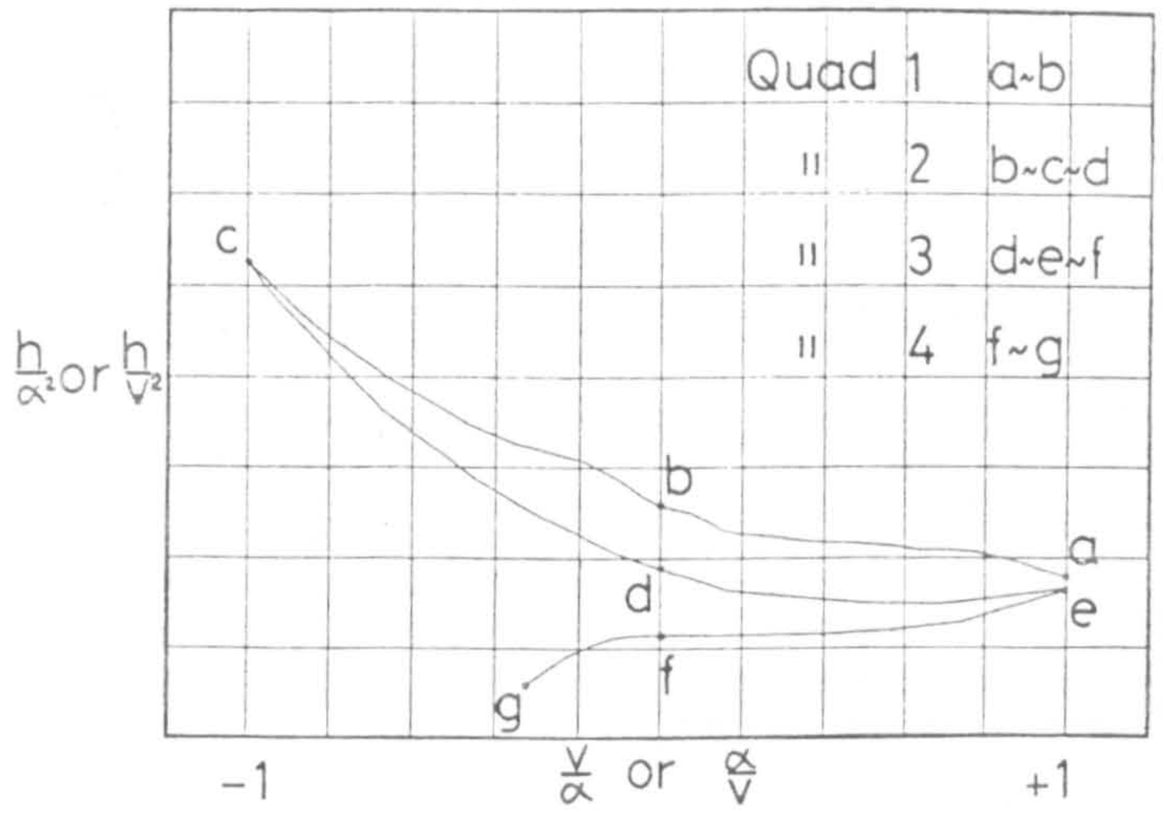

Fig. 2 Dimensionless homologous representation of machine characteristic for a single guide vane opening

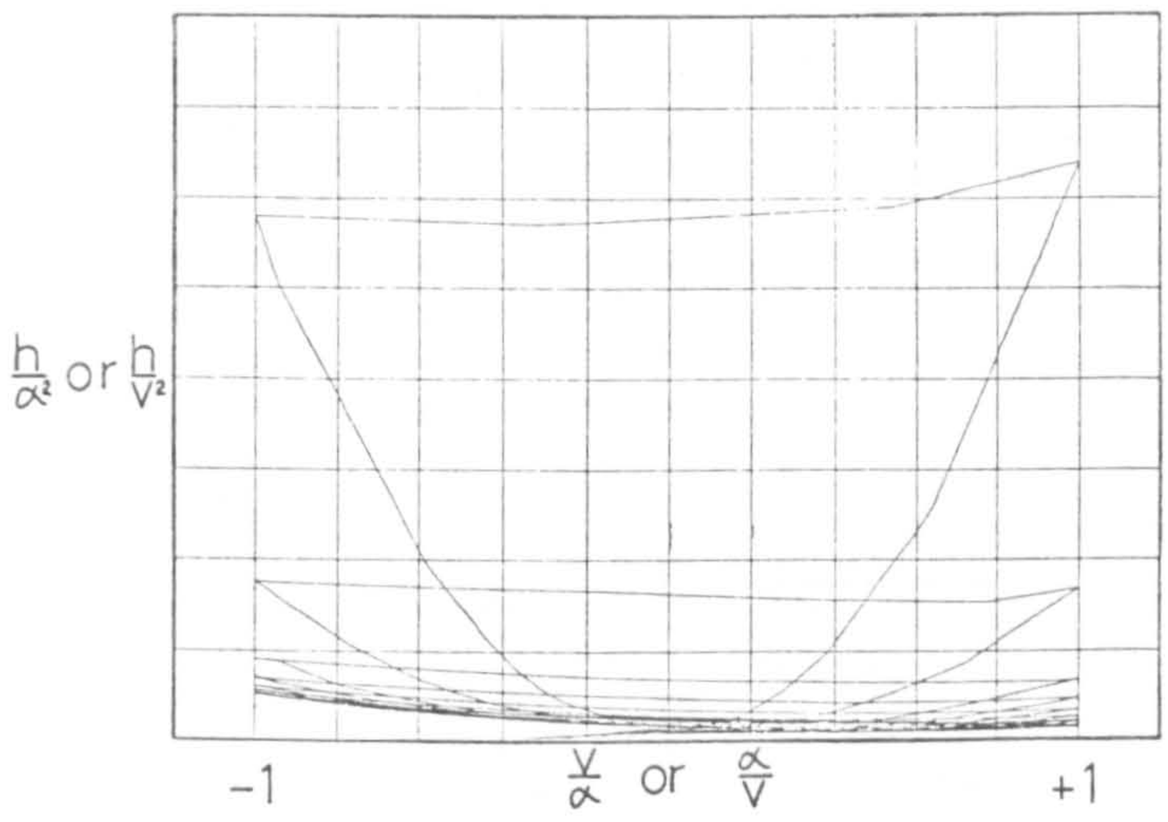

Fig. 3 Dimensionless homologous representation of machine characteristics.

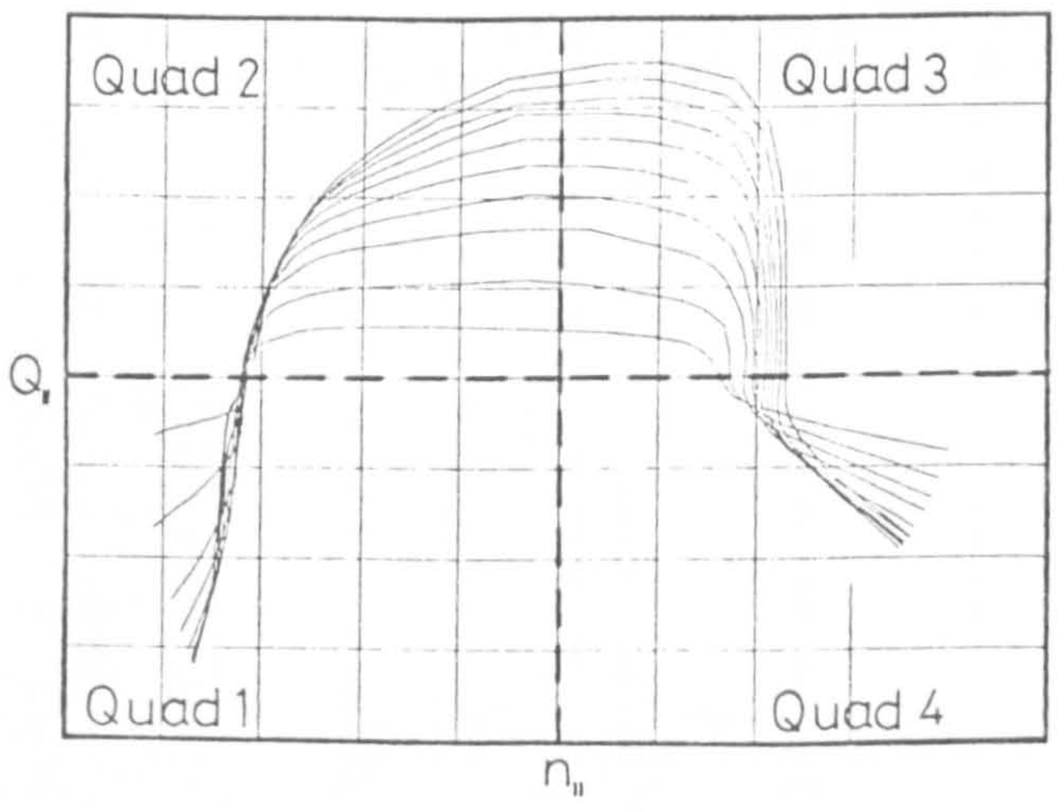

Fig. 4 Unit parameter representation of machine characteristics.

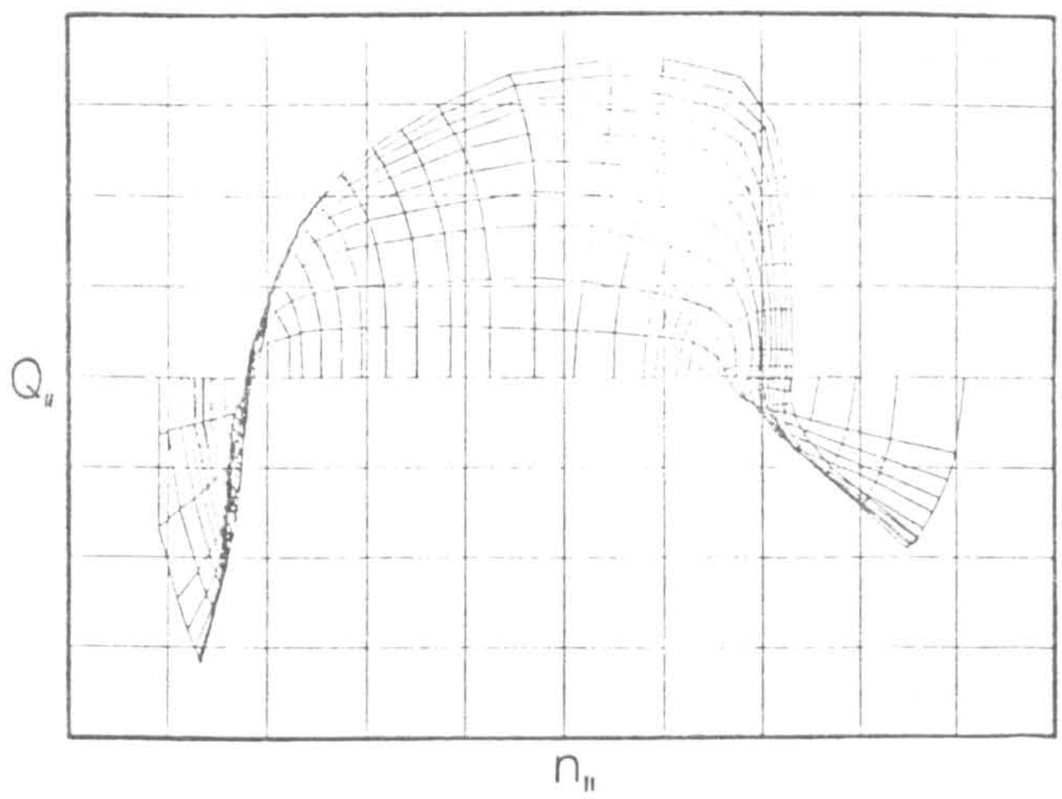

Fig. 5 Curvilinear mesh superimposed on the unit parameter representation of Fig.4.

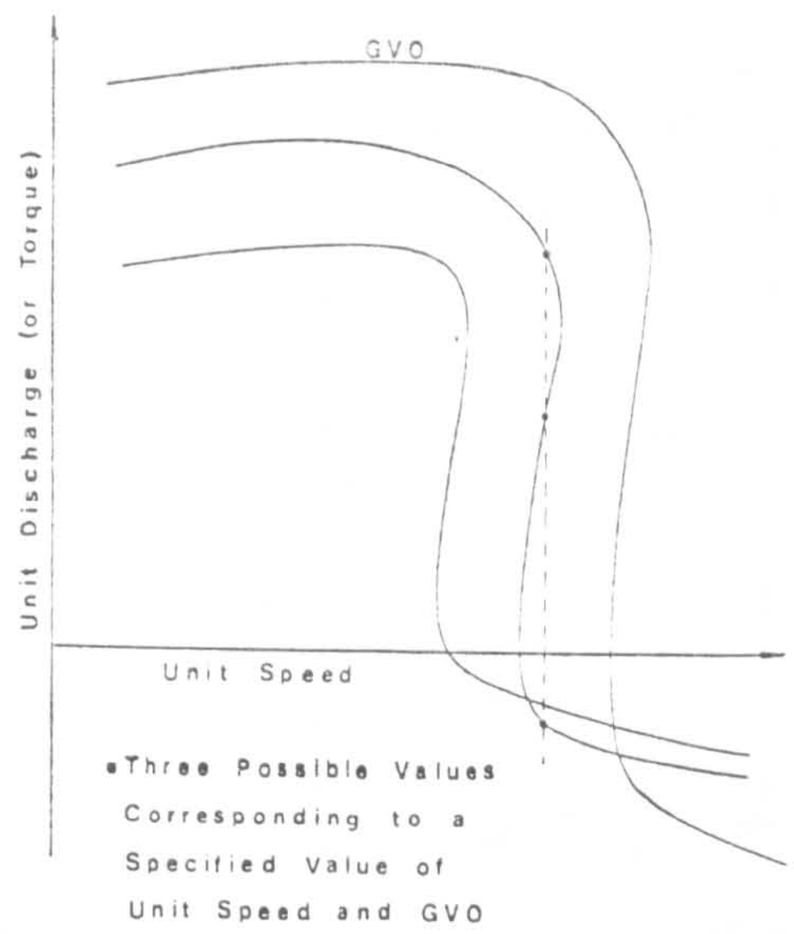

Fig. 6 Multivalved instability region represented in the unit parameter plane.

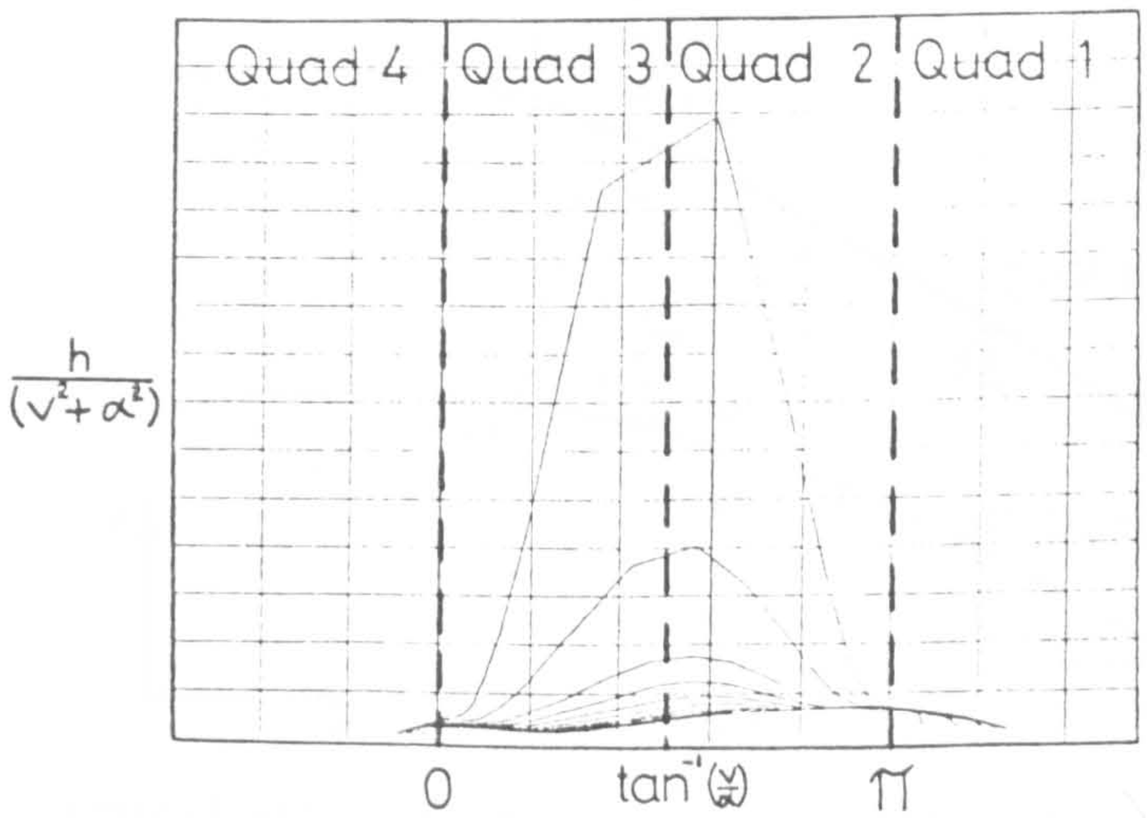

Fig. 7 Suter plane representation of machine characteristics.

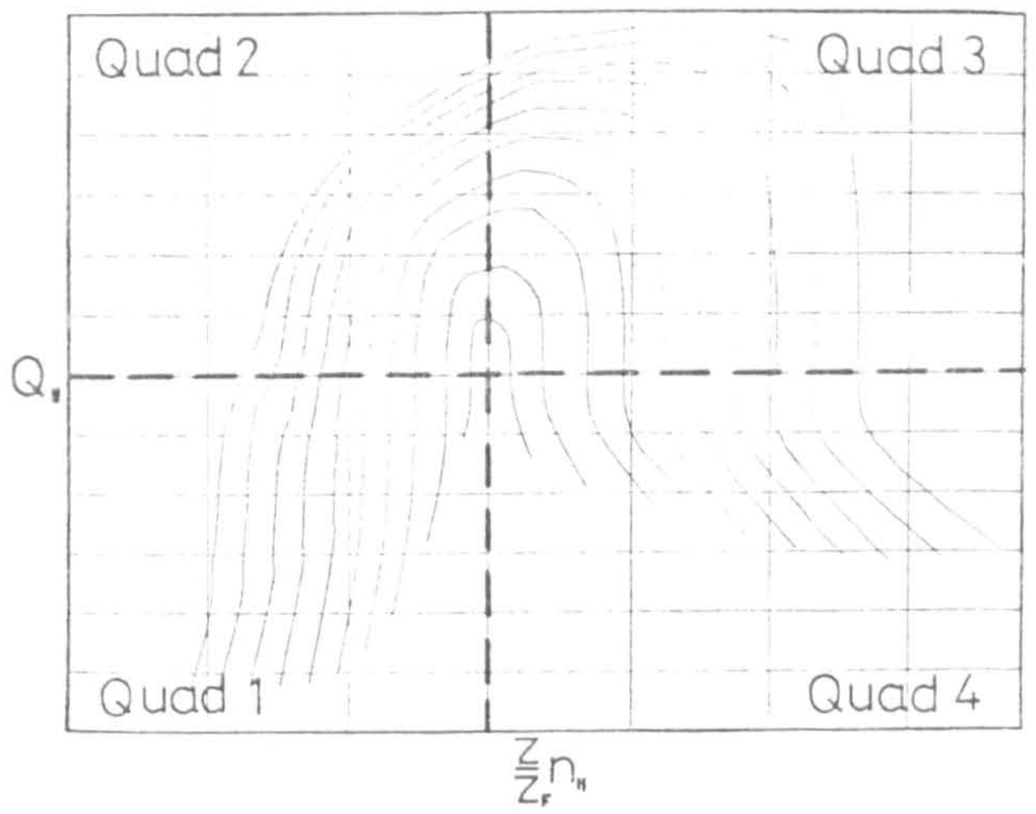

Fig. 8 Exploded unit parameter representation of machine characteristics.

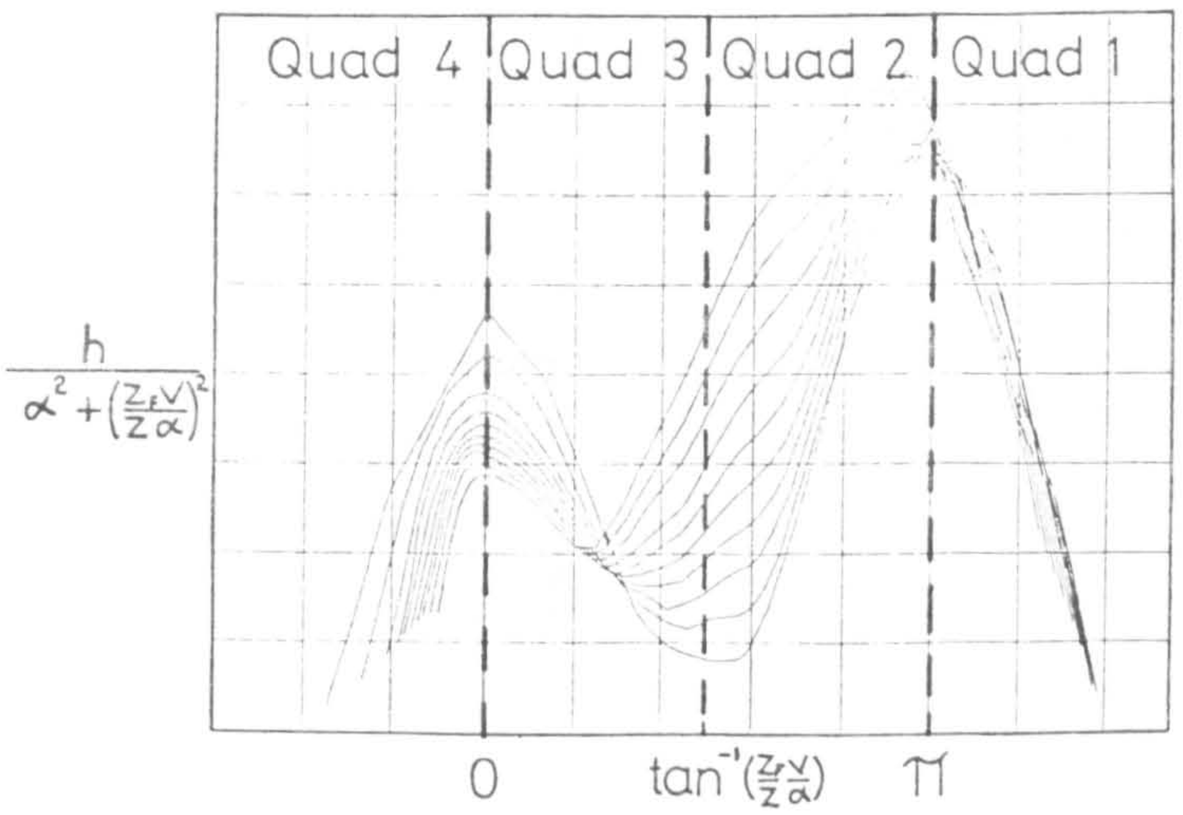

Fig. 9 Modified suter plane representation of machine characteristics.

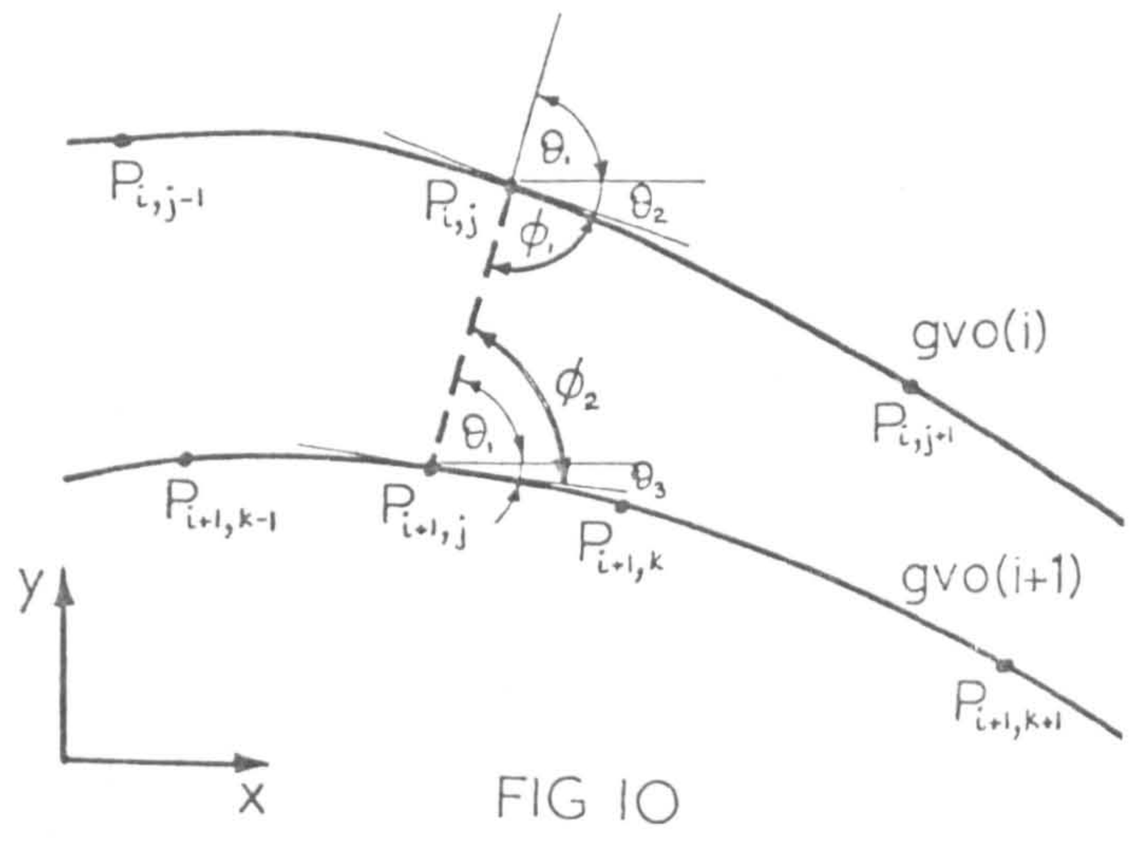

Fig.10 Approximation of the curvilinear mesh superimposed on the machine characteristics.